NOTE TO USERS

SYNTHESIS, SPECIATION, AND APPLICATIONS OF LANTHANIDE POLYOXOMETALATES: VERSATILE NANOSTRUCTURED BUILDING BLOCKS

By

Cheng Zhang

A dissertation submitted to the graduate Faculty in Chemistry in partial fulfillment of the requirements for the degree of Doctor of Philosophy, The City University of New York

2005

INFORMATION TO USERS

The quality of this reproduction is dependent upon the quality of the copy submitted. Broken or indistinct print, colored or poor quality illustrations and photographs, print bleed-through, substandard margins, and improper alignment can adversely affect reproduction.

In the unlikely event that the author did not send a complete manuscript and there are missing pages, these will be noted. Also, if unauthorized copyright material had to be removed, a note will indicate the deletion.

ProQuest Information and Learning Company
300 North Zeeb Road
P.O. Box 1346
Ann Arbor, MI 48106-1346

This manuscript has been read and accepted for the Graduate Faculty in Chemistry in satisfaction of the dissertation requirement for the degree of Doctor of Philosophy.

Dec 29, 2004
Date

Chair of Examining Committee

Jan. 3, 2005
Date

Gerald Kaplan
Executive Officer

Klaus Grohmann

Z. Conrad Zhang

Malgorzata Ciszkowska

Supervisory Committee

The City University of New York

Abstract

SYNTHESIS, SPECIATION, AND APPLICATIONS OF LANTHANIDE POLYOXOMETALATES: VERSATILE NANOSTRUCTURED BUILDING BLOCKS

By

Cheng Zhang

Adviser: Professor Lynn C. Francesconi

Polyoxometalates (POMs) are robust, early transition metal oxide anions that are presently widely used in catalysis, predominantly in heterogeneous catalysis. Incorporation of lanthanide (Ln) ions can lead to potential applications in homogeneous catalysis and new applications and improved performances in heterogeneous catalysis, development of luminescent materials and separation media. To realize these applications, it is critical to understand the speciation chemistry of lanthanide ions and POMs. Therefore, our objective is to identify parameters that impact the solution and solid-state chemistry of lanthanide polyoxometalates. My research focuses on the lanthanide chemistry of two families of polyoxometalates. 1) The α-$PW_9O_{34}^{9-}$ polyoxometalate, derived from the parent, Keggin POM, and 2) the α_1 and α_2 isomers of the monovacant $P_2W_{17}O_{61}^{10-}$, derived from the parent Wells-Dawson POM. These polyoxometalates can also serve as versatile nanostructured building blocks.

In these two major areas of research, the following conclusions can be made:

1) The reaction products of $PW_9O_{34}^{9-}$ with Eu(III) in aqueous solution, identified by multinuclear NMR spectroscopy and X-ray crystallography, are highly dependent on the counter cation, pH , and stoichiometry. To unambiguously assign the species in our solution studies, we optimized reaction conditions of Eu(III) and $PW_9O_{34}^{9-}$ to isolate the

four nano-sized compounds that are observed in the speciation studies. The solid-state crystal structures not only are consistent with the solution species, but also reveal the unique abilities of the countercations to influence speciation and structure.

2) The α_1 and $\alpha 2$ -$P_2W_{17}O_{61}^{10-}$ isomers are distinguished by the position of the defect in the belt or cap, respectively. The basicity of the four oxygen atoms in the vacancy offers unique possibilities to tailor synthetic chemistry. The stability constants, K_1, for the 1:1 Ln: $\alpha_1P_2W_{17}O_{61}^{10-}$ complexes, determined by a competitive method monitoring ^{31}P NMR with EDTA as the reference competing ligand, increase significantly as the lanthanide series is traversed, reflecting the high basicity and lack of flexibility of the $\alpha 1$ site. The 1:2 Ln: $\alpha_1P_2W_{17}O_{61}^{10-}$ complexes are much less stable than the 1:1 Ln: $\alpha_1P_2W_{17}O_{61}^{10-}$ complexes, as shown by the stability constant, K_2, and are countercation dependent. The log K_1/log K_2 ratios suggest that the 1:1 complexes can be isolated cleanly compared to the α_2-$P_2W_{17}O_{61}^{10-}$ analogs and indeed, we find this is the case. We used this information to define the synthesis of hybrid inorganic-organic Ln $\alpha_1P_2W_{17}O_{61}^{10-}$ complexes, which led to the production of Ln POMs that react with organic ligands, some that highly sensitize the luminescence of the lanthanide ion. The solution behavior is very different for the α_2-$P_2W_{17}O_{61}^{10-}$ isomer that possesses a vacancy in the "cap" position. In this family, the polyoxometalates appear to associate to form 1:2 Ln: $\alpha_2P_2W_{17}O_{61}^{10-}$ complexes and 2:2 Ln: $\alpha_2P_2W_{17}O_{61}^{10-}$ complexes that are dimers in the solid state. The 2:2 Ln: $\alpha_2P_2W_{17}O_{61}^{10-}$ complexes show structural differences across the Ln series that is a function of lanthanide ion size.

Acknowledgements

First of all, my deep appreciation extends to all those who were involved in the research covered by this thesis.

My most heartfelt thanks go to my research advisor, Professor Lynn C. Francesconi, for her guidance, inspiration, encouragement, understanding and support through these years.

I want to thank Professor Klause Grohmann from Hunter College, Professor Malgorzata Ciszkowska from Brooklyn College and Dr. Conrad Zhang from Akzon Nobel Inc. for serving on my thesis committee, especially Dr. Conrad Zhang, for his strong interest in the work, thoughtful comments and encouragement.

I am very grateful to the two VIPs (very important person) in chemistry program, Professor Koeppl and Prof. Grohmann, for their dedication and patience in helping us graduate students.

I am very grateful to Dr. Louis Todaro, for his expert help in using X-ray crystallography and valuable advises both in science and in life.

A special thank you goes to Prof. Lazaridis, for his encouragement, kindness and helping me adjust to the new environment as I just came to the United States.

I appreciate the extraordinary effort of Graduate Center of the City University of New York, chemistry department at Hunter College and our lab to provide a congenial working environment. And my special gratitude to Dr. Robertha Howell for solving the crystal structures and guidance for luminescence project; Dr. Cliff Soll for his expert help in using analytical instruments and valuable advices; Dr. Michael Blumenstein for the help in using the NMR instrument; Professor Craig Hill for his remarkable contribution

to the paper we published together; Melchor Cantoria, Donna, Laurence for their help in the lab.

I owe special thanks to Dr. Gertrude Elion for her inspirational and financial support, the prestigious Gertrude Elion Fellowship Award, and to Dr. Rose K. Rose for the outstanding Rose Kfar Rose Dissertation Award.

The last but not the least gratitude must be extended to my husband, Qinghai Gao, for his support, my son, Yuan Gao, who always makes me proud, and for being so understanding when the demands of my work limited the time we spent together; my Mom and Dad, for their endless love and support.

To my son, my mom and my dad.

Table of Contents

List of Figures

Chapter 1

Chapter 2

Chapter 3

Chapter 4

Chapter 5

Chapter 6

List of Tables

Chapter 2

Chapter 3

Chapter 4

Chapter 5

List of Schemes

Chapter 1

Chapter 2

Chapter 5

Chapter 6

Chapter 1. Overview

1.1 General

Polyoxometalates (POMs) are early transition metal oxygen anion clusters, more specifically, they are oligomeric aggregates of metal cations (usually the d^0 species V(v), Nb(v), Ta(v), Mo(VI) and W(VI)) bridged by oxide anions that form by self-assembly processes.[1] They are a rapidly growing class of compounds. The first compound of this class were reported over 150 years ago, and today more than 70 different elements have been reported as POMs constituents.[2]

Properties that are essential for applications in catalysis, medicine, and material science can be readily tailored in POMs through rational design.[3] These properties include molecular composition, size, shape, charge density, redox potentials, acidity, and solubility. POMs can be rendered soluble in nearly all media from H_2O (inorganic) to hydrocarbons (organic) by choice of countercations.

A remarkably attractive feature with POMs lies in their versatility because most of the elements in the periodic table can be incorporated into the structure of these compounds. An increasing number of synthetic reactions exist that allow for the substitution of one or more metal centers (P-, d-, or f-block), organic functions, or organometallic groups into a parent POM structure. Metals in POMs are in highest Valent State (no d electrons), therefore oxygen atoms can donate electrons to Metal unfilled orbital to form strong bonding. Scheme1 shows examples of organic - inorganic hybrid molecules. In scheme 1, for example, the transition metal Ti atom of $[TiOPh]^{3+}$ replaces

one W atoms from $[W_6O_{19}]^{2-}$ to form $[(OPh)TiW_5O_{18}]^{3-}$. Organic ligands can also bond to a nonmetallic heteroatom, e.g., terminal oxygen atom, or directly bond to the metals throughσ, π, 2π- bonding ligands, such as oxo, organoimido, cyclopentadienyl, nitrido and carbyne groups.[4]

Small metal-oxygen heteropolyoxometalates can serve as building blocks. Simple metal-oxygen building blocks or quasi-preoganized building blocks can be linked together to form new structures. A large variety of linking units combined with the

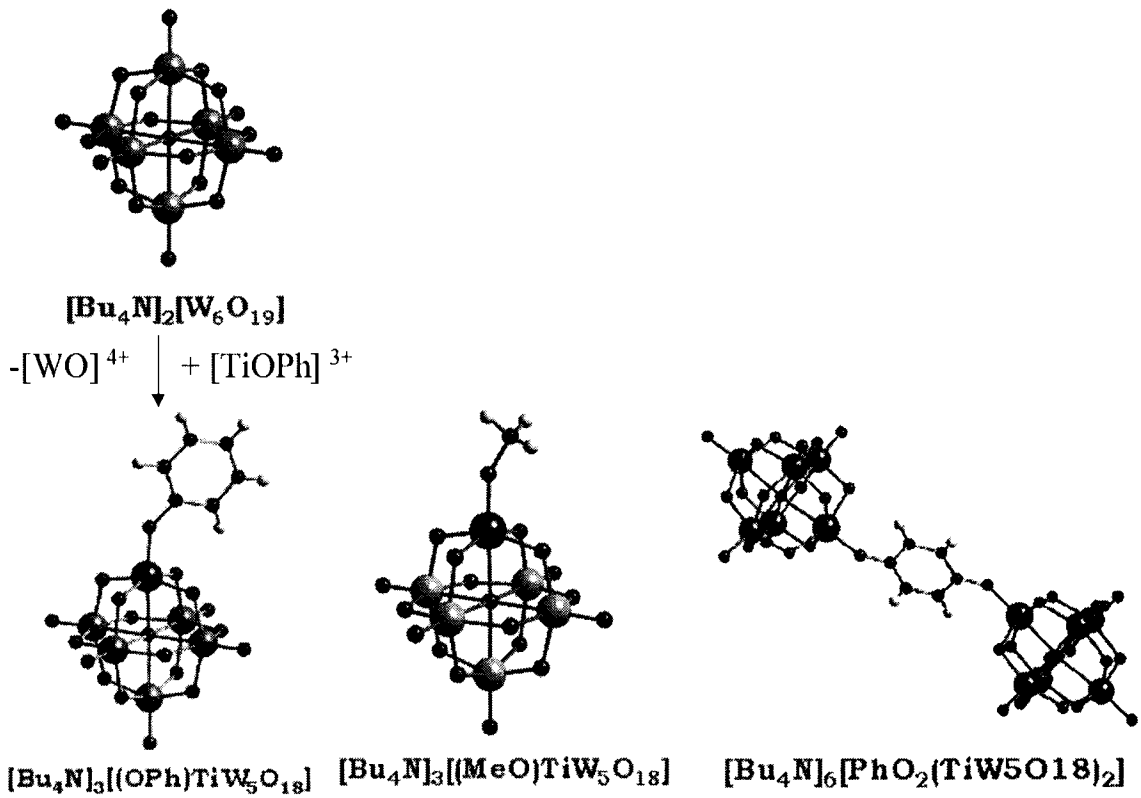

Scheme 1. Formation of organic – inorganic hybrid molecules

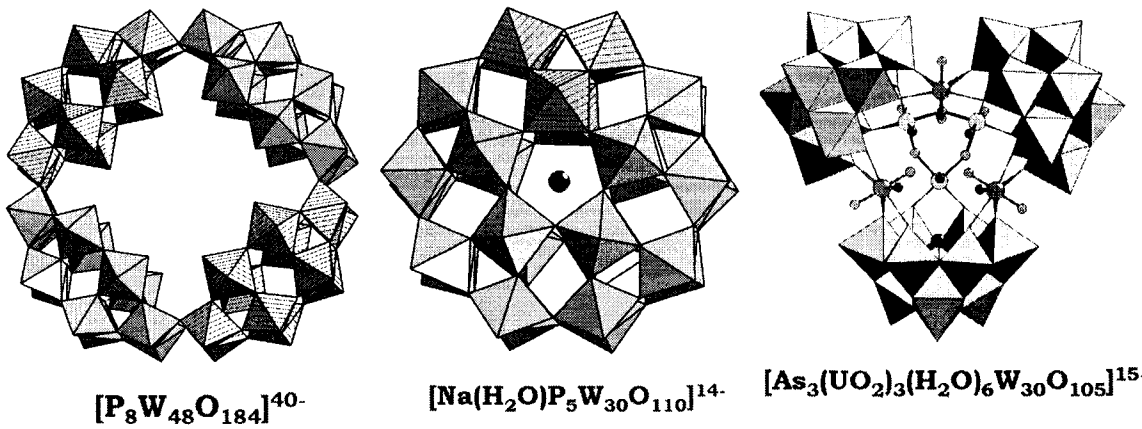

Figure 1. The structures of a: $[P_8W_{48}O_{184}]^{40-}$, b: $[Na(H_2O)P_5W_{30}O_{110}]^{14-}$, C: $[As_3(UO_2)_3(H_2O)_6W_{30}O_{105}]^{15-}$

abundant building blocks provide the possibility of producing a wide range of POMs structures through various linking geometries. Figure 1 shows structures of different shapes and sizes of POMs linked by smaller metal-oxygen POMs units. 4 $\{P_2W_{12}\}$ building blocks are connected to each other to form an approximately ring shaped anion. The crystal structure of $\{P_8W_{48}\}$ reveals that the central cavity of the anion contains a number of potassium cations.[5] Structure of the anion $[Na(H_2O)P_5W_{30}O_{110}]^{14-}$ can be regarded as a cyclic assembly of five $\{PW_6\}$ groups.[6] The central Na^+ can be replace by other cations of similar size, e.g. Ca^{2+}, most Ln^{III}, and U^{IV}.[7,8] The central cation is coordinated by a H_2O molecule that is enclosed in the central cavity.[9] The sodium derivative has been evaluated as a catalyst for the oxidation of H2S to sulfur, and was the best of the POMs examined.[10] The anion, $[(UO_2)_3(H_2O)_5As_3W_{29}O_{104}]^{19-}$ has the structure shown in Figure 1 which contains three $\{AsW_{10}\}$ fragments bridged by three pentagonal-bipyramidal $\{UO_2\}^{3+}$ cations.[11]

1.2 The lacunary Keggin and Wells-Dawson polyoxometalates containing Lanthanide

Polyoxometalates (POMs) containing Keggin and Wells-Dawson moieties are of fundamental and practical interest. These species are chemically robust, easily modified with respect to incorporation of transition metal ions, charge, size, potential, and can be rendered soluble in water or organic solution. Due to these features that can alter their molecular and electronic properties, these species may be useful in diverse disciplines such as catalysis, and material science.[4] They also have found varying applications in such areas as nuclear waste disposal and in medicine as antiviral and anti-tumor agents.[12] Different types of POMs are preferred depending on their particular stability. For example, the Wells Dawson structure, $[P_2W_{18}O_{62}]^{6-}$, and the Keggin structure $[PW_{12}O_{40}]^{3-}$ are particularly stable and have been used as oxidation catalysts in industry. The "keggin" deviations especially are known as thermal catalysts and, recently, photocatalysts, for oxidation transformation of various organic molecules in solution.[13]

1.2.1 Keggin tri-vacant $[PW_9O_{34}]^{9-}$ containing Lanthanide

Many studies have been performed on the reactions of transition metal ions with tri-vacant A/B-$[PW_9O_{34}]^{9-}$. A $[PW_9O_{34}]^{9-}$ (**A**) moiety derives from the removal of three WO_6 octahedra from the parent α keggin structure, $[PW_{12}O_{40}]^{3-}$ (**B**). Removing a triad of edge-sharing WO_6 octahedra results in a B-$[PW_9O_{34}]^{9-}$,[14,15] while removing three corner-sharing WO_6 octahedra from three separate W_3O_{13} triads results in an A-$[PW_9O_{34}]^{9-}$.[14,16] The A- and B-$[PW_9O_{34}]^{9-}$ moieties coordinate the central d-electron transition metal ions in the sandwich polyoxoanions in different ways, giving rise to structurally distinct complexes. For example, either 2:1 type[14, 17-18] of tetranuclear sandwich complexes

$[M_4(H_2O)_2(PW_9O_{34})_2]^{10-}$ or 3:2 typeof trinuclear complex of $[M_3(H_2O)_3(PW_9O_{34})_2]^{12-}$ are known with various transition metal ions (M^{2+}= Mn, Fe, Co, Ni, Cu, Zn, M^{3+}= Fe) due to using different A or B $[PW_9O_{34}]^{9-}$.[19-20] The larger anion $[Co_9(OH)_3(H_2O)_6(HPO_4)_2(PW_9O_{34})_3]^{16-}$, which contains a nonanuclear Co(II) cluster, was also identified by weakley [21] as a byproduct in the preparation of $[Co_4(H_2O)_2(PW_9O_{34})_2]^{10-}$.

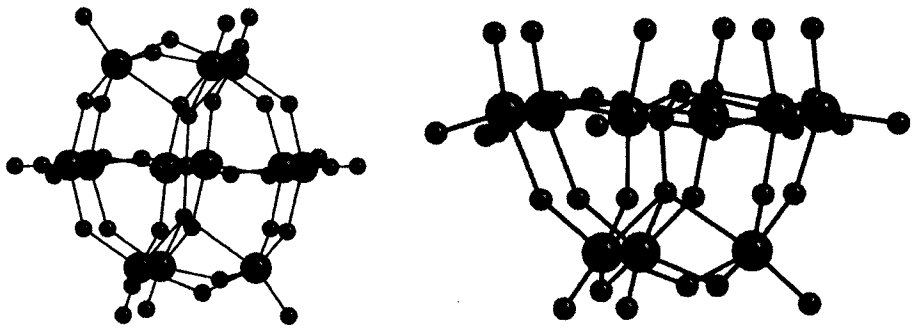

Figure 2. Structure of trivacant annion $[PW_9O_{34}]^{9-}$ (A) and parent Keggin annion $[PW_{12}O_{34}]^{3-}$ (B). The large size balls represent tungsten atoms. The medium size balls represent phorsphorus atoms, and the small size balls represent oxygen atoms.

In an attempt to rationally design lanthanide polyoxometalate materials, we are studying the unique behavior of A-$[PW_9O_{34}]^{9-}$ and lanthanides. In this study, we examine the speciation of A-$[PW_9O_{34}]^{9-}$. We find 4 Ln POMs form upon changing reaction conditions (pH, counterions, ratio of reactants). We present in this paper two novel polyoxometalate complexes of lanthanide $(NH_4)_{15}Na_6(H_3O)[Eu_2PW_{10}O_{38}]_4(W_3O_{14})]$, $[Eu(H_2O)_2(PW_{11}O_{39})]_n^{4n-}$, and two structure published complexes $Cs_{11}[Eu(PW_{11}O_{39})_2]$, $K_{14}[Eu(\alpha\text{-}2\text{-}P_2W_{17}O_{61})]_2$ but from two synthetic methods different from the literatures[22-

[23]. The four species have been thoroughly characterized by spectroscopic methods (IR, multinulear ^{31}P and ^{183}W NMR, Fluorescence) and by x-ray crystallography.

1.2.2 Mono-vacant $[P_2W_{17}O_{61}]^{10-}$ polyoxometalates containing Lanthanide

The Wells-Dawson mono-vacant lacunary polyoxometalates, specifically, $(\alpha_2\text{-}P_2W_{17}O_{61})^{10-}$ and $(\alpha_1\text{-}P_2W_{17}O_{61})^{10-}$ isomers, derived from the plenary Wells-Dawson ion, $[\alpha\text{-}P_2W_{18}O_{62}]^{6-}$, by removal of a WO unit from the "cap" and "belt" regions, respectively.[24] Figure 3 shows the structure of the parent Wells-Dawson anion and its two lacunary α-1 and α-2 $[P_2W_{17}O_{61}]^{10-}$. The shaded oxygen atoms present the four oxygen atoms available to bind to metal ions. Two recent studies suggest the dependence of structure and equilibria on the lanthanide ionic radius and solution conditions. In one study by Sadakane, the solid-state X-ray crystallography shows that the [Ce $(\alpha_2$-

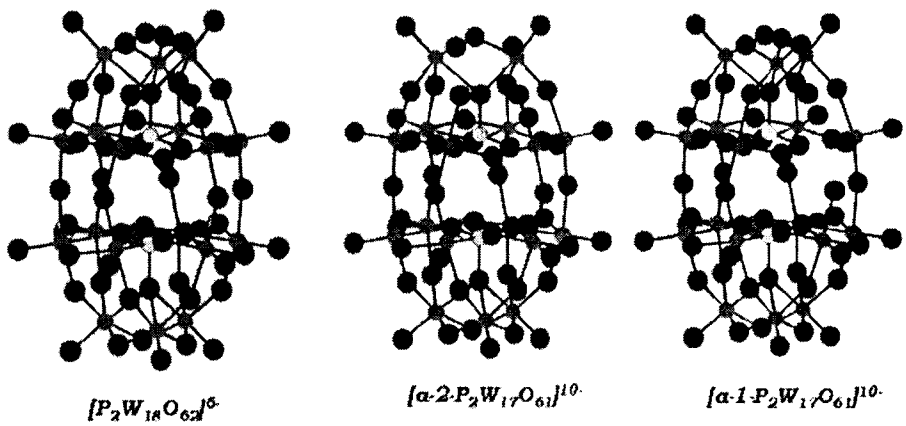

Figure 3. Structures of Wells Dawson anion $[a\text{-}P_2W_{18}O_{62}]^{6-}$ (C), monovacant $[a\text{-}1\text{-}P_2W_{17}O_{61}]^{10-}$ (D) and $[a\text{-}2\text{-}P_2W_{17}O_{61}]^{10-}$ (E). The large size balls represent tungsten atoms. The medium size balls represent phorsphorus atoms, and the small size balls represent oxygen atoms.

$P_2W_{17}O_{61})]^{7-}$ species is actually a 2:2 dimer wherein the Ce(III) is nine-coordinate, exhibiting a capped square antiprismatic coordination geometry and is bound to four oxygen atoms of the $(\alpha_2\text{-}P_2W_{17}O_{61})^{10-}$ unit, four water molecules and an adjacent terminal W=O bond of an adjacent $[Ce(\alpha_2\text{-}P_2W_{17}O_{61})]^{7-}$ unit.[24h] In solution, the "dimer" dissociates to form a monomeric species, as demonstrated by ^{183}W NMR spectroscopy. ^{31}P NMR experiments in water showed an equilibrium between the 1:1 and 1:2 Ce(III): $\alpha_2\text{-}P_2W_{17}O_{61}{}^{10-}$ species.

The mid-late lanthanides behave differently. We reported the Eu(III) analog where the Eu(III) is 8-coordinate, bound to four oxygen atoms of the $\alpha_2\text{-}P_2W_{17}O_{61}{}^{10-}$, three water molecules and to a terminal W-O of the "belt" region of an adjacent [α_2-$P_2W_{17}O_{61}$], forming a "cap to belt" 2:2 dimer. ^{183}W NMR and luminescence experiments suggest that the dimer dissociates in solution to form a monomeric 1:1 species. We did not observe an equilibrium between the 1:1 and 1:2 Eu(III): $\alpha_2\text{-}P_2W_{17}O_{61}{}^{10-}$ complexes.[24e]

The structural and electronic features of the α_1 defect contribute to unique electron transfer properties in the Wells-Dawson ion, $P_2W_{18}O_{62}{}^{6-}$[25] and in transition metal complexes of the $\alpha_1\text{-}P_2W_{17}O_{61}{}^{10-}$ isomer.[26] Previously, we reported the isolation of the 1:1 $[(H_2O)_4Ln(\alpha_1\text{-}P_2W_{17}O_{61})]^{7-}$ complexes in solution and solid-state.[27] We are using the findings described here for the purpose of producing pure 1:1 Ln: POMs that should be useful precursors for ternary complexes wherein the solvent (water) molecules are replaced by organic ligands. This is a non-trivial task because the well-known 1:2 Ln: POM species are commonly formed for Ln complexes of $\alpha\text{-}XW_{11}O_{39}{}^{n-}$ (Keggin derivatives) and the $\alpha_2\text{-}P_2W_{17}O_{61}{}^{10-}$ species (vacancy in the "cap" region) and it is

difficult to cleanly isolate 1:1 Ln: POM species, free of the 1:2 species. This is especially problematic when trying to produce organic soluble 1:1 species by metathesis reactions.

1.3 Applications

POMs have been found wide applications in many fields such as catalysis, medicine, materials with magnetic and luminescent properties, and radioactive waste treatment. [28-32]

Catalysis: Several catalytic processes involving POMs in both homogeneous and heterogeneous systems have recently been commercialized.[3] About 70% of catalytic applications use the Keggin type heteropolyacids (HPA) and their salts.[30] HPAs have several advantages as catalysts that make them economically and environmentally attractive. 1) They are strong Bronsted acids. 2) They have reversible redox properties and have the ability to activate O_2, H_2O_2, organic peroxides, etc. 3) They are thermally stable; 4) They are highly soluble in polar solvents and transferable into hydrocarbons by changing counter ions. These properties render HPAs potentially as promising acid, redox, and bifunctional catalysts in homogeneous as well as in heterogeneous or biphasic systems.[33] Some lanthanide complexes of POMs produced in our lab show both Bronsted and Lewis acid active sites, which attract wide attention, have great promises in the application of catalysis. Further investigation and studies are in process.

Medicine: POMs play important roles in antiviral and antitumoral activities. POMs can penetrate cell membranes and localize intracellularly. The reasons for biological activity may include ionic size and charge. For example, molecular mechanics studies suggest that $[(O_3POPO_3)_4W_{12}O_{36}]^{16-}$ inhibits HIV-1RT via docking at the DNA

binding region of the enzyme through electrostatic interactions. Redox and electron-transfer and reservoir properties may also contribute to biological activities.[33]

Materials: Increasing attention is currently being paid to POMs in the domain of material science due to their chemical, structural and electronic versatility. The preparation of new materials using polyoxometalates as building blocks is a very rich area for research. In the Francesconi group, we have identified new families of heteropolyoxometalates containing lanthanide (Ln) ions of various nuclearities (from Sm to Lu)[27a, 34] These materials are stable in solid state and in aqueous solution at varying pH values. Lanthanide ions are very useful to connect up polyoxometalate units into novel materials for two reasons. First, lanthanides have multiple coordination requirements and oxophilicity and can bind to more than one polyoxometalate unit, thus linking polyoxometalate units together. Second, lanthanides have interesting and useful physical properties, such as magnetism and luminescence. Polyoxometalate complexes of lanthanides can be exited using simple UV lamps; excitation into the tungsten-oxygen framework results in energy transfer to the Ln. These properties may be exploited in the preparation of new magnetic and luminescent materials. The preliminary luminescence studies of lanthanid complexes of POMs with organic ligands in chapter 5 of this report has combined aqueous and organic solution studies with solid state X-ray crystallography to understand the complex solution chemistry of lanthanide polyoxometalates. This work leads to the production of Ln POMs that react with organic ligands, some that highly sensitize the luminescence of the lanthanide ion. When the organic species is a sensitizing ligand, the resulting ternary complex can be employed as functional building blocks for luminescent materials.[35]

Radioactive waste treatment: POMs may be useful to mimic colloids and mineral species found in radioactive wastes. The sorption of actinides to minerals and colloids is particularly problematic in radioactive waste tanks and waste streams. The isomer, $[\alpha\text{-}2\text{-}P_2W_{17}O_{61}]^{10-}$, found application to selected aspects of actinide separations science in high-level nuclear waste processing. This anion stabilizes the otherwise very reactive tetravalent oxidation states of americium, curium, berkelium, and californium. The $[P_2W_{17}O_{61}]^{10-}$ anion has also been tested in a separation strategy using biphasic system based on PEG-poly(ethylene glycol) — wherein it facilitates the transport of An(III) and An(IV) ions into the PEG-rich phase. While the radiochemistry shows that polyoxometalates facilitate extraction of radionuclides, important structural and solution chemistry of POMs that is critical to the deployment of POMs in separation strategies is lacking. A study of the solution chemistry and structures of Ln and An POMs, therefore, is critical to realize the potential of these unique anions for separation of radiometals from the bulk of radioactive waste.

Some fundamental research subjects on POM systems reported in recent literature include the genesis of metal oxides and the chemistry of self-assembly, electron transfer in solutions and at metal oxide interfaces, magnetic behaviors of large multicomponent systems, catalytic performances, involving interfacial redox chemistry, chemical/physical phenomena of mixed valent structures and excited-state metal oxide-like materials, molecular recognition by complex multicenter inorganic species, and chemotherapeutic agent efficacy.[3]

1.4 Speciation studies of polyoxometalates

Polyoxometalate chemistry is very complex in aqueous and, especially, in organic solution. It is critical to understand the aqueous and organic solution chemistry in order to take polyoxometalate chemistry to the level where POMs can be used as functional building blocks for new materials, homogeneous catalysts, and for separation strategies.

In the studies of $[PW_9O_{34}]^{9-}$, this anion has six oxygen atoms available for bonding, while lanthanides have multiple coordination requirements and oxophilicity and can bind to more than one polyoxometalate unit, therefore, the aqueous and organic chemistry for both $[PW_9O_{34}]^{9-}$ and lanthanides are complex. $[PW_9O_{34}]^{9-}$ composition in aqueous solution is dynamic, which are multiequilibria exist depending on pH, countercation, concentration and aging of the solution. Lanthanide ions also show complex dynamic behavior in aqueous solution. If we want to rationally prepare lanthanide $[PW_9O_{34}]^{9-}$ compounds as building blocks for new materials, it is critical to understand the effects of pH, concentration, countercation on the species that exist in solution and how these parameters impact on the species that are isolated in the solid state. After thoroughly study the speciation of lanthanide complexes of $[PW_9O_{34}]^{9-}$ as a function of solution conditions, the specific nanostructured complex with controlled size, shape and composition can be rationally tuned in a predictable manner.[36]

In the studies of α_1-$P_2W_{17}O_{61}{}^{10-}$ and α_2-$P_2W_{17}O_{61}{}^{10-}$, we try to understand how the solution conditions, structural, and electronic features of the α_1-$P_2W_{17}O_{61}{}^{10-}$ and α_2-$P_2W_{17}O_{61}{}^{10-}$ isomers impact the speciation and stabilities of their Ln complexes.[37, 38] The objective of this work is to understand the parameters that influence the complexes formed in solution and their chemistry. These parameters include the electronic and steric properties of the defect site of the POM, the lanthanide ion because the lanthanide

contraction has a profound effect on the chemistry, and solution components, such as pH, countercation, and concentration of species.

This dissertation describes the detailed solution and solid state studies of Lanthanide tri-vacant Keggin and mono-vacant Wells-Dawson polyoxometalates and exploration of possible applications in luminescence materials.

1.5 References

(1) Jeffrey T. Rhuce, Craig L. Hill, Deborah A. Juad. *Chem. Rev.*,**1998**, 98, 327-357

(2) Pierre Gouzerh, Anna Proust, *Chem. Rev.*, **1998**, 98, 77-111

(3) Hill, C. L., *Chem Review*. 1998, 98, 3

(4) Gouzerh, P.; Proust, A., *Chem. Rev*. 1998, 98, 77.

(5) Contant, R.; Teza, A. *Inorg. Chem.* **1985**, 24, 4610.

(6) Jeannin, Y. *J. Cluster. Sci.* **1992**, 3, 55

(7) Creaser, I.; Heckel, M. C.; Neitz, R. J.; Pope, M. T. *Inorg. Chem.* **1993**, 32, 1573.

(8) Antonio, M. R.; Soderholm, L. *J. Cluster Sci.* **1996**, 7, 585.

(9) Dickman, M. H.; Gama, G. J.; Kim, K. C.; Pope, M. T. *J. Cluster Sci.* **1996**, 7, 567.

(10) Harrup, M. K.; Hill, C. L. *Inorg. Chem.* **1994**, 33, 5448.

(11) Kim, K.; Pope, M. T. *Inorg. Chem.*, **1999**,

(12) Kim, G.S.; Judd, D.A.; Hill, C. L.; Schinazi, R. F.; J. Med. Chem. **1994**, 37, 816

(13) Bartis J.; Dankova M.; Lessmann J.; Luo Q-H.; Horrocks, Jr.; W. Dew.; Francesconi L. C., *Inorganic. Chem.*, **1999**, 38, 1042-1053

(14) Zhang, X.; Chen, Q.; Duncan,D. C.; Lachiotte, R. J.; Hill, C. L. *Inorg. Chem.* 1997, 36, 4381.

(15) Finke, R. G.; droege, M.; Hutchinso, J. R.; gansow, O. *J. Am. Chem. Soc.* 1981, 103, 1587-1589.

(16) Massart, R.; Contant, R.; Fruchart, J.-M.; Ciabrini, J. –P.; Fournier, M. *Inorg. Chem.* 1977, 16, 2916-2921.

(17) (a) Weakley, T. J. R.; Finke, R. G. *Inorg. Chem.* 1990, 29, 1235-1241. (b) Weakley, T. J. R.; Evans, H. T., Jr.; Showell, J. S.; Tourne, C. M. *J. Chem. Soc., Chem.*

Commun. 1973, 139-140. (c) Evans, H. T.; Tourne, G. F.; Tourne, C. M.; Weakly, T. J. R.; *J. Chem. Soc., Dalton Trans.* 1986, 2699. (d) Finke, R. G.; Droege, M. W.; Domaile, P. J. *Inorg. Chem.* 1987, 26, 3886.

(18) (a) Coronado, E.; Gomez-Garcia, C. J. *Comments Inorg. Chem.* 1995, 17, 255. (b) Gomez-Garcia, C.; Coronado, E.; Gomez-Romero, P.; Casan-Pastor, N. Inorg. Chem. 1993, 32, 3378.

(19) (a) Zhang, X.; Jameson, G. B.; O'Connor, C. J.; Pope, M. T. *Polyhedron* 1996, 15, 917.

(20) (a) Knoth, W. H.; Domaille, P. J.; Harlow, R. L. *Inorg. Chem.* 1986, 25, 1577. (b) Knoth, W. H.; Domaille, P. J.; Farlee, R. D. *Organometallics* 1985, 4, 62.

(21) Weakley, T. J. R. *J. Chem. Soc. Chem. Commun.* 1984, 1406.

(22) Luo, Q. H.; Howell, R. C.; Bartis, J.; Dankova, M.; Horroks, W. D. Jr.; Rheingold, L.; Francesconi, L. C., *Inorg.Chem.* Accepted.

(23) S. K. Yun and T. Pinnavaia, *Inorg. Chem.* 1996, 35, 6853-6860.

(24) Luo, Q.; Howell, R. C.; Bartis, J.; Dankova, M.; Horrocks, W. D., Jr.; Rheingold, A. L.; Francesconi, L. C. *Inorg. Chem.* 2002, *41*, 6112-6117.

(25) a. Kozik, M.; Hammer, C. F.; Baker, L. C. W.,*J. Am. Chem. Soc.* **1986,** *108*, 2748-2749. b.Kozik, M.; Baker, L. C. W.,*J. Am. Chem. Soc.* **1990,** *112*, 7604-7611. c. Keita, B.; Levy, B.; Nadjo, L.; Contant, R.,*New. J. Chem.* **2002,** *26*, 1314-1319. d. Lopez, X.; Bo, C.; Poblet, J. M.,*J. Am. Chem. Soc.* **2002,** *124*, 12574-12582.

(26) Contant, R.; Abbessi, M.; Canny, J.; Belhouari, A.; Keita, B.; Nadjo, L., *Inorg. Chem.* **1997,** *36*, 4961-4967. b. Contant, R.; Richet, M.; Lu, Y. W.; Keita, B.;

Nadjo, L.,*Eur. J. Inorg. Chem.* **2002,** c. Keita, B.; Girard, F.; Nadjo, L.; Contant, R.; Canny, J.; Richet, M.,*J. Electroanal. chem.* **1999,** *478*, 76-82.

(27) a. Bartis, J.; Dankova, M.; Lessmann, J. J.; Luo, Q.-H.; Horrocks, W. D., Jr.; Francesconi, L. C., *Inorg. Chem* **1999,** *38*, 1042-1053. b. Luo, Q.; Howell, R.C.; Bartis, J.; Dankova, M.; Williams, C.; Horrocks, W.DeW., Jr.; Young, V.C., Jr,; Rheingold, A.L.; Francesconi, L.C.; Antonio, M.R.*Inorg. Chem.* **2001**, *40*, 1894.

(28) For key references to lanthanide luminescence: a.Bunzli, J.-C. G. "Luminescent Probes" in Lanthanide Probes in Chemistry, Biology and Earth Sciences; Bunzli, J.-C.G.; Choppin, G. Eds.; 1989; Elsevier, Amsterdam. b. Kido, J.; Okamoto, Y. *Chem. Rev.* **2002**, *102*, 2357-2368. c. Bruce, J. I.; Dickins, R. S.; Govenlock, L. J.; Gunnlaugsson, T.; Lopinski, S.; Lowe, M. P.; Parker, D.; Peacock, R. D.; Perry, J. J. B.; Aime, S.; Botta, M., *J. Am. Chem. Soc.* **2000**, *122*, 9674-9684. d. Dickins, R. S.; Aime, S.; Batsanov, A. S.; Beeby, A.; Botta, M.; Bruce, J. I.; Howard, J. A. K.; Love, C. S.; Parker, D.; Peacock, R. D.; Puschmann, H.*J. Amer. Chem. Soc.* **2002**, *124*, 12697-12705. e. Parker, D.; Dickins, R. S.; Puschmann, H.; Crossland, C.; Howard, J. A. K. *Chem. Rev.* **2002**, *102*, 1977-2010..

(29) For key reviews on new functional materials, particularly electrochromic, electroluminescent, photochromic and photoluminescent materials, a. Katsoulis, D.E. *Chem. Rev.*, **1998**, *98*, 359-387. b.Yamase, T. *Chem. Rev.*, **1998**, *98*, 307-325. *For recent applications of lanthanide polyoxometalates incorporated into materials: electrochromic device preparation*, c. Liu, S.; Kurth, D. G.; Mohwald, H.; Volkmer, D.*Advanced Materials* **2002**, *14*, 225-228. *photoluminescent films*, d. Mo, Y.-G.; Dillon, R. O.; Snyder, P. G.; Tiwald, T. E. *Thin Solid Films* **1999**, *355-356*, 1-5. e.

Xu, L.; Zhang, H.; Wang, E.; Kurth, D. G.; Li, Z. *J. Mater. Chem.* **2002**, *12*, 654-657. f. Xu, L.; Zhang, H.; Wang, E.; Wu, A.; Li, Z. *Materials Chemistry and Physics* **2002**, *77*, 484-488. g. Wang, Y.; Wang, X.; Hu, C.; Shi, C. *J. Mater. Chem.* **2002**, *12*, 703-707. h. Wang, J.; Liu, F.; Fu, L.; Zhang, H. *Materials Lett.* **2002**, *56*, 300-304. i. Wang, Y.; Wang, X.; Hu, C. *Journal of Colloid and Interface Science* **2002**, *249*, 307-315. j. Wang, J.; Wang, H. S.; Fu, L. S.; Liu, F. Y.; Zhang, H. J. *Thin Solid Films* **2002**, *414*, 256-261.

(30) For key references to lanthanide Lewis Acid catalysis: a. Aspinall, H. C. *Chem. Rev.* **2002**, *102*, 1807-1850. b. Molander, G. A. *Chemtracts-Organic Chemistry* **1998**, *11*, 237-263. c. Molander, G. *Chem. Rev.* **1992**, *92*, 29-68. d. Shibasaki, M.; Yoshikawa, N. *Chem. Rev.* **2002**, *102*, 2187-2209. e. Kobayashi, S.; Kawamura, M. *J. Am. Chem. Soc.* **1998**, *120*, 5840-5841. f. Kobayashi, S. *Pure and Appl. Chem.* 1998, *70*, 1019-1026. g. Aspinall, H. C.; Dwyer, J. L. M.; Greeves, N.; McIver, E. G.; Woolley, J. C. *Organometallics* **1998**, *17*, 1884-1888. h. Xie, W.-H.; Yu, L.; Chen, D.; Li, J.; Ramirez, J.; Miranda, N. F.; Wang, P. G . in *Environmentally Benign Chemistry: Green Chemistry*; Anastas, P. T. and Williamson, T. C., Ed.; Oxford University Press: Oxford, UK, **1998**; Vol. , pp 129-149.

(31) Sadakane, M.; Dickman, M. H.; Pope, M. T. *Angew. Chem. Int. Ed.* **2000**, *39*, 2914-2916.

(32) Mialane, P.; Lisnard, L.; Mallard, A.; Marrot, J.; Antic-Fidancev, E.; Aschehoug, P.; Vivien, D.; Secheresse, F. *Inorg. Chem.* **2003**, *42*, 2102-2108.

(33) Luo, Q-H., Doctoral Dissertation, Chemistry Department of the City University of New york, **2002**.

(34) a. Jeffrey T. Rhuce, Craig L. Hill, Deborah A. Juad. *Chem. Rev.*,**1998**,98,327-357, b. Pierre Gouzerh, Anna Proust, *Chem. Rev.*, **1998**, 98, 77-111, c. Kim, G.S.; Judd, D.A.; Hill, C. L.; Schinazi, R. F.; J. Med. Chem. **1994**, 37, 816

(35) Zhang, C.; Howell, R. C.; Francesconi, L. C., *J. cluster. Sci.*, **2004**, in press.

(36) Zhang, C.; Howell, R.C.; Perez, F.; Scotland, K.; Todaro L. J., Francesconi, L.C., ***Inorg. Chem.***, **2004**, 43, 7691-7701.

(37) Zhang C.; Fang X.; Luo, Q-H; Howell R. C.; Hill, C. L.; Francesconi L. C., ***Inorg. Chem.***, submitted, **2004**.

(38) Zhang, C.; Howell, R. C.; Luo, Q-H; Fieselmann, H. L.; Todaro, L. J.; Francesconi, L. C., ***J. Am. Chem. Soc.***, accepted, **2004**.

Chapter 2. Influence of pH, counter cation, and stoichiometric ratio on the aqueous speciation of Eu^{3+} with tri-vacant $[PW_9O_{34}]^{9-}$ POM

2.1 Introduction

Polyoxometalates (POMs, for convenience) are robust, early transition metal oxide anions with fascinating properties and great potential applications in many fields such as catalysis, material science and medicine, as well as their unusual topological properties.[1-5] Lanthanide, Ln, ions offer unique functionality, such as luminescence and magnetic properties, when combined with polyoxometalates. However, the aqueous and organic chemistry for both POMs and lanthanides are complex. Polyoxometalate composition in aqueous solution is dynamic, that is multiequilibria exist depending on pH, countercation, concentration and aging of the solution. Lanthanide ions also show complex dynamic behavior in aqueous solution.

While many solid state and solution structures have been determined for POMs and recently, for Ln POMs, in attempts to achieve "massive" polyoxometalates,[6] complete understanding of the solution species and dynamics for POMs, in general, is lacking. If we want to rationally prepare lanthanide POM compounds as building blocks for new materials, it is critical to understand the effects of pH, concentration, countercation on the species that exist in solution and how these parameters impact on the species that are isolated in the solid state.

Our group has studied the mono-vacant lacunary polyoxometalates, specifically, $(\alpha_2\text{-}P_2W_{17}O_{61})^{10-}$ and $(\alpha_1\text{-}P_2W_{17}O_{61})^{10-}$ isomers, where the lanthanide ion is incorporated

into the "cap" and "belt" regions of the POM, respectively. We have isolated the 1:1 complexes and the 1:2 complexes and examined their stabilities in aqueous solution. A study of equilibrium constants in aqueous solution reveals that the defect site in the (α_1-$P_2W_{17}O_{61}$) $^{10-}$ species is very selective for the later, heavier lanthanides with high charge/size ratio.[7]

The tri-vacant polyoxotungstate, $XW_9O_{34}^{n-}$, has the potential to support lanthanide clusters. $XW_9O_{34}^{n-}$ is derived from the Keggin structure (X=P, n=9; X=Si, n=10; X=As(V), n=9) and this anion has six oxygen atoms available for bonding (in the Aα form) and seven (in the Bα form). We isolated a unique Ln_8 cluster tied together by $PW_9O_{34}^{9-}$ under neutral to basic conditions.[18] This species is very stable in water at pH 6.5-9. Examination of the solution chemistry of Eu(III) and $PW_9O_{34}^{9-}$ revealed interesting and complex behavior of lanthanide phosphotungstates that is reported herein.

The objective of this work is to examine the solution speciation of lanthanide complexes of $PW_9O_{34}^{9-}$ as a function of solution conditions. To this end, we studied the variations of Eu(III) and $PW_9O_{34}^{9-}$ with respect to pH, countercation and stoichiometry, parameters that are well known to influence POM and Ln POM speciation. We employ Eu(III) in these studies because the shift properties allow convenient monitoring by ^{31}P NMR.

To unambiguously assign the species in our solution studies, we optimized reaction conditions of Eu(III) and $PW_9O_{34}^{9-}$ to isolate the four compounds that are observed in the speciation studies. These compounds were characterized by appropriate solution and solid-state techniques, including multinuclear NMR and X-ray crystallography. The solid-state crystal structures not only are consistent with the

solution species, but also reveal the unique abilities of the countercations to influence speciation and structure.

2.2 Experimental Section

2.2.1 General

All reagents were commercially available and used without further purification. Nanopure water was obtained from a Millipore Reverse Osmosis Direct-Q System. Elemental analyses were carried out by Inductive Coupled Plasma Atomic Emission Spectrometry (ICP-AES, SECTROFLAME M120E) as described below. IR spectra were recorded on a Perkin-Elmer 1625 FT-IR at room temperature from KBr pellets. Sodium 9-tungstophosphate (Na_9 A-PW_9O_{34} $\cdot 16H_2O$) was prepared according to a published method [19] and identified by infrared spectroscopy.

2.2.2 Reaction Chemistry

2.2.2.1 Reaction of the polyoxometalate A-α-$PW_9O_{34}^{9-}$ as a function of countercation and pH.

i) Buffer solutions of LiAc (0.5M), NaAc(0.5M), KAc(0.5M) and CsAc(0.5M) were each prepared at pH 4.75 (30% D_2O). Na_9 A-$PW_9O_{34}^{9-}$ (Sodium salt) (0.1g) was added with vigorous stirring into four vials each containing 3 ml of buffer. ii) 3 ml of A-$PW_9O_{34}^{9-}$ (sodium salt) (0.1g) aqueous solution (30% D_2O) was prepared at pH 1, 3, 5, 7.3, 8, 10.35 by using HCl or NaOH to adjust the pH. The solutions from both i) and ii) were heated to 90°C for 2 min. The solutions were cooled to room temperature, and then placed into 10 mm NMR tubes. The ^{31}P NMR spectra were recorded and the data are tabulated in **Table 3**.

2.2.2.2 Reaction of A-$PW_9O_{34}^{9-}$ with Eu^{3+} (1:1 stoichiometry) as a function of pH monitored by ^{31}P NMR.

0.056 mmol Eu^{3+} (50 µl of 1.12 M) was added into four vials each containing 3 ml of H_2O (30% D_2O) respectively, A-PW_9 (0.1527 g, 0.056 mmol) was added slowly to the above solutions with vigorous stirring; the pH of resulting solutions were adjusted to 1, 3, 7 and 9 by adding diluted HCl or NaOH, followed by heating to 90 °C for 2 mins. The solutions were cooled to room temperature, and then placed into 10 mm NMR tubes. The ^{31}P NMR spectrum was recorded and is shown in **Figure 2**. The pH recorded after the NMR measurements did not change significantly.

2.2.2.3 A-$PW_9O_{34}^{9-}$ with Eu^{3+} (1:1 stoichiometry) as a function of countercation and pH.

Buffer solutions of LiAc (0.5 M), NaAc (0.5 M), and KAc (0.5 M) were prepared at three pH values (4.5, 5.5, 6.5) (30%D_2O). Preparation of solutions: 0.056 mmol Eu^{3+} (50 µl of 1.12 M) was added into nine vials each containing 3 ml of buffer. A-$PW_9O_{34}^{9-}$ (0.1527 g, 0.056 mmol) was added slowly with vigorous stirring to obtain slightly cloudy solutions that were heated at 90 °C for 2 min to form clear solutions. The solutions were cooled to room temperature, and then placed into 10 mm NMR tubes. The ^{31}P NMR spectra were recorded and are shown in **Figures 3** and **4**.

2.2.2.4 Expanded study of A-$PW_9O_{34}^{9-}$ with Eu^{3+} (1:1 stoichiometry) as a function of counter cation, including Cs^+ and Al(III).

0.056 mmol Eu^{3+}(50 µl of 1.12 M) was added into four vials containing 3 ml of H_2O (30% D_2O). A-$PW_9O_{34}^{9-}$ (0.1527 g, 0.056 mmol) was added slowly to the above

solutions with vigorous stirring; the resulting solutions were heated to 90 °C for 2 mins. NaCl (0.990g,0.56 M), KCl (0.125g, 0.56 M), CsCl (0.113g, 0.22M) and $AlCl_3$ (0.135 g, 0.19M) were added to each of the vials during the heating stage. The vials were cooled to room temperature, the pH of the solutions was measured and found in all cases except Al(III) to be ca 7; for Al(III), the pH was 2-3. The solutions were placed into 10 mm NMR tubes. The ^{31}P NMR spectra were recorded and the spectra are shown in **Figure 5**. The pH after the experiment did not change significantly.

2.2.2.5 Reaction of A-$PW_9O_{34}^{9-}$ with Eu^{3+} as a function of organic countercations, tetrabutylammonium (TBA) bromide and tetraethylammonium (TEA) bromide. (The following reaction performed in 1:1 or 2:1 Eu: A-$PW_9O_{34}^{9-}$ stoichiometry yields the same product.)

To $EuCl_3.6H_2O$ (0.32g, 0.87 mmol) dissolved in H_2O (25 ml) was added $Na_9PW_9O_{34}.15H_2O$ (2.44 g, 0.87 mmol) to form a cloudy solution. After heating at 90 °C for 10 min, cooling and filtering off a small amount of insoluble material, tetrabutylammonium bromide (2.78g, 8.7 mmol) was added to form a white precipitate. This crude precipitate can be collected by filtration. Further purification can be achieved by extracting three times with CH_2Cl_2 (50 ml). The organic layer was collected and the solvent evaporated and dried under vacuum.

2.2.2.6 Reaction of A-$PW_9O_{34}^{9-}$ with Eu^{3+} as a function of stoichiometry (Eu: A-$PW_9O_{34}^{9-}$= 0.5 : 1, 1:1; 2:1).

The reaction of Eu^{3+} and A-$PW_9O_{34}^{9-}$ in 2:1, 1:1 and 0.5:1 ratio was carried out in buffer solution NaAc (0.5 M, pH 6.5). 50 μl (0.056 mmol) of 1.12 M Eu^{3+} each was

added into three vials containing 3 ml of NaAc (0.5 M, pH 6.5) (30% D_2O). 0.3054 g (0.112 mmol), 0.1527 g (0.056 mmol) and 0.07635 g (0.028 mmol)of A-PW_9 was added slowly to the above solutions with vigorous stirring. The resulting solutions were heated to 90 °C for 2 mins, followed by cooling to room temperature, and then placement into 10 mm NMR tubes. The ^{31}P NMR spectrum was recorded and is shown in **Figure 6**. When the experiment was carried out in water, not NaAc buffer, the same results are obtained with a few more unidentified peaks for the 1:2 Eu: $PW_9O_{34}^{9-}$ combination (not shown).

2.2.3 Preparation and crystallization of the individual species that are observed in speciation experiments.

To unambiguously identify the species observed from the ^{31}P NMR experiments, the syntheses of complexes 1,2,3 and 4 from Eu(III) and A-$PW_9O_{34}^{9-}$ were optimized and the complexes were isolated and characterized by X-ray crystallography, elemental analysis, Infrared Spectroscopy, and multinuclear NMR.

2.2.3.1 Preparation and crystallization of $(NH_4)_{22}\{(Eu_2PW_{10}O_{38})_4(W_3O_8(H_2O)_2(OH)_4\}\cdot 44H_2O$, 1.

1 was prepared by a modification of the procedure used earlier.[18] Solid Na_9 A-$PW_9O_{34}\cdot 16H_2O$ (4.90 g, 1.8 mmol) was added slowly to a solution of $EuCl_3\cdot 6H_2O$ (0.66 g, 1.8 mmol) in 15 ml of H_2O. The resulting cloudy solution was heated to about 80°C, within a few seconds, a clear solution formed. Solid NH_4Cl (5.16 g, 54 mmol) was added to the hot solution, a white precipitate was formed immediately, and the solution heated for an additional 5 minutes. The resulting solution turned clear, and then was cooled in an ice bath. The crystallized solid was collected by filtration, and recrystallized from hot

water. Yield: 2.78 g, 76%. X-ray quality crystals were obtained at 4°C by recrystallizing 1 g of the white crystalline solid from 8 ml of hot water. Anal. Calcd for $(NH_4)_{22}\{Eu_2PW_{10}O_{38})_4(W_3O_8(H_2O)_2(OH)_4\}\cdot 44H_2O$: W, 60.11; Eu, 9.25; P, 0.94. Found: W, 60.10; Eu, 9.30; P, 0.88. IR (KBr, cm^{-1}) metal-oxygen stretching region: 1092 (m), 1055(m), 1025(m), 951(s), 935(s), 820(vs), 790 (s).

2.2.3.2 Preparation and crystallization of $Al(H_3O)\{Eu(H_2O)_2PW_{11}O_{34}\}\cdot 20H_2O$, 2.

To a solution of $EuCl_3\cdot 6H_2O$ (0.66 g, 1.8 mmol) in 15 ml of H_2O Na_9 A-PW_9O_{34} $\cdot 16H_2O$ (2.45 g, 0.9 mmol) was added slowly with vigorous stirring to form a slightly cloudy solution. Heating at 80 °C and addition of $AlCl_3$ (1.74 g, 7.2 mmol) resulted in a clear solution. Stirring at room temperature was continued for 20 min. Traces of a precipitate were removed by filtration. The solution was stored in a beaker and allowed to slowly evaporate. After a week, needle-like crystals were obtained. Yield: 1.2 g, 45%. X-ray quality crystals were selected from the bulk crystals and cut into 0.1 X 0.12 X 0.25 mm^3 blocks. Anal. Calcd for $Al(H_3O)\{Eu(H_2O)_2PW_{11}O_{34}\}\cdot 20H_2O$: W, 61.51; Eu, 4.62; P, 0.94; Al, 0.82. Found: W, 61.59; Eu, 4.67; P, 0.95; Al, 0.88. IR (KBr, cm^{-1}), metal-oxygen stretching region: 1093 (m), 1051(m), 957(s), 833 (s).

2.2.3.3 Preparation and crystallization of Cs_{11} $Eu(PW_{11}O_{34})_2$ $\cdot 28H_2O$, 3.

Solid Na_9 A-PW_9O_{34} $\cdot 16H_2O$ (2.45 g, 0.9 mmol) was added slowly to a solution of $EuCl_3\cdot 6H_2O$ (0.33 g, 0.9 mmol) in 7.5 ml of H_2O to obtain a slightly cloudy solution. Heating to 80°C resulted in a clear solution within a few minutes. Solid CsCl (2.27 g, 13.5 mmol) was added to the hot solution resulting immediately in the formation of a white precipitate. Heating was continued for an additional 5 min, then the resulting slurry was cooled in an ice bath. The solid was collected by filtration. Yield: 1.86 g, 82%. X-ray

quality crystals were obtained by recrystallizing 0.5 g of the white solid from 6 ml of warm water (50°C). Anal. Calcd for Cs_{11} $Eu(PW_{11}O_{34})_2 \cdot 28H_2O$: W, 53.02; Eu, 1.99; P, 0.81. Found: W, 53.64; Eu, 2.13; P, 0.81. IR (KBr, cm^{-1}), metal-oxygen stretching region: 1084 (m), 1056(m), 1023(m), 943(s), 776 (s).

2.2.3.4 Preparation and crystallization of $Al_2(H_3O)_8\{Eu(H_2O)_3(\alpha\text{-}2\text{-}P_2W_{17}O_{61})\}_2 \cdot 29H_2O$, 4.

Solid Na_9 A-PW_9O_{34} $\cdot 16H_2O$ (2.45 g, 0.9 mmol) was added slowly to a solution of $EuCl_3 \cdot 6H_2O$ (0.33 g, 0.9 mmol) in 7.5 ml of H_2O to form a cloudy solution. Heating to 80°C resulted in a clear solution within seconds. Solid $AlCl_3$ (4.34 g, 18 mmol) was added and the resulting clear solution was heated for an additional 3 min. Traces of a precipitate were removed by filtration. The solution was stored in a vial at room temperature. After a month, small thick rectangular-like crystals were grown, and x-ray quality crystals were selected from the bulk crystals. Yield: 0.7 g, 53%. Anal. Calcd for $Al_2(H_3O)_8\{Eu(H_2O)_3(\alpha\text{-}2\text{-}P_2W_{17}O_{61})\}_2 \cdot 29H_2O$: W, 65.84; Eu, 3.20; P, 1.31; Al, 0.57. Found: W, 64.71; Eu, 3.21; P, 1.10; Al, 0.56. IR (KBr, cm^{-1}), metal-oxygen stretching region: 1100 (m), 1046(m), 954(vs), 893(m), 820(s), 773 (vs), 722 (s).

2.2.4 Analytical techniques

2.2.4.1 Elemental analysis by ICP.

i) Standard solution preparation. The standard solution of P (0.2, 0.4, 0.6, 0.8, 1.2 ppm), Eu (1, 2, 4, 6 ppm), W (20, 40, 60, 80, 120 ppm), Al (0.5, 1, 1.5, 2.5 ppm), Na (1, 3, 5, 7 ppm), and K (1, 3, 5, 7 ppm) was prepared by diluting 1000 ppm ICP standard solution (GFS Chemicals, Inc.) with distilled water. ii) Sample preparation. Crystals of complex **1-4** were collected by filtration, air dried and then further dried in a dessicator

over $CaSO_4$, under vacuum for 1.5 hour. The samples were left in the closed dessicator overnight. Afterwards, 0.0508 g of **1**, 0.0470 g of **2**, 0.0526 g of **3**, and 0.0510 g of **4** were each dissolved in 50 ml of distilled water. 1 and 2 ml of solution from each stock solution were diluted to 25 ml with water and used for ICP measurements. iii) Measurement method: The maximum wavelength for different element was selected (P: 213.618 nm; Eu: 381.970 nm; W: 239.709 nm; Al: 308.215 nm; Na: 589.592 nm; K: 766.496 nm). A calibration curve for each element was constructed. After the calibration curve of each element was completed, the concentrations (in ppm) were determined for the two solutions of each sample (40.64 μg/ml, 81.28 μg/ml of **1**, 37.60 μg/ml, 75.20 μg/ml of **2**, 42.08 μg/ml, 84.16 μg/ml of **3**, 40.80 μg/ml, 81.60 μg/ml of **4**). The concentrations, in ppm, were converted to weight percent of each element.

2.2.4.2 Collection of NMR Data.

All NMR spectra were recorded on a JEOL GX-400 spectrometer with 5 or 10 mm tubes. Resonance frequencies are 161.8 MHz for ^{31}P and 16.7 for ^{183}W. Chemical shifts are given with respect to external 85% H_3PO4 for ^{31}P and 2.0 M Na_2WO_4 for ^{183}W. Typical acquisition parameters for ^{31}P spectra included the following: spectral width, 10000 Hz; acquisition time, 0.8 s; pulse delay, 1 s; pulse width, 15 μs (50° tip angle). From 200 to 1000 scans were required. For ^{183}W spectra, typical conditions included the following: spectral width, 10000 Hz; acquisition time, 1.6 s; pulse delay, 0.5 s; pulse width, 50 μs (45° tip angle). From 1000 to 30000 scans were acquired. For all spectra, the temperature was controlled to ± 0.2 deg. For both ^{31}P and ^{183}W chemical shifts, the convention used is that the more negative chemical shifts denote more upfield resonances.

2.2.4.3 Single-Crystal X-ray Structure Determination.

Crystals of 1-4 were examined under a thin layer of mineral oil using a polarizing microscope. Selected crystals were mounted on a glass fiber and quickly placed in a stream cold nitrogen on a Bruker SMART CCD diffractometer equipped with a sealed tube Mo anode (K_∂ radiation, λ=0.71073 Å) and graphite monochromator or Nonius Kappa CCD diffractometer. The data were collected at around 100K. Data collection, indexing, and initial cell refinements were all handled using SHELXTL software. The SHELX package of software was used to solve and refine the restructures.[20] The heaviest atoms were located by direct methods, and the remaining atoms were found in subsequent Fourier difference syntheses. For the ammonium salt 1, the data did not support discrimination between oxygen and nitrogen atoms. All refinements were full-squares on F^2. Crystal data and structure refinement parameters for 1-4 are listed in Table 1 and 2. Selected bond distances for 1, 2, 3 and 4 are given in Table 3.

2.3 Results

2.3.1 Solution chemistry.

2.3.1.1 Solution Speciation of $PW_9O_{34}^{9-}$

A-$PW_9O_{34}^{9-}$ is formed from Na_2WO_4 and H_3PO_4 at pH 9.[21,22] Hill and co-workers examined the fundamental stability of A- and B-$PW_9O_{34}^{9-}$ under buffered neutral (physiological pH 7.4) aqueous media by ^{31}P NMR spectroscopy and found that, at equilibrium conditions, predominantly the monolacunary α-$PW_{11}O_{39}^{7-}$ species formed in the presence of two buffers (sulfite and tris).[23] Also, unidentified phosphorus containing

Table 1. Crystal Data and Structure Refinement for species **1** and **2**

	1	**2**
empirical formula	Eu8 O228 P4 W43	Al Eu O41 P W11
fw	12893.11	2888.26
cryst syst	triclinic	triclinic
space group	P-1(no.2)	P-1(no.2)
temp, K	109 (2)	100 (2)
wavelength, Å	0.71073	0.71073
a, Å	20.2000 (0)	11.4280(23)
b, Å	22.6951(6)	11.5930(23)
c, Å	25.3200(7)	19.754 (4)
α, deg	65.6760(10)	103.66(3)
β, deg	88.5240(10)	95.29(3)
γ, deg	86.0360(10)	102.31(3)
Vol, $Å^3$	10550.0 (5)	2456.4(9)
Z	2	2
calcd density, g/cm^3	4.058	3.905
abs coeff, mm^{-1}	25.816	27.029
F (000)	11140	2466
θ range, deg	1.77 to 27.50	1.89 to 27.45
limiting indices	$-26 \le h \le 26$ $-29 \le k \le 29$ $-32 \le l \le 32$	$-14 \le h \le 14$ $-14 \le k \le 15$ $-25 \le l \le 25$
reflns collected/unique	141901/48396, [R(int)=0.0386]	21306/11183, [R(int)=0.0286]
Refinement meth	full-matrix least- squares on F^2	full-matrix least-squares on F^2
data/ restraints/ parameters	48396/0/1408	11183/0/491
GOF on F^2	1.071	1.096
final R indices [$I>2\sigma(I)$]	R1= 0.0534, wR2=0.1292	R1=0.0572, wR2= 0.1624
R indices (all data)	R1=0.0624, wR2= 0.1347	R1=0.0687, wR2= 0.1770
largest diff.peak and hole	5.373 and –4.87 $eÅ^{-3}$	11.94 and –3.807 $eÅ^{-3}$

Table 2. Crystal Data and Structure Refinement for species **3** and **4**

	3	**4**
empirical formula	Cl Cs11 Eu K O93 P2 W22	K2 Al4 Eu2 O168 P4 W34
fw	7283.16	9552.82
cryst syst	triclinic	triclinic
space group	P-1(no.2)	P-1(no.2)
temp, K	100 (2)	100 (2)
wavelength, Å	0.71073	0.71073
a, Å	12.8663(14)	12.649(6)
b, Å	19.8235(22)	16.230(8)
c, Å	21.7060(23)	21.518(9)
α, deg	114.57(0)	111.223(16)
β, deg	91.86(0)	94.182(18)
γ, deg	102.91(0)	107.581(17)
Vol, $Å^3$	4858.3(9)	3842(3)
Z	2	1
calcd density, g/cm^3	4.979	4.129
abs coeff, mm^{-1}	30.832	26.373
F (000)	6212	4136
θ range, deg	1.04 to 28.40	1.04 to 28.74
limiting indices	$-16 \le h \le 16$ $-26 \le k \le 22$ $0 \le l \le 28$	-14<=h<=16 -21<=k<=13 -27<=l<=28
reflns collected/unique	18777/18777 [R(int)=0.0000]	27206 / 16035 [R(int)=0.0500]
Refinement meth	full-matrix least-squares on F^2	full-matrix least-squares on F^2
data/ restraints/ parameters	18777/0/705	16035 / 0 / 519
GOF on F^2	0.986	1.055
final R indices [I>2σ(I)]	R1= 0.0818 wR2= 0.2135	R1= 0.0778, wR2= 0.2158
R indices (all data)	R1= 0.1170 wR2= 0.2391	R1= 0.0946 wR2= 0.2293
largest diff.peak and hole	8.071 and -7.938 $eÅ^{-3}$	9.386 and -8.749 $eÅ^{-3}$

Table 3. Selected Bond Lengths (Å) for species **1**, **2**, **3**, and **4**

1					
Eu(1)-O(1)	2.436(10)	Eu(3)-O(1)	2.396(13)	Eu(3)-O(16B)	2.377(13)
Eu(1)-O(13)	2.346(11)	Eu(3)-O(15)	2.479(11)	Eu(3)-O(19B)	2.451(11)
Eu(2)-O(13)	2.391(13)	Eu(3)-O(16)	2.318(11)	Eu(4)-O(18)	2.314(13)
Eu(2)-O(19B)	2.383(11)	Eu(3)-O(13)	2.539(11)	Eu(4)-O(12B)	2.374(13)
Eu(2)-O(16B)	2.557 (11)	Eu(3)-O(14B)	2.369(10)		
Eu(1)-Eu(3)	5.907 (13)	Eu(4)-Eu(3)	5.827 (12)	Eu(1)-Eu(6)	3.910 (13)
Eu(2)-Eu(4)	6.146 (10)	Eu(1)-Eu(4)	6.146 (13)	Eu(4)-Eu(4)	6.536 (12)
Eu(1)-Eu(8)	4.426 (13)	Eu(4)-Eu(6)	6.557(12)	Eu(2)-Eu(3)	4.392 (10)
2					
Eu(1)-O(1)	2.431(39)	Eu(1)-O(5A)	2.392(20)	Eu(1)-O(2A)	2.456(57)
Eu(1)-O(6)	2.369(23)	Eu(1)-O(3A)	2.362(21)	Eu(1)-O(34)	2.499(21)
Eu(1)-O(4A)	2.362 (23)	Eu(1)-O(40)	2.407(21)	Al(1)-O(27)	2.871(30)
Eu(1)-Eu(1A)	6.288(88)				
3					
Eu(1)-O(1)	2.423 (1)	Eu(1)-O(5)	2.362 (5)	Eu(1)-O(2)	2.350 (2)
Eu(1)-O(6)	2.346 (2)	Eu(1)-O(3)	2.428 (0)	Eu(1)-O(7)	2.421 (3)
Eu(1)-O(4)	2.373 (1)	Eu(1)-O(8)	2.380 (1)		
4					
Eu(1)-O(1)	2.460(11)	Eu(1)-O(5)	2.419(10)	Eu(1)-O(2)	2.571(13)
Eu(1)-O(6)	2.437(13)	Eu(1)-O(3)	2.479(11)	Eu(1)-O(7)	2.447(11)
Eu(1)-O(4)	2.324(11)	Eu(1)-O(51A)	2.380(11)	Eu(1)-Eu(1A)	5.366 (12)

products were formed that were buffer dependent. In the present study, we examined the solution behavior of the A-$PW_9O_{34}^{9-}$, at equilibrium, under different pH (1-10) and counter cation (Li^+, Na^+, K^+, Cs^+, Al^{3+}) conditions by ^{31}P NMR (**Table 4**). In acidic solution the major species formed are H_3PO_4, the Keggin anion $PW_{12}O_{40}^{3-}$ and the mono-lacunary Keggin anion, $PW_{11}O_{39}^{7-}$. In buffer (0.5 M, LiAc, NaAc, KAc) at pH 4.75, only two species H_3PO_4 and $PW_{11}O_{39}^{7-}$ exist in the solution. Under neutral conditions, $PW_{11}O_{39}^{7-}$ along with PO_4^{3-} and unidentified species were present, similar to the previous study [23]. In basic solutions, the major species formed are PO_4^{3-} and WO_4^{2-} (according to

^{183}W NMR data), consistent with decomposition of the A-$PW_9O_{34}^{9-}$. The addition of the Al^{3+} to the solution of A- $PW_9O_{34}^{9-}$ results in a lowering of the pH to about 2-3 and the observation of two equal intensity peaks at –10.7, -11.45 ppm that may indicate a Wells-Dawson anion, for example, the β-Wells-Dawson anion or an Al(III) adduct of the α-$P_2W_{18}O_{62}^{6-}$ or possibly incorporation of the Al(III) into the α2- $P_2W_{17}O_{61}^{10-}$. These two peaks were in small concentration (13 %); the majority of the species observed in the case of Al(III) addition, are $PW_{11}O_{39}^{7-}$ and $PW_{12}O_{40}^{3-}$.

2.3.1.2 Solution Speciation of $PW_9O_{34}^{9-}$ with Eu^{3+}- After mixing and before heating

The speciation reactions of $PW_9O_{34}^{9-}$ with Eu^{3+} involve adding the polyoxometalate to a solution containing Eu(III) at the appropriate pH and countercation content. The solutions are heated for two minutes at 90°C; after this heating step, the ^{31}P NMR does not change over a period of days. Before the heating step, ^{31}P NMR analysis shows that there are unidentified, broad ^{31}P peaks that are likely due to chemical exchange processes of different species. For example, **Figure 1** shows the ^{31}P NMR

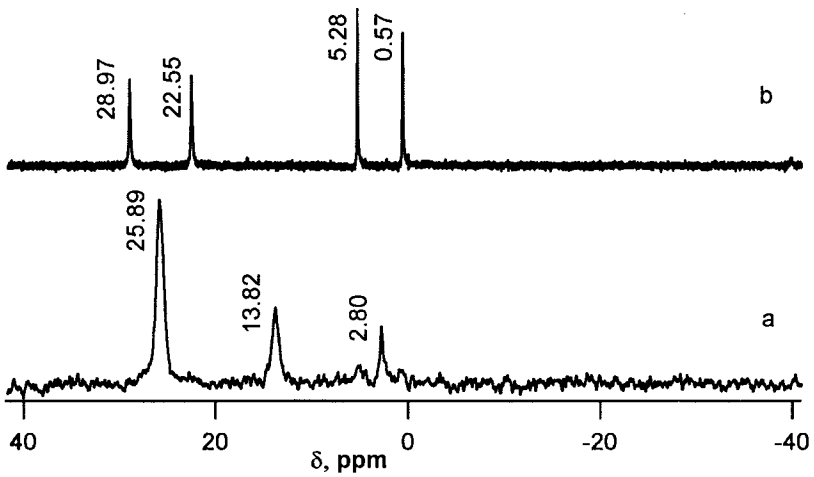

Figure 1. ^{31}P NMR spectra of reaction of $PW_9O_{34}^{9-}$ + NEu^{3+} a) before heat, b) after heat at 90°C

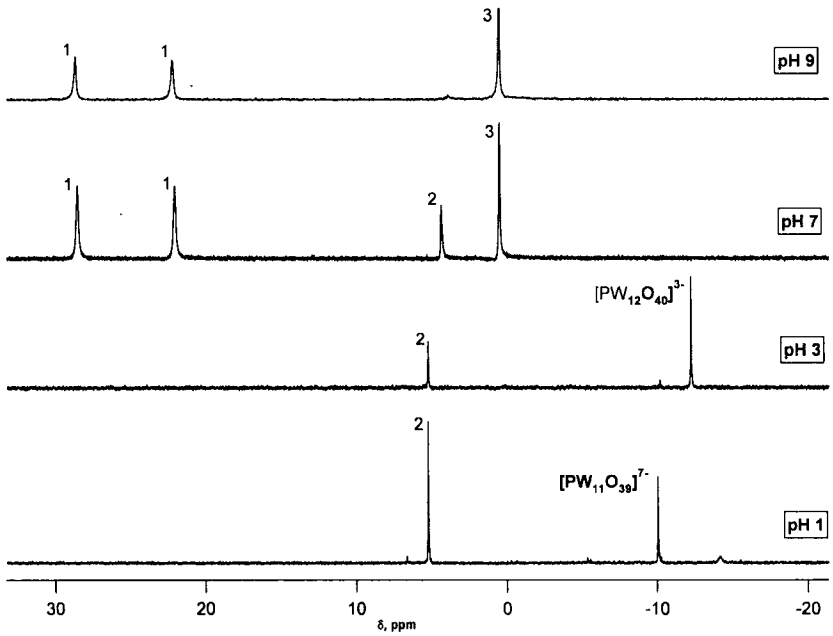

Figure 2. The ^{31}P NMR spectra for reactions of $PW_9O_{34}^{9-}$ + Eu^{3+} (1:1 stoichiometry) as a function of pH. The numbers represent the species, see text, that give rise to the designated ^{31}P NMR resonances.

spectra for a typical reaction of $PW_9O_{34}^{9-}$ and Eu(III), 1:1 stoichiometry, pH ca 6-7, before heating and after heating at 90°C. Before heating, the spectrum is broad and the peak positions do not correspond to any of the identified species. However, it is apparent that the broad peaks represent dynamic behavior of species that are in chemical exchange. For example, the peak at 25.89 ppm is clearly the largest peak and likely represents an average of the peaks of species **1**, $\{(Eu_2PW_{10}O_{38})_4(W_3O_8)(H_2O)_2(OH)_4\}^{22-}$ (28.97, 22.55 ppm) where the two chemically inequivalent ($Eu_2PW_{10}O_{38}$) lobes of the molecule are engaged in a dynamic process. The other peaks at 13.82 and 2.80 ppm are also broad and may represent chemical exchange as well. The peak at 2.80 ppm appears to be an average between species **2** and **3** $Eu(PW_{11}O_{39})^{4-}$ (5.28 ppm) and $Eu(PW_{11}O_{39})_2^{11-}$ (0.57 ppm) reflecting an exchange process involving these species. The peak at 13.82 possibly represents exchange between all three species. Heating this solution results in clear

conversion to species **1** (28.97, 22.55 ppm) and species **2** and **3** ($Eu(PW_{11}O_{39})^{4-}$ (5.28 ppm) and $Eu(PW_{11}O_{39})_2^{11-}$ (0.57 ppm), respectively.

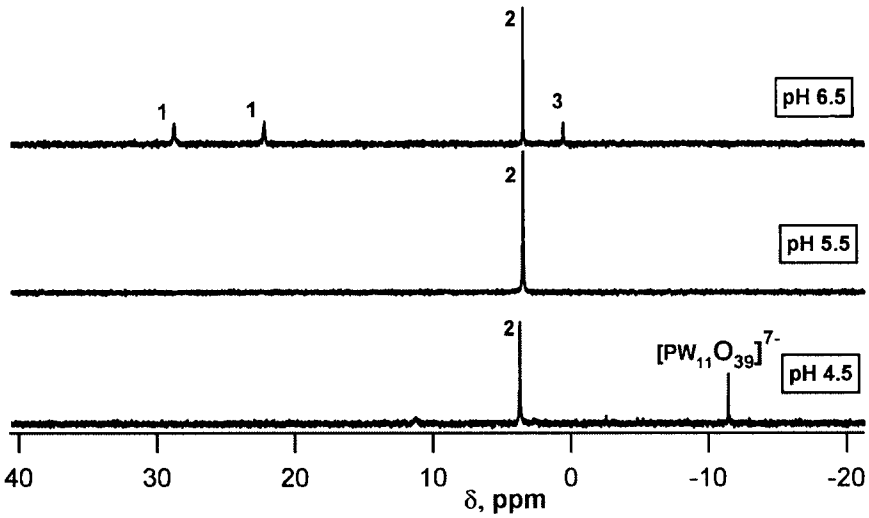

Figure 3. ^{31}P NMR spectra of control experiment of $PW_9O_{34}^{9-}$ + NEu^{3+} at up) LiAc buffer (0.5 M), bottom) NaAc buffer (0.5 M) with different pH

Conversion of the broad peaks (**Figure 1**) to species **1**,**2** and **3** also occurs if the solution is allowed to age for 12 hours at room temperature. Aging experiments of the heated solutions show that the spectra do not change during a period of days, suggesting that the system has reached equilibrium.

2.3.1.3 Reaction of $PW_9O_{34}^{9-}$ with Eu^{3+} (1:1 stoichiometry) at different pH

The ^{31}P NMR spectra (Figure 2) for the reaction carried out at low pH (1-3) shows two peaks at 5.23 ppm and –11.93 ppm, that correspond to species 2, Eu(PW11O39)4-, and PW11O397- respectively. Decomposition to PW12O403- is also observed. Three species are observed at pH 7, these are **1** $(Eu_2PW_{10}O_{38})_4(W_3O_8(H_2O)_2(OH)_4)^{22-}$ (δ, ppm:28.55, 22.07), **2** $Eu(PW_{11}O_{39})^{4-}$

(δ,ppm:5.25 ppm) and **3** $Eu(PW_{11}O_{39})_2^{11-}$ (δ, ppm: 0.5 ppm). The spectrum at pH 9 is dominated by species **1** and **3**.

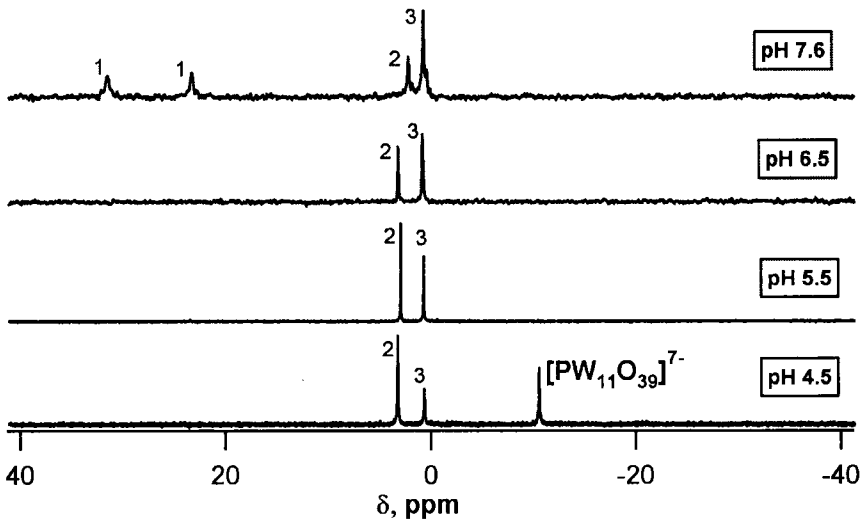

Figure 4. ^{31}P NMR spectra of control experiment of $PW_9O_{34}^{9-}$ + NEu^{3+} at KAc buffer (0.5 M) with different pH

The reaction of $PW_9O_{34}^{9-}$ with Eu^{3+} under varying pH (4.5, 5.5 and 6.5) was examined in the presence of different cations (Li^+, Na^+, K^+) (**Figures 3 and 4**). This experiment provides the opportunity to evaluate both the pH and counterion influence on speciation. With Li acetate or Na acetate buffer (0.5M) at pH 4.5 (**Figure 3**), the ^{31}P NMR of $PW_9O_{34}^{9-}$ and Eu^{3+} in a 1:1 mole ratio showed that **2** was the major solution species with the $PW_{11}O_{39}^{7-}$ ligand as a minor species. At pH 5.5, only species **2** was observed, while at pH 6.5, two additional species **1** and **3** were present in the solution in low concentration.

Different behavior is observed with K^+ counterions (KAc, 0.5M). For example, at pH 4.5, the major species observed in solution are **2**, $Eu(PW_{11}O_{39})^{4-}$ and free $PW_{11}O_{39}^{7-}$, with **3**, $Eu(PW_{11}O_{39})_2^{11-}$, in significant concentration (**Figure 4**). Increasing the pH results in no observable free $PW_{11}O_{39}^{7-}$ and a significant increase in the concentration of species **3**. In contrast to the Li^+ and Na^+ case, species **3** grows in significantly at the lower pH values with K^+ as the buffer, until it is the dominant species at pH 7.6. Species **1** begins to appear at a higher pH of 7.6 compared to 6.5 found for the Li^+ and Na^+ buffers.

2.3.1.4 Expanded study of $PW_9O_{34}^{9-}$ with Eu^{3+} (1:1 stoichiometry) as a function of countercation

To further test the effect of countercations on speciation, a study of the speciation of $PW_9O_{34}^{9-}$ + Eu^{3+} (1:1 stoichiometry, pH 7) with an expanded series of countercations, was carried out (**Figure 5**). With Na^+ (not shown), K^+ or NH_4^+ (not shown), three species corresponding to **1** (28.8, 22.2 ppm), **2** (5.2 ppm) and **3** (0.5 ppm) can be identified, similar to studies reported above. Addition of Cs^+ into the aqueous solution of $PW_9O_{34}^{9-}$ + Eu^{3+} (1:1 stoichiometry, pH 7) results in exclusively one species, **3**, $Eu(PW_{11}O_{39})_2^{11-}$.

Solutions containing the countercation Al(III) show the presence of species **4**, that has been identified as $Eu(\alpha\text{-}2\text{-}P_2W_{17}O_{61})^{7-}$ by ^{31}P NMR and crystallography, *vide infra*.[15] This phenomenon was only seen in the presence of Al^{3+} and is possibly due to the acidity that Al^{3+} confers upon the solution; generally, the pH after treatment with $AlCl_3$ was ca 2-

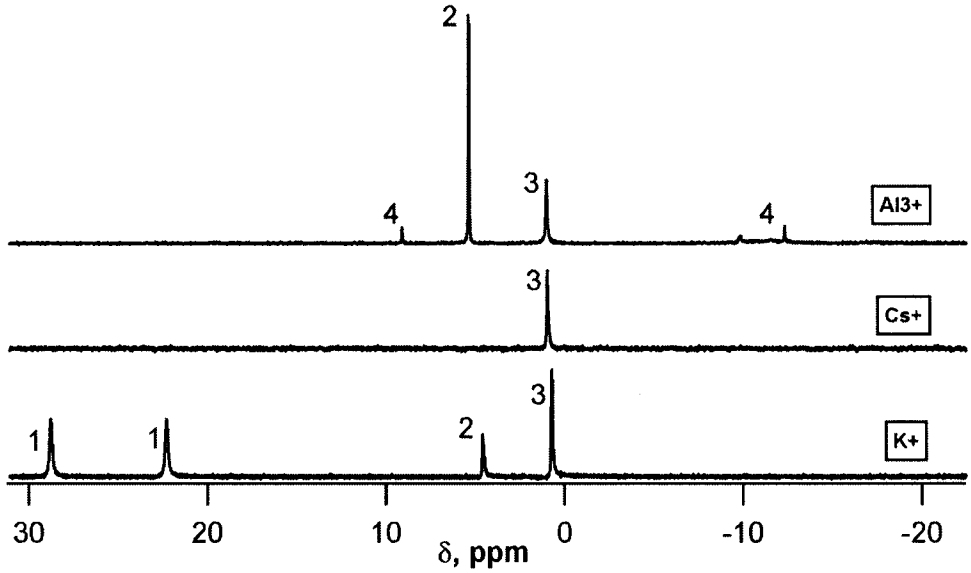

Figure 5. ^{31}P NMR spectra of reactions of $PW_9O_{34}^{9-}$ + Eu^{3+} (1:1 stoichiometry) with different counter cations (see text for concentrations of countercations, pH 7, except for Al(III), where the pH 2-3). The numbers represent the species, see text, that give rise to the designated ^{31}P NMR resonances.

3. Also, the ability of Al(III) to bind to oxygen atoms of polyoxometalates may influence the formation of this species. Species **2** and **3**, the 1:1 $Eu(PW_{11}O_{39})^{4-}$ and 1:2 $Eu(PW_{11}O_{39})_2^{11-}$, respectively, are also found as the majority species in this solution (**Figure 5**).

The reaction of Eu(III) and A- $PW_9O_{34}^{9-}$ in H_2O, in both 1:1 or 2:1 Eu: A-$PW_9O_{34}^{9-}$ stoichiometry, with the addition of TBA^+ or TEA^+, resulted in isolation, by extraction into organic solution, of species **2**, $Eu(PW_{11}O_{39})^{4-}$, exclusively. The ^{31}P NMR of the TBA salt (δ, ppm, 5.3, H_2O; δ,ppm, 9.6, CH_3CN) was identical to that for a genuine sample of $TBA_3H\{EuPW_{11}O_{39}\}$ that was prepared directly by two methods (metathesis of the potassium salt of $Eu(PW_{11}O_{39})^{4-}$, prepared by direct reaction of Eu(III) and $PW_{11}O_{39}^{7-}$, or by reaction of $Eu(ClO_4)_3$ and $TBA_4H_3(PW_{11}O_{39})^{24}$ in CH_3CN). The

samples of $TBA_3H\{EuPW_{11}O_{39}\}$ prepared directly have been analyzed by elemental analysis, thus far.

2.3.1.5 Reaction of $PW_9O_{34}^{9-}$ with Eu^{3+} under different stoichiometries.

The reaction of Eu^{3+} and A- $PW_9O_{34}^{9-}$ in 0.5:1, 1:1 and 2:1 Eu: POM stoichiometric ratios were studied in NaAc buffered solution (0.5 M, pH 6.5) and the ^{31}P NMR data is shown in **Figure 6**. ^{31}P NMR spectra show that at 0.5: 1 Eu: $PW_9O_{34}^{9-}$, species **3**, $Eu(PW_{11}O_{39})_2^{11-}$, dominates while **2**, $Eu(PW_{11}O_{39})^{4-}$, and an unknown species at 1.99 ppm, possibly due to decomposition of PW_9^{9-} in solution [25], are present in smaller quantities. At 1:1 Eu: $PW_9O_{34}^{9-}$ stoichiometry, three distinct species coexist in solution; according to ^{31}P NMR, these species are **1**, $\{(Eu_2PW_{10}O_{38})_4(W_3O_8(H_2O)_2(OH)_4\}^{22-}$, **2**,

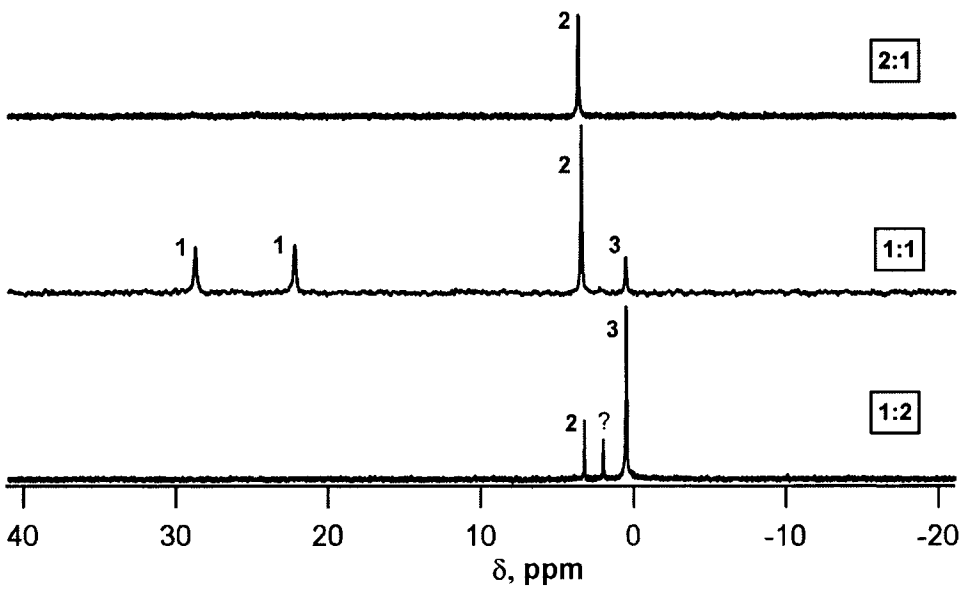

Figure 6. Up. ^{31}P NMR Spectra of Reactions of $PW_9O_{34}^{9-}$ + Eu^{3+} as a function of stoichiometry. Bottom. The boxed ratios represent the stoichiometric ratio of Eu: POM; therefore, the bottom spectrum represents the 1:2 Eu: $PW_9O_{34}^{9-}$ stoichiometry; the middle spectrum represents the 1:1 Eu: $PW_9O_{34}^{9-}$ stoichiometry; the top spectrum represents 2:1 Eu: $PW_9O_{34}^{9-}$ stoichiometry. The solution species are indicated by the numbers above the resonances, see text.

and **3**. At 2:1 Eu: $PW_9O_{34}^{9-}$, one species, **2,** is observed in the aqueous solution. The same speciation behavior is observed when the experiment is run in water and not buffer, except that there are a few more small unidentified peaks in the 1:2 Eu: $PW_9O_{34}^{9-}$ sample, probably due to decomposition of PW_9^{9-} in solution. Addition of $AlCl_3$ to solutions of 1:1 Eu: $PW_9O_{34}^{9-}$ stoichiometry resulted in the small amount $Eu(\alpha\text{-}2\text{-}P_2W_{17}O_{61})_2^{14-}$ (**Figure 5**). In contrast, upon addition of Al to 2:1 Eu: $PW_9O_{34}^{9-}$ stoichiometry, the $Eu(PW_{11}O_{39})^{4-}$ species was isolated as crystals in 45 % yield, *vide infra.*

2.3.2 Isolation, characterization of the four complexes observed in solution speciation studies and description of crystal structures.

From careful analysis of the reactions reported above, we chose appropriate conditions to optimize the syntheses and isolate the four species **1**, **2**, **3** and **4** from reactions of $PW_9O_{34}^{9-}$ with Eu^{3+}. This is important to confidently identify the species and understand their formation. The procedures are summarized in Scheme 1.

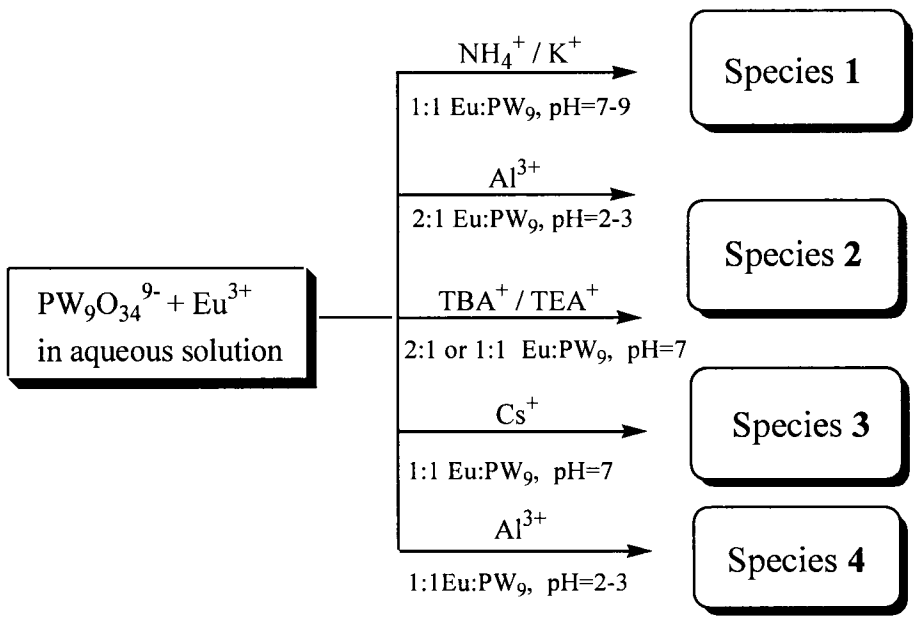

Scheme 1. Synthetic strategy for isolation of species **1**, **2**, **3**, and **4** from Eu(III) and of $PW_9O_{34}^{9-}$.

Species 1. The addition of NH_4^+ at pH 7-9 to a solution of $PW_9O_{34}^{9-}$ and Eu^{3+} results in the isolation of **1** as chunky colorless rectangular blocks. The ^{31}P NMR chemical shifts (**Table 5**) for isolated crystalline samples of **1** are observed at 31.53, 23.22 ppm and are dependent on solution conditions; in solution with different countercations present, the resonances are shifted upfield. We have recently reported the identical structure of the Y(III) and Eu(III) analogs of **1**.[18] Y(III) and Eu(III) also behave similarly with respect to solution speciation of $PW_9O_{34}^{9-}$ and thus, the Y(III) analogs are useful for solution characterization using ^{183}W NMR because resonances corresponding to all W atoms can be observed. The resonances corresponding to W atoms close to the site of substitution are often not observed in the Eu(III) analogs.

Species **1**, forms easily with $PW_9O_{34}^{9-}$ at pH 6.5-9 in 76% yield, and is uniquely stable in basic solution. From our previous work, multinuclear NMR and luminescence excitation spectra provide evidence that the cluster remains intact in aqueous solution and the ^{31}P NMR data, provided in this study, shows that the cluster remains intact under basic conditions and different countercation content. Increasing the acid content sets up an equilibrium with complex **2,** $Eu(PW_{11}O_{39})^{4-}$, that can be monitored by ^{31}P NMR, **Figure 7**. The Y(III) analog shows the same equilibrium and ^{183}W NMR of the Y(III) + $PW_9O_{34}^{9-}$ solution at pH 4.6 shows 6 peaks, of appropriate integration, that correspond to the 1:1 $Y(PW_{11}O_{39})^{4-}$ species, consistent with our assignment of $Eu(PW_{11}O_{39})^{4-}$.

1 can be viewed as the confluence of four $PW_{10}O_{37}^{9-}$ units each incorporating 2 Eu(III) ions to create four Keggin-like anions that are further tied together by three

Table 4. ^{31}P NMR chemical shift (δ, ppm) of A-$PW_9O_{34}^{9-}$ at different pH, buffer and counter cation

pH	Counter cation	δ, ppm	Assignment
pH 1	Na	.6410	PO_4^{3-}
		-11.8417	PW_{11}^{7-}
		-14.5522	PW_{12}^{3-}
pH 3	Na	.5091	PO_4^{3-}
		-10.8308	PW_{11}^{7-}
		-11.8197	?
		-12.7501	?
		-14.8379	PW_{12}^{3-}
pH 4.75	Cs	2.8806	PO_4^{3-}
		-10.1104	PW_{11}^{7-}
	K	2.8257	PO_4^{3-}
		-10.0958	PW_{11}^{7-}
	Na	2.9355	PO_4^{3-}
		-10.0958	PW_{11}^{7-}
	Li	2.9941	PO_4^{3-}
		-10.3778	PW_{11}^{7-}
pH 3	Al	-10.6049	PW_{11}^{7-}
		-10.7074	$P_2W_{18}^{10-}$?
		-11.4546	$P_2W_{18}^{10-}$?
pH 2	Al	-10.9260	PW_{11}^{7-}
		-12.1128	?
		-13.0065	?
		-13.2995	?
pH 5	Na	.7875	PO_4^{3-}
		-1.6812	?
		-10.1129	PW_{11}^{7-}
pH 7.3	Na	3.0364	PO_4^{3-}
		-1.6812	?
		-8.9994	?
		-10.1056	PW_{11}^{7-}
pH 8	Na	3.2708	PO_4^{3-}
pH 10.35	Na	3.4467	PO_4^{3-}

Table 5. Multinuclear NMR Data for **1**, **2**, **3**, **4**.

Compounds	^{31}P NMR data (δ ppm)
$[Eu_2PW_{10}O_{38})_4(W_3O_{14})]^{30-}$, **1**[a]	31.53, 23.22
$[Eu(H_2O)_xPW_{11}O_{39}]^{7-}$, **2**	5.25
$[Eu(PW_{11}O_{39})_2]^{11-}$, **3**	0.34
$[Eu(H_2O)_x(\alpha\text{-}2\text{-}P_2W_{17}O_{61})]^{14-}$, **4**	8.72, -12.23
$[Y(H_2O)_xPW_{11}O_{39}]^{7-}$	-12.04
$[Y(PW_{11}O_{39})_2]^{11-}$	-12.28
	^{183}W NMR data (δ ppm, integration)
$[Y_2PW_{10}O_{38})_4(W_3O_{14})]^{30-}$ [b]	-30.8(2), -99.8(2), -103.4(2), -110.8(2), -124.2(2), -129.8(2), -131.1(2), -133.8(2), -134.6(2), -135.8(2), -139.2(2), -141.3(1), -145.9(2), -149.7(2), -157.9(2), -159.8(2), -174.7(2), -187.8(2), -225.7(2)
$[Y(H_2O)_xPW_{11}O_{39}]^{4-}$ [c]	-107.36(2), -116.79(1), -126.47(2), -144.94(2), -145.47(2), -155.00(2)
$[Eu(H_2O)_x(PW_{11}O_{39})]^{4-}$ [c]	-123.93(1), -131.45(2), -138.44(2), -187.69(2)
$[Y(PW_{11}O_{39})_2]^{11-}$ [c]	-130.00 (1), -132.02 (1), -143.93 (1), -149.42(1), -150.64(1), -155.53 (1), -166.64(1), -172.38(1), 173.23(1), -174.76(1), -206.99(1)

a. Chemical shifts for crystalline sample of (1) in water. The chemical shifts for samples with high concentrations of counterions and other species are found slightly upfield at 28.55, 22.07 ppm.

b. Howell, R. C.; Perez, F. G.; Jain, S.; Horrocks, W. D.; Rheingold, A. L.; Francesconi, L. C. *Angew. Chew. Int. Ed.* **2001**, 40(21), 4031-4034.

c. The samples were prepared directly from $PW_{11}O_{39}^{7-}$ for ^{183}W NMR. The ^{31}P NMR for these samples was identical with samples prepared via $PW_9O_{34}^{9-}$.

additional tungstate units, **Figure 8**. The central core consists then of the eight Eu(III) ions coordinated to tungstate units, shown in **Figure 9**. Bond valence sums [26,27] (**Table 6**) performed on all of the oxygen atoms in this core suggest that four oxygen atoms O13, O14, O16 and O18, each bridging two Eu(III) ions, are hydroxides and two oxygen atoms, O15 and O17 are water molecules bound to Eu(III) centers. This hydroxo/oxo core is expected given the neutral to basic pH required for the formation of this complex and the general Lewis acidity of the lanthanides.

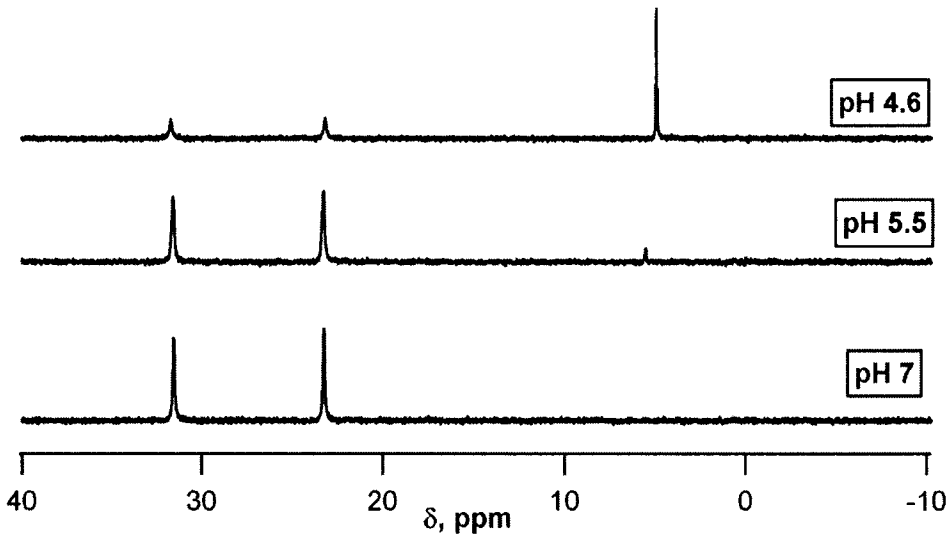

Figure 7. ^{31}P NMR spectra of species **1** at different pH

Species 2. The addition of Al^{3+} into the solution of $PW_9O_{34}^{9-}$ with Eu^{3+} (2:1 Eu: POM) results in a drop in pH from 7 to 2.8. As the predominant polyoxotungstate species is the monovacant $PW_{11}O_{39}^{9-}$ at lower pH (**Table 4**), it is very reasonable that addition of Eu(III) will form $Eu(H_2O)_4W_{11}O_{39}^{4-}$ especially in this case, with an excess of Eu(III). ^{31}P NMR and elemental analysis are consistent with this formulation. As shown in **Figure 10**, in the solid-state, **2** is an infinite one dimensional polymer, similar to the $Eu(H_2O)_2(SiW_{11}O_{39})^{5-}$ (K^+ salt) species published by Mialane recently.[5] The structure is similar also to $Ce(H_2O)_3(\alpha\text{-}SiW_{11}O_{39})^{5-}$ that also forms a one dimensional polymer.[4] Due to the smaller size of Eu^{3+} than Ce^{3+}, it is reasonable that only two water molecules are coordinated to the Eu^{3+} rather than three water molecules that are found coordinated to Ce^{3+}. The Eu^{3+} is coordinated to four oxygen atoms of the defect site of $\alpha\text{-}PW_{11}O_{39}$, to two water molecules, and to two neighboring $\alpha\text{-}PW_{11}O_{39}$ units through terminal oxygen atoms. As observed for most lanthanide complexes of monovacant polyoxometalates, the

Eu(III) ion is in a distorted monocapped square antiprism environment. The Al(III) ion sits in the space between the α-$PW_{11}O_{39}$ units and shows a weak connection (average Al-O: 2.87 (3) Å) to a terminal oxygen atom of an adjacent polyoxometalate. The structure contains 35.3% solvent accessible space.[28] Therefore, it is likely that water is located in this interstitial space as well. The Eu(III)-O bond lengths to the four oxygen atoms in the Keggin defect are similar (average: 2.371Å) and the average Eu(III)-oxygen bond lengths to the two neighboring $PW_{11}O_{39}$ moieties is longer at 2.453 Å. The Eu-O (H_2O) distance is 2.455 Å within the range of Eu-O (H_2O) bond distances.[5,15] The interatomic distances between the europium centers are 6.288 Å. The bond lengths for the atoms in the tungsten-oxygen framework of $Eu(H_2O)_2(PW_{11}O_{39})^{4-}$ compare favorably with other Keggin structures. Although **2** exits as an oligomer in the solid state, it is soluble in aqueous solution and the ^{31}P NMR is identical to a sample of $Eu(PW_{11}O_{39})^{4-}$, suggesting that the polymer dissociates into the monomeric form.

Species 3. Addition of Cs^+ to $PW_9O_{34}^{9-}$ and Eu^{3+} (1:1 stoichiometry) at pH 7 results in **3** as small colorless thick rectangular crystals. The crystal structure, **Figure 11**, shows that this species is a 1:2 Eu: $PW_{11}O_{39}^{7-}$ complex, originally isolated by Peacock and Weakley.[29] The ^{31}P NMR shows one peak at 0.34 ppm that is identical with the 1:2 Eu: $PW_{11}O_{39}^{7-}$ complex, prepared directly. The ^{183}W NMR of 1:2 analog $Y(PW_{11}O_{39})_2^{11-}$ shows 11 peaks [12,30] (**Table 5**), consistent with the C_2 structure revealed by X-ray crystallography.

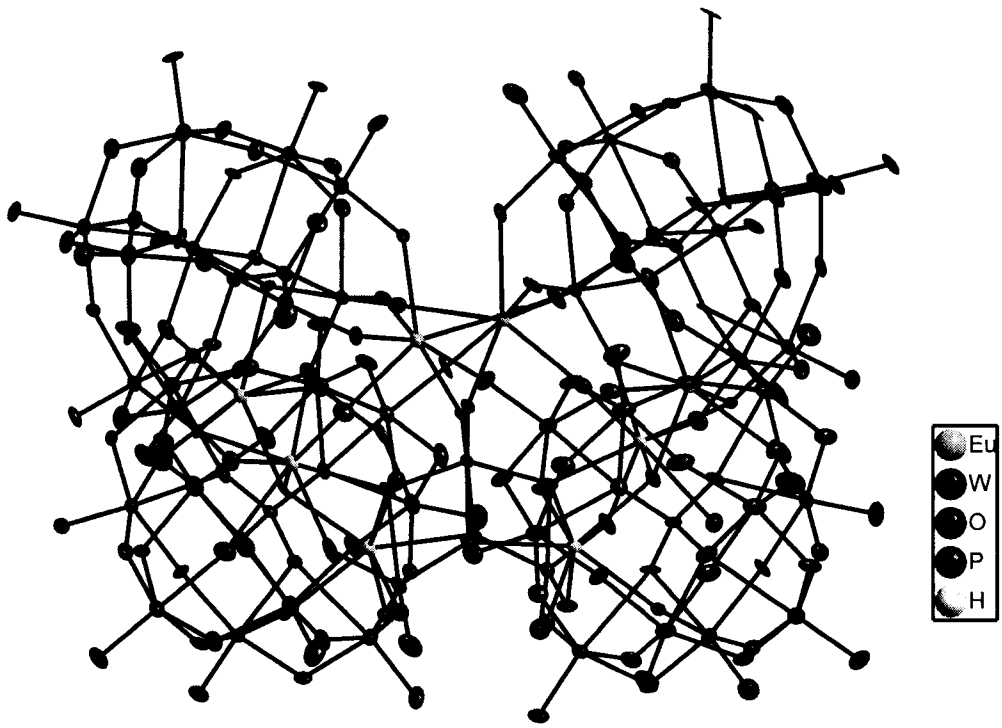

Figure 8. Representation as 50% ellipsoids of the asymmetric unit of 1. Uncoordinated water molecules and hydrogen atoms removed for clarity.

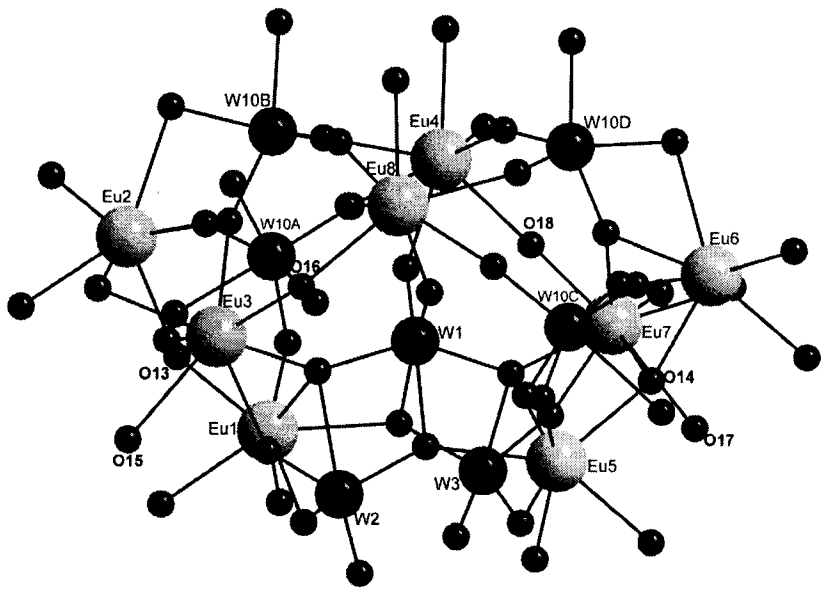

Figure 9. Structure of the central $W_8Eu_8(H_2O)_2(OH)_4O_{40}$ unit in $\{Eu_2PW_{10}O_{38})_4(W_3O_8(H_2O)_2(OH)_4)\}^{22-}$, **1** Uncoordinated H_2O molecules have been removed for clarity (The large size balls represent europium atoms, The medium size balls represent tungsten atoms, and the small size balls represent oxygen atoms). Hydroxide and water oxygen atoms are labeled, see text.

Table 5. Bond Valence Sum (BVS) for the oxygen atoms in the core $[Eu_2PW_{10}O_{38})_4(W_3O_8(H_2O)_2(OH)_4)]^{22-}$

	Oxygen	BVS		Oxygen	BVS
Terminal	W(2)-O(8)	1.707		W(7C)-O(14C)-Eu(5)	2.126
	W(3)-O(11)	1.579		W(8C)-O(16C)-Eu(5)	1.934
	Eu(3)-O(15)	0.335		W(10C)-O(18C)-Eu(6)	1.879
	Eu(7)-O(17)	0.350		W(10C)-O(19C)-Eu(5)	1.942
	W(6A)-O(11A)	1.657		W(10C)-O(20C)-Eu(4)	1.957
	W(7A)-O(13A)	1.657		W(4C)-O(36C)-W(10C)	1.863
	W(8A)-O(15A)	1.600		W(9C)-O(37C)-W(10C)	1.820
	W(9A)-O(17A)	1.721		W(5B)-O(10B)-Eu(4)	1.862
				W(6B)-O(12B)-Eu(4)	1.884
μ_2-Bridge	W(1)-O(5) –Eu(8)	1.957		W(7B)-O(14B)-Eu(3)	1.820
	W(1)-O(6)-Eu(4)	1.928		W(8B)-O(16B)-Eu(3)	1.765
	W(2)-O(7)-Eu(1)	1.842		W(10B)-O(18B)-Eu(4)	1.992
	W(2)-O(9)-Eu(3)	1.814		W(10B)-O(20B)-Eu(8)	1.987
	W(3)-O(10)-Eu(5)	2.163		W(4B)-O(36B)-W(10B)	1.896
	W(3)-O(12)-Eu(7)	1.839		W(9B)-O(37B)-W(10B)	1.567
	Eu(1)-O(13)-Eu(2)	0.904		W(5D)-O(10D)-Eu(8)	1.851
	Eu(5)-O(14)-Eu(6)	0.927		W(6D)-O(12D)-Eu(8)	1.852
	Eu(3)-O(16)-Eu(4)	1.040		W(7D)-O(14D)-Eu(7)	1.766
	Eu(7)-O(18)-Eu(8)	1.010		W(8D)-O(16D)-Eu(8)	1.980
	W(5A)-O(10A)-Eu(2)	1.902		W(10D)-O(20D)-Eu(4)	1.956
	W(6A)-O(12A)-Eu(2)	1.896		W(4D)-O(36D)-W(10D)	1.931
	W(7A)-O(14A)-Eu(1)	1.845		W(9D)-O(37D)-W(10D)	1.616
	W(8A)-O(16A)-Eu(1)	1.987			
	W(10A)-O(18A)-Eu(2)	1.927	μ_3 - Bridge	μ3-O1, Eu1, Eu3, W1	1.894
	W(10A)-O(19A)-Eu(1)	2.062		μ3-O2, Eu5, W1, W2	2.060
	W(10A)-O(20A)-Eu(8)	2.006		μ3-O3, W3, W1, Eu1	2.094
	W(4A)-O(36A)-W(10A)	1.829		μ3-O4, W1, Eu5, Eu7	1.847
	W(9A)-O(37A)-W(10A)	1.789		μ3-O19B, W10B, Eu2, Eu3	2.066
	W(5C)-O(10C)-Eu(6)	1.929		μ3-O19D, W10D, Eu6, Eu7	2.021
	W(6C)-O(12C)-Eu(6)	1.973			

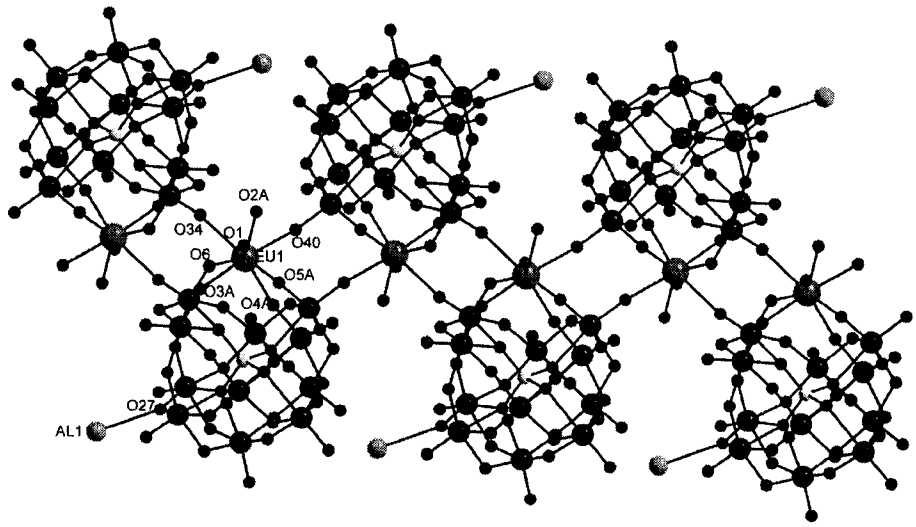

Figure 10. Ball and stick structure of $Al\{Eu(H_2O)_2(PW_{11}O_{39})\}^-$, **2**. Uncoordinated H_2O molecules have been removed for clarity. Legend: W: large dark balls; O: small dark balls; Eu: large gray balls; P: small gray balls; Al: medium gray balls

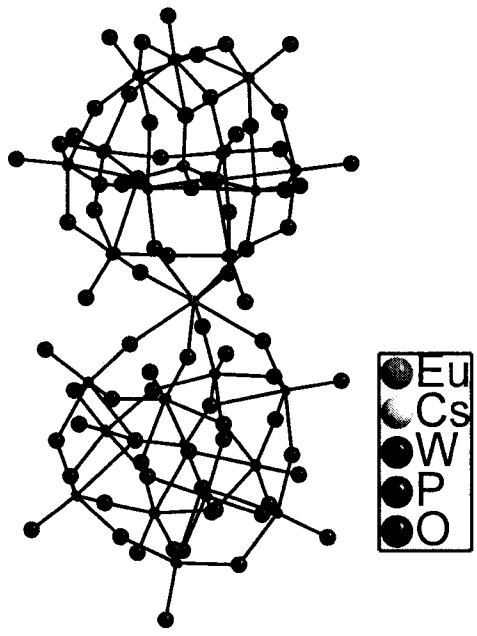

Figure 11. Ball and stick structure of $Eu(PW_{11}O_{39})_2^{11-}$, **3**. Uncoordinated H_2O molecules have been removed for clarity. Legend: W: blue; O: red; Eu: green; P: yellow; Al: blue

dimeric structure $\{Eu(H_2O)_3(\alpha\text{-}2\text{-}P_2W_{17}O_{61})\}_2^{14-}$ (**Figure 12**) that we have observed before from the reaction of excess Eu(III) with $\alpha\text{-}2\text{-}P_2W_{17}O_{61}^{10-}$ in a KCl medium.[15]

However, in this case, the Al(III) serves as a counterion and forms weak connections with the terminal W-O bonds of adjacent $\{Eu(H_2O)_3(\alpha\text{-}2\text{-}P_2W_{17}O_{61})\}_2^{14-}$ units, seen in **Figures 13 and 14**.

The extended structure is composed of the anions of **4** linked together by surface bound Al^{3+} cations. The Al^{3+} ions, in a distorted trigonal prismatic coordination environment, bind to terminal oxygen atoms of two dimers (average Al-O distances: 2.77(5) Å) giving rise to chains along the crystallographic a axis (**Figure 13**), while down the c axis, Al^{3+} links three $\{Eu(H_2O)_3(\alpha\text{-}2\text{-}P_2W_{17}O_{61}\}_2^{14-}$ units giving rise to the formation of discrete channels forming a porous 3D structure (pore size: 17 Å x 6 Å, **Figure 14**). This compound is less soluble in water than anions of similar size, probably due to the covalent bonding of the Eu^{3+} to a terminal oxygen of an adjacent polyoxoanion, and to the surface bonding of the Al^{3+} cations. Both ^{31}P and ^{183}W NMR show good evidence to support the notion that the dimeric complex $\{Eu(H_2O)_3(\alpha\text{-}2\text{-}P_2W_{17}O_{61})\}_2^{14-}$ in the solid state dissociates in aqueous solution to form the monomeric form $Eu(\alpha\text{-}2\text{-}P_2W_{17}O_{61})^{7-}$ (**Table 5**).

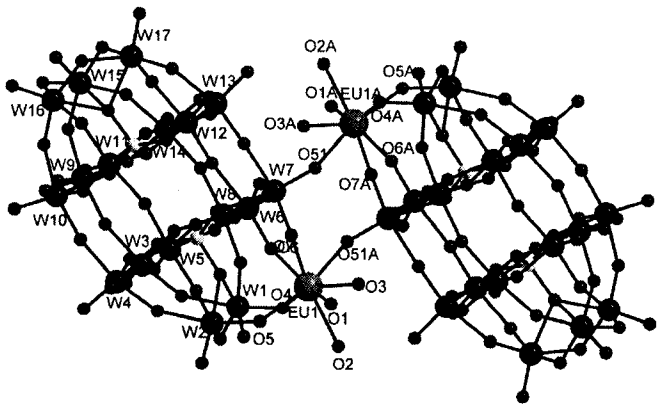

Figure 12. Left: ball and stick structure of $\{Eu(H_2O)_3(\alpha\text{-}2\text{-}P_2W_{17}O_{61})\}_2^{14-}$, **4.** Uncoordinated H_2O molecules have been removed for clarity. Legend: W: large dark balls; O: small dark balls; Eu: large gray balls; P: small gray balls.

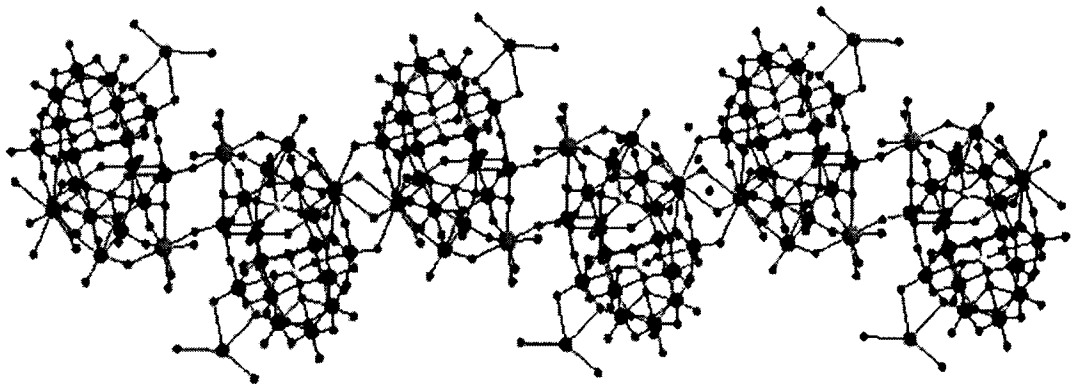

Figure 13. Packing diagram of **4**, viewed along a axis. Uncoordinated H_2O molecules have been removed for clarity. Legend: W: large dark balls; O: small dark balls; Eu: large gray balls; Al: medium gray balls; P: small gray balls.

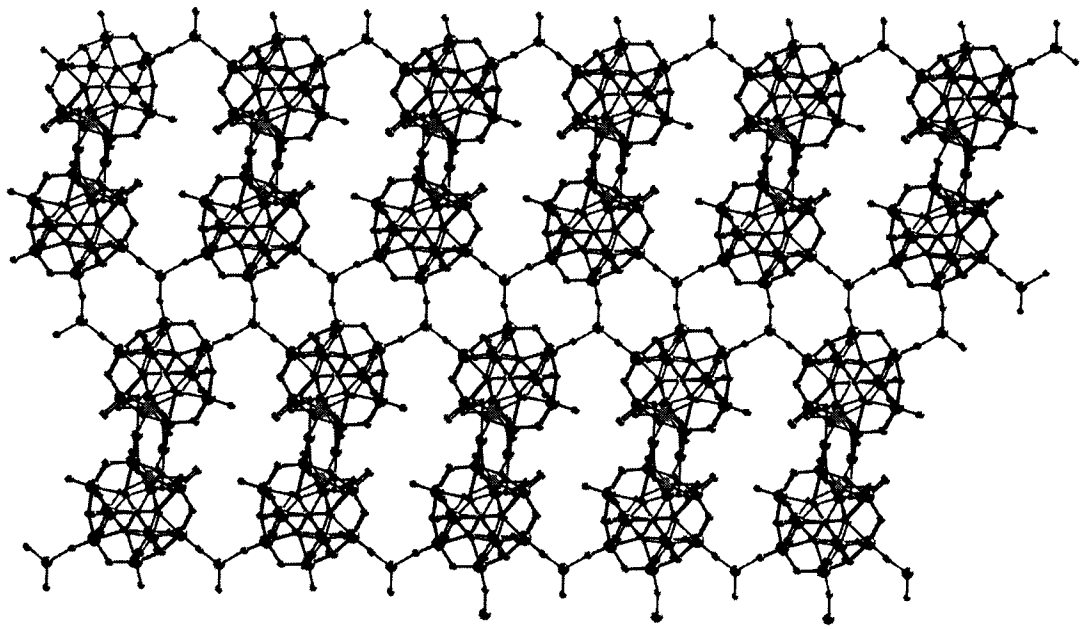

Figure 14. Packing diagram of **4**, viewed along c axis. Uncoordinated H_2O molecules have been removed for clarity. Legend: W: large dark balls; O: small dark balls; Eu: large gray balls; Al: medium gray balls; P: small gray balls.

2.4 Discussion

The three parameters, pH, countercation, and stoichiometry, have an important impact on the aqueous speciation of $PW_9O_{34}^{9-}$ and Eu^{3+}. The pH influences the speciation of the polyoxometalate $PW_9O_{34}^{9-}$, alone, to form primarily $PW_{11}O_{39}^{7-}$ ligand [23] and

decomposition products (**Table 4**) to which the Eu(III) can bind. The countercations modulate the reactivity and may be instrumental in anchoring polyoxometalate units together for assembling larger structures, such as the "sandwich" complex, $Eu(PW_{11}O_{39})_2^{11-}$, **3** and the hydroxo/ oxo cluster, **1**. [31]

Under low pH conditions, the high acid content stabilizes the $PW_{11}O_{39}^{7-}$ ligand as well as species **2**, $Eu(PW_{11}O_{39})^{4-}$, the 1:1 species. As the base is increased, and proton competition with the $PW_{11}O_{39}^{7-}$ ligand and $Eu(PW_{11}O_{39})^{4-}$(**2**) decreases, the concentration of the 1:2 complex, $Eu(PW_{11}O_{39})_2^{11-}$, (**3**) is increased. Eventually at high pH, where $PW_9O_{34}^{9-}$ decomposes to $PW_{11}O_{39}^{7-}$, lower nuclearity phosphotungstates, as well as WO_4^{2-}, species **3** and **1** become major components of the solution, as seen in **Figures 2, 3** and **4**. Species **1** is comprised of the $PW_{10}O_{38}^{11-}$ fragment and monotungstate units bound to Eu(III).

Cations have a significant effect on the speciation of $PW_9O_{34}^{9-}$ and Eu(III). The hypothesis that large, less extensively hydrated alkali metal cations bind to the surfaces of the polyoxometalates and "anchor" the POM units in place for assembly into larger structures, such as the 1:2 sandwich structures, has been put forward. [32,33] Ion pairing of large cations (Rb^+) to POM surfaces was proposed by Kirby and Baker in a study to understand the solution "syn" structure of $Th(\alpha\text{-}2\text{-}P_2W_{17}O_{61})_2^{16-}$.[32] The formation of a 1:2 K^+: $SiW_{11}O_{39}$ species in a Cs^+ environment has been reported recently by Laronze [33]. In this latter study, similar to ours, treatment of the trivacant $A\text{-}\alpha\text{-}SiW_9O_{34}^{10-}$ with K^+ and excess Cs^+ results in isolation of Cs_{15} $K(SiW_{11}O_{39})_2$, where K^+ is bound in the cavity. This molecule is similar to **3**, with cubic coordination about the K^+ rather than square antiprismatic coordination geometry that is prevalent with the lanthanides. They propose,

according to the solid-state crystal structure, that the Cs^+ anchors the $SiW_{11}O_{39}^{8-}$ species in place for the formation of the 1:2 K^+: POM complex. To substantiate this proposal, the solid-state structure of Cs_{15} $K(SiW_{11}O_{39})_2$, shows that three Cs^+ ions are bound to terminal oxygen atoms of each $SiW_{11}O_{39}^{10-}$ unit (with Cs-O distances of ca. 3.2 Å) perhaps stabilizing the $K(SiW_{11}O_{39})_2^{15-}$ solid-state structure. The molecule dissociates in aqueous solution.

Similarly, we have observed that in aqueous solution K^+ and Cs^+ promote the formation of the 1:2 $Eu(PW_{11}O_{39})_2^{11-}$ species. The formation of species **3**, 1:2 $Eu(PW_{11}O_{39})_2^{11-}$, in significant concentration, is observed at low pH (4.5) for solutions containing K^+ buffer (**Figure 4**). In contrast **3** appears only at higher pH (6.5) with Li^+ and Na^+ containing buffers and in very low quantities (**Figures 3** and **5**). When Cs^+ is employed as a counterion, **3** is the only species formed (**Figure 5**). These observations are consistent with ion pairing of K^+ and Cs^+ to the $PW_{11}O_{39}$ lobes, thus anchoring the $PW_{11}O_{39}$ lobes in position to form the 1:2 complex.

Considering the solid-state structure of $Cs_{11}Eu(PW_{11}O_{39})_2$, one Cs^+ (Cs7) is in close contact with the terminal W-O and bridging W-O oxygen atoms (3.2 Å) from both lobes and may be a prototype as to the role large cations have in stabilizing this structure. The remaining 10 Cs^+ ions surround the sandwich complex. The Cs^+ ions may insulate and stabilize the sandwich $Eu(PW_{11}O_{39})_2$ ions in crystal. Similar interaction of Cs^+ ions with the metal oxygen surfaces may stabilize this structure in solution as well.

Ion pairing of alkali metal cations to polyoxometalates has been quantitated in recent studies. The larger and less extensively solvated alkali-metal cations form smaller (more intimate) association complexes with the $\{X^{n+}VW_{11}O_{40}\}^{(9-n)-}$ (X=P(V), Si(IV),

Al(III)) family of polyoxometalates.[34,35] The smaller association complexes impact physical properties of the polyoxometalates, for example the diffusion coefficients and electron transfer rates of organic oxidation reactions. The countercation effect can be further substantiated by our observations on the solution speciation of the 1:2 Ln(α-1-$P_2W_{17}O_{61})_2^{14-}$ species.[36] We find that countercations are critical to the formation of 1:2 Ln(α-1-$P_2W_{17}O_{61})_2^{14-}$ species in aqueous solution. In these studies, ^{31}P NMR shows clearly that in aqueous solution the 1:2 species is maintained in Cs^+ buffer, whereas an equilibrium between the 1:1 and 1:2 is set up with K^+. Li^+ buffer result in complete dissociation of the 1:2 Ln(α-1-$P_2W_{17}O_{61})_2^{14-}$ species into the 1:1 Ln(α-1-$P_2W_{17}O_{61})^{7-}$ species and (α-1-$P_2W_{17}O_{61})^{10-}$ ligand. We suspect that the Cs^+ ions and to an extent, the K^+ ions are binding to surface sites of POMs and thus stabilize the 1:2 structures in solution.

In contrast, the addition of large organic counterions such as tetrabutylammonium (TBA^+) chloride or tetraethylammonium (TEA^+) chloride into the solution of $PW_9O_{34}^{9-}$ + Eu^{3+} (2: 1 and 1:1 Eu: $PW_9O_{34}^{9-}$ stoichiometry) results in formation of exclusively species **2**, $Eu(PW_{11}O_{39})^{4-}$. It has been demonstrated recently, in ion pairing experiments, that large organic countercations do not bind to the surface of POMs to form ion pairs. [35] The stabilization of the 1:1 $Eu(PW_{11}O_{39})^{4-}$ over the 1:2 $Eu(PW_{11}O_{39})_2^{11-}$ species with TBA and TEA, then, are consistent with their lack of binding to the POM surfaces.

The effect of Al(III) as a counterion has also been probed. To understand the formation of the Eu(α-2-$P_2W_{17}O_{61})_2^{14-}$ species, **4**, with the addition of Al(III), we analyzed solutions of the $PW_9O_{34}^{9-}$ ligand in the presence of Al^{3+}. Treatment of $PW_9O_{34}^{9-}$ with Al(III) results in a lowering of the pH to 2-3 and it is possible that

condensation of two α-A- $PW_9O_{34}^{9-}$ moieties can occur. The ^{31}P NMR reveals small, equal intensity peaks that likely correspond to a Wells-Dawson molecule, possibly a β-$P_2W_{18}O_{62}$ molecule, an α-$P_2W_{18}O_{62}$ with Al(III) bonded unsymmetrically to its faces or the mono lacunary α2-$P_2W_{17}O_{61}^{10-}$ with Al(III) occupying the vacancy or near the vacancy (**Table 4**). It is likely that the Eu(III) binds into the vacancy to form the small amount of complex **4** observed in the solution (**Figure 5**).

The stoichiometry of Eu and $PW_9O_{34}^{9-}$ play an important role in the speciation of Eu polyoxometalates, as shown in **Figure 6**. In an excess of $PW_9O_{34}^{9-}$ at pH 7, decomposition to primarily $PW_{11}O_{39}^{7-}$ with some unidentified P containing products, and phosphate as well as tungstate (**Table 4**), results in formation of both $Eu(PW_{11}O_{39})_2^{11-}$, **3**, and $Eu(PW_{11}O_{39})^{4-}$, **2**. With more Eu(III) present, as in 1:1 stoichiometry, under neutral conditions and with Na^+, K^+ and NH_4^+, $PW_{11}O_{39}^{7-}$ and lower nuclearity phosphotungstates (such as $PW_{10}O_{38}^{11-}$) can be trapped by the excess Eu(III) ions and monotungstate groups to form the Eu_8 hydroxo/oxo cluster, **1**. The 2:1 Eu: $PW_9O_{34}^{9-}$ stoichiometry provides an excess of Eu(III) ions to promote formation of $Eu(PW_{11}O_{39})^{4-}$, **2**

The crystal structure of species **2**, and **4**, shown in **Figures 10**, **12**, **13** and **14**, are instructive to examine the potential interaction of oxophilic Al(III) counterions with polyoxometalate surfaces. Species **2** and **4** show weak interactions of the Al(III) ions with terminal oxygen atoms of the polyoxometalate. The interaction, although weak, allows connection of the polyoxometalates and buildup of a porous material, as seen in species **4**.

We have investigated only the effects of pH and countercation in this study. However, other ions also can serve as templates or structure directing groups. This was seen clearly in a recent report by Hill wherein the addition of carbonate to an aqueous solution of $Y(III)Cl_3$ followed by addition of Na_8H A-α- PW_9O_{34} and workup forms 33% of a new complex that consists of a $Y_3(PW_9O_{34})_2$ sandwich complex wherein CO_3^{2-} anchors the Y(III) ions and the two POM units[37]. We find that species **1** forms without the addition of CO_3^{2-}. In this case, carbonate appears to template the formation of this sandwich complex. The structure is reminiscent of the $Cu_3(PW_9O_{34})_2$ templated by nitrate anion. [38]

2.5 Conclusion

We have focused this study on understanding speciation chemistry of lanthanide complexes of the tri-vacant polyoxometalate, $PW_9O_{34}^{9-}$ in aqueous solution. The A-α-$PW_9O_{34}^{9-}$ has 6 basic oxygen atoms that are available for bonding. The reaction products are highly dependent on the pH, countercation, and stoichiometry between Eu(III) and $PW_9O_{34}^{9-}$. The four species that have been observed in solution speciation studies have been synthesized and thoroughly characterized in the solid state and in solution. The pH has a profound effect on the speciation; at low pH, the $(PW_{11}O_{39})^{7-}$ predominates and the 1:1 $Eu(PW_{11}O_{39})^{4-}$,**2**, forms. As the pH is increased, the 1:2 Weakley complex, $Eu(PW_{11}O_{39})_2^{11-}$ species, **3** and a Eu_8 hydroxo/oxo cluster,**1**, forms. The countercations modulate this effect. Large countercations, such as K^+ and Cs^+, with low hydrodynamic radii (compared to Li^+ and Na^+) promote the formation of the 1:2 $Eu(PW_{11}O_{39})^{4-}$, **3** species and **1**, at low pH values. We postulate that these large countercations can interact with the polyoxometalate surface and position one $Eu(PW_{11}O_{39})^{4-}$ unit for binding by a

second $(PW_{11}O_{39})^{7-}$ moiety. The formation of $\{Eu(H_2O)_3(\alpha\text{-}2\text{-}P_2W_{17}O_{61})\}_2$, **4**, with Al(III) ions bound to terminal W-O bonds, is observed when Al(III) is employed as a countercation.

2.6 References

(1) For key references to lanthanide luminescence: a.Bunzli, J.-C. G. "Luminescent Probes" in Lanthanide Probes in Chemistry, Biology and Earth Sciences; Bunzli, J.-C.G.; Choppin, G. Eds.; 1989; Elsevier, Amsterdam. b. Kido, J.; Okamoto, Y. *Chem. Rev.* **2002**, *102*, 2357-2368. c. Bruce, J. I.; Dickins, R. S.; Govenlock, L. J.; Gunnlaugsson, T.; Lopinski, S.; Lowe, M. P.; Parker, D.; Peacock, R. D.; Perry, J. J. B.; Aime, S.; Botta, M., *J. Am. Chem. Soc.* **2000**, *122*, 9674-9684. d. Dickins, R. S.; Aime, S.; Batsanov, A. S.; Beeby, A.; Botta, M.; Bruce, J. I.; Howard, J. A. K.; Love, C. S.; Parker, D.; Peacock, R. D.; Puschmann, H.*J. Amer. Chem. Soc.* **2002**, *124*, 12697-12705. e. Parker, D.; Dickins, R. S.; Puschmann, H.; Crossland, C.; Howard, J. A. K. *Chem. Rev.* **2002**, *102*, 1977-2010..

(2) For key reviews on new functional materials, particularly electrochromic, electroluminescent, photochromic and photoluminescent materials, a. Katsoulis, D.E. *Chem. Rev.*, **1998**, *98*, 359-387. b.Yamase, T. *Chem. Rev.*, **1998**, *98*, 307-325. *For recent applications of lanthanide polyoxometalates incorporated into materials*: *electrochromic device preparation*, c. Liu, S.; Kurth, D. G.; Mohwald, H.; Volkmer, D.*Advanced Materials* **2002**, *14*, 225-228. *photoluminescent films*, d. Mo, Y.-G.; Dillon, R. O.; Snyder, P. G.; Tiwald, T. E. *Thin Solid Films* **1999**, *355-356*, 1-5. e. Xu, L.; Zhang, H.; Wang, E.; Kurth, D. G.; Li, Z. *J. Mater. Chem.* **2002**, *12*, 654-657. f. Xu, L.; Zhang, H.; Wang, E.; Wu, A.; Li, Z. *Materials Chemistry and Physics* **2002**, *77*, 484-488. g. Wang, Y.; Wang, X.; Hu, C.; Shi, C. *J. Mater. Chem.* **2002**, *12*, 703-707. h. Wang, J.; Liu, F.; Fu, L.;

Zhang, H. *Materials Lett.* **2002**, *56*, 300-304. i. Wang, Y.; Wang, X.; Hu, C. *Journal of Colloid and Interface Science* **2002**, *249*, 307-315. j. Wang, J.; Wang, H. S.; Fu, L. S.; Liu, F. Y.; Zhang, H. J. *Thin Solid Films* **2002**, *414*, 256-261.

(3) For key references to lanthanide Lewis Acid catalysis: a. Aspinall, H. C. *Chem. Rev.* **2002**, *102*, 1807-1850. b. Molander, G. A. *Chemtracts-Organic Chemistry* **1998**, *11*, 237-263. c. Molander, G. *Chem. Rev.* **1992**, *92*, 29-68. d. Shibasaki, M.; Yoshikawa, N. *Chem. Rev.* **2002**, *102*, 2187-2209. e. Kobayashi, S.; Kawamura, M. *J. Am. Chem. Soc.* **1998**, *120*, 5840-5841. f. Kobayashi, S. *Pure and Appl. Chem.* 1998, *70*, 1019-1026. g. Aspinall, H. C.; Dwyer, J. L. M.; Greeves, N.; McIver, E. G.; Woolley, J. C. *Organometallics* **1998**, *17*, 1884-1888. h. Xie, W.-H.; Yu, L.; Chen, D.; Li, J.; Ramirez, J.; Miranda, N. F.; Wang, P. G . in *Environmentally Benign Chemistry: Green Chemistry*; Anastas, P. T. and Williamson, T. C., Ed.; Oxford University Press: Oxford, UK, **1998**; Vol. , pp 129-149.

(4) Sadakane, M.; Dickman, M. H.; Pope, M. T. *Angew. Chem. Int. Ed.* **2000**, *39*, 2914-2916.

(5) Mialane, P.; Lisnard, L.; Mallard, A.; Marrot, J.; Antic-Fidancev, E.; Aschehoug, P.; Vivien, D.; Secheresse, F. *Inorg. Chem.* **2003**, *42*, 2102-2108.

(6) Muller, A.; Peters, F.; Pope, M. T.; Gatteschi, D. *Chemical Reviews* **1998**, *98*, 239-271.

(7) Muller, A.; Krickemeyer, E.; Bogge, H.; Schmidtmann, M.; Peters, F. *Angew. Chem. Int. Ed.* **1998**, *37*, 3360-3365.

(8) Muller, A.; Sarkar, S.; Shah, S. Q. N.; Bogge, H.; Schmidtmann, M.; Sarker, S.; Kogerler, P.; Hauptfleish, B.; Trautwein, A. X.; Schunemann, V. *Angew. Chem. Int. Ed.* **1999**, *38*, 3238-3241.

(9) Wassermann, K.; Dickman, M. H.; Pope, M. T. *Angew. Chem. Int. Ed. Engl.* **1997**, *36*, 1445-1448.

(10) Belai, N.; Sadakane, M.; Pope, M. T. *J. Am. Chem. Soc.* **2001**, *123*, 2087-2088.

(11) Bartis, J.; Dankova, M.; Blumenstein, M.; Francesconi, L. C. *Journal of Alloys and Compunds* **1997**, *249*, 56-68.

(12) Bartis, J.; Sukal, S.; Dankova, M.; Kraft, E.; Kronzon, R.; Blumenstein, M.; Francesconi, L. C. *J. Chem. Soc., Dalton Trans* **1997**, 1937-1944.

(13) Bartis, J.; Dankova, M.; Lessmann, J. J.; Luo, Q.-H.; Horrocks, W. D., Jr.; Francesconi, L. C. *Inorganic Chemistry* **1999**, *38*, 1042-1053.

(14) Luo, Q.; Howell, R. C.; Dankova, M.; Bartis, J.; Williams, C. W.; Horrocks, W. D., Jr.; Young, J., V.G.; Rheingold, A. L.; Francesconi, L. C.; Antonio, M. R. *Inorg. Chem.* **2001**, *40*, 1894-1901.

(15) Luo, Q.; Howell, R. C.; Bartis, J.; Dankova, M.; Horrocks, W. D., Jr.; Rheingold, A. L.; Francesconi, L. C. *Inorg. Chem.* **2002**, *41*, 6112-6117.

(16) Sadakane, M.; Dickman, M. H.; Pope, M. T. *Inorg. Chem.* **2001**, *40*, 2715-2719.

(17) Sadakane, M.; Ostuni, A.; Pope, M. T. *J. Chem. Soc. Dalton Trans.* **2002**, 63-67.

(18) Howell, R. C.; Perez, F. G.; Jain, S.; Horrocks, W. D., Jr.; Rheingold, A. L.; Francesconi, L. C. *Angew. Chem. Int. Ed.* **2001**, *40*, 4301-4304.

(19) Domaille, P. J. *Inorg. Synth.* **1990**, *27*, 100-101.

(20) SHELXTL, Brucker AXS, Inc., Bruker Advanced X-ray Solutions, **1999**

(21) Contant, R. *Inorg. Synth.* **1990**, *27*, 71.

(22) Contant, R.; Herve, G. *Reviews in Inorganic Chemistry* **2002**, *22*, 63-111.

(23) Hill, C. L.; Weeks, M. S.; Schinazi, R. F. *J. Med. Chem.* **1990**, *33*, 2767-2772.

(24) Ho, R. K. C.; Klemperer, W. G. *J. Amer. Chem. Soc.* **1978**, *100*, 6772-6774.

(25) When A-α- $PW_9O_{34}^{9-}$ was directly dissolved in NaAc (0.5 M, pH 6.5, 30% D_2O), the peak at 1.99 ppm along with other small peaks was observed.

(26) Thorp, H. H. *Inorg. Chem.* **1992**, *31*, 1585-1588.

(27) Brown, I. D.; Altermatt, D. *Acta Cryst.* **1985**, *B41*, 244-247.

(28) Spek, A. L. *Acta Cryst.* **1990**, *A 46*, C34.

(29) Peacock, R. D.; Weakley, T. J. R. *J. Chem. Soc.* **1971**, *A*, 1836-39.

(30) Fedotov, M. A.; Pertsikov, B. Z.; Danovich, D. K. *Polyhedron* **1990**, *9*, 1249-1256.

(31) We have also observed Eu(III)and Eu(III)-OH-Eu(III) dimeric units serving as countercations. These moieties bind to terminal W=O bonds of polyoxometalates. (Zhang, C.; Howell, R.C.; Francesconi, L.C., manuscript in preparation).

(32) Kirby, J. F.; Baker, L., C.W. *Inorganic Chemistry* **1998**, *37*, 5537-5545.

(33) Laronze, N.; Marrot, J.; Herve, G. *Inorg. Chem.* **2003**, *42*, 5857-5862.

(34) Grigoriev, V. A.; Hill, C. L.; Weinstock, I. A. *J. Am. Chem. Soc.* **2000**, *122*, 3544-3545.

(35) Grigoriev, V. A.; Cheng, D.; Hill, C. L.; Weinstock, I. A. *J. Am. Chem. Soc.* **2001**, *123*, 5292-5307.

(36) Cheng, Z.; Howell, R. C.; Luo, Q.; Fieselmann, H. L.; Todaro, L.; Francesconi, L. C., manuscript in preparation.

(37) Fang, X.; Anderson, T. M.; Neiwert, W. A.; Hill, C. L. *Inorg. Chem.* **2003**, *42*, 8600-8602.

(38) Knoth, W. H.; Domaille, P. J.; Harlow, R. L. *Inorg. Chem.* **1986**, *25*, 1577-1584.

Chapter 3. Influence of steric and electronic properties of the defect site, lanthanide ionic radii and solution conditions on the composition of lanthanide and mono-vacant $[\alpha_1\text{-}P_2W_{17}O_{61}]^{10-}$

3.1 Introduction

Polyoxometalates (POMs) are transition metal oxide clusters that have most applications in heterogeneous and homogeneous oxidation catalysts.[1,2] We envision that incorporation of lanthanide (Ln) ions into POMs offer additional useful functionality, for example, in the creation of luminescent, magnetic and Lewis Acid catalytic centers. The potential for creative Ln POM synthesis exists; for example, lanthanide ions can link polyoxometalates into oligomers and large wheel structures [3] and they can serve as connectors and transfer agents for different monolacunary POMs.[4] However, rational assembly of lanthanide polyoxometalates has not been accomplished due to the difficulty in controlling the multiple coordination requirements of Lns coupled with the often multiple basic sites of lacunary polyoxometalates. To design rational synthetic procedures it is critical to understand the principles that govern the formation of lanthanide polyoxometalates.

This study addresses the formation and stability of a class of lanthanide POMs that can be used as synthons in aqueous and organic reactions. We focus specifically on lanthanide interactions with the monovacant $\alpha_1\text{-}P_2W_{17}O_{61}^{10-}$ isomer, derived from the Wells-Dawson anion, $P_2W_{18}O_{62}^{6-}$, where the vacancy is located in the "belt" region. The structural and electronic features of the α_1 defect contribute to unique electron transfer

properties in the Wells-Dawson ion, $P_2W_{18}O_{62}^{6-}$[5] and in transition metal complexes of the α_1-$P_2W_{17}O_{61}^{10-}$ isomer.[6] Previously, we reported the isolation of the 1:1 $[(H_2O)_4Ln(\alpha_1\text{-}P_2W_{17}O_{61})]^{7-}$ complexes in solution and solid-state.[7] Here we try to understand how the structural and electronic features of the α_1-$P_2W_{17}O_{61}^{10-}$ isomer impact the speciation and stability of its Ln complexes. We are using the findings described here for the purpose of producing pure 1:1 Ln: POMs that should be useful precursors for ternary complexes wherein the solvent (water) molecules are replaced by organic ligands. This is a non-trivial task because the well-known 1:2 Ln: POM species are commonly formed for Ln complexes of α-$XW_{11}O_{39}^{n-}$ (Keggin derivatives) and the α_2-$P_2W_{17}O_{61}^{10-}$ species (vacancy in the "cap" region) and it is difficult to cleanly isolate 1:1 Ln: POM species, free of the 1:2 species. This is especially problematic when trying to produce organic soluble 1:1 species by metathesis reactions.

3.2 Experimental Section

3.2.1 General

All reagents were commercially available and used without further purification. $K_{10}[\alpha\text{-}1\text{-}P_2W_{17}O_{61}]$ was prepared following the method of Contant.[8] Elemental analyses were carried out by Inductive Coupled Plasma Atomic Emission Spectrometry (ICP-AES, SECTROFLAME M120E).

3.2.2 Synthesis and Crystallization of $[Ln(\alpha\text{-}1\text{-}P_2W_{17}O_{61})_2]^{17-}$ (Ln=La^{3+}, Eu^{3+}, Nd^{3+}, Dy^{3+}, Ho^{3+}, Er^{3+})

$K_9Li[\alpha\text{-}1\text{-}P_2W_{17}O_{61}]$ (1g, 0.20 mmol) was dissolved in 12 ml of buffer solution of LiAc (0.285 M) at pH 4.75 at room temperature, 0.115 ml of 0.90 M $LaCl_3$ solution (0.10 mmol) was added slowly to the above solution with vigorous stirring, The solution was

stirred vigorously for 15 mins, followed by addition of KCl (0.32 g, 4.29 mmol). A white precipitate formed and was collected by filtration. The white solid was redissolved in a minimum amount of buffer solution of LiAc (0.285 M) pH 4.75 and then was placed in the freezer (4°C). After three days, colorless rectangular crystals had formed. Elemental anal. Calcd for $K_{14}(H_3O)_3[La(\alpha\text{-}1\text{-}P_2W_{17}O_{61})_2]\cdot 64H_2O$: La, 1.23; W, 55.23; P, 1.09; K, 4.84. Found: La, 1.25; W, 57.29; P, 1.22; K, 4.84. Elemental anal. Calcd for $K_{14}(H_3O)_3[Eu(\alpha\text{-}1\text{-}P_2W_{17}O_{61})_2]\cdot 64H_2O$: Eu, 1.34; W, 55.17; P, 1.09; K, 4.83. Found: Eu, 1.34; W, 55.19; P, 1.11; K, 4.80. The crystals of $[Ln(\alpha\text{-}1\text{-}P_2W_{17}O_{61})_2]^{17-}$ ($Ln=Eu^{3+}$, Nd^{3+}, Dy^{3+}, Ho^{3+}, Er^{3+}) were grown in the same fashion. The crystal shapes are all similar except the size and color. The Eu, Dy analog crystals are colorless, the Nd analog crystals are light blue, while the Ho and Er crystals are very light pink.

3.2.3 Titration of $[\alpha\text{-}1\text{-}P_2W_{17}O_{61}]^{10-}$ into Eu^{3+} solution in 0.04 M KCl results in the observation of 1:2 Euα1 species monitored by ^{31}P NMR

To the solution of 17.5 μl of 1.12 M Eu^{3+} (0.056 mmol) in 2.5 ml of 0.04 M KCl (30% D_2O), 0.0629 g, 0.03145 g, 0.03145 g and 0.03145 g of $(\alpha\text{-}1\text{-}P_2W_{17}O_{61})^{10-}$ in 1:1, 1:1.5, 1:2 and 1:2.5 stoichiometric ratio was added respectively, shaken for 2 mins each time and then was placed into 10 mm NMR tube. The recorded ^{31}P NMR spectrum was shown in Figure 5.

3.2.4 Conditional Stability Constant Determination

3.2.4.1 Determination of K_1

3.2.4.1.1 Sample Preparation

All lanthanides were standardized by EDTA (standard solution, Aldrich) with xylenol orange as indicator. The molecular weight of the ligand $K_{10}[\alpha\text{-}1\text{-}P_2W_{17}O_{61}]$ was

obtained by titrating $[\alpha\text{-}1\text{-}P_2W_{17}O_{61}]^{10-}$ with $CoCl_2$ (0.2979 M) (standardized by EDTA) monitoring by UV-vis (the absorbance was recorded at 544 nm). The procedure of the ^{31}P NMR sample was prepared as follow: 0.0425 g of $K_{10}[\alpha\text{-}1\text{-}P_2W_{17}O_{61}]$ was dissolved in 2 ml of lithium acetate buffer (pH=4.72, 0.5 M, 20% D_2O), 31.0 μl of $LnCl_3$ (0.2004M) and 25 μl of EDTA (0.0974 M) was added. The solution was clear. After 8 hours at room temperature the solution reached its equilibrium. ^{31}P NMR spectrum was recorded. An external standard, phosphoric acid (0.009-0.013 M), which is placed in a smaller tube inside of 10mm NMR tube, was used to quantitatively monitor the concentrations of $[\alpha\text{-}1\text{-}P_2W_{17}O_{61}]^{10-}$. At least four determinations were performed for each lanthanide.

3.2.4.1.2 Standard Curve Preparation and Use

Calibration curve of $[\alpha\text{-}1\text{-}P_2W_{17}O_{61}]^{10-}$ vs. STD were obtained by monitoring ^{31}P NMR of four concentrations, 0.5 mM, 1.2 mM, 2.0 mM and 3.0 mM under the same conditions as for the above competition experiments. The intensity of $[\alpha\text{-}1\text{-}P_2W_{17}O_{61}]^{10-}$ /STD plotted against the concentration of $[\alpha\text{-}1\text{-}P_2W_{17}O_{61}]^{10-}$ gives a straight line, which means the intensity of $[\alpha\text{-}1\text{-}P_2W_{17}O_{61}]^{10-}$ (the peak at -8.4 ppm, for example) I_L vs. intensity of STD I_{STD} is proportional to the concentration of $[\alpha\text{-}1\text{-}P_2W_{17}O_{61}]^{10-}$. $S_g = \frac{I_L}{I_{STD}} = \kappa[L]_t$, S_g is obtained from the ^{31}P NMR spectra. Thus $[L]_t$ = Sg / k, can be used directly for the calculation of K_{eq}.

Sample ^{31}P NMR Data

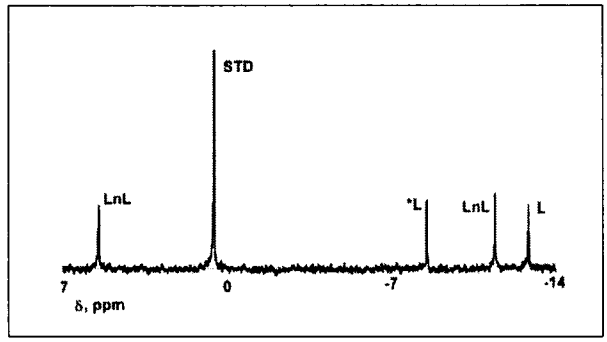

Equilibrium solution of Eu^{3+}, $(\alpha\text{-}1\text{-}P_2W_{17}O_{61})^{10-}$ and competitive ligand EDTA at LiAc (0.5 M) pH 4.75. STD= standard, LnL= $Eu(\alpha\text{-}1\text{-}P_2W_{17}O_{61})^{10-}$

Table 1. Conditional Stability Constants of LnEDTA at pH 4.72

Ln	La	Nd	Eu	Er	Lu
LogK' [a]	14.56	16.56	17.32	18.83	19.80
$Log\alpha_L$' [b]	-6.90	-6.90	-6.90	-6.90	-6.90
LogK'cond [c]	8.56	9.66	10.42	11.93	12.90

a. Martell, A. E. and Smith, R. M., *Critical stability constants*, Vol. 1, P205, Plenum Press, New York, 1974

b. EDTA has five protonation constants: log K_1^H: 10.19, log K_2^H: 6.13, log K_3^H: 2.69, log K_4^H: 2, log K_5^H: 1.5. (Martell, A. E.; Motekaits, R. J., *Determination and use of stability constants*, New York, VCH Publishers, 1992). At pH 4.72, $[H^+] = 10^{-4.72}$ M, substituted into equations (6) and (7), $Log\alpha_L' = -6.9$ was obtained.

c. Based on equations (4) and (5), LogK'cond = Log K' + Log α_L' (The number of the equations was seen in Luo's Doctoral Dissertation (page 132-133)). [9]

3.2.4.1.3 Data Analysis:

Determination of conditional formation constants for Ln (III) α-1 1:1 complexes obtained from Ligand-Ligand competition studies, the equations of the data analysis in detail were described in Luo's Doctoral Dissertation (page 132-136).[9]

3.2.4.1.4 Sample of Calculations to obtain K_{eq} and K_{cond} .

This is one of the four determinations for the conditional formation constants of Euα1 1:1 complex. 0.0425 g of α1 in 2 ml of LiOAC buffer (pH 4.72, 0.5 M, 20% D_2O) + 31.0 μl of Eu (0.275 M) + 25 μl of EDTA (0.1 M), Mw of α1= 5826.35 g/mol.

Initial concentration:

$[\alpha 1]_i$ = 0.0425/5826.35/(2000+31+25)*1000000= 0.0040637 M

$[Eu]_i$ = 31*0.275/(2000+31+25)= 0.004146 M

$[EDTA]_i$ = 25*0.1/(2000+31+25)= 0.001216 M

The integration from ^{31}P NMR spectra: STD: 0.86931, α1: 0.23505, α1/STD=0.27038. From calibration curve of α1, Sg=α1/STD=k*[α1]t, k=305.59, thus [α1]t=0.27038/305.59=0.000885 M.

Equilibrium concentration: Euα1 + EDTA ⇔ EuEDTA + α1

mass equations [α1]i =[Euα1]t + [α1]t, [Eu]i = [Euα1] + [EuEDTA], [EDTA]i = [EDTA]t + [EuEDTA]

[Euα1]t= [α1]i - [α1]t =0.0040637-0.000885=0.003179 M

[EuEDTA]= [Eu]i – [Euα1]= 0.004146-0.003179=0.0009675 M

[EDTA]t= [EDTA]i – [EuEDTA]= 0.001216-0.0009675=0.000248 M

Keq = [EuEDTA]t[α1]t/([Euα1]t[EDTA]t)= 0.0009675*0.000885/(0.003179*0.000248)=1.084145, Log Keq= 0.035088

From equation (2), Log Keq= Log Kcon(EuEDTA)-Log Kcon(Euα1), LogK'con(EuEDTA)= 10.42, thus Log Kcon(Euα1)= 10.42-0.035088= 10.38

3.2.4.2 Determination of K_2:

3.2.4.2.1 Equilibrium constant measurement of $[Ln(\alpha\text{-}1\text{-}P_2W_{17}O_{61})_2]^{17-}$ (Ln = La^{3+}, Nd^{3+}, Eu^{3+}, Dy^{3+}, Ho^{3+}, Er^{3+}) at different counter cation monitored by ^{31}P NMR.

The buffer solution of LiAc (0.02 M), NaAc (0.02M), KAc (0.02 M) and CsAc (0.02 M) (30% D_2O) at pH 4.85±0.10 was prepared respectively. In 10 mm NMR tube, 0.06 g of $(\alpha\text{-}1\text{-}P_2W_{17}O_{61})^{10-}$ was dissolved in 2 ml of above buffer solution respectively, and then different Ln^{3+} ($(\alpha\text{-}1\text{-}P_2W_{17}O_{61})^{10-}$ / Ln^{3+} stiochiometric ratio = 2.2) was added

separately, the resulting solution was shaken for about 30 min, and then was placed at room temperature for 5 hour. ^{31}P NMR spectrum was recorded afterwards. The external standard was phosphoric acid (0.009-0.013 M) in a small tube, which was placed inside a 10 mm NMR tube. The calibration curve $(\alpha\text{-1-}P_2W_{17}O_{61})^{10-}$ vs. STD was obtained at four different concentrations, 0.5 mM, 1.0 mM, 2.0 mM, and 3.0 mM by monitoring ^{31}P NMR. The equilibrium constants of $[Ln(\alpha\text{-1-}P_2W_{17}O_{61})_2]^{17-}$ at different counter cation, Li^+, Na^+, K^+, Cs^+ was displayed in Figure 1 and Table 2. At least four determinations were performed for each analysis.

3.2.4.2.2 Sample Standard Curve

The calibration curve of $(\alpha\text{-1-}P_2W_{17}O_{61})^{10-}$ is the same as in determination of K_1

Sample Spectrum

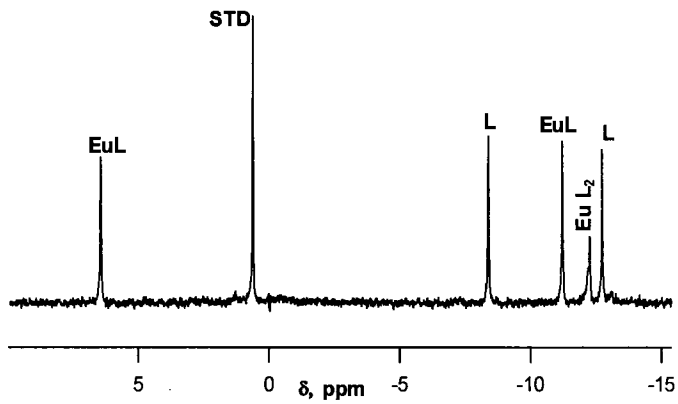

^{31}P NMR spectrum of equilibrium solution of Eu^{3+}, $(\alpha\text{-1-}P_2W_{17}O_{61})^{10-}$ in 1:2 ratio at NaAc (0.04 M) pH 4.75. STD is the external standard (0.01228 M of H_3PO_4 in H_2O). EuL is $[Eu(\alpha\text{-1-}P_2W_{17}O_{61})]^{7-}$, L is ligand $(\alpha\text{-1-}P_2W_{17}O_{61})^{10-}$, EuL_2 is $[Eu(\alpha\text{-1-}P_2W_{17}O_{61})_2]^{17-}$.

In these NMR spectra, we find that the downfield ^{31}P peak for EuL_2 (close to Eu) is broad and not easily observed, especially when in low concentration (see Figure 5). The equilibrium expression is written in terms of the initial Eu concentration and the

POM concentration (see below), the concentrations are higher for these species and the resonances are sharp and thus can be successfully integrated.

3.2.4.2.3 Data Analysis:

$Eu + L \rightarrow EuL + L \Leftrightarrow EuL_2$ (1)

$[Eu]_0 = [EuL]_t + [EuL_2]_t + [Eu]_t$ (2)

$[L]_0 = [EuL]_t + [L]_t + 2[EuL_2]_t$ (3)

Hence:

$[EuL]_t = [Eu]_0 - [EuL_2]_t$ (4) and

$[EuL]_t = [L]_0 - [L]_t - 2[EuL_2]_t$ (5) therefore

$[Eu]_0 - [EuL_2]_t = [L]_0 - [L]_t - 2[EuL_2]_t$ (6)

$[EuL_2]_t = [L]_0 - [L]_t - [Eu]_0$ (7)

$[EuL]_t = [L]_t - [L]_o + 2[Eu]_0$ (8)

$$K = \frac{[EuL_2]_t}{[EuL]_t[L]_t} = \frac{[L]_0 - [L]_t - [Eu]_0}{([L]_t - [L]_0 + 2[Eu]_0)[L]_t}$$

Assumptions: The 1:1 complex of LnL forms immediately, $Ln + L \rightarrow LnL$, thus there are no non- coordinated Ln ions present in the solution.

3.2.4.2.4 Sample of Data Analysis

For example: 0.0686 g of α1 in 2 ml of KOAC buffer (pH 4.85, 0.02 M, 20% D_2O) + 30.0 µl of Eu (0.1897 M), this is just one of the four determinations for the conditional formation constants of Euα1 1:2 complex. Mw of α1= 4948.51 g/mol

Initial concentration:

$[Eu]_0$= 30*0.1897/(2000+30)= 0.003 M

$[L]_0$= 0.0686/4948.51/(2000+30)*1000000= 0.00683 M

The integration from ^{31}P NMR: STD = 0.80724, L= 0.55813, L/STD=0.69141. From calibration curve of α1, Sg=L/STD=k*$[L]_t$, k=318.77, thus

$[L]_t$=0.69141/318.77=0.002169 M.

Equilibrium concentration: EuL + L ⇔ EuL_2

From equations (7) and (8) above, $[EuL_2]_t = [L]_0 - [L]_t - [Eu]_0$ = 0.00683-0.002169-0.003=0.00168 M,

$[EuL]_t = [L]_t - [L]_0 + 2[Eu]_0$ = 0.002169-0.00683+2*0.003=0.0013 M

Thus, $K_2 = [EuL2]_t/([EuL]_t[L]_t)$= 0.00168/(0.0013*0.002169)= 597.3269, $LogK_2$ = 2.78

3.2.5 Elemental analysis by ICP

i) Standard solution preparation. The standard solution of P (0.2, 0.4, 0.6, 0.8, 1.2 ppm), Eu (1, 2, 4, 6 ppm), La (1, 2, 4, 6 ppm), W (20, 40, 60, 80, 120 ppm), Al (0.5, 1, 1.5, 2.5 ppm), Na (1, 3, 5, 7 ppm), and K (1, 3, 5, 7 ppm) was prepared by diluting 1000 ppm ICP standard solution (GFS Chemicals, Inc.) with distilled water. ii) Sample preparation. Crystals of complex $[Ln(\alpha\text{-}1\text{-}P_2W_{17}O_{61})_2]^{17-}$ ($Ln=La^{3+}$, Eu^{3+}) were collected by filtration, and were placed in uncovered, carefully labeled, small vials, then were put into a dessicator ($CaSO_4$ as drying agent), vacuum for 1.5 hour. The samples were left in the closed evacuated dessicator overnight. Afterwards, 0.0148 g of $[Eu(\alpha\text{-}1\text{-}P_2W_{17}O_{61})_2]^{17-}$ and 0.0106 g of $[La(\alpha\text{-}1\text{-}P_2W_{17}O_{61})_2]^{17-}$ was dissolved in a 25 ml volumetric flask with distilled water. 2 and 4 ml of solution from each flask was filled in to 25 ml of volumetric flask individually to make ICP samples. iii) Method: The sensitive wavelength for different element was selected (P: 213.618 nm; Eu: 381.970 nm; La:

379.478 nm, W: 239.709 nm; Na: 589.592 nm; K: 766.496 nm). A calibration curve for each element was constructed. The measurement of each sample was then performed.

3.2.6 Collection of NMR Data

All NMR spectra were recorded on a JEOL GX-400 spectrometer with 5 or 10 mm tubes. Resonance frequencies are 161.8 MHz for ^{31}P and 16.7 for ^{183}W. Chemical shifts are given with respect to external 85% H_3PO4 for ^{31}P and 2.0 M Na_2WO_4 for ^{183}W. Typical acquisition parameters for ^{31}P spectra included the following: spectral width, 10000 Hz; acquisition time, 0.8 s; pulse delay, 1 s; pulse width, 15 μs (50° tip angle). From 200 to 1000 scans were required. For ^{183}W spectra, typical conditions included the following: spectral width, 10000 Hz; acquisition time, 1.6 s; pulse delay, 0.5 s; pulse width, 50 μs (45° tip angle). From 1000 to 30000 scans were acquired. For all spectra, the temperature was controlled to 25 ± 0.2 deg. For both ^{31}P and ^{183}W chemical shifts, the convention used is that the more negative chemical shifts denote upfield resonances.

3.2.7 Single Crystal X-ray Structure Determination

Block-like crystals of $[La(\alpha\text{-}1\text{-}P_2W_{17}O_{61})_2]^{17-}$ were isolated from solution and examined under a thin layer of mineral oil using a polarizing microscope. A suitable crystal was chosen and mounted on a glass fiber while still coated in oil; the crystal was then immediately frozen to 100K on a Bruker Nonius Kappa CCD diffractometer equipped with a sealed tube Mo anode (K_∂ radiation, λ=0.71073 Å) and graphite monochromator. Since crystals of $[Eu(\alpha\text{-}1\text{-}P_2W_{17}O_{61})_2]^{17-}$ turned dark or broke into pieces once out of the oil, the selected crystals were mounted in the loop to make sure the crystals stay in the oil and then quickly placed in a stream cold nitrogen. Data collection, indexing, and initial cell refinements were all handled using accompanying proprietary

Nonius software. The SHELX package of software was used to solve and refine the restructures. The heaviest atoms were located by direct methods, and the remaining atoms were found in subsequent Fourier difference. Data for crystals of $K_{14}(H_3O)_3[Ln(\alpha\text{-}1\text{-}P_2W_{17}O_{61})_2]\cdot nH_2O$ (Ln = Nd^{3+}, Eu^{3+}, Er^{3+}) were collected using a cryoloop which was then frozen at 100 K. These crystals decomposed easily upon removal from the freezer and during the X-ray experiment.

To solve the solvent disorder problem, Platon/SQUEEZE was used to determine the void volume in each of the three structures approximating to an additional 50 hydrogen bonded water molecules per unit cell.[10] The void volumes present were for 1899 $Å^3$ La, 2016 $Å^3$for Nd and 2054 $Å^3$for Eu representing 12.1 %, 12.6 % and 24.5 % of the unit cell volumes respectively.

It is typical to observe peaks adjacent to the W atoms in polyoxometalates, as seen in these structures.[11] The large residual peaks and high R_{int} observed in the Eu and Nd analogs may also be due to decomposition of the crystals as the data is being collected.

3.3 Results and Discussion

The stepwise stability constants, K_1 and K_2, equations 1 and 2, and the log K_1/log K_2 ratio is an indicator to forming stable 1:1 Ln: POM complexes.

$$Ln + (\alpha_1\text{-}P_2W_{17}O_{61})^{10-} \rightleftharpoons (H_2O)_4Ln(\alpha_1\text{-}P_2W_{17}O_{61})^{7-} \qquad K_1 \quad (1)$$

$$(H_2O)_4Ln(\alpha_1\text{-}P_2W_{17}O_{61})^{7-} + (\alpha_1\text{-}P_2W_{17}O_{61})^{10-} \rightleftharpoons Ln(\alpha_1\text{--}P_2W_{17}O_{61})_2^{14-} \quad K_2 \quad (2)$$

The conditional stability constants, log K_1 (eq 1) and log K_2 (eq 2), for Ln complexes of $(\alpha_1\text{-}P_2W_{17}O_{61})^{10-}$, shown in **Table 2**, were determined using ^{31}P NMR spectroscopy that gives direct determination of concentrations and allows the exact

speciation to be monitored. The increase of K_1, as the lanthanide series is traversed, is consistent with our synthetic observations that isolation of the 1:1 Ln: $(\alpha_1\text{-}P_2W_{17}O_{61})^{10-}$

Table 2. Conditional Stability Constants for Lanthanide Complexes of $\alpha_1\text{-}P_2W_{17}O_{61}{}^{10-}$

Lanthanide	La	Nd	Eu	Dy
Log K_1[a]	8.00 ± 0.17	8.63± 0.22	10.35± 0.22	11.08± 0.15
Log K_2 (Li^+)[b]	2.190 ±0.017	2.069± 0.025	2.177± 0.003	2.132± 0.008
LogK_2 (Na^+)[b]	2.257 ± 0.03	2.559± 0.009	2.421± 0.022	2.493± 0.009
Log K_2 (K^+)[b]	2.609± 0.015	2.788± 0.005	2.785± 0.008	2.677± 0.018
Log K_2 (Cs^+)[b]	3.139± 0.026	3.321± 0.023	3.220± 0.041	3.099± 0.014
Log K_1/LogK_2	3.65	4.17	4.75	5.19

Table 2. Conditional Stability Constants for Lanthanide Complexes of $\alpha_1\text{-}P_2W_{17}O_{61}{}^{10-}$ (continue)

Lanthanide	Er	Yb	Lu
Log K_1[a]	11.62± 0.09	12.21± 0.12	12.50± 0.09
Log K_2 (Li^+)[b]	2.233± 0.006	2.043± 0.033	1.874± 0.007
LogK_2 (Na^+)[b]	2.264± 0.021	2.313± 0.054	2.042± 0.008
Log K_2 (K^+)[b]	2.351± 0.024	2.464± 0.012	2.139± 0.026
Log K_2 (Cs^+)[b]	2.517± 0.006	2.521± 0.003	2.185± 0.006
Log K_1/LogK_2 [c]	5.20	5.98	6.67

a. K_1 determined from competition experiments, monitored by ^{31}P NMR, using EDTA as competitive ligand, pH=4.7, 0.5M $LiNO_3$, 25°C. See supporting material for details.

b. K_2 determined by ^{31}P NMR measurements, described in supporting material. Conditions: pH=4.85; 0.02M Macetate (M=Li,Na,K,Cs); 25°C.

c. K_2: 0.02M LiOAc

species is facile for the later lanthanides.[7a] The data support the notion that the high basicity of the α1 vacancy, ascribed to the orientation of the PO_4^{3-} tetrahedron, positioning a basic oxygen atom near the α1 site, requires high charge/size cations for stabilization.[12] The α1 defect also is rigid, compared to the α2 defect that

accommodates lanthanide ions across the Ln series with similar K_1 and K_2 stability constants. Stability constants (thermodynamic) have been reported for Ln complexes of α_2-$P_2W_{17}O_{61}^{10-}$, and although these are limited to Ce(III), Nd(III) and Eu(III), they lead to the conclusion that K_1 and K_2 are constant across the series at between 10.35 - 12.7 and 7-8.1, respectively. The ratio log K_1/log K_2 = 1.47- 1.57.[13] Our own data, using NMR competition methods luminescence titrations, are consistent with these studies. We find that for Ln complexes of α_2-$P_2W_{17}O_{61}^{10-}$, log K_1 (thermodynamic) is constant for lanthanides spanning the Ln series (La-Lu) at ca 11.3-12.0 and log K_2 is also constant, ranging from 5.8 to 6.6 and the log K_1/log K_2 ratio = 1.95-2.00.[14] Ciabrini reported conditional constants for Ce(III) α2 $P_2W_{17}O_{61}^{10-}$ (log K_1: 8.8; log K_2: 6.0; log K_1/log K_2=1.47).[12] Recent determination of conditional stability constants measured for Eu(III) and other lanthanides also support the constant K_1 across the Ln series.[15]

The conditional log K_2 constants for Ln complexes of $(\alpha_1$-$P_2W_{17}O_{61})^{10-}$, as a function of countercation (Li^+, Na^+, K^+, and Cs^+), are much lower than K_1 and are dependent on the lanthanide ionic radius as well as on the countercation. Our data (K_1, K_2, log K_1/log K_2) are consistent with the conditional stability constants reported by Contant for Ce(III) complexes of the α1 $P_2W_{17}O_{61}^{10-}$ isomer (1M $LiNO_3$, log K_1: 6.6; log K_2: 1.5; log K_1/log K_2= 4.4) using spectrophotometric and potentiometric techniques.[8]

Synthesis, crystallization and X-ray crystallographic analyses of the 1:2 Ln: $(\alpha_1$-$P_2W_{17}O_{61})^{10-}$ (Ln= La, Nd, Eu, Er) species were compromised by the lack of stability, as expected by the low stability constants, and the Yb and Lu analogs could not be isolated. Crystal decomposition hindered the X-ray diffraction analysis.

All of the crystals showed the 1:2 formulation, Figure 2; As shown in Table 3, the La(III) analog gave the highest quality data. The formulation of $K_{14}(H_3O)_3[Ln(\alpha_1\text{-}P_2W_{17}O_{61})_2]\cdot xH_2O$ for La and Eu was also confirmed by elemental analysis of crystals.

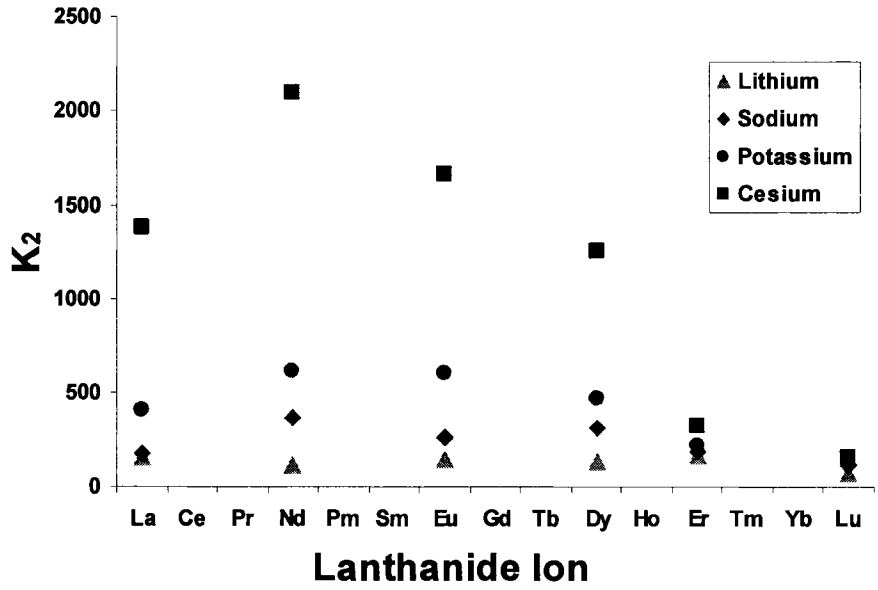

Figure 1. K_2 for formation of $[Ln(\alpha\text{-}1\text{-}P_2W_{17}O_{61})_2]^{17-}$ as a function of lanthanide ion and countercation

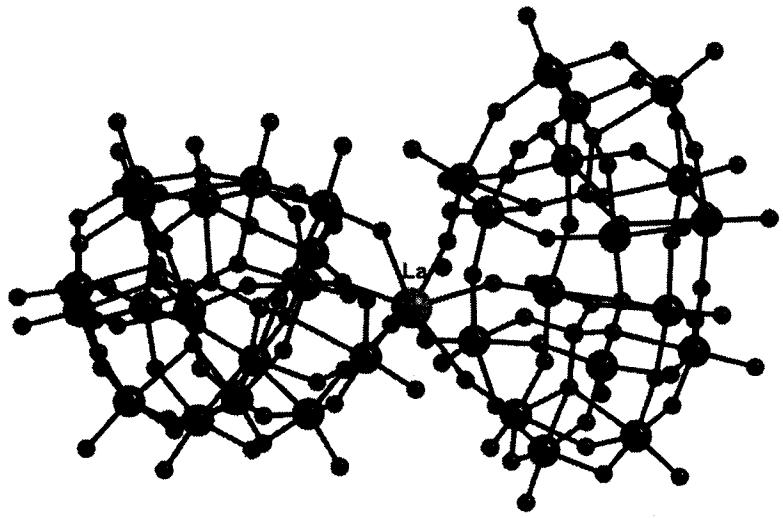

Figure 2. Ball and Stick representation of $[La(\alpha\text{-}1\text{-}P_2W_{17}O_{61})_2]^{17-}$ (La: large gray balls; P: small gray balls; W: large dark balls; O: small dark balls.)

Table 3. Crystal data and Structure Refinement for $K_{14}(H_3O)_3[La(\alpha\text{-}1\text{-}P_2W_{17}O_{61})_2]\cdot nH_2O$

empirical formula	$K_{14}LaP_4W_{34}O_{158}$	$H_{82}K_5Cl_3EuP_4W_{34}O_{155.5}$	$H_{92}K_4Cl_4Na_4NdP_4W_{34}O_{162}$
Formula weight	9589.09	9399.25	9593.92
crystal system	Monoclinic	Triclinic	Monoclinic
space group	C2/c	$P\bar{1}$	C2/c
temp, K	100 K	100K	100 K
wavelength, Å	0.71073	0.71073	0.71073
a, Å	41.339(8)	16.432(3)	41.072(8)
b, Å	15.636(3)	21.204(4)	16.152(3)
c, Å	24.988(5)	25.860(5)	24.933(5)
α, deg	90	88.82(3)	90
β, deg	104.53(3)	82.32(3)	104.63(3)
γ, deg	90	69.61(3)	90
Vol, $Å^3$	15635(5)	8367(3)	16004(6)
Z	4	2	4
calcd density, g/cm^3	4.074	3.731	3.982
abs coeff, mm^{-1}	25.692	23.947	24.980
F (000)	16652	8222	16848
θ range, deg	1.40 to 27.57 deg	2.91 to 27.49	2.90 to 27.32 deg
limiting indices	-53<=h<=53, -20<=k<=20, -32<=l<=32	-21<=h<=21, -27<=k<=27, -33<=l<=33	-52<=h<=52, -20<=k<=20, -30<=l<=30
reflns collected/unique	34400/17934 [R(int)=0.0557]	117898/38252 [R(int)=0.1603]	59874/17288 [R(int)=0.2791]
Refinement meth	Full-matrix least squares on F^2	Full-matrix least squares on F^2	Full-matrix least squares on F^2
data/ restraints/ parameters	17934 / 0 / 568	38252/3/1047	17288 / 0 / 540
GOF on F^2	1.070	1.053	1.044
final R indices [I>2σ(I)]	R_1 = 0.0744, wR_2 = 0.1953	R_1 = 0.1125, wR_2 = 0.2761	R_1 = 0.1232, wR_2 = 0.2800
R indices (all data)	R_1 = 0.1162, wR_2 = 0.2360	R_1 = 0.1786, wR_2 = 0.3158	R_1 = 0.1861, wR_2 = 0.3100
largest diff.peak and hole ($eÅ^{-3}$)	10.493 and -7.549	25.827 and -17.214	6.804 and -6.403

Table 4. Selected Bond Lengths and Angles for $[Ln(\alpha_1\text{-}P_2W_{17}O_{61})_2]^{17-}$

La1 - O9 2.480 (11)	Nd – O2N 2.467(4)	Eu – O11E 2.402 (25)
La1 - O21 2.471 (5)	Nd – O6N 2.445(8)	Eu – O2E 2.351 (35)
La1 - O39 2.506 (7)	Nd – O11N 2.378(11)	Eu – O9E 2.402 (47)
La1 - O61 2.445 (10)	Nd – O9N 2.475(10)	Eu – O6E 2.411 (36)
Eu – O22E 2.397 (15)		
Eu – O26E 2.365 (18)		
Eu – O31E 2.356 (56)		
Eu – O27E 2.378 (26)		

The X-ray crystallography structure, shown in Figure 2, reveals the source of the instability of the 1:2 complex. The Ln(III) center is bound, in a square antiprismatic coordination geometry, to two $(\alpha_1\text{-}P_2W_{17}O_{61})^{10-}$, with Ln-O bond lengths that decrease as the Ln series is traversed (Table 4). As a response to the decreasing bond lengths, the angle, that represents the spreading apart of the two $(\alpha_1\text{-}P_2W_{17}O_{61})^{10-}$ moieties, opens significantly across the series: 64.5° (La), 77.2 (Nd), 81.6° (Eu). The acute angle results in closer contact of the POM lobes, resulting in steric encumbrance.

Orientation of the $(\alpha_1\text{-}P_2W_{17}O_{61})^{10-}$ units is shown in Figure 3. The relative orientation of the two α-1 lobes can be described by two angles. The first angle describes the "rotation" of the units relative to each other. This angle can be assessed by constructing a plane through both phosphorous atoms and the lanthanide atom in each unit and then calculating the angle between these planes. This angle does not show significant variation, varying from 111, 108, and 112 for La, Nd, and Eu, respectively. The second angle, that shows significant variation, can be aptly described as an "opening up" of the units. This angle is assessed by constructing planes through both phosphorous atoms, the apical phosphorous oxygen atoms, and a bridging oxygen in the cap region. This angle changes from La, 64.5; Nd, 77.2; Eu 81.6; and reflects the spreading apart of the POM lobes.

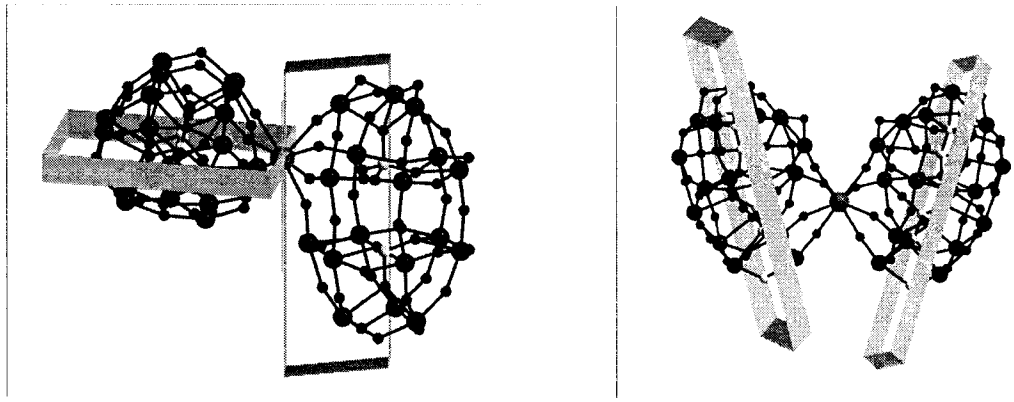

Planes that describe Rotation Planes that describe Spreading Apart of POMs

Figure 3. Display of angles between two $(\alpha\text{-}1\text{-}P_2W_{17}O_{61})^{10-}$ units in $[La(\alpha\text{-}1\text{-}P_2W_{17}O_{61})_2]^{17-}$

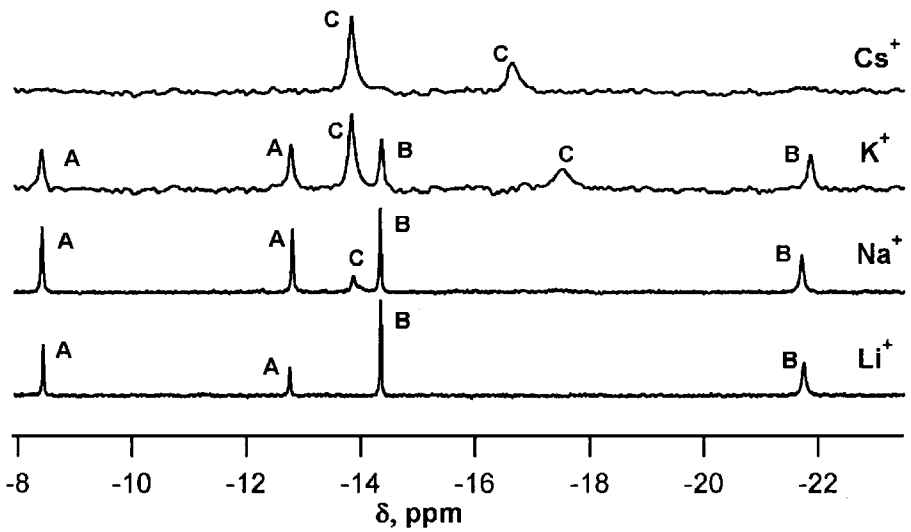

Figure 4. Speciation dependence of 0.01 mmol of $[Nd(\alpha_1\text{-}P_2W_{17}O_{61})_2]^{17-}$ on counteraction (0.04 M) in water monitored by ^{31}P NMR spectroscopy. A. Ligand $[\alpha\text{-}1\text{-}P_2W_{17}O_{61}]^{10-}$; B. 1:1 $[Nd(\alpha_1\text{-}P_2W_{17}O_{61})]^{7-}$, C. 1:2 $[Nd(\alpha_1\text{-}P_2W_{17}O_{61})_2]^{17-}$.

The ^{31}P NMR and ^{183}W spectra can only be obtained in D_2O that is high in salt content, KCl or CsCl, and it appears that there are two species in solution. The NMR data are consistent with two species in solution (See Luo's Doctoral Dissertation, Figure 5.4, 5.5, and 5.6).[9] The ^{31}P NMR data is summarized in Table 5. The downfield chemical

shifts for La and Nd are unsymmetrical, showing a broad peak and a possible doublet. The two peaks are spread out in the Eu(III) analog. The major species shows two resonances consistent with equivalence of each $(\alpha\text{-}1\text{-}P_2W_{17}O_{61})^{10-}$ unit. The minor species appears to show a "doublet" in the downfield region, possibly consistent with the C_1 symmetry of the 1:2 species, as isolated in the crystal structure. The observation of $[Eu(\alpha\text{-}1\text{-}P_2W_{17}O_{61})_2]^{17-}$ was obtained in our lab by titrating Eu^{3+} with ligand $(\alpha\text{-}1\text{-}P_2W_{17}O_{61})^{10-}$ in 0.04 M KCl solution (see Figure 5). It is clear to show that there is more than one type of 1:2 complexes exist in the solution. In this case, K2 calculations have almost certainly been made on several 1:2 complexes and this could tie in with the high observed K2 for Nd and the counter cation effect mentioned above (Figure 1 and table 2).

Speciation of 1:2 Lnα_1 complexes is highly counter cation dependent. Crystals of the $[Nd(\alpha_1\text{-}P_2W_{17}O_{61})_2]^{17-}$ dissolved in aqueous buffer, clearly show the speciation dependence on the counterion (Figure 1). The 1:2 complex is stabilized by Cs^+ (0.04M); an equilibrium between the 1:2, 1:1 complexes and $(\alpha_1\text{-}P_2W_{17}O_{61})^{10-}$ is observed in 0.04 M K^+ and only 1:1 complex and ligand are observed in 0.04 M Li^+ or Na^+ buffer. Luminescence lifetime measurements taken in D_2O and H_2O for the Eu(III) analog show that no water molecules are bound to the Eu(III) center,[16] consistent with the 1:2 formulation.

The ^{183}W NMR, showing 16 peaks, (2 overlap at –215 ppm) is consistent with the major species, as observed in the ^{31}P NMR spectrum, representing a species where the two $(\alpha\text{-}1\text{-}P_2W_{17}O_{61})^{10-}$ units are equivalent. The resonances for the minor species are likely buried in the noise of the spectrum. (See Luo's Doctoral Dissertaion, Figure 5.7).[9]

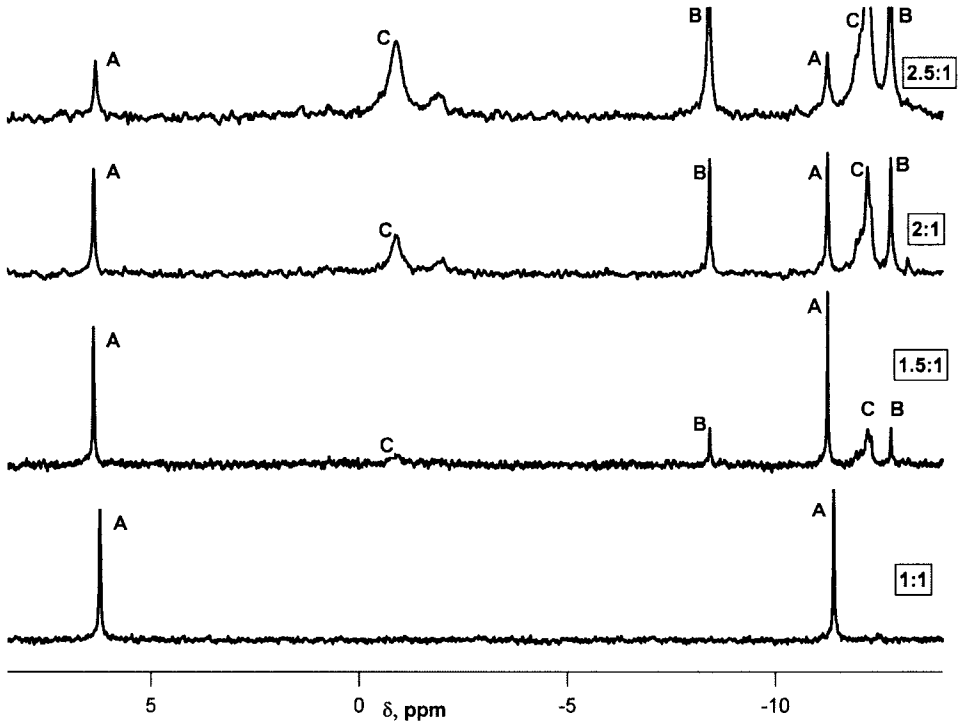

Figure 5. Titration of $[\alpha\text{-1-}P_2W_{17}O_{61}]^{10-}$ into 17.5 µl of 0.728 M Eu^{3+} solution in 0.04 M KCl monitored by ^{31}P NMR.A. 1:1 $[Eu(\alpha\text{-1-}P_2W_{17}O_{61})]^{7-}$, B. Ligand $[\alpha\text{-1-}P_2W_{17}O_{61}]^{10-}$, C. 1:2 $[Eu(\alpha\text{-1-}P_2W_{17}O_{61})_2]^{17-}$.

Table 5. ^{31}P NMR chemical shift of $[Ln(\alpha\text{-1-}P_2W_{17}O_{61})_2]^{17-}$

Ln	δ, ppm
La	-9.56 (m), -12.96 (m)
Nd	-13.96 (d), -16.32(s)
Eu	-0.919(s), -2.01(d), -11.94 (d), -12.19 (s)

m= multiplet, d= doublet, s= singlet

3.4 Conclusions

In summary, stabilization of the 1:1 Ln: $(\alpha_1\text{-}P_2W_{17}O_{61})^{10-}$ complex with respect to the 1:2 complex is due to the high conditional stability constant, K1 and the very low K2. K2 is dependent on solution conditions and is derived from the severe steric strain due to the proximity of the $(\alpha_1\text{-}P_2W_{17}O_{61})^{10-}$ lobes. We have produced organic soluble 1:1 Ln:

$(\alpha_1\text{-}P_2W_{17}O_{61})^{10-}$ complex, free of the 1:2 and other impurities. These and their reactivity in organic solvents will be reported in chapter 5.

3.5 References

1) a. Katsoulis, D. E.,*Chem. Rev.* **1998,** *98*, 359-387. b. Mizuno, N.; Misono, M.,*Chem. Rev.* **1998,** *98*, 199-217.

2) Weinstock, I. A.; Barbuzzi, E. M. G.; Wemple, M. W.; Cowan, J. J.; Reiner, R. S.; Sonnen, D. M.; Heintz, R. A.; Bond, J. S.; Hill, C. L.,*Nature* **2001,** *414*, 191-195.

3) a. Sadakane, M.; Dickman, M. H.; Pope, M. T.,*Angew. Chem. Int. Ed.* **2000,** *39*, 2914-2916. b. Mialane, P.; Lisnard, L.; Mallard, A.; Marrot, J.; Antic-Fidancev, E.; Aschehoug, P.; Vivien, D.; Secheresse, F.,*Inorg. Chem.* **2003,** *42*, 2102-2108. c. Wassermann, K.; Dickman, M. H.; Pope, M. T.,*Angew. Chem. Int. Ed. Engl.* **1997,** *36*, 1445-1448.

4) Belai, N.; Sadakane, M.; Pope, M. T.,*J. Am. Chem. Soc.* **2001,** *123*, 2087-2088.

5) a. Kozik, M.; Hammer, C. F.; Baker, L. C. W.,*J. Am. Chem. Soc.* **1986,** *108*, 2748-2749. b.Kozik, M.; Baker, L. C. W.,*J. Am. Chem. Soc.* **1990,** *112*, 7604-7611. c. Keita, B.; Levy, B.; Nadjo, L.; Contant, R.,*New. J. Chem.* **2002,** *26*, 1314-1319. d. Lopez, X.; Bo, C.; Poblet, J. M.,*J. Am. Chem. Soc.* **2002,** *124*, 12574-12582.

6) Contant, R.; Abbessi, M.; Canny, J.; Belhouari, A.; Keita, B.; Nadjo, L.,*Inorg. Chem.* **1997,** *36*, 4961-4967. b. Contant, R.; Richet, M.; Lu, Y. W.; Keita, B.; Nadjo, L.,*Eur. J. Inorg. Chem.* **2002,** c. Keita, B.; Girard, F.; Nadjo, L.; Contant, R.; Canny, J.; Richet, M.,*J. Electroanal. chem.* **1999,** *478*, 76-82.

7) a. Bartis, J.; Dankova, M.; Lessmann, J. J.; Luo, Q.-H.; Horrocks, W. D., Jr.; Francesconi, L. C., *Inorg. Chem* **1999,** *38*, 1042-1053. b. Luo, Q.; Howell, R.C.; Bartis, J.; Dankova, M.; Williams, C.; Horrocks, W.DeW., Jr.; Young, V.C., Jr,; Rheingold, A.L.; Francesconi, L.C.; Antonio, M.R.*Inorg. Chem.* **2001**, *40*, 1894.

8) Contant, R., *Inorg. Synth*, 1990, 27, 71

9) Luo, Q-H., Doctoral Dissertation, Chemistry Department of the City University of New york, **2002**.

10) Sluis & Spek, *Acta Cryst.* **1990**, *A46*, 194

11) Ortega, F.; Pope, M. T.; Evans, J., H.G. *Inorg. Chem.* **1997**, *36*, 2166-2169., Sazani, G.; Dickman, M. H.; Pope, M. T. *Inorg. Chem.* **2000**, *39*, 939-943; Wasserman, K.; Lunck, H. J.; Palm, R.; Fuchs, J.; Steinfeldt, N.; Stoesser, R.; Pope, M. T. *Inorg. Chem.* **1996**, *35*, 3273-9; Xin, F.; Pope, M. F. *Inorg. Chem.* **1996**, *35*, 5693-5695; Zhang, X. Y.; O'Connor, C. J.; Jameson, G. B.; Pope, M. T. *Inorg. Chem.* **1996**, *35*, 30-34).

12) Ciabrini, J.-P.; Contant, R.,*J. Chem. Research (M).* **1993,** 2720-2744.

13) Bion, L.; Mercier, F.; Decambox, P.; Moisy, P.,*Radiochim. Act*a **1999**; 161-166.

14) Luo, Q.-H.; Zhang, C.; Howell, R.C.; Francesconi, L.C., manuscript in preparation.

15) Van Pelt, C. E.; Crooks, W. J., III; Choppin, G. R.,*Inorg. Chim. Acta.* **2003,** 1-8.

16) q= 0.34, 0.5M KCl; Horrocks, W. D., Jr.,*Methods in Enzymology* **1993,** *226*, 495-538.

Chapter 4. Influence of the lanthanide and solutions conditions on formation of lanthanide complexes of mono-vacant [α_2-$P_2W_{17}O_{61}]^{10-}$ POMs.

4.1 Introduction

Lanthanide (Ln) ions can offer unique functionality when combined with polyoxometalates. The use of lanthanide ions to "link" POMs into solid-state oligomers [1] and large wheel structures [2] has been observed in solid-state X-ray crystal structures. Solution studies demonstrate that lanthanide ions can also serve as connectors and transfer agents for different monolacunary POMs.[3] In addition to the potential for creation of new materials, we envision that incorporation of lanthanide ions into POMs offer additional useful functionality, for example, in the creation of luminescent,[4] magnetic, Lewis acid catalytic centers.[5]

In order to realize the potential of Ln POMs, it is critical to understand the speciation chemistry. Polyoxometalate composition in aqueous solution is dynamic; multiequilibria exist depending on pH, countercation, concentration and aging of the solution. Lanthanide ions also show complex dynamic behavior in aqueous solution. Such an understanding of the complex solution speciation and dynamics for POMs, in general, and Ln POMs, specifically, is lacking.

We and others have studied the aqueous chemistry of lanthanide complexes of the mono-vacant lacunary polyoxometalates, specifically, $(\alpha_2\text{-}P_2W_{17}O_{61})^{10-}$ and $(\alpha_1\text{-}P_2W_{17}O_{61})^{10-}$ isomers, derived from the Wells-Dawson ion, $[\alpha\text{-}P_2W_{18}O_{62}]^{6-}$, where the

defect is incorporated into the "cap" and "belt" regions of the POM, respectively.[[6] Two recent studies suggest the dependence of structure and equilibria on the lanthanide ionic radius and solution conditions. In one study by Sadakane, the solid-state X-ray crystallography shows that the $[Ce(\alpha_2\text{-}P_2W_{17}O_{61})]^{7-}$ species is actually a 2:2 dimer wherein the Ce(III) is nine-coordinate, exhibiting a capped square antiprismatic coordination geometry and is bound to four oxygen atoms of the $(\alpha_2\text{-}P_2W_{17}O_{61})^{10-}$ unit, four water molecules and an adjacent terminal W=O bond of an adjacent $[Ce(\alpha_2\text{-}P_2W_{17}O_{61})]^{7-}$ unit.[7] In solution, the "dimer" dissociates to form a monomeric species, as demonstrated by ^{183}W NMR spectroscopy. ^{31}P NMR experiments in water showed an equilibrium between the 1:1 and 1:2 Ce(III): $\alpha_2\text{-}P_2W_{17}O_{61}{}^{10-}$ species.

The mid-late lanthanides behave differently. We reported the Eu(III) analog where the Eu(III) is 8-coordinate, bound to four oxygen atoms of the $\alpha_2\text{-}P_2W_{17}O_{61}{}^{10-}$, three water molecules and to a terminal W-O of the "belt" region of an adjacent $[\alpha_2\text{-}P_2W_{17}O_{61}]$, forming a "cap to belt" 2:2 dimer. ^{183}W NMR and luminescence experiments suggest that the dimer dissociates in solution to form a monomeric 1:1 species. We did not observe an equilibrium between the 1:1 and 1:2 Eu(III): $\alpha_2\text{-}P_2W_{17}O_{61}{}^{10-}$ complexes.[8]

The objective of this work is to identify parameters that impact the solid-state structure and the solution chemistry, specifically, parameters that influence the 1:1 to 1:2 equilibria processes. In this study, we note the influence of the lanthanide ionic radii, the solution conditions such as pH, countercation and concentration.

4.2 Experimental Section

4.2.1 General

All reagents were commercially available and used without further purification. Nanopure water was obtained from a Millipore Reverse Osmosis Direct-Q System. The following lacunary anions salts were prepared according to published methods and were identified by ^{31}P NMR: $K_{10}[\alpha_1\text{-}P_2W_{17}O_{61}]$ and $Li_{10}[\alpha_2\text{-}P_2W_{17}O_{61}]$.[9] Elemental analyses were carried out by Inductive Coupled Plasma Atomic Emission Spectrometry (ICP-AES, SPECTROFLAME M120E).

4.2.2 1. Preparation and crystallization of the 1:1 $[Ln(H_2O)_x(\alpha_2\text{-}P_2W_{17}O_{61})]_2$ complexes. $K_{13}(H_3O)[Ln(H_2O)_x(\alpha_2\text{-}P_2W_{17}O_{61})]_2\cdot 2KCl\cdot nH_2O$ (x=4 for Ln = La, Ce, Pr; x=3 for Ln = Nd, Y, Lu). The 1:1 complexes were prepared by three methods. **Method A** (Ln=La, Ce, **Pr**, **Nd**) is a modification of the synthesis reported earlier.[8] The lacunary $K_{10}[\alpha_2\text{-}P_2W_{17}O_{61}]$ (2g, 0.43 mmol) was dissolved in 20 ml of 0.5 M sodium acetate buffer at pH 5.0 or lithium acetate at pH 5.5 (Lu) at 70°C to form a clear solution. The lanthanide as the chloride salt (1.50 mmol), dissolved in a minimum amount of water, was added dropwise to the stirring $K_{10}[\alpha_2\text{-}P_2W_{17}O_{61}]$ solution. KCl (2g) was added to the reaction mixture, within a few seconds for the early lanthanides and a few minutes for the later lanthanides, precipitate formed and was collected. X-ray quality crystals were obtained by recrystallizing 0.05 g of the solid from a minimum amount of warm water (50°C). The quality of the crystals of La, Ce and Pr analogues is not good using this synthetic method. **Method B** (Ln=La) is a modification of the synthesis reported by Pope.[6] $K_{10}[\alpha_2\text{-}P_2W_{17}O_{61}]$ (2 g, 0.403 mmol) was dissolved in 20 ml of H_2O at 80°C and was added dropwise over a period of 30 min to a hot (80°C) solution of $LnCl_3\cdot 6H_2O$ (0.66g, 1.62 mmol) in 2 ml of H_2O, cloudy solution was formed. After stirring the solution at 80°C for an additional 5 min, 20 ml of 3.7 M NH_4Cl was added.

The reaction mixture turned into a clear solution which was stirred at the same temperature for an additional 5 min before the solution was cooled to room temperature (pH=3.0). The X-ray quality crystals were obtained after a few hours. The final products were collected the next day, yielding 1.84 g of colorless crystals, 92% (based on W). Elemental analysis (%) calc. for $(NH_4)_{13}(H_3O)[La_2(\alpha_2\text{-}P_2W_{17}O_{61})_2]\cdot 26H_2O\cdot 10NH_4Cl$: La 2.82, P 1.27, W 63.85; found: La 2.88, P 1.26, W 63.60. **Method C** $K_5Na_2(H_3O)_7[Y_2(\alpha_2\text{-}P_2W_{17}O_{61})_2]\cdot 34H_2O$: In a 100 mL flask, $YCl_3\cdot 6H_2O$ (1.1 g, 3.63 mmol) was dissolved in 50 mL H_2O. $Na_{12}[\alpha\text{-}P_2W_{15}O_{56}]\cdot 18H_2O$ (5 g, 1.16 mmol) was added with vigorous stirring. The mixture was then heated at 80 °C for 15 min and KCl 7.5 g was added to solution. After the solution was cooled in an ice water slurry for 1 h, the white precipitate was collected and dried under suction. The crude product was then dissolved in 60 °C H_2O 50 mL upon addition of 4 M HCl (about 1.25 mL). After filtration, the solution was cooled in a refrigerator at 5 °C for 1 d, yielding 2.10 g colorless crystals, 43.3% (based on W). IR (KBr disk, 600 – 1100 cm^{-1}): $\tilde{\nu}$ = 711 (s), 783 (s), 924 (sh), 943 (s), 1016 (w), 1028 (w), 1059 (sh), 1086 (s) cm^{-1}. ^{31}P NMR (161.9MHz, D_2O) (refer to 85% H_3PO_4): δ = –7.82, –13.46 ppm.

4.2.3 Synthesis and Crystallization of $[Ln(\alpha\text{-}2\text{-}P_2W_{17}O_{61})_2]^{17-}$ ($Ln=La^{3+}$, Gd^{3+}, Eu^{3+}, Lu^{3+}).

The 1:2 complexes were prepared by two methods. **Method A** is a modification of the synthesis reported earlier.[8] $K_{10}[\alpha_2\text{-}P_2W_{17}O_{61}]$ (2g, 0.43 mmol) was dissolved in 20 ml of buffer solution of LiAc (0.285 M) at pH 4.75 at room temperature, $LnCl_3$ (0.215 mmol) was dissolved in minimum amount of water and was added slowly to the above solution with vigorous stirring, The resulting clear solution was stirred vigorously for 15

mins, followed by addition of KCl (2.72 g, 3.66 mmol). A white precipitate formed and was collected by filtration. The white solid was redissolved in a minimum amount of buffer solution of LiAc (0.285 M) pH 4.75 and then was placed in the freezer (4°C). After three days, colorless block-like crystals had formed. **Method B.** $K_5Na_6(H_3O)_6[La(\alpha_2\text{-}P_2W_{17}O_{61})_2]\cdot 49H_2O$: In a 250 ml flask, $LaCl_3\cdot 7H_2O$ (1 g, 2.69 mmol) is dissolved in 120 mL 60 °C 1 M pH 4.7 sodium acetate buffer. $Na_{12}[\alpha\text{-}P_2W_{15}O_{56}]\cdot 18H_2O$ (12 g, 2.69 mmol) is added with vigorous stirring. Any insoluble material is removed by centrifugation after the mixture is stirred for 2 h. NaCl 28 g and KCl 8 g is added to the centrifugate, followed by cooling in a refrigerator at 5 °C for 1 d. The resulting crystals are collected on a medium glass frit and recrystallized in 10 mL H_2O at 5 °C, yielding 8.7 g product, 74.8% (based on W). X-ray quality crystals of **1** were grown at 5 °C from a clear solution of **1** in H_2O for two days. Elemental analysis (%) calcd (based on crystal structure) for $K_5Na_6(H_3O)_6[La(\alpha_2\text{-}P_2W_{17}O_{61})_2]\cdot 49H_2O$: La 1.42, P 1.27, W 63.85; found: La 1.43, P 1.35, W 61.60. IR (KBr disk, 600 – 1100 cm^{-1}): $\tilde{\nu}$ = 769 (s), 823 (s), 919 (sh), 941 (s), 1017 (m), 1056 (m), 1085 (s) cm^{-1}. ^{31}P NMR (161.9MHz, D_2O) of **1** (refer to 85% H_3PO_4): δ = –7.48, –13.50; ^{183}W NMR (16.7MHz, D_2O, refer to 2M $NaWO_4$): δ = –134.86 (s, 4W), –139.84 (s, 4W), –175.54 (s, 6W), –186.60 (broad, 4W), –210.32 (s, 4W), –214.96 (s, 4W), –217.14 (s, 4W), –233.50 (s, 4W). The peak at –175.54 ppm, which integrates for 6W, corresponds to the two sharp resonances at –178.97 (4W) and –180.51 ppm (2W) in NMR spectrum for Li salt in reference.

4.2.4 Standardization of $Li_{10}[\alpha_2\text{-}P_2W_{17}O_{61}]$

The standardization procedure by titration with Co(II) has been reported.[9] 0.5 ml of the $Li_{10}[\alpha_2\text{-}P_2W_{17}O_{61}]$ solution was placed in a UV-vis cuvette with 2 ml of the lithium acetate buffer (0.5 M, pH 4.75). To this solution $CoCl_2$ (0.2455 M) was added in 20 μl increments and the absorbance was recorded at 544 nm. The absorbance plotted against the volume of $CoCl_2$ added gives a sharp breakpoint when all the $Li_{10}[\alpha_2\text{-}P_2W_{17}O_{61}]$ reacted with the $CoCl_2$ in 1:1 stoichiometric ratio. Three titrations were run for each standardization, the agreement was within 1%.

4.2.5 Standardization of $PrCl_3$.

Standardization of Pr(III) was accomplished by complexometric titration using xylenol orange as an indicatior.[10]

4.2.6 Stability Constant Measurements.

4.2.6.1 Determination of $K_{eq}(1)$ and Log(K2*K1):

Sample Preparation: All lanthanides were standardized by EDTA (standard solution, Aldrich) with xylenol orange as indicator. Stock concentration (0.005396 M) of $K_{10}[\alpha\text{-}2\text{-}P_2W_{17}O_{61}]$ was obtained by titrating $[\alpha\text{-}2\text{-}P_2W_{17}O_{61}]^{10-}$ with $CoCl_2$ (0.08 M) (standardized by EDTA) monitoring by UV-vis (the absorbance was recorded at 544 nm). 0.2176 M EDTA at pH 6.6 was obtained by adding diluted NaOH to a standard EDTA solution (pH4.00, 0.5M) and by titrating $CoCl_2$ (0.2979 M) with xylenol orange as indicator. The procedure of a ^{31}P NMR sample (for example Eu^{3+}) was prepared as follow: 1000 μL of 0.005396 M α2 (in 0.5 M NaOAC buffer, pH 6.6) was placed in a 10mm NMR tube, 400 μL D_2O and 11.5 μl Eu^{3+} (0.22875 M) was then added, after shaken for about 15 minutes, 600 μL of EDTA (pH 6.6, 0.2176 M) was added, shaken for another 15 minutes. The solution was clear. After 18 hours at room temperature the

solution reached its equilibrium. ^{31}P NMR spectrum was recorded. An external standard, phosphoric acid (0.009-0.013 M), which is placed in a smaller tube inside of 10mm NMR tube, was used to quantitatively monitor the concentrations of $[\alpha\text{-}2\text{-}P_2W_{17}O_{61}]^{10-}$. At least four determinations were performed for each lanthanide, the final pH was measured after taking the ^{31}P NMR.

Sample ^{31}P NMR Data

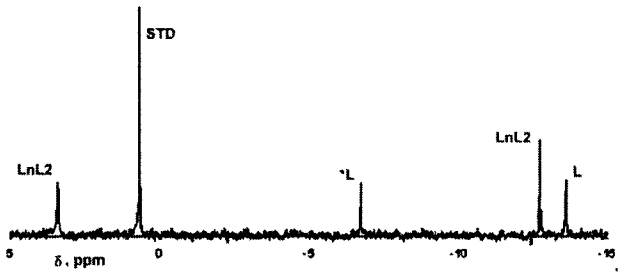

Equilibrium solution of Eu^{3+}, $(\alpha\text{-}2\text{-}P_2W_{17}O_{61})^{10-}$ and competitive ligand EDTA at NaOAc (0.5 M), pH 6.53, (Initial concentration: $2[Ln]_i=[L]$), STD is the external standard (85% H_3PO_4), LnL_2 is $Eu(\alpha\text{-}2\text{-}P_2W_{17}O_{61})_2^{17-}$, L is $(\alpha\text{-}2\text{-}P_2W_{17}O_{61})^{10-}$.

4.2.6.2 Determination of $K_{eq}(2)$ and Log(K2/K1)

Sample preparation: The molecular weight of the ligand $K_{10}[\alpha\text{-}2\text{-}P_2W_{17}O_{61}]$ was obtained by titrating $[\alpha\text{-}2\text{-}P_2W_{17}O_{61}]^{10-}$ with $CoCl_2$ (0.2979 M) (standardized by EDTA) monitoring by UV-vis (the absorbance was recorded at 544 nm). The procedure of a ^{31}P NMR sample (for example Eu^{3+}) was prepared as follow: 0.0522g of $K_{10}[\alpha\text{-}2\text{-}P_2W_{17}O_{61}]$ was dissolved in 1600ul of NaOAC buffer (0.5M, pH 3.5), 400 μL D_2O and 49.2 μL Eu^{3+} (0.22875 M) was added, after shaken for about 15 minutes, 40 μL EDTA (0.1M, pH 4.0) was added, shaken for another 15 minutes. The solution was clear. After about 18 hours at room temperature the solution reached its equilibrium. ^{31}P NMR spectrum was recorded. An external standard, phosphoric acid (0.009-0.013 M), which is placed in a smaller tube inside of 10mm NMR tube, was used to quantitatively monitor the

concentrations of $[\alpha\text{-}2\text{-}P_2W_{17}O_{61}]^{10-}$. At least four determinations were performed for each lanthanide, the final pH was measured after taking the ^{31}P NMR.

4.2.6.3 Standard Curve Preparation and Use

Calibration curve of $[\alpha\text{-}2\text{-}P_2W_{17}O_{61}]^{10-}$ vs. STD were obtained by monitoring ^{31}P NMR of four concentrations, 0.5 mM, 1.2 mM, 2.0 mM and 3.0 mM under the same conditions as for the above competition experiments. The intensity of $[\alpha\text{-}2\text{-}P_2W_{17}O_{61}]^{10-}$ /STD plotted against the concentration of $[\alpha\text{-}2\text{-}P_2W_{17}O_{61}]^{10-}$ gives a straight line, which means the intensity of $[\alpha\text{-}2\text{-}P_2W_{17}O_{61}]^{10-}$ (the peak at -6.4 ppm, for example) I_L vs. intensity of STD I_{STD} is proportional to the concentration of $[\alpha\text{-}2\text{-}P_2W_{17}O_{61}]^{10-}$. $S_g = \frac{I_L}{I_{STD}} = \kappa[L]_t$, S_g is obtained from the ^{31}P NMR spectra. Thus $[L]_t$ = Sg / k, can be used directly for the calculation of K_{eq}.

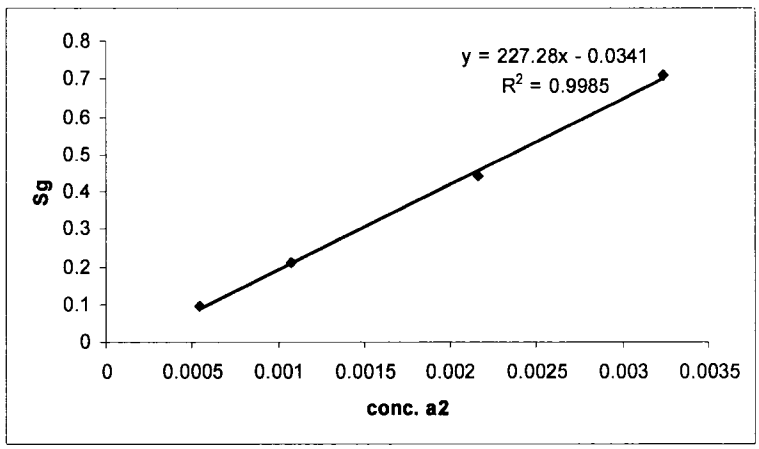

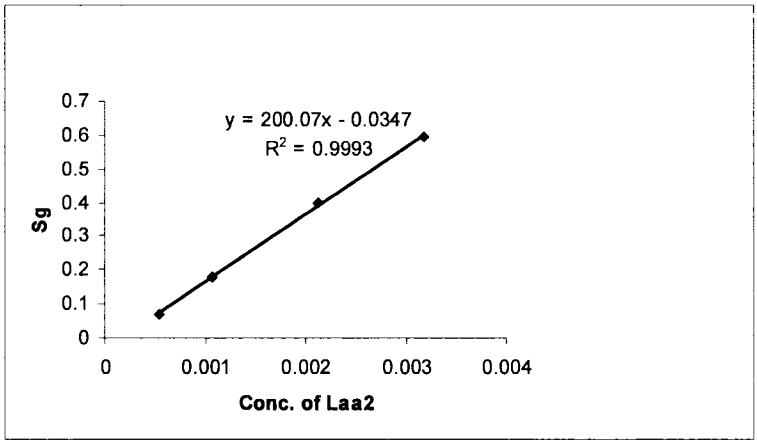

up: Standard curve of $(\alpha\text{-}2\text{-}P_2W_{17}O_{61})^{10-}$ (peak at -13 ppm), bottom: Standard curve of $La(\alpha\text{-}2\text{-}P_2W_{17}O_{61})$ (peak at -13 ppm)

Sample ^{31}P NMR Data

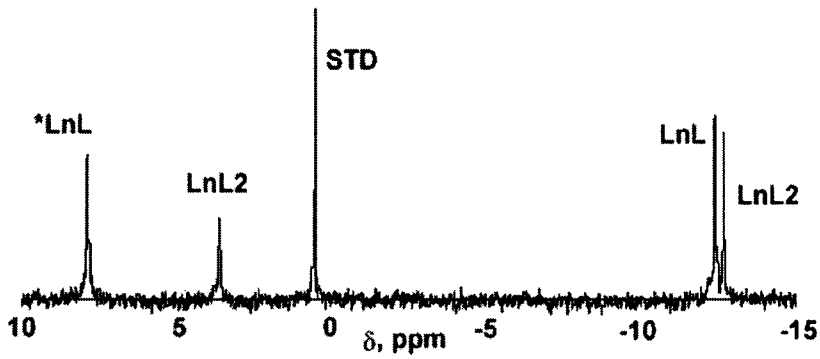

Equilibrium solution of Eu^{3+}, $(\alpha\text{-}2\text{-}P_2W_{17}O_{61})^{10-}$ and competitive ligand EDTA at NaOAc (0.5 M), pH 3.46, (Initial concentration: $[Ln]_i=[L]_i$), STD is the external standard (85% H_3PO_4), LnL_2 is $Eu(\alpha\text{-}2\text{-}P_2W_{17}O_{61})_2^{17-}$, LnL is $Eu(\alpha\text{-}2\text{-}P_2W_{17}O_{61})^{7-}$.

Calibration curve of $Ln[\alpha\text{-}2\text{-}P_2W_{17}O_{61}]^{7-}$ vs. STD and the concentration of $Ln[\alpha\text{-}2\text{-}P_2W_{17}O_{61}]^{7-}$ were obtained from the same manner. The intensity of LnL peak (always chose the same peak for each experiment) I_{LnL} *vs.* intensity of STD peak I_{STD} is proportional to the concentration of and LnL ($Ln(\alpha\text{-}2\text{-}P_2W_{17}O_{61})$).

Table 1. Conditional Stability Constants of LnEDTA at different pH

Ln	La		Pr		Nd		Eu		Ho		Yb		Lu	
LogK' [a]	14.56		16.36		16.56		17.32		18.60		19.48		19.80	
pH	2.2	6.6	3.31	6.84	3.34	6.6	3.46	6.53	3.35	6.38	3.34	6.15	3.29	6.09
$Log\alpha_L$' [b]	-12.73	-3.72	-9.80	-3.43	-9.69	-3.72	-9.47	-3.81	-9.71	-4.00	-9.73	-4.33	-9.84	-2.42
LogK'cond [c]	8.56	11.74	6.56	12.93	6.87	12.84	7.85	13.51	8.89	14.60	9.75	15.15	9.96	17.81

a. Martell, A. E. and Smith, R. M., *Critical stability constants*, Vol. 1, P205, Plenum Press, New York, 1974

b. EDTA has five protonation constants: log K_1^H: 10.19, log K_2^H: 6.13, log K_3^H: 2.69, log K_4^H: 2, log K_5^H: 1.5. (Martell, A. E.; Motekaits, R. J., *Determination and use of stability constants*, New York, VCH Publishers, 1992). An example to calculate LogK'cond(EuEDT): at pH 3.46, $[H^+] = 10^{-3.46}$ M, substituted into equations (6) and (7), (The numbers of the equations were seen in Luo's Doctoral Dissertation (page 133)).[10] $Log\alpha_L' = -9.47$ was obtained.

c. LogK'cond = Log K' + Log α_L' = 17.32

4.2.6.4 Sample of Calculations to obtain $K_{eq}(1)$ and Log(K2*K1)

EuL2 + EDTA ⇆ EuEDTA + 2L (pH=6.53) (where L=α2)

For example:

1000 μL of 0.005396 M α2 (in 0.5 M NaOAC buffer, pH 6.6) + 600 μL of EDTA (pH 6.6, 0.2176 M) + 400 μL D_2O + 11.5 μl Eu^{3+} (0.22875 M) (This is just one of the four determinations for Log(K2*K1))

Initial concentration: $[L]_i = 1000*0.005396/(1000+11.5+600+400) = 2.68258E\text{-}03$ M

$[Eu]_i = 11.5*0.22875/(1000+11.5+600+400) = 1.30779E\text{-}03$ M

$[EDTA]_i = 600*0.2176/(1000+11.5+600+400) = 6.49068E\text{-}02$ M

The integration from ^{31}P NMR: STD = 0.82607, L= 0.16500, L/STD=0.19974. From calibration curve of α2, Sg=L/STD=k*$[L]_t$, k=227.28, thus $[L]_t$=(0.16500+0.0341)/ 227.28=1.02887E-03 M.

Equilibrium concentration: **EuL2 + EDTA ⇆ EuEDTA + 2L (pH=6.53) (where L=α2)**

Mass equations:

$[L]_i = 2[EuL_2]_t + [L]_t$,

$[Eu]_i = [EuL]_t + [EuEDTA]_t$,

$[EDTA]_i = [EDTA]_t + [EuEDTA]_t$

Therefore, $[L]_t$ = 1.02887E-03 M

$[EuL_2]_t = 0.5([L]_i - [L]_t) = 0.5$ (2.68258E-03 -1.02887E-03) =8.26854E-04 M

$[EuEDTA]_t = [Eu]_i - [EuL_2]_t$ = 1.30779E-03 - 8.26854E-04 = 4.80939E-04 M

$[EDTA]_t = [EDTA]_i - [EuEDTA)]_t$ = 6.49068E-02-4.80939E-04 = 6.44258E-02 M

Thus $K_{eq}(1) = [EuEDTA]_t [L]_t^2 / ([EuL_2]_t[EDTA]_t)$= 4.80939E-04*(1.02887E-03)^2 /(8.26854E-04 *6.44258E-02)= 9.5570E-06, $LogK_{eq}(1)$ = -5.02. From equation (5), LogKeq(1)=Log'(EuEDTA)-$Log(K_{2con}*K_{1cond})$, thus, $Log(K_{2con}*K_{1cond})$ = Log'(EuEDTA)-LogKeq(1) = 13.51-(-5.02) = 18.53.

At pH 6.53, Logβ = -4.38E-04, therefore $Log(K_2*K_1)$= 18.53-2*(-4.38E-04) =18.53, the average of $Log(K_2*K_1)$= 18.43

4.2.6.5 Sample of Calculations to obtain $K_{eq}(2)$ and Log(K2/K1)

2EuL + EDTA ⇆ EuEDTA + EuL2 (pH=3.46) (where L=α2)

This is one of the four determinations for $K_{eq}(2)$ and Log(K2/K1).

0.0522g of a2 ligand + 1600ul of NaOAC buffer (0.5M, pH 3.5) + 400 μL D_2O + 49.2 μL Eu^{3+} (0.22875M) + 40 μL EDTA (0.1M, pH 4.2), Final pH 3.46. (Mw of α1= 4633 g/mol)

Initial concentration:

$[L]_i$ = 0.0522g /4633/(1600+400+49.2+40)*1000000= 5.39297E-03 M

$[Eu]_i$ = 49.2*0.22875/(1600+400+49.2+40)= 5.38699E-03 M

$[EDTA]_i$ = 40*0.1/(1600+400+49.2+40)= 1.91461E-03 M

The integration from ^{31}P NMR spectra: STD: 0.9661, EuL: 0.49221, I_{EuL}/I_{STD}=0.50948. From calibration curve of EuL, Sg = I_{EuL}/I_{STD} =k*[α2]t, k=269.21, thus [EuL]t=(0.50948+0.0494)/269.21=2.07601E-03 M. (where L = α2).

Equilibrium concentration:

2EuL + EDTA ⇆ EuEDTA + EuL_2 (pH=3.46) (where L=α2)

Mass equations $[L]_i = [EuL]_t + 2[EuL_2]_t$,

$[Eu]_i = [EuL]_t + [EuEDTA]_t + [EuL_2]_t$,

$[EDTA]_i = [EDTA]_t + [EuEDTA]_t$

$[EuL_2]_t = 0.5[L]_i - 0.5[EuL]_t$ =0.5 (5.39297E-03 -2.07601E-03)= 1.65848E-03 M

$[EuEDTA]_t$= $[Eu]_i$ – $[EuL]_t$- $[EuL_2]_t$= 5.38699E-03 - 2.07601E-03 - 1.65848E-03 =1.65250E-03 M

$[EDTA]_t = [EDTA]_i - [EuEDTA]_t$= 1.91461E-03 -1.65250E-03 =2.62107E-04 M

Keq=$[EuEDTA]_t[EuL_2]_t/([EuL]^2_t[EDTA]_t)$=1.65250E-03*1.65848E-03/(2.07601E-03)^2*2.62107E-04)= 2426.1, Log Keq= 3.385

From equation (6), Log Keq= Log K'cond(EuEDTA)+Log(K2cond/K1cond), LogK'con(EuEDTA)= 7.85 (see Table S3), thus Log(K2cond/K1cond) = 3.385-7.85 = -4.46, and therefore Log(K2/K1) = -4.46, the average of Log(K2/K1) = -4.46

Based on Log(K2/K1) = -4.46 and $Log(K_2*K_1)$= 18.43, LogK1 = 11.45, LogK2 = 6.99

4.2.7 Reaction of Pr^{3+} with $[\alpha_2\text{-}P_2W_{17}O_{61}]^{10-}$ (1:1 stiochiometry) as a function of counter cation monitored by ^{31}P NMR.

Buffer solutions of LiOAc (1M), NaOAc(1M), KOAc(1M) and CsOAc(0.5M) were each prepared at pH 4.75. 0.09 ml of standardized $Li_{10}[\alpha_2\text{-}P_2W_{17}O_{61}]$ solution (0.2311M), 0.0181 ml of standardized $PrCl_3$ solution (1.15M) and 0.192 ml of D_2O were

each placed into five 5 mm NMR tubes, followed by 0.3 ml of either H_2O or buffer. The final ion concentration was 0.5M in each solution containing Li^+, Na^+ or K^+ and 0.25 M for Cs^+. The solutions were shaken for 5 minutes, incubated at room temperature for 30 minutes, after which the ^{31}P NMR spectra were recorded. The data are shown in **Figure 3**. [Pr] = $[\alpha_2\text{-}P_2W_{17}O_{61}]$= 34.6 mM, $[Li^+]$= 0.35M; $[Na^+]$= 0.5M. Reactions of Eu^{3+} or Yb^{3+} with $[\alpha_2\text{-}P_2W_{17}O_{61}]^{10-}$ (1:1 stiochiometry) as a function of counter cation were carried out in the similar manner; the NMR data are shown in **Figure 8** and **9**.

4.2.8 Reaction of Pr^{3+} with $[\alpha_2\text{-}P_2W_{17}O_{61}]^{10-}$ (1:1 stiochiometry) as a function of pH monitored by ^{31}P NMR at constant ionic strength, with Na^+ counterion.

Solutions of NaOAc (0.5M) at five different pH values were each prepared (2, 4, 6, 8, 10) (30% D_2O) (pH 2 and 10 were adjusted by dilute HCl and NaOH respectively). Standardized $Li_{10}[\alpha_2\text{-}P_2W_{17}O_{61}]$ solution (0.09 mL, 0.2311M) and 0.0181 mL of standardized $PrCl_3$ solution (1.15M) were placed into five 5 mm NMR tubes, and 0.5 mL of one of the above NaOAc solutions was added into the NMR tubes to give five samples buffered at the five pH values. The NMR tubes were shaken for 5 minutes and incubated at room temperature for 30 minutes, then the ^{31}P NMR spectra were recorded and the data are shown in **Figure 4**. The pH recorded after the NMR measurements did not change significantly. $[Na^+]$ = 0.41M; $[Li^+]$= 0.34M . [Pr] = $[\alpha_2\text{-}P_2W_{17}O_{61}]$= 34 mM. Reactions of Eu^{3+} or Yb^{3+} with $[\alpha_2\text{-}P_2W_{17}O_{61}]^{10-}$ (1:1 stiochiometry) as a function of pH were carried out in the similar manner; the NMR data are shown in **Figure 7** and **10**.

4.2.9 Reaction of Pr^{3+} with $[\alpha_2\text{-}P_2W_{17}O_{61}]^{10-}$ (1:1 stiochiometry) as a function of concentration of counter cation monitored by ^{31}P NMR.

Solutions of NaOAc (0.04 M, 0.2 M, 0.5 M, 1.0 M, 2.0 M) at pH 4.75 were prepared. Standardized $Li_{10}[\alpha_2\text{-}P_2W_{17}O_{61}]$ solution (0.09 ml, 0.2311M), 0.0181 ml of $PrCl_3$ (1.15M) solution and 0.192 ml of D_2O were placed into five 5 mm NMR tubes followed by the addition of 0.3 ml of each buffer solution into the above five 5mm NMR tubes individually. The solution in the NMR tubes were shaken for 5 minutes and incubated at room temperature for about 30 minutes. The ^{31}P NMR spectra were recorded; the data are shown in **Figure 5**. $[Li^+]$= 0.34M. [Pr] = $[\alpha_2\text{-}P_2W_{17}O_{61}]$= 34.7 mM $[Na^+]$ = varies from 0.02M to 1.0M

4.2.10 Reaction of Pr^{3+} with $[\alpha_2\text{-}P_2W_{17}O_{61}]^{10-}$ (1:1 stiochiometry) as a function of concentration monitored by ^{31}P NMR.

Solutions of $Li_{10}[\alpha_2\text{-}P_2W_{17}O_{61}]$ and $PrCl_3$ of 1:1 stoichiometry were prepared at 50mM, 100mM, 150mM, 200mM, 250 mM and 300mM concentration. The pH ranged from 5.77 (50 mM) to 4.92 (300 mM). The ^{31}P NMR data are shown in **Figure 6**. [Pr] = $[\alpha_2\text{-}P_2W_{17}O_{61}]$ ranges from 50 mM, 100 mM, 150 mM, 200 mM, 250 mM; [Li+]: 500 mM, 1M, 1.5M, 2.0M, 2.5 M, 3.0M

4.2.11 Reaction of Pr^{3+} with $[\alpha_2\text{-}P_2W_{17}O_{61}]^{10-}$ (1:1 stiochiometry) as a function of counter cation and temperature monitored by ^{31}P NMR.

Buffer solutions of LiOAc (1M), NaOAc(1M), KOAc(1M) and CsOAc(0.5M) were each prepared at pH 4.75. Standardized $Li_{10}[\alpha_2\text{-}P_2W_{17}O_{61}]$ solution (0.09 ml , 0.2311M), 0.0181 ml of 1.15M of $PrCl_3$ solution and 0.192 ml of D_2O were added to five 5 mm NMR tubes, followed by 0.3 mL of either H_2O or one of the four buffer solutions. The NMR tubes were shaken for 5 minutes, incubated for 30 minutes, and then the ^{31}P NMR spectra were recorded at various temperatures ranging from 0~90°C. The

data are shown in **Figure 11-16**. Due to the formation of the precipitate, the sample with KOAc (**Figure 14**) and CsOAc (**Figure 15**) was taken at 25°C and higher.

The samples were prepared with $Li_{10}[\alpha_2\text{-}P_2W_{17}O_{61}]$ and therefore contain 0.35M Li^+ in addition to the countercation of the buffer (0.5M). To examine the effect of varying the K^+ and Li^+ concentrations, and thus to compare with the sample represented in **Figure 14**, prepared with $Li_{10}[\alpha_2\text{-}P_2W_{17}O_{61}]$ and KOAc, a sample was prepared using $K_{10}[\alpha_2\text{-}P_2W_{17}O_{61}]$ in LiOAc buffer. Standardized $K_{10}[\alpha_2\text{-}P_2W_{17}O_{61}]$ (0.405 g) and 0.076 ml of 1.15M of $PrCl_3$ were placed into a 10 mm NMR tube, 2.3 ml of LiOAc buffer solution (0.5M, pH 4.75) (30% D_2O) was added into the tube. The solution in the NMR tubes was shaken for about 5 minutes, and then the ^{31}P NMR spectra were recorded at different temperature range from 0~90°C and the data are shown in **Figure 16**.

4.2.11 Elemental analysis by ICP

The methods used for elemental analyses by ICP were described in a previous publication (Zhang, 2004).[11]

4.2.12 Collection of NMR Data

All NMR spectra were recorded on a JEOL GX-400 spectrometer with 5 or 10 mm tubes. Resonance frequencies are 161.8 MHz for ^{31}P and 16.7 for ^{183}W. Chemical shifts are given with respect to external 85% H_3PO4 for ^{31}P and 2.0 M Na_2WO_4 for ^{183}W. Typical acquisition parameters for ^{31}P spectra included the following: spectral width, 10000 Hz; acquisition time, 0.8 s; pulse delay, 1 s; pulse width, 15 μs (50° tip angle). From 200 to 1000 scans were required. For ^{183}W spectra, typical conditions included the following: spectral width, 10000 Hz; acquisition time, 1.6 s; pulse delay, 0.5 s; pulse width, 50 μs (45° tip angle). From 1000 to 30000 scans were acquired. For all spectra, the

temperature was controlled to 25 ± 0.2 deg. For both ^{31}P and ^{183}W chemical shifts, the convention used is that the more negative chemical shifts denote upfield resonances.

4.2.13 Single Crystal X-ray Structure Determination

Block-like crystals of 2:2 and 1:2 complexes **1** and **2** were isolated from solution and examined under a thin layer of mineral oil using a polarizing microscope. A suitable crystal was chosen and mounted on a glass fiber while still coated in oil; the crystal was then immediately frozen to 100K on a Bruker Nonius Kappa CCD diffractometer equipped with a sealed tube Mo anode (K_∂ radiation, λ=0.71073 Å) and graphite monochromator. Data collection, indexing, and initial cell refinements were all handled using accompanying proprietary Nonius software. The SHELX package of software was used to solve and refine the restructures. The heaviest atoms were located by direct methods, and the remaining atoms were found in subsequent Fourier difference. Single-crystal X-ray data for $[Y_2(\alpha_2\text{-}P_2W_{17}O_{61})_2]^{14-}$ and $[La(\alpha_2\text{-}P_2W_{17}O_{61})_2]^{17-}$ was collected on a Bruker D8 SMART APEX CCD area detector system at 100(2) K. Structure solution and refinement were carried out by using SHELXTL V5.10 program. Crystal data of 2:2 complexes and bond lengths were shown in **Table 2** and **Table 3**.

4.3 Results and Discussion

4.3.1 Solid-State Crystal Structures

4.3.1.1 2:2 Ln: $[\alpha_2\text{-}P_2W_{17}O_{61}]^{10-}$

Interestingly, two structural types are observed in the solid-state structures of the 1:1 Ln(III): $[\alpha_2\text{-}P_2W_{17}O_{61}]^{10-}$ complexes. The early lanthanides, La (III), Ce(III), and Pr (III), show "cap to cap" dimers. The Ce(III) structure was reported by Pope. We found the

Table 2. Crystal data and Structure Refinement for $[M_2(\alpha\text{-}2\text{-}P_2W_{17}O_{61})_2]^{14-}$ (M = La, Nd, Lu and Y) and $[La(\alpha\text{-}2\text{-}P_2W_{17}O_{61})_2]^{17-}$

empirical formula	LaN6.5O77P2 W 17	K8NdO81P2 W17	$K_5LuO89.5P2$ W17	$K_5Na_2O_{80.5}P_2$ $W_{17}Y$	$K_5LaNa_6O_{171}P$ $_4W_{34}$
Formula weight	4649.37	4940.43	4989.86	4805.78	9583.13
crystal system	Monoclinic	Triclinic	Triclinic	Triclinic	Triclinic
space group	C2/c	P-1	P-1	P-1	P-1
temp, K	100 (2)	100 (2)	100(2)	100 (2)	100 (2)
wavelength, Å	0.71073	0.71073	0.71073	0.71073	0.71073
a, Å	45.825(9)	12.922(3)	12.670(3)	12.657(1)	14.579(2)
b, Å	12.702(3)	14.635(3)	16.263(3)	16.270(1)	24.505(3)
c, Å	26.349(5)	23.300(5)	21.588(4)	21.670(2)	26.087(3)
α, deg	90(3)	72.21(3)	101.62(3)	101.927(2)	66.094(4)
β, deg	93.50(3)	81.67(3)	106.46(3)	106.378(2)	87.836(4)
γ, deg	90(3)	75.69(3)	107.74(3)	107.591(1)	74.849(4)
Vol, $Å^3$	15308(5)	4053.9(14)	3856.3(13)	3867.6(5)	8199.6(17)
Z	8	2	2	2	2
calcd density, g/cm^3	4.035	4.047	4.297	4.127	3.881
abs coeff, mm^{-1}	26.132	25.198	26.947	26.343	24.292
F (000)	16052	4296	4340	4176	8324
θ range, deg	3.06 to 27.94	2.93 to 27.62	1.04 to 27.53	1.39 to 33.16	1.45 to 33.07
limiting indices	-59<=h<=59, -15<=k<=16, -33<=l<=34	-16<=h<=16, -18<=k<=19, -30<=l<=30	-16<=h<=16, -21<=k<=21, -28<=l<=28	-19<=h<=19, -25<=k<=24, -33<=l<=32	-21<=h<=21, -36<=k<=37, -39<=l<=39
reflns collected/unique	23872/15813 [R(int)=0.0823]	32576/18471 [R(int)=0.0446]	30483/17525 [R(int)=0.0634]	80294/27489 [R(int)=0.0614]	145879/57624 [R(int)=0.0864]
Refinement meth	Full-matrix least squares on F^2	Full-matrix least squares on F^2	Full-matrix least squares on F^2	Full-matrix least squares on F^2	Full-matrix least squares on F^2
data/ restraints/ parameters	15813/0/515	18741/0/572	17525/0/578	27489 / 0 / 648	57624 / 0 / 1163
GOF on F^2	1.050	1.116	1.123	1.034	1.025
final R indices [I>2σ(I)]	R_1 =0.1181 wR_2 = 0.2829	R_1 = 0.0767 wR_2 = 0.1932	R_1 = 0.0906 wR_2 = 0.2407	R_1 = 0.0523, wR_2 = 0.1109	R_1 = 0.0588, wR_2 = 0.1354
R indices (all data)	R_1 =0.1853 wR_2 = 0.3352	R_1 = 0.0967 wR_2 = 0.2040	R_1 = 0.1311 wR_2 = 0.2791	R_1 = 0.0674, wR_2 = 0.1173	R_1 = 0.0978, wR_2 = 0.1495
largest diff.peak and hole ($eÅ^{-3}$)	6.798 and -5.154	7.165 and -4.807	7.262 and -5.514	5.397 and -3.033	5.924 and -5.338

Table 3. Selected Bond Lengths and Angles for the 1:1 $[La2(\alpha\text{-}2\text{-}P_2W_{17}O_{61})_2]^{14-}$ and 1:2 $[Ln(\alpha 1\text{-}P_2W_{17}O_{61})_2]^{17-}$ complexes.

$[La_2(\alpha\text{-}2\text{-}P_2W_{17}O_{61})_2]^{14-}$	$[Nd_2(\alpha\text{-}2\text{-}P_2W_{17}O_{61})_2]^{14-}$	$[Lu_2(\alpha\text{-}2\text{-}P_2W_{17}O_{61})_2]^{14-}$
La – O(3) 2.556(26)	Nd(1)-O(68W) 2.465(27)	Lu(1)-O(64W) 2.282(24)
La – O(10) 2.500(2)	Nd(1)-O(40W) 2.512(27)	Lu(1)-O(62W) 2.378(58)
La – O(25W) 2.509(9)	Nd(1)-O(59W) 2.498(6)	Lu(1)-O(63W) 2.311(21)
La – O(27W) 2.625(4)	Nd(1)-O(52) 2.380(43)	Lu(1)-O(44) 2.286(29)
La – O(32) 2.576(18)	Nd(1)-O(44) 2.388(29)	Lu(1)-O(17) 2.286(32)
La – O(38W) 2.590(23)	Nd(1)-O(63) 2.407(32)	Lu(1)-O(50) 2.262(35)
La – O(57) 2.503(6)	Nd(1)-O(38) 2.406(27)	Lu(1)-O(38) 2.303(40)
La – O(59W) 2.637(39)	Nd(1)-O(60A) 2.435(46)	Lu(1)-O(33A) 2.326(67)
La – O(61A) 2.549(27)	Ave. Nd-O 2.436 (29)	Ave. Lu–O 2.304(30)
Ave. La – O 2.560 (17)		
$[Y_2(\alpha\text{-}2\text{-}P_2W_{17}O_{61})_2]^{14-}$	$[Ce_2(\alpha\text{-}2\text{-}P_2W_{17}O_{61})_2]^{14-}$	$[Eu(\alpha\text{-}2\text{-}P_2W_{17}O_{61})_2]^{17-}$
Y(1)-O(53) 2.313(8)	Ce(18)– O(63W) 2.646(35)	Eu(1)-O(1A) 2.375(4)
Y(1)-O(54) 2.332(8)	Ce(18)– O(75W) 2.464(3)	Eu(1)-O(2A) 2.463(6)
Y(1)-O(59) 2.347(8)	Ce(18)– O(74W) 2.514(17)	Eu(1)-O(3A) 2.407(3)
Y(1)-O(61) 2.314(8)	Ce(18)– O(7W) 2.759(41)	Eu(1)-O(4A) 2.361(4)
Y(1)-O(1W) 2.358(9)	Ce(18)– O(68) 2.384(20)	Eu(1)-O(1B) 2.378(3)
Y(1)-O(2W) 2.409(9)	Ce(18)– O(1) 2.430(46)	Eu(1)-O(2B) 2.375(3)
Y(1)-O(3W) 2.346(9)	Ce(18)– O(3) 2.529(74)	Eu(1)-O(3B) 2.356(4)
Y(1)-O(14) 2.365(9)	Ce(18)– O(26) 2.524(29)	Eu(1)-O(4B) 2.386(5)
Ave. Y–O 2.348(8)	Ce(18)– O(61A) 2.675(62)	Ave. Eu - O 2.388(4)
	Ce(19)– O(39) 2.653(16)	
$[La(\alpha\text{-}2\text{-}P_2W_{17}O_{61})_2]^{17-}$	Ce(19)– O(52) 2.656(32)	$[Gd(\alpha\text{-}2\text{-}P_2W_{17}O_{61})_2]^{17-}$
La(1) – O(32) 2.449(9)	Ce(19)– O(68) 2.281(21)	Gd(1)-O(87) 2.371(2)
La(1)– O(23) 2.466(9)	Ce(19)– O(51) 2.351(55)	Gd(1)-O(11) 2.383(2)
La(1)– O(51) 2.482(9)	Ave. Ce - O 2.528(35)	Gd(1)-O(10) 2.341(2)
La(1)– O(42) 2.489(9)		Gd(1)-O(85) 2.384(3)
La(1) – O(12) 2.491(10)		Gd(1)-O(13) 2.465(4)
La(1)– O(93) 2.497(9)		Gd(1)-O(88) 2.396(3)
La(1)– O(47) 2.499(9)		Gd(1)-O(205) 2.326(2)
La(1)– O(83) 2.526(9)		Gd(1)-O(22) 2.389(2)
Ave. La-O 2.480(9)		Ave. Gd - O 2.382(2)

same cap to cap structure using their preparation conditions where the pH is maintained at 2.0 and also, following conditions where the pH is kept at 4.5. The La (III), and Pr (III) show identical unit cells and the structures are isomorphous with the Ce(III) analog. In these structures, the lanthanide ion is 9-coordinate, exhibiting a capped square antiprismatic coordination geometry. The Ln is bound to four oxygen atoms of the

polyoxometalate, four water molecules and also to a terminal W-O bond in the "cap" region of an adjacent [α_2-$P_2W_{17}O_{61}$] unit, thus forming the 2:2 dimers.

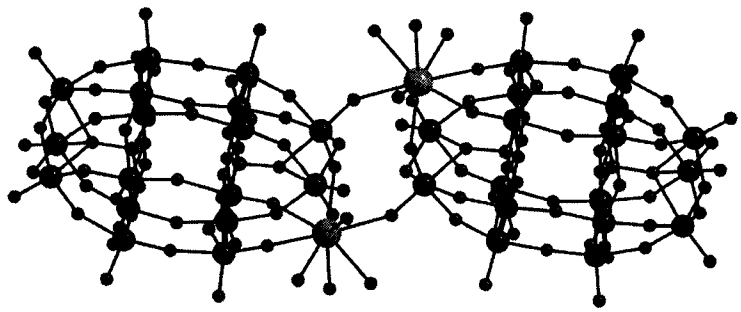

Figure 1. Ball and stick structure of 2:2 complex "cap tp cap", $\{Ln(H_2O)_4(\alpha\text{-}2\text{-}P_2W_{17}O_{61})\}_2^{14-}$ (Ln = La, Ce, Pr), **1.** Uncoordinated H_2O molecules have been removed for clarity. Legend: W: large dark balls; O: small dark balls; Eu: large gray balls; P: small gray balls.

The 2:2 Ln: [α_2-$P_2W_{17}O_{61}$] complexes for the mid-late lanthanides show a different connectivity. We reported the Eu(III) analog previously.[8] In these species, the Ln is 8-coordinate, bound to four oxygen atoms of the α_2-$P_2W_{17}O_{61}^{10-}$, three water molecules and to a terminal W-O of the "belt" region of an adjacent [α_2-$P_2W_{17}O_{61}$], forming a "cap to belt" 2:2 dimer.

While in solution, the 1:1 species are monomeric, the solid-state crystal structures show a "2:2 dimer formation" where one Ln is bound to a terminal tungsten oxygen of an adjacent polyoxometalate. There is a distinct structural change across the lanthanide series. The structural change from a "cap-to-cap" structure, found with the early lanthanides, to the "cap-to-belt" structure occurs at Nd. The cap-to-cap motif allows the early lanthanides with larger ionic radii, more room to accommodate their Ln-O bond lengths, which are significantly larger than the mid-late lanthanide analogs. Also, the 9-

coordination that is often found for the early lanthanides is best accommodated by the cap-to-cap structures.

The decrease in ionic radii across the lanthanide series results in shorter bond lengths for the mid-late lanthanides and often 8-coordination. The cap-to-belt motif apparently is sufficient to accommodate the eight coordination of the mid-late lanthanide: α_2-$P_2W_{17}O_{61}^{10-}$ dimers. Generally, the Ln-O_{H2O} bonds are slightly longer than the Ln-O_{POM} bonds. We have observed this previously in a study comparing single crystal diffraction and X-ray Absorption Spectroscopy experiments for $[Lu(H_2O)_4(\alpha_2\text{-}P_2W_{17}O_{61})]^{7-}$ and $[Ln(\alpha_2\text{-}P_2W_{17}O_{61})_2]^{17-}$ complexes.[8] **Table 3** shows the average bond length decrease for the La (III), Ce(III), Nd (III), Y (III) (Ho(III) analog), and Lu (III) complexes (2.560 Å, 2.528 Å, 2.436 Å, 2.348 Å, and 2.304 Å, respectively). The bond lengths for the Ce(III) analog reported here are similar to that reported by Pope. [7]

4.3.1.2 1:2 Ln: $[\alpha_2\text{-}P_2W_{17}O_{61}]^{10-}$

The 1:2 $[Ln(\alpha_2\text{-}P_2W_{17}O_{61})_2]^{17-}$ crystal structures for Ln= La, Gd, Eu were solved in this study. The Lu(III) analog was published previously.[8] All of the analogs show similar solid-state X-ray structures. These are also similar to the partial structure reported for the Ce (IV) analog. The POM lobes are oriented in a "cis" position and the Ln(III) ion is bound to four oxygen atoms of the cap region of both (α_2-$P_2W_{17}O_{61}$) units. As expected, the bond lengths decrease across the lanthanide series (see **Table 3**).

The crystal structures of the 1:2 Ln(III): $[\alpha_2\text{-}P_2W_{17}O_{61}]^{10-}$ ($[Ln(\alpha_2\text{-}P_2W_{17}O_{61})_2]^{17-}$) analogs, **Figure 2** and **Tables 1** and **2** demonstrate that the Ln(III) ion substitutes for two $[WO]^{4+}$ units in the "cap" regions of two $[\alpha_2\text{-}P_2W_{17}O_{61}]^{10-}$. The Ln(III) are in square

antiprismatic coordination environments bound to eight oxygen atoms, four from each POM unit. The two polyoxometalate lobes are disposed in a "syn" fashion. Average Ln-O bond lengths are consistent with the decreasing ionic radii across the lanthanide series and are slightly shorter than the average bond lengths for the 1:1 complexes because there are no water molecules bound to the Ln(III). Therefore, the average Ln(III)-O bond lengths observed are La: 2.480 (9) Å; Eu: 2.388(4) Å, Gd: 2.382(2) Å, and Lu: 2.30(2)Å [8].

The details of the bond lengths and angles of the W-O framework of the $[\alpha_2\text{-}P_2W_{17}O_{61}]^{10-}$ in all molecules in this study are consistent with other structures previously reported.

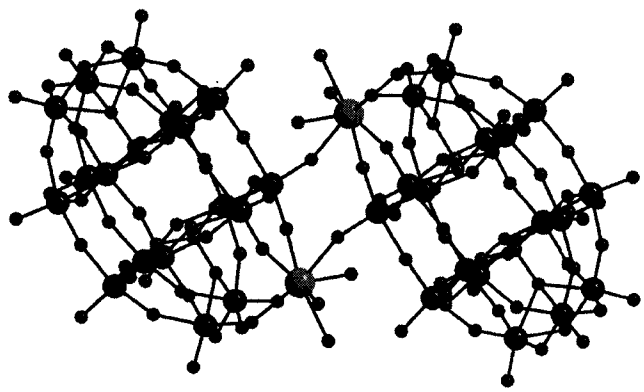

Figure 2. Ball and stick structure of 2:2 complex "cap tp cap", $\{Ln(H_2O)_3(\alpha\text{-}2\text{-}P_2W_{17}O_{61})\}_2^{14-}$ (Ln = Nd, Eu, Y, Lu), **2.** Uncoordinated H_2O molecules have been removed for clarity. Legend: W: large dark balls; O: small dark balls; Eu: large gray balls; P: small gray balls.

4.3.2 Solution Speciation Chemistry: Impact of counterion, pH and concentration.

4.3.2.1 NMR Experiments: General.

In order to understand the effect of solution conditions on the 1:1 to 1:2 Ln(III): $\alpha_2\text{-}P_2W_{17}O_{61}^{10-}$ equilibria for the early, mid and late lanthanides, we have designed ^{31}P NMR studies that probe variation in pH, counterion and concentration. We use Pr (III),

Eu (III) and Yb(III), as representative lanthanides for the ^{31}P NMR experiments because, as paramagnetic lanthanides, they result in chemical shift dispersion that allows clear observation and identification of the solution species. Pr(III) is representative of the early lanthanides as it forms the head to head dimer similar to Ce (III) and La (III) and shows the equilibrium between the 1:1 and 1:2 Pr: α_2-$P_2W_{17}O_{61}^{10-}$ species in the ^{31}P NMR. Eu(III) and Yb(III) are representative of the mid-late lanthanides. In order to perform these studies, the chemical shift values for the 1:1 and 1:2 complexes must be known first. These were determined in this and previous work [8,9,11] and are shown in **Table 3**.

Moreover, the dissociation of the 2:2 dimer in aqueous solution to form a 1:1 monomer in solution has been verified by combinations of ^{183}W NMR spectroscopy for the Ce(III) [7] and Nd(III) and Lu(III) analogs and luminescence spectroscopy for the Eu(III) analogs. [8]

Table 4. Multinuclear NMR chemical shifts (δ, ppm) for the 1:1 and 1:2 Ln:[α-2-$P_2W_{17}O_{61}]^{10-}$ complexes at 0.5 M sodium Acetate Buffer at pH 4.75, 25°C.

	1:1 Ln: :[α-2-$P_2W_{17}O_{61}]^{10-}$		1:2 Ln: :[α-2-$P_2W_{17}O_{61}]^{10-}$	
Ln	P1	P2	P1	P2
La	-7.52	-13.56	-7.42	-13.58
Ce	-14.40	-17.26	-13.92	-13.98
Pr	-11.91	-13.47	-8.41	-13.11
Nd	-20.74	-14.66	-18.50	-14.36
Eu	7.32	-12.43	3.73	-12.73
Yb	32.78	-9.92	39.15	-8.28
Lu	-8.03	-13.52	-7.72	-13.42

4.3.2.3 Solution Speciation Chemistry: Result

Figure 3 shows the ^{31}P NMR data for the reaction of Pr(III) with $Li_{10}[\alpha_2\text{-}P_2W_{17}O_{61}]^{10-}$ in 1:1 stoichiometry as a function of countercation. The Li^+, Na^+ and K^+ countercations are in 0.5M concentration with Cs^+ in 0.05M concentration. In D_2O without additional countercation, the 1:1 species shows ^{31}P resonances at –14.12 and –16.14 ppm. The peak marked a2 is assigned to the P that is closest to the Pr; this peak is broader than a1, presumably due to the proximity to the paramagnetic lanthanide. It is clear that the countercation has an effect on the speciation. For example, addition of Li^+, Na^+ and K^+ results in a shift of both a1 and a2 upfield with a2 experiencing the most pronounced shifts. Also, with Na^+ and K^+, the appearance of the 1:2 peaks are observed; these are marked b1 and b2. The 1:2 species have been independently identified in 0.5M Na^+ and K^+ by mixing Pr and $Li_{10}[\alpha_2\text{-}P_2W_{17}O_{61}]^{10-}$ in 1:2 stoichiometry. It is likely that b1 represents the P closest to the Pr(III) center due to its broadness compared to b2. This peak also shifts upon changing countercation. When Cs^+ is used, precipitation occurs, requiring a lower concentration for these experiments to keep all species in solution. Therefore, the ^{31}P NMR chemical shifts are similar to the case where no counterion is added. Under identical conditions, the Eu(III) analog showed similar behavior, presented in **Figure 8**; in this case, the 1:2 species is clearly observed upon addition of Li^+, Na^+ and K^+ and the quantity of 1:2 complex increases with the larger countercation. In contrast, Yb(III) showed exlusively the 1:1 species, **Figure 9**.

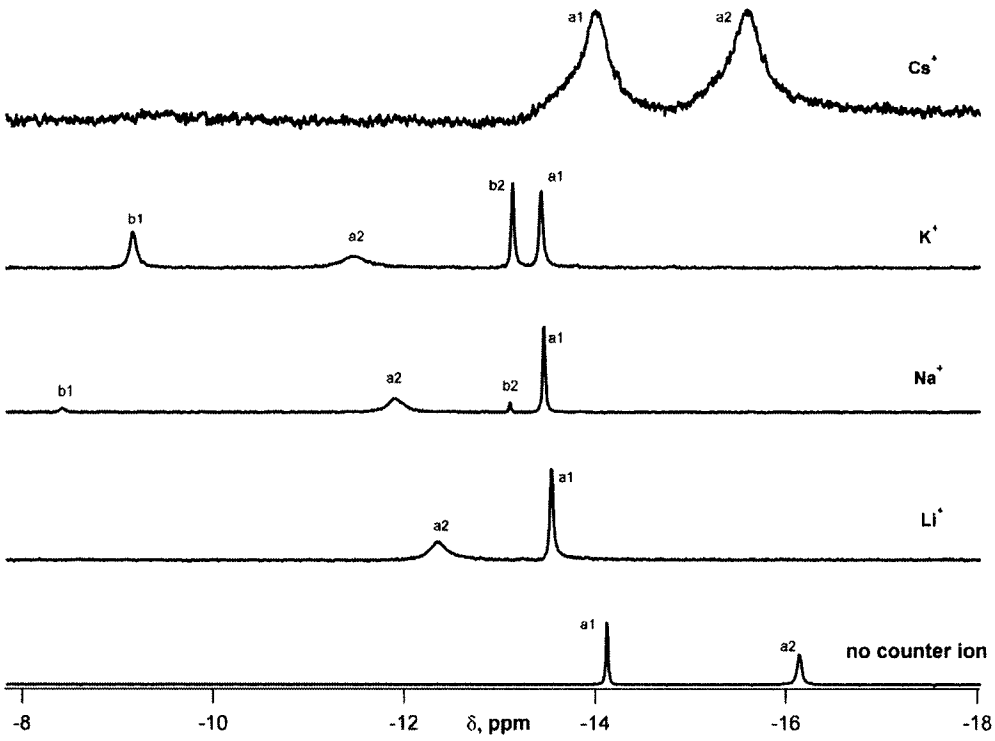

Figure 3. Reaction of Pr^{3+} with $Li_{10}[\alpha_2\text{-}P_2W_{17}O_{61}]$ (1:1 stiochiometry) as a function of counter cation, pH 4.75, the concentration of Li^+, Na^+, K^+ = 0.5M . Concentratin of Cs^+ = 0.05M.

The 1:1 Ln: $(\alpha_2\text{-}P_2W_{17}O_{61})^{10-}$ (Ln=Pr, Eu, Yb) were further investigated in 0.5M Na^+ as a function of pH, shown in **Figures 3, 7** and **10**, respectively. Samples of Pr(III) (**Figure 3**)and Eu(III) (**Figure 7**), at all pH values, show the 1:1 and 1:2 species with little variation from pH 4 to pH 10. The increase in the amount of the 1:2 species at basic pH is very likely due to the competition between OH^- ions and the polyoxometalate for the lanthanide(III). Lanthanide ions form hydroxides and oxides with high stability, thus liberating a $(\alpha_2\text{-}P_2W_{17}O_{61})^{10-}$ that can bind to the 1:1 Pr: $(\alpha_2\text{-}P_2W_{17}O_{61})^{10-}$ species to form the 1:2 species and some colloidal Ln oxides. We did not note the formation of precipitates in the NMR tubes, however colloidal lanthanides are often undetectable by the eye. The Yb(III) analog behaves in a similar fashion, **Figures 10**.

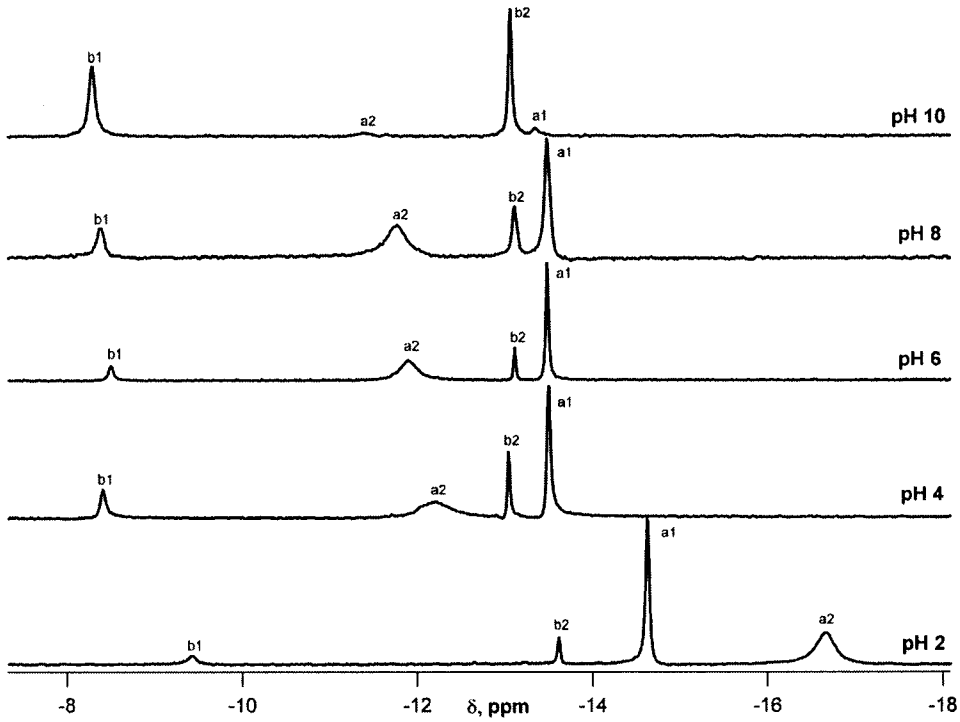

Figure 4. Reaction of Pr^{3+} with $Li_{10}[\alpha_2\text{-}P_2W_{17}O_{61}]$ (1:1 stiochiometry) as a function of pH.

The effect of the sodium ion concentration is examined in **Figure 5**, where the concentration of the 1:1 Pr: $(\alpha_2\text{-}P_2W_{17}O_{61})^{10-}$ is 35M in pH=4.75. It is clear that the concentration of Na^+ impacts the speciation. First the a2 peak shifts downfield and broadens upon increase of Na^+. Second, as the Na^+ concentration is increased, peaks that represent the 1:2 species (b1 and b2) appear. The severe broadening at 0.5 M and 1.0 M Na^+ may be due to the combined effects of paramagnetism and increasing ionic strength.

Increasing the concentration of the complex, shown in **Figure 6**, results in appearance of the 1:2 species at 100 mM and higher. This behavior is consistent with the concentration dependence of the Ce(III) analog reported previously, suggesting the 1:1 $\rightleftharpoons$ 1:2 equilibrium. [7]

$$2\,[Ln(\alpha_2\text{-}P_2W_{17}O_{61})]^{7-} \rightleftharpoons [Ln(\alpha_2\text{-}P_2W_{17}O_{61})_2]^{17-} + Ln$$

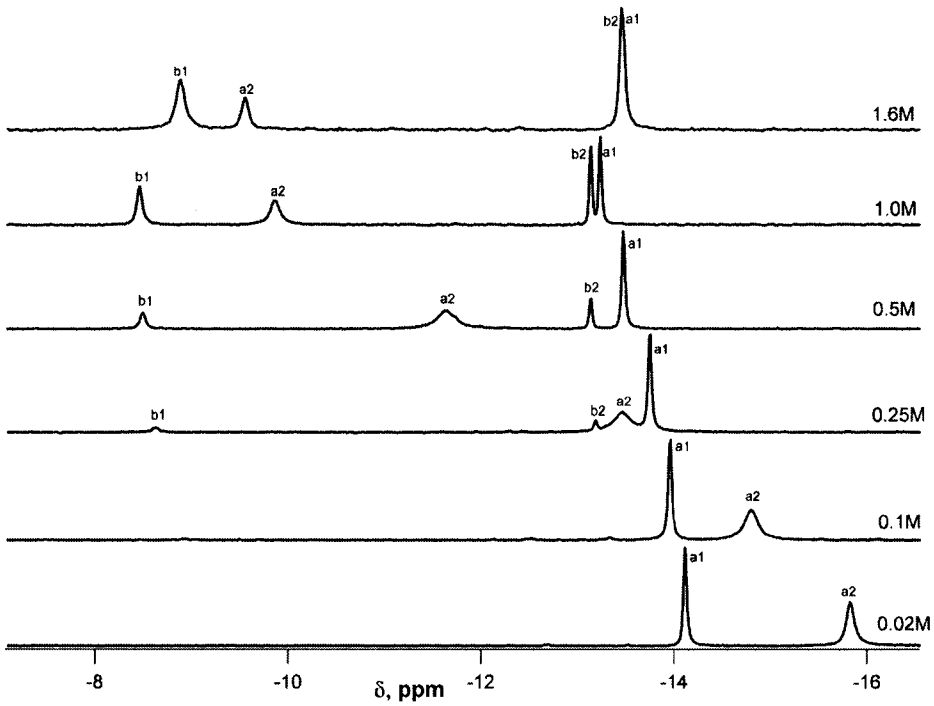

Figure 5. Reaction of Pr^{3+} with $Li_{10}[\alpha_2\text{-}P_2W_{17}O_{61}]$ (1:1 stiochiometry) as a function of concentration of NaOAC.

Figures 11-16 show the ^{31}P NMR spectra for the reaction of Pr(III) with $Li_{10}[\alpha_2\text{-}P_2W_{17}O_{61}]^{10-}$ as a function of both countercation and temperature. The absence of added countercation is shown in **Figure 11** and **Figures 12**, and **Figures 13-15** show the temperature dependence of the reaction with added countercation, Li^+, Na^+, K^+, and Cs^+, respectively. In all cases, upfield shifts are observed for the a2 and b1 resonances (corresponding to P atoms close to site of substitution, for the 1:1 and 1:2 complexes, respectively) and slight downfield shifts are observed for a1 and b2 resonances (corresponding to P atoms remote to the substitution site for the 1:1 and 1:2 complexes, respectively). The variable temperature spectra for the reaction of Pr(III) with $Li_{10}[\alpha_2\text{-}$

$P_2W_{17}O_{61}]^{10-}$ with no added countercation (**Figure 11**) shows that the 1:1 Pr: [α_2-$P_2W_{17}O_{61}]^{10-}$ species is the only species present in this solution, consistent with our earlier results (**Figure 3)**

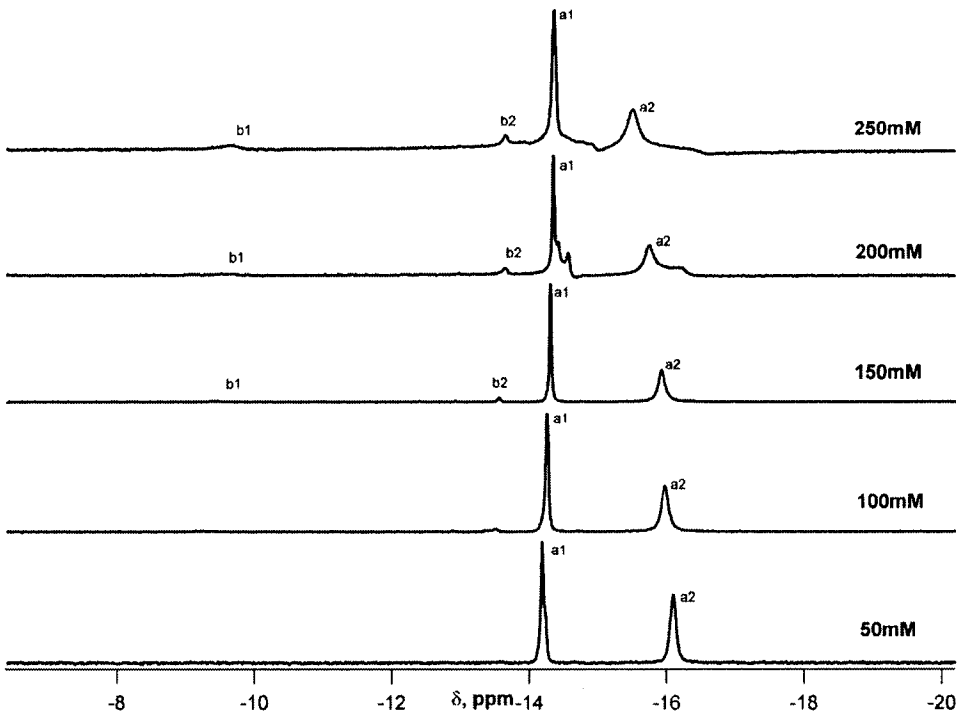

Figure 6. Reaction of Pr^{3+} with $Li_{10}[\alpha_2$-$P_2W_{17}O_{61}]$ (1:1 stiochiometry) as a function of concentration of Pr(α_2-$P_2W_{17}O_{61}$) complex (pH 4.92-5.77)

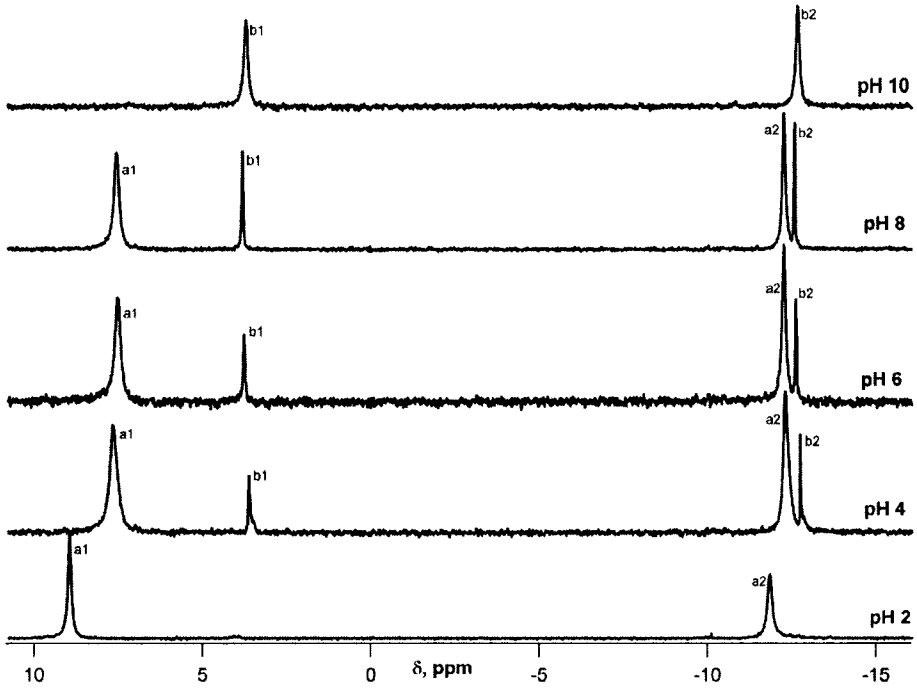

Figure 7. Reaction of Eu3+ with $Li_{10}[\alpha_2\text{-}P_2W_{17}O_{61}]$ (1:1 stiochiometry) as a function of pH at constant ionic strength, with Na+ counterion. ([Li+]= 0.34 M, [Na+] =0.41 M, [Eu3+] = $[\alpha_2\text{-}P_2W_{17}O_{61}10\text{-}]$= 34mM

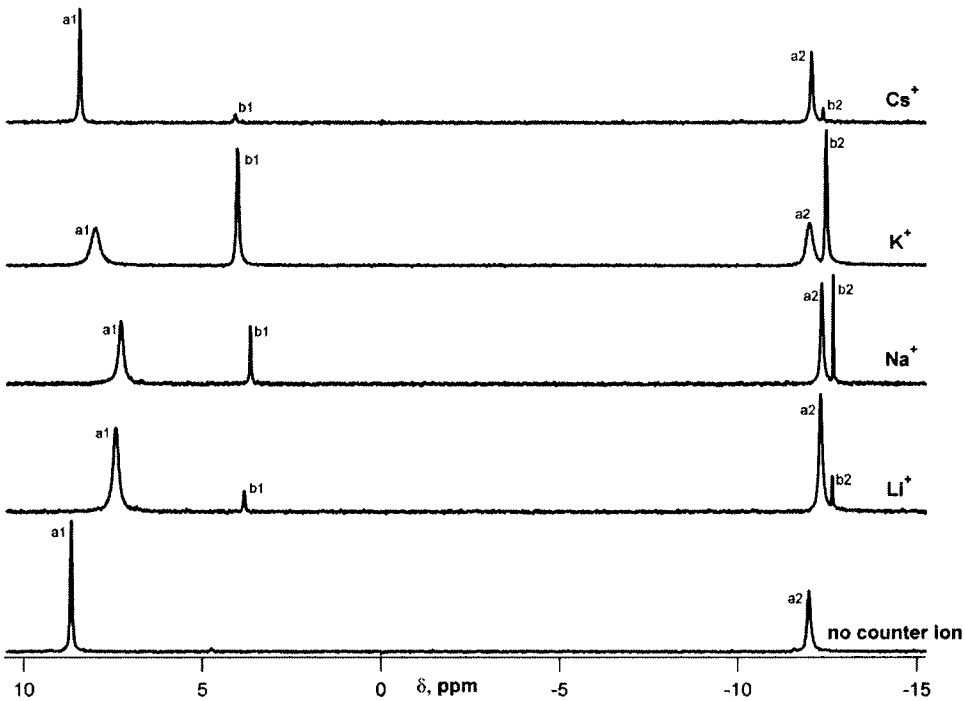

Figure 8. Reaction of Eu3+ with $Li_{10}[\alpha_2\text{-}P_2W_{17}O_{61}]$ (1:1 stiochiometry) as a function of counter cation, pH 4.75, the concentration of Li+, Na+, K+ = 0.5M . Concentratin of Cs+ = 0.05M.

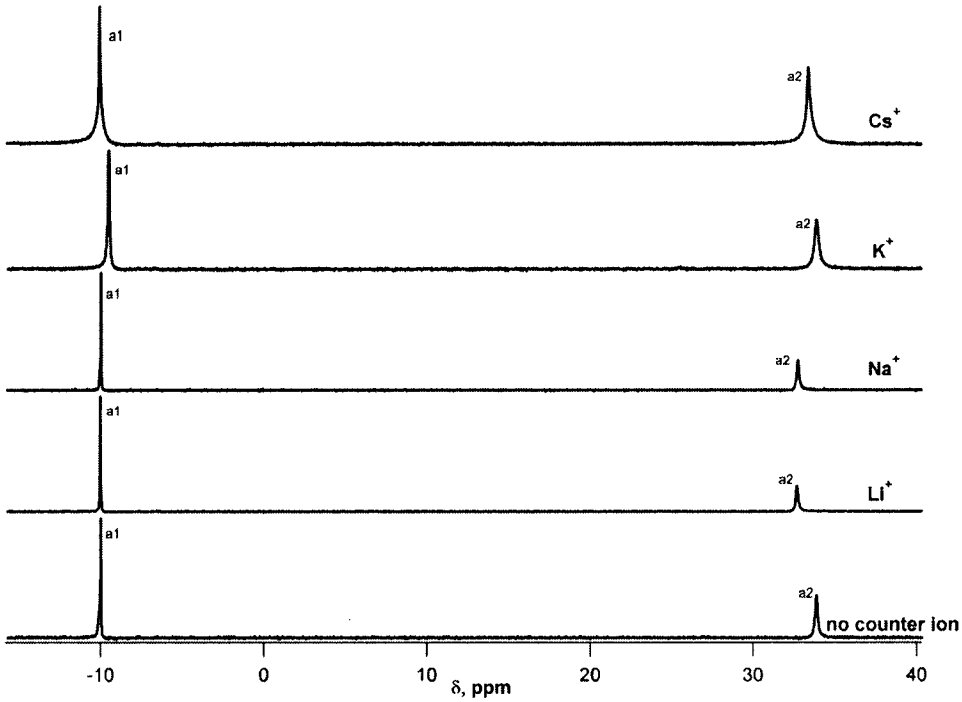

Figure 9. Reaction of Yb3+ with $Li_{10}[\alpha_2\text{-}P_2W_{17}O_{61}]$ (1:1 stiochiometry) as a function of counter cation, pH 4.75, the concentration of Li+, Na+, K+ = 0.5M . Concentratin of Cs+ = 0.05M.

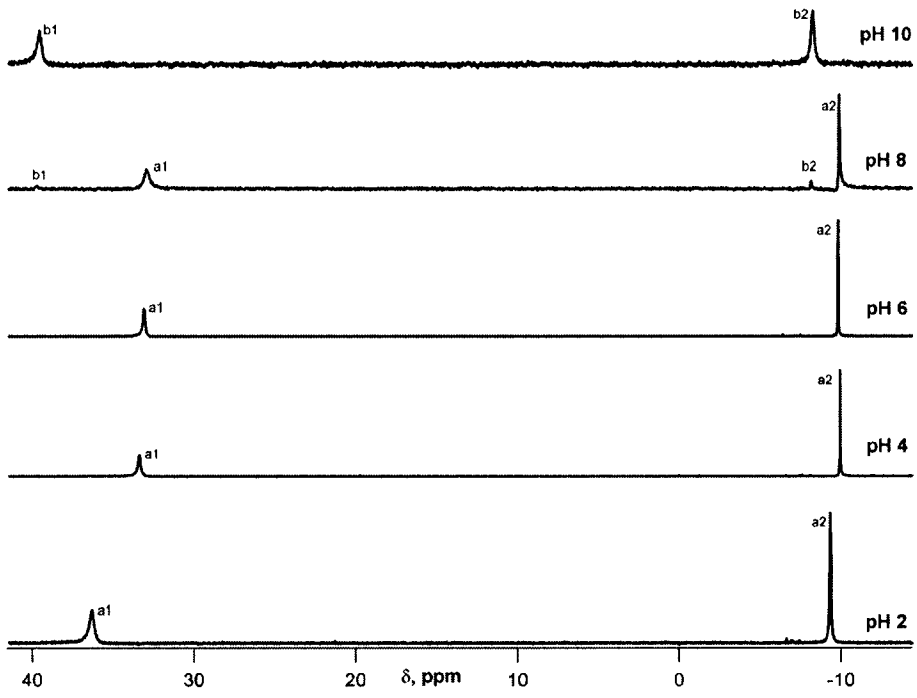

Figure 10. Reaction of Yb3+ with $Li_{10}[\alpha_2\text{-}P_2W_{17}O_{61}]$ (1:1 stiochiometry) as a function of pH at constant ionic strength, with Na+ counterion. ([Li+]= 0.34 M, [Na+] =0.41 M, [Yb3+] = $[\alpha_2\text{-}P_2W_{17}O_{61}10\text{-}]$= 34 mM)

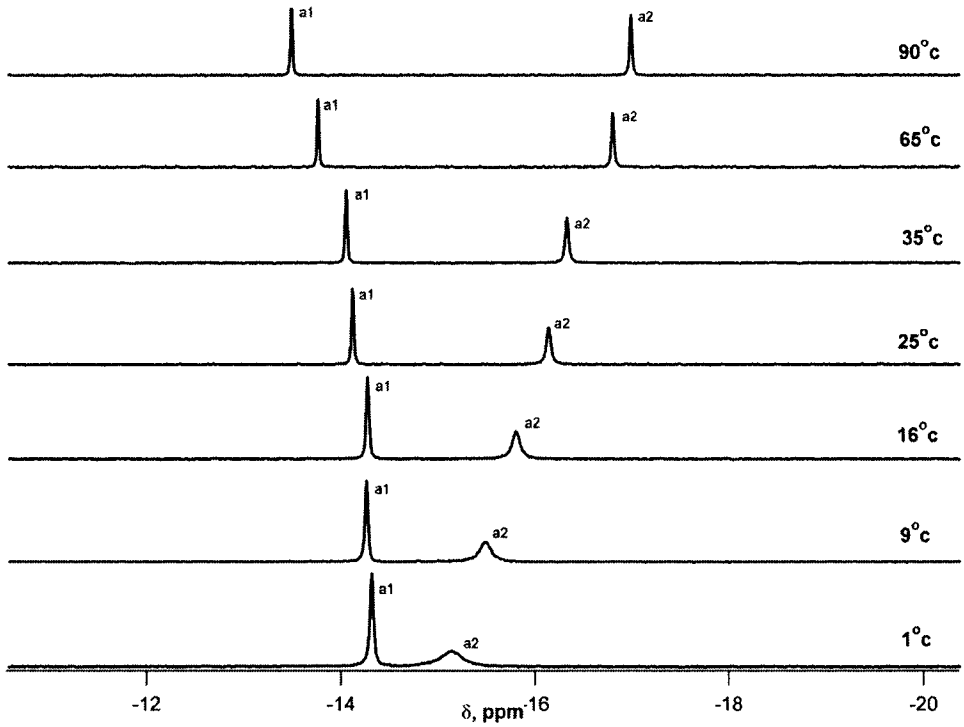

Figure 11. Reaction of Pr^{3+} with $Li_{10}[\alpha_2\text{-}P_2W_{17}O_{61}]$ (1:1 stiochiometry) (no excess counter cation) as a function off temperature

Figure 12 shows the reaction of Pr(III) with $Li_{10}[\alpha_2\text{-}P_2W_{17}O_{61}]^{10-}$ in a LiOAC buffer, as a function of temperature. Here also, consistent with Li^+ stabilizing the 1:1 species, **Figure 3,** only the 1:1 species is observed and the peak that represents the P close to the Pr(III), a2, is highly temperature dependent, shifting upfield with increasing temperature. Both processes represented in **Figures 11** and **13** are reversible.

The temperature dependence for the reaction of Pr(III) with $Li_{10}[\alpha_2\text{-}P_2W_{17}O_{61}]^{10-}$ in a Na^+ and K^+ buffer as a function of temperature, shown in **Figure 13** and **14**, are complicated due to the appearance of both 1:1 and 1:2 species. **Figure 13** shows the reaction of Pr(III) with $Li_{10}[\alpha_2\text{-}P_2W_{17}O_{61}]^{10-}$ in a NaOAc buffer as a function of

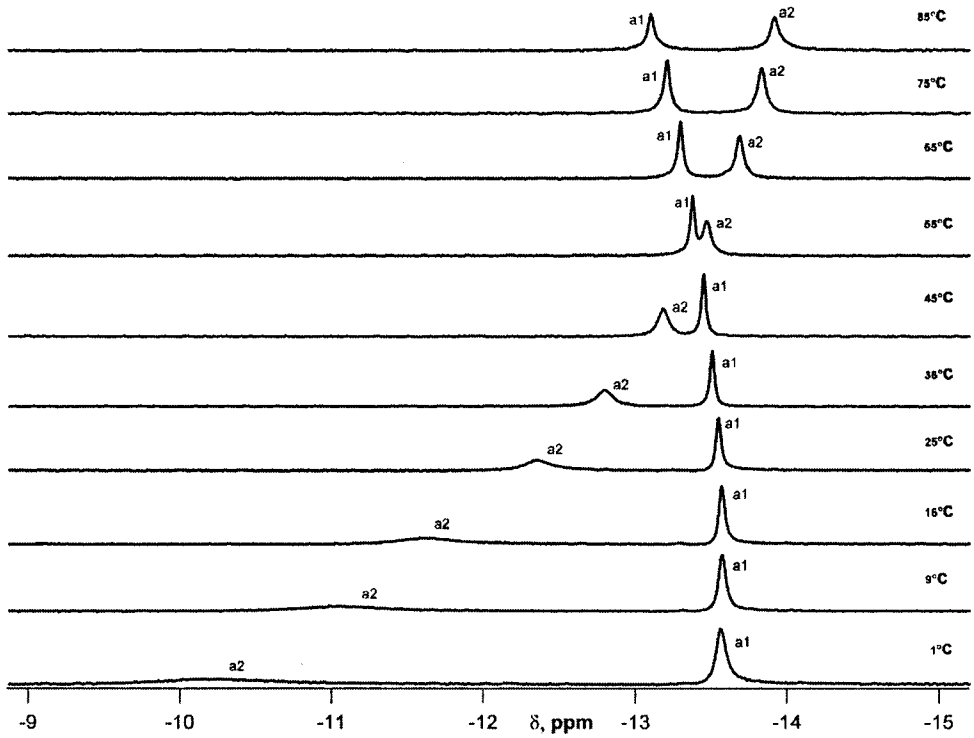

Figure 12. Reaction of Pr^{3+} with $Li_{10}[\alpha_2\text{-}P_2W_{17}O_{61}]$ (1:1 stiochiometry) with LiOAc as a function of temperature

temperature. Consistent with Na^+ promoting the 1:2 formation (**Figures 3** and **5**), at 35°C and lower, both the 1:1 and 1:2 species, are observed. The a2 resonance (1:1 species, P close to paramagnetic center) is highly temperature sensitive, shifting upfield, and b1 (1:2 complex, P close to paramagnetic center) is shifted slightly downfield, while b2 (remote P for 1:2 complex) does not shift significantly. The K^+ buffer promotes significant amounts of the 1:2 complex, shown in **Figure 14**; The peaks for the P atoms of the 1:2 complex do not seem to shift much with temperature, in contrast to the peaks for the 1:1 complex.

Figure 15 shows the temperature dependence for the reaction of Pr(III) with $Li_{10}[\alpha_2\text{-}P_2W_{17}O_{61}]^{10-}$ in a Cs^+ buffer. This is similar to the experiment in pure water, with no added counteraction, **Figure11**, due to the low concentration of Cs^+.

Figure 16 shows the reaction of Pr(III) with $K_{10}[\alpha_2\text{-}P_2W_{17}O_{61}]^{10-}$, in Li^+ buffer, as a function of temperature. This experiment can be compared with **Figure 14**. In both experiments, the K^+ that is at concentrations of 0.34 M or 0.5 M promotes the formation of the 1:2 species.

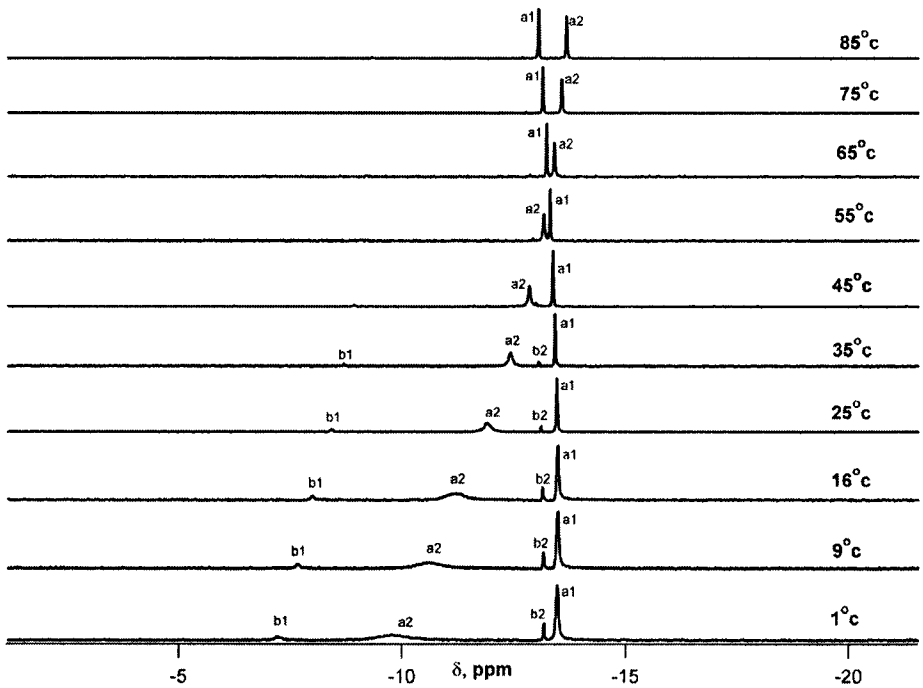

Figure 13. Reaction of Pr^{3+} with $Li_{10}[\alpha_2\text{-}P_2W_{17}O_{61}]$ (1:1 stiochiometry) with NaOAc as a function of temperature.

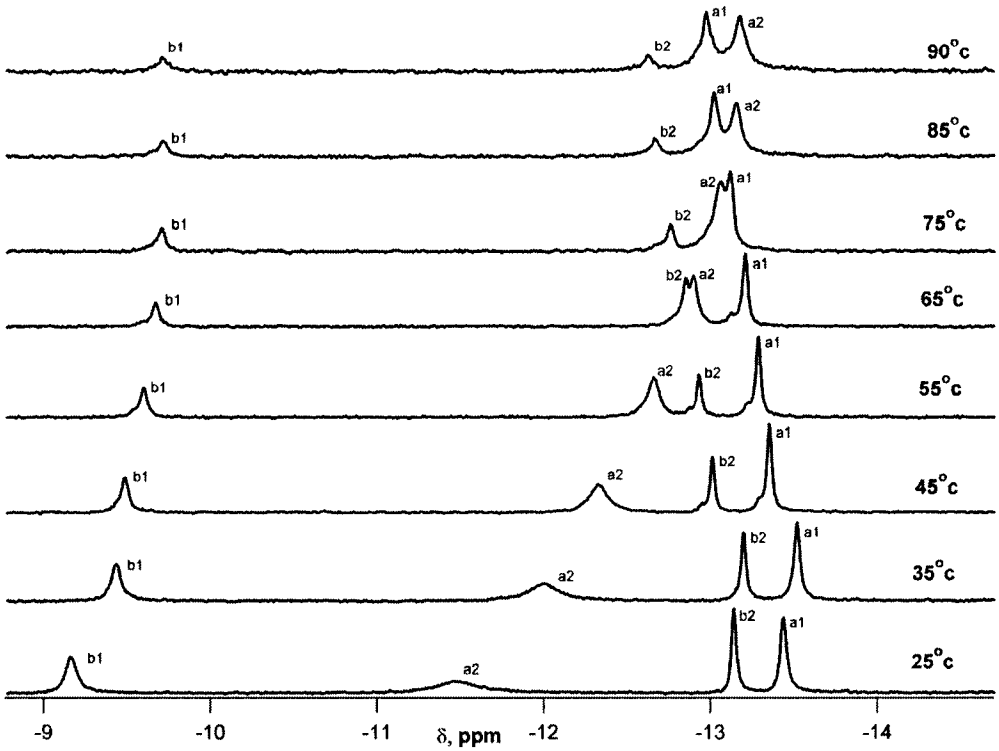

Figure 14. Reaction of Pr^{3+} with $Li_{10}[\alpha_2\text{-}P_2W_{17}O_{61}]$ (1:1 stiochiometry) with KOAc as a function of temperature

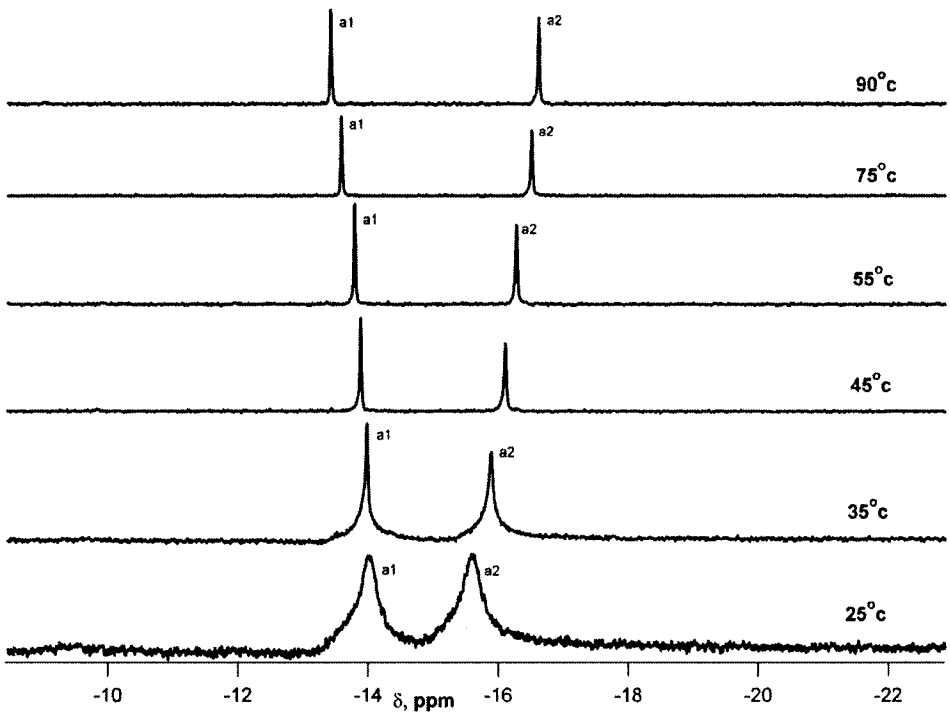

Figure 15. Reaction of Pr^{3+} with $Li_{10}[\alpha_2\text{-}P_2W_{17}O_{61}]$ (1:1 stiochiometry) with CsOAc as a function of temperature

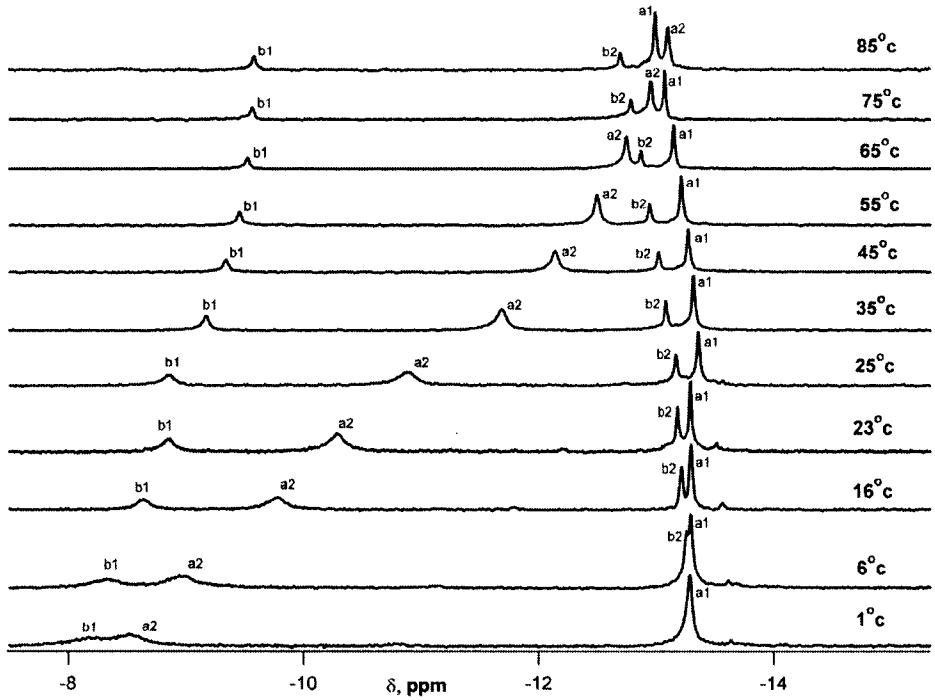

Figure 16. Reaction of Pr3+ with K10[α2-P2W17O61] (1:1 stiochiometry) with LiOAc as a function of temperature

4.3.2.4 Solution Speciation Chemistry: Discussion

It was established by ^{183}W NMR and luminescence studies that the 2:2 Ln (III) : α_2-$P_2W_{17}O_{61}^{10-}$ solid-state dimeric species, both the "cap-to-cap" and the "cap-to-belt" analogs, dissociated into a 1:1 species that can be conveniently represented as $[Ln(H_2O)_4(\alpha_2\text{-}P_2W_{17}O_{61})]^{7-}$. Using ^{31}P NMR spectroscopy, Sadakane observed an equilibrium between this 1:1 species and the 1:2 $[Ce(\alpha_2\text{-}P_2W_{17}O_{61})_2]^{17-}$ species in aqueous solution (pH not specified, countercation, ionic strength not identified) with an equilibrium constant 1.46.[7] The pH, ionic strength and counteractions were not considered in that study. These parameters can have significant effects on the speciation. In our previous report on the mid-late lanthanide complexes of the α_2-$P_2W_{17}O_{61}^{10-}$ species, we observed equilibrium between the 1:1 and 1:2 species in the the luminescence

spectroscopy in water at pH 6.0.[37] This bracketed the 1:1 to 1:2 Eu: α_2-$P_2W_{17}O_{61}^{10-}$ equilibrium to be on the order of micromolar under those aqueous pH 6.0 conditions. [8]

Investigating the equilibria further by ^{31}P NMR spectroscopy under controlled conditions here, we observed that the ^{31}P NMR taken on aqueous solutions of the crystals of the Ce(III) 2:2 analog, prepared via the method reported in reference [7], with no additional electrolyte, showed a pH dependence. The ^{31}P NMR spectrum taken on crystals at neutral to slightly basic pH showed exclusively the 1:1 species, whereas small amounts of the 1:2 species were present at low pH (2). The lanthanides Pr(III) and Nd(III) behave similarly. This behavior was not observed for the 1:1 analogs of the mid to late lanthanides. In the ^{31}P NMR experiment for the mid-late lanthanides, (Eu(III) and Lu(III)) at 10-30 mM of crystalline material, at acidic to neutral pH, exclusively the 1:1 species were found.

An investigation of the speciation of the 1:1 Ln: α_2-$P_2W_{17}O_{61}^{10-}$, across the lanthanide series, employing ^{31}P NMR spectroscopy, was undertaken to understand the speciation properties. Following that, stability constant measurements were determined to fully understand the speciation properties for lanthanide (III) complexes of α_2-$P_2W_{17}O_{61}^{10-}$.

Speciation of Pr(III), Eu(III) and Yb(III) followed by ^{31}P NMR studies, shown in **Figures 3**, **8** and **9**, revealed the significant role of the countercation in the speciation of the 1:1 Ln: α_2-$P_2W_{17}O_{61}^{10-}$ species. For the early (Pr) and mid (Eu) lanthanides, the larger, less extensively hydrated alkali metal cations promote the formation of the 1:2 $[Ln(P_2W_{17}O_{61})_2]^{17-}$. The late lanthanides (Yb) maintain the 1:1 stoichiometry with all counteractions. The hypothesis that large, less extensively hydrated alkali metal cations

bind to the surfaces of the polyoxometalates and "anchor" the POM units in place for assembly into larger structures, such as the 1:2 sandwich structures, has been put forward. Ion pairing of large cations (Rb^+) to POM surfaces was proposed by Kirby and Baker in a study to understand the solution "syn" structure of $Th(\alpha\text{-}2\text{-}P_2W_{17}O_{61})_2^{16-}$. [12] We and others have observed the role of cations on the speciation of $XW_9O_{34}^{n-}$ (X=P,n=9; X=Si, n=10). [11,13] K^+ and Cs^+ exclusively promote 1:2 $[Ln(PW_{11}O_{39})_2]^{13-}$ and $Cs_{15}K(SiW_{11}O_{39})_2$, where K^+ is bound in the cavity. Laronze et al.[13] propose, according to the solid-state crystal structure, that the Cs^+ anchors the $SiW_{11}O_{39}^{8-}$ species in place for the formation of the 1:2 K^+: POM complex. To substantiate this proposal, the solid-state structure of $Cs_{15}K(SiW_{11}O_{39})_2$, shows that three Cs^+ ions are bound to terminal oxygen atoms of each $SiW_{11}O_{39}^{10-}$ unit (with Cs-O distances of ca. 3.2 Å) perhaps stabilizing the $K(SiW_{11}O_{39})_2^{15-}$ solid-state structure. The molecule dissociates in aqueous solution.

Ion pairing of alkali metal cations to polyoxometalates has been quantitated in recent studies. The larger and less extensively solvated alkali-metal cations form smaller (more intimate) association complexes with the $\{X^{n+}VW_{11}O_{40}\}^{(9-n)-}$ (X=P(V), Si(IV), Al(III)) family of polyoxometalates.[14,15] The smaller association complexes impact physical properties of the polyoxometalates, for example the diffusion coefficients and electron transfer rates of organic oxidation reactions. The countercation effect can be further substantiated by our observations on the solution speciation of the 1:2 $Ln(\alpha\text{-}1\text{-}P_2W_{17}O_{61})_2^{14-}$ species.[16] We find that countercations are critical to the formation of 1:2 $Ln(\alpha\text{-}1\text{-}P_2W_{17}O_{61})_2^{14-}$ species in aqueous solution. In these studies, ^{31}P NMR shows clearly that in aqueous solution the 1:2 species is maintained in Cs^+ buffer, whereas an equilibrium between the 1:1 and 1:2 is set up with K^+. Li^+ buffer result in complete

dissociation of the 1:2 $Ln(\alpha\text{-}1\text{-}P_2W_{17}O_{61})_2^{14-}$ species into the 1:1 $Ln(\alpha\text{-}1\text{-}P_2W_{17}O_{61})^{7-}$ species and $(\alpha\text{-}1\text{-}P_2W_{17}O_{61})^{10-}$ ligand. We suspect that the Cs^+ ions and to an extent, the K^+ ions are binding to surface sites of POMs and thus stabilize the 1:2 structures in solution.

It is likely that the ion pairing process gives rise to the temperature dependence of the chemical shift shown in **Figures 11-16**.

Ion pairing effects of organic phthalamide species have been examined by variable temperature NMR studies and Ks, ΔH, and Δ S values can be calculated for the process.[17] For the NMR experiments that involve only one species, i.e. the 1:1 species (**Figures 6** and **11**), this is straightforward. For the experiments where both the 1:1 and 1:2 species are present this may be more complicated. The equilibrium constant, K, for the process can be calculated.[59] Plotting ln K vs 1/T gives the ΔH and ΔS of the process. These are collected in **Table 5**. The ΔH values increase as the countercation concentration increases (from no countercation added to 0.5M Li^+, K^+ or 0.02M Cs^+). The ΔH values increase also from Li^+ and K^+; this is consistent with the increased binding strength of the larger, less extensively hydrated countercations that was found for substituted Keggin ions. [14,15]

The equilibrium constant, K, for the process can be related to the resonance shifts using the equation:

$$\ln\{(\delta_u - \delta)/(\delta - \delta_l)\} = \ln K = \Delta H / RT - \Delta S / R$$

Where δu = upper chemical shift limit

δl = lower chemical shift limit

δ = temperature dependent chemical shift of reference peak

ΔH = process enthalpy

ΔS = process entropy

Data of lnk under different temperature is shown in **Table 6**. Plots of ln K vs 1/T are given in Figure **17** (multiple parts) and ΔH and ΔS values given in **Table 5**.

Table 5. ΔH and ΔS for the reaction of Pr^{3+} with $[\alpha_2\text{-}P_2W_{17}O_{61}]^{10-}$ (1:1 stiochiometry) as a function of counter cation

	No counterion	LiOAc[1]	KOAc[1]	CsOAc[1]	K+LiOAc[2]
ΔH(kJ/mol)	-48.99	-54.15	-65.15	-65.95[1]	-63.99
ΔS(KJ/mol,K)	0.163	0.183	0.210	0.207	0.211

[1] $[Li^+]=[K^+]=0.5M$; $[Cs^+]=0.02M$ and $[Li^+]$ from POM= 0.34M

[2] $[Li^+]$ =0.5M and $[K^+]$ from POM= 0.34M

Table 6. Temperature dependence of Lnk for different counterions

No counterion		Li^+		K^+		Cs^+		$Li^+ + K^+$	
T (K)	lnk	T(K)	lnk	T(K)	lnk	T(K)	lnk	T(K)	lnk
282	1.445123	274	-10.0268	301.2	0.658511	309.3	0.807012	279	2.566805
289.1	0.713098	282	-10.9852	309.4	-0.01391	319.4	-0.05712	289.1	0.966116
301.2	-0.17134	289.1	-11.6079	319.4	-0.72121	329.5	-0.72747	295.7	0.462722
309.4	-0.59598	297.5	-12.3466	329.5	-1.38919	349.5	-2.16569	309.3	-0.80654
339.7	-2.17515	309.4	-12.7983	339.6	-2.10057			319.4	-1.32693
		319.4	-13.1829	349.7	-3.07648			329.5	-1.8836
		329.6	-13.4698					338.5	-2.47414
		339.6	-13.6835					348.6	-3.41188
		349.7	-13.8361						
		359.8	-13.9216						

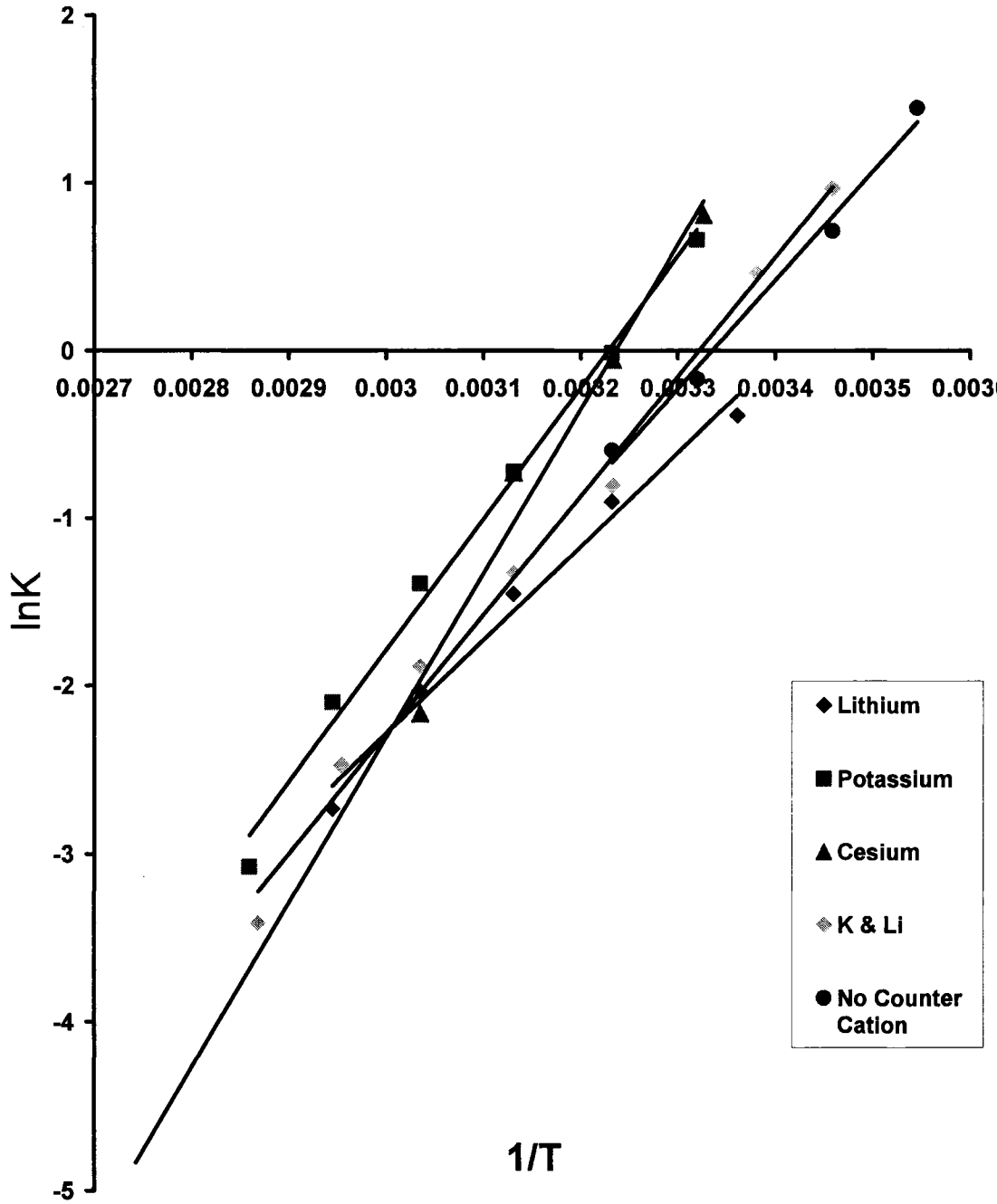

Figure 17. Plot of lnK vs 1/T for different countercation

4.3.2.5 Stability Constant Measurements

To provide more comprehensive understanding of factors that govern complex formation and disposition of the equilibria processes, we sought to measure the formation constants of the lanthanide $[P_2W_{17}O_{61}]^{10-}$ species. Stability constant data will extend and explain the observations made from the ^{31}P NMR solution studies and yield specific information so that we can choose conditions to form 1:1 species, that are important in the rational design of hybrid materials for catalytic and materials applications. Moreover, knowledge of the stability constants and the selectivity of the $[\alpha\text{-}2\text{-}P_2W_{17}O_{61}]^{10-}$ and the $[\alpha\text{-}1\text{-}P_2W_{17}O_{61}]^{10-}$ ligand (following paper) for different lanthanide ions should be transferable to actinide polyoxometalates as models for actinide mineral interactions.

A competitive method, vide supra, using EDTA as the competitive ligand at pH 4.7 was developed to measure K_1 and K_2 for the following equilibria processes. The detailed method development was described in Luo's Ph.D. dissertation.[18] The stability constant data for Ln(III): $\alpha_2\text{-}P_2W_{17}O_{61}$ 1:1 and 1:2 complexes are shown in **Table 6**. The stability constants for Ln(III): $\alpha_2\text{-}P_2W_{17}O_{61}$ 1:1 and 1:2 complexes after acidic and Na^+ corrections are shown in **Table 7**.

$$Pr + (\alpha_2\text{-}P_2W_{17}O_{61})^{10-} \rightleftharpoons [Pr(\alpha_2\text{-}P_2W_{17}O_{61})]^{7-} \quad K_1 \quad (1)$$

$$[Pr(\alpha_2\text{-}P_2W_{17}O_{61})]^{7-} + (\alpha_2\text{-}P_2W_{17}O_{61})^{10-} \rightleftharpoons [Pr(\alpha_2\text{-}P_2W_{17}O_{61})_2]^{14-} \quad K_2 \quad (2)$$

Table 6. Thermodynamic formation constants for Ln(III): $(\alpha_2\text{-}P_2W_{17}O_{61})^{10-}$ 1:1 and 1:2 complexes obtained from ligand-ligand competition studies.

Ln	La	Pr	Nd	Eu
Log K_1	9.27±0.24	9.72±0.10	10.59±0.18	11.38±0.12
Log K_2	8.06±0.22	7.70±0.10	7.67±0.20	6.73±0.10
Log K_1/LogK_2	1.15	1.26	1.38	1.69
Log β2	17.33		18.26	18.01

Table 6. Thermodynamic formation constants for Ln(III): $(\alpha_2\text{-}P_2W_{17}O_{61})^{10-}$ 1:1 and 1:2 complexes obtained from ligand-ligand competition studies (continue).

Ln	Ho	Yb	Lu
Log K_1	12.59±0.10	12.87±0.11	13.76 ±0.14
Log K_2	6.27±0.12	5.60 ±0.10	3.98 ±0.11
Log K_1/LogK_2	2.01	2.30	3.46
Log β2	18.86	18.47	17.74

K1 and *K2* determined from competition experiments, monitored by ^{31}P NMR, using EDTA as a competitive ligand, 25°C. The determination of K1 and K2 was carried out at different pH. For early Ln analogs, the determination of K1 was carried out at pH 2. 2-3.3, for K2, at pH 6.6-6.8. For mid to late Ln analogues, the determination of K1 was carried out at pH 3.3-3.5, for K2, at pH 6.0-6.5.

Although there have been few stability constant determination for lanthanide polyoxometalates, the $XW_{11}O_{39}^{n-}$ and $[\alpha\text{-}2\text{-}P_2W_{17}O_{61}]^{10-}$ (one with $[\alpha\text{-}1\text{-}P_2W_{17}O_{61}]^{10-}$) have received the most attention allowing comparison with this work. Stability constant determination has been achieved previously by absorption spectroscopy[19][20] and potentiometric titrations coupled with electrochemical techniques for the Ce(III)/Ce(IV) couple.[20] There have been two reports using luminescence for Eu(III) analogs: Bion developed a luminescence assay based on emission spectra of Eu(III) / $[\alpha\text{-}2\text{-}P_2W_{17}O_{61}]^{10-}$ combinations.[21] Van Pelt reported determination of stability constants for lanthanide polyoxometalates by using the $^7F_0 \rightarrow {}^5D_0$ selective excitation spectra of solutions containing millimolar concentration of Eu with varying POM concentration.[22] The stability constants of the Eu(III) complexes of the POMs were calculated from the excitation spectra using a modified version of the program SQUAD, originally developed by D.J. Leggett, to calculate stability constants from absorption data. Recently Li reported a competitive method using arsenazo, monitoring the absorption using visible spectroscopy.

Our results show an increase in K1 across the lanthanide series and slight decrease for K2 across the series. The further explaination and investigation of this in terms of previous results and what these data mean in terms of our solution NMR data are in process.

Table 7. Formation constants for Ln(III): α_2-$P_2W_{17}O_{61}$ 1:1 and 1:2 complexes after acidic and Na^+ corrections. Comparison with some published literature values.

Ln	This work			Ref.1			Ref.2 and 3			Ref.4		
	$\log\beta_1$	$\log K_2$	$\log\beta_2$	$\log\beta_1$	$\log K_2$	$\log\beta_2$	$\log\beta_1$	$\log K_2$	$\log\beta_2$	$\log\beta_1$	$\log K_2$	$\log\beta_2$
La	11.07	9.86	2.093	9.34	7.25	16.59	8.25[2]					
Ce				9.66	6.6	16.26	12.4[3]	8.8	21.2[3]	11.5-12.2		
Pr	11.38	9.36	20.75	10.09	6.28	16.37						
Nd	12.41	9.49	21.90	9.73	6.31	16.04	9.30[2]			10.7-12.7		
Sm				8.97	7.29	16.26						
Eu	13.40	8.94	22.34	9.86	8.35	18.21	9.91[2]		18.30[2]	10.35	8.05	18.4
Gd				9.65	7.41	17.06						
Tb				9.84	7.85	17.69						
Dy				10.06	8.55	18.61						
Ho	14.54	8.22	22.75	10.84	17.15	17.99						
Er							9.55[2]					
Yb	15.05	7.83	22.89	9.74	8.19	17.93	9.59[2]					
Lu	15.98	6.22	22.20									

Ref. 1 Y.W.Lu, B. Keita, L. Nadjo, *Polyhedron* 23 (2004) 1579-1586.
Ref. 2 C.E. VanPelt, W.J. Crooks III, G.R. Choppin, *Inorganica Chimica Acta*, 340(2002) 1-7.
Ref. 3 J. P. Ciabrint and R. Contant, xxxx, 1993, 2720-2744
Ref. 4 L. Bion, F. Mercier, P. Decambox, P. Moisy, *Radiochim. Acta*, 1999, 87, 161-166.

4.4 References

(1) a. Sadakane, M.; Dickman, M. H.; Pope, M. T. *Angew. Chem. Int. Ed.* 2000, *39*, 2914-2916. b. Mialane, P.; Lisnard, L.; Mallard, A.; Marrot, J.; Antic-Fidancev, E.; Aschehoug, P.; Vivien, D.; Secheresse, F. *Inorg. Chem.* 2003, *42*, 2102-2108.

(2) a. Muller, A.; Krickemeyer, E.; Bogge, H.; Schmidtmann, M.; Peters, F. *Angew. Chem. Int. Ed.* 1998, *37*, 3360-3365. b. Muller, A.; Sarkar, S.; Shah, S. Q. N.; Bogge, H.; Schmidtmann, M.; Sarker, S.; Kogerler, P.; Hauptfleish, B.; Trautwein, A. X.; Schunemann, V. *Angew. Chem. Int. Ed.* 1999, *38*, 3238-3241. c. Wassermann, K.; Dickman, M. H.; Pope, M. T. *Angew. Chem. Int. Ed. Engl.* 1997, *36*, 1445-1448.

(3) Belai, N.; Sadakane, M.; Pope, M. T. *J. Am. Chem. Soc.* 2001, *123*, 2087-2088.

(4) For key references to lanthanide luminescence: a.Bunzli, J.-C. G. "Luminescent Probes" in Lanthanide Probes in Chemistry, Biology and Earth Sciences; Bunzli, J.-C.G.; Choppin, G. Eds.; 1989; Elsevier, Amsterdam. b. Kido, J.; Okamoto, Y. *Chem. Rev.* **2002**, *102*, 2357-2368. c. Bruce, J. I.; Dickins, R. S.; Govenlock, L. J.; Gunnlaugsson, T.; Lopinski, S.; Lowe, M. P.; Parker, D.; Peacock, R. D.; Perry, J. J. B.; Aime, S.; Botta, M.,*J. Am. Chem. Soc.* **2000**, *122*, 9674-9684. d. Dickins, R. S.; Aime, S.; Batsanov, A. S.; Beeby, A.; Botta, M.; Bruce, J. I.; Howard, J. A. K.; Love, C. S.; Parker, D.; Peacock, R. D.; Puschmann, H*J. Amer. Chem. Soc.* **2002**, *124*, 12697-12705. e. Parker, D.; Dickins, R. S.; Puschmann, H.; Crossland, C.; Howard, J. A. K. *Chem. Rev.* **2002**, *102*, 1977-2010..

(5) For key references to lanthanide Lewis Acid catalysis: a. Aspinall, H. C. *Chem. Rev.* **2002**, *102*, 1807-1850. b. Molander, G. A. *Chemtracts-Organic Chemistry*

1998, *11*, 237-263. c. Molander, G. *Chem. Rev.* **1992**, *92*, 29-68. d. Shibasaki, M.; Yoshikawa, N. *Chem. Rev.* **2002**, *102*, 2187-2209. e. Kobayashi, S.; Kawamura, M. *J. Am. Chem. Soc.* **1998**, *120*, 5840-5841. f. Kobayashi, S. *Pure and Appl. Chem.* 1998, *70*, 1019-1026. g. Aspinall, H. C.; Dwyer, J. L. M.; Greeves, N.; McIver, E. G.; Woolley, J. C. *Organometallics* **1998**, *17*, 1884-1888. h. Xie, W.-H.; Yu, L.; Chen, D.; Li, J.; Ramirez, J.; Miranda, N. F.; Wang, P. G . in *Environmentally Benign Chemistry: Green Chemistry*; Anastas, P. T. and Williamson, T. C., Ed.; Oxford University Press: Oxford, UK, **1998**; Vol. , pp 129-149.

(6) a. Bartis, J.; Dankova, M.; Blumenstein, M.; Francesconi, L. C. *Journal of Alloys and Compunds* 1997, *249*, 56-68. b. Bartis, J.; Sukal, s.; Dankova, M.; Kraft, E.; Kronzon, R.; Blumenstein, M.; Francesconi, L. C. *J. Chem. Soc., Dalton Trans* 1997, 1937-1944. c. Bartis, J.; Dankova, M.; Lessmann, J. J.; Luo, Q.-H.; Horrocks, W. D., Jr.; Francesconi, L. C. *Inorganic Chemistry* 1999, *38*, 1042-1053. e. Luo, Q.; Howell, R. C.; Dankova, M.; Bartis, J.; Williams, C. W.; Horrocks, W. D., Jr.; Young, J., V.G.; Rheingold, A. L.; Francesconi, L. C.; Antonio, M. R. *Inorg. Chem.* 2001, *40*, 1894-1901. f. Luo, Q.; Howell, R. C.; Bartis, J.; Dankova, M.; Horrocks, W. D., Jr.; Rheingold, A. L.; Francesconi, L. C. *Inorg. Chem.* 2002, *41*, 6112-6117.

(7) Sadakane, M.; Ostuni, A.; Pope, M. T. *J. Chem. Soc. Dalton Trans.* 2002, 63-67.

(8) Luo, Q.; Howell, R. C.; Dankova, M.; Bartis, J.; Williams, C. W.; Horrocks, W. D., Jr.; Young, J., V.G.; Rheingold, A. L.; Francesconi, L. C.; Antonio, M. R. *Inorg. Chem.* 2001, *40*, 1894-1901.

(9) Bartis, J.; Dankova, M.; Lessmann, J. J.; Luo, Q.-H.; Horrocks, W. D., Jr.; Francesconi, L. C. *Inorganic Chemistry* 1999, *38*, 1042-1053.

(10) Vogel, A. I. *A text-book of quantitative inorganic analysis_including elementary instrumental analysis*; 3rd edition ed.; Longmans, 1961.

(11) Zhang, C.; Howell, R. C.; Scotland, K. B.; Perez, F. G.; Todaro, L.; Francesconi, L. C. *Inorg. Chem.* 2004, *43*, 7691-7701.

(12) Kirby, J. F.; Baker, L., C.W. *Inorganic Chemistry* 1998, *37*, 5537-5545.

(13) Laronze, N.; Marrot, J.; Herve, G. *Inorg. Chem.* 2003, *42*, 5857-5862.

(14) Grigoriev, V. A.; Hill, C. L.; Weinstock, I. A. *J. Am. Chem. Soc.* 2000, *122*, 3544-3545.

(15) Grigoriev, V. A.; Cheng, D.; Hill, C. L.; Weinstock, I. A. *J. Am. Chem. Soc.* 2001, *123*, 5292-5307.

(16) Cheng, Z.; Howell, R. C.; Luo, Q.; Fieselmann, H. L.; Todaro, L.; Francesconi, L. C. 2004.

(17) Barrett, D. M. Y.; Kawha, I. A.; Mague, J. T.; McPherson, G. L. *J. Org. Chem.* 1995, *60*, 5946-5953

(19) Peacock, R. D.; Weakley, T. J. R. *J. Chem. Soc.* 1971, *A*, 1836-1839.

(20) Ciabrini, J.-P.; Contant, R. *J. Chem. Research (M).* 1993, 2720-2744.

(21) a. Bion, L.; Moisy, P.; Madic, C. *Radiochimica Acta* 1995, *69*, 251-257. b. Bion, L.; Moisy, P.; Vaufrey, F.; Meot-Reymond, S.; Simoni, E.; Madic, C. *Radiochim. Acta* 1997, *78*.

(22) Van Pelt, C. E.; Crooks, W. J., III; Choppin, G. R. *Inorg. Chim. Acta.* 2003, *346*, 215-222.

Chapter 5. Characterization and luminescence studies of ternary complexes of lanthanide polyoxometalates with organic ligands

5.1 Introduction

Complex **1**, $[Eu(H_2O)_3(\alpha_2\text{-}P_2W_{17}O_{61})(Eu_2(H_2O)_7]_4^{4-}$, isolated in this study is a cluster of Eu(III) ions tied together by the $[Eu(\alpha_2\text{-}P_2W_{17}O_{61})]^{7-}$ polyoxometalate, that is formed in a high yield, highly reproducible reaction. We thought that this material would be an excellent crystalline framework to study the effect of the reaction with organic ligands to form ternary complexes that may sensitize the lanthanide luminescence.

Photosensitization of lanthanides is a strategy to produce new sensor materials. Indeed, $EuCl_3$ and $TbCl_3$ have been tested in viscous solution, imbedded in organic ligands, supported on materials or in polymers as sensors for detecting nerve agents[11] , dipicolinic acid (the chemical marker for bacterial spores) [12] and other biological and chemical entities.[13] Polyoxometalates and metal oxides, in general, may offer useful matrices or support materials for lanthanides.

Lanthanide emission bands are very sharp (often a few cm^{-1} in width), yielding pure colors, and are largely independent of coordination environment due to the shielding of the f electrons. The absorption coefficients of lanthanides are very low due to the Laporte-forbidden and often spin-forbidden *f-f* transitions and therefore, lanthanides require direct excitation or photosensitization to observe high luminescence. [14-16]

One way to obtain relatively high luminescence yields is through photoexcitation of the metal oxygen framework of the polyoxometalates with UV light. Using this

technique, Yamase has studied the intramolecular energy transfer processes in polyoxometalloeuropate complexes. Photoexcitation of the O→M (M=Nb,Mo,W) ligand to metal charge transfer (LMCT) bands of the polyoxometalates leads to Eu^{III} emission with single exponential decay. [17] The quantum yield for $[Eu(W_5O_{19})_2]^{9-}$ is the highest found for Eu(III) polyoxometalates. [18]

We propose the use of photosensitizing organic ligands to sensitize the lanthanide luminescence in lanthanide polyoxometalates. In this case, the chromophore absorbs UV light efficiently (large ε) and is excited to the singlet state; intersystem crossing to the triplet state occurs and energy transfer to the lanthanide occurs by a Dexter mechanism[19], resulting in emission from the Ln ion, Scheme 1.

The position of the organic ligand triplet state energy must be 2000 cm^{-1} above the receiving lanthanide 4f state to ensure a fast and irreversible energy transfer.[20] This restricts the range of chromophores to those with high triplet energy and a small S-T energy gap if excitation is to be achieved in the 315 – 430 nm range. The quantum yield depends on the efficiency of the individual steps: the intersystem crossing efficiency, the energy transfer efficiency and the Ln(III) luminescence quantum yield (Scheme 1).

High frequency oscillators, like the O-H, N-H vibrations of the solvent and ligands, play an important role in removing energy nonradiatively from the lanthanide excited state, thus quenching the luminescence. Deactivation of the luminescence from excited Ln^{3+} ions in solution occurs by a vibrational energy-transfer process, involving high-energy vibrations of water molecules- both bound and closely diffusing- or of ligand (N-H) oscillators. To prevent this nonradiative quenching, Ln ions should be shielded by the ligand from their environment.

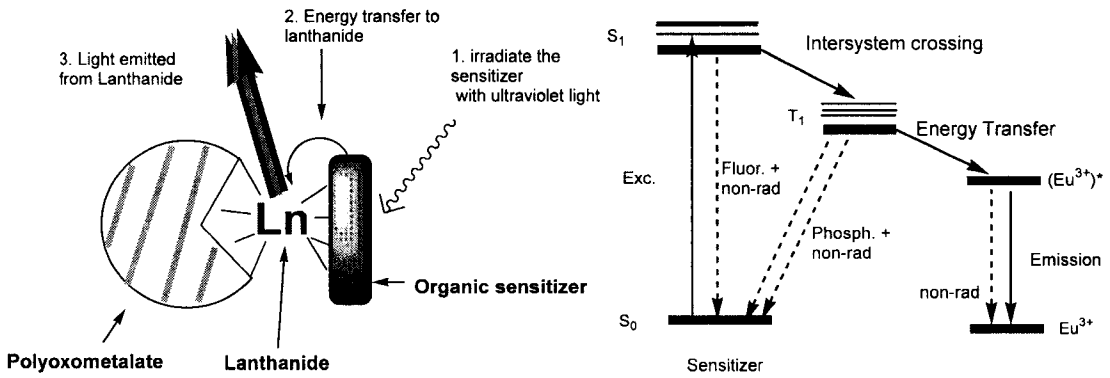

Scheme 1. Left: Concept of Ternary Complex for sensitization of lanthanide luminescence. Right: Energy level diagram of Sensitizer-Eu^{3+} energy transfer process.

Polyoxometalates and metal oxides, in general, may offer excellent matrices or support materials to shield the lanthanide ion/ions from non-radiative removal of energy from the solvent. Much longer lifetimes for excited Er^{3+} ($^4I_{13/2}$), Nd^{3+} ($^4F_{3/2}$) and Yb^{3+} ($^2F_{5/2}$) species have been found in inorganic matrices. We and others have seen that the 1:2 Eu: POM (in our work, the α-1 and α-2 $P_2W_{17}O_{61}^{10-}$) complexes effectively shield the Eu^{3+} from the water solvent and exhibit lifetimes in the millisecond range.

The objective of this work is to incorporate sensitizing organic molecules into lanthanide polyoxometalate complexes to test if the luminescence is enhanced. To achieve this objective we attempted to prepare stable systems wherein the H_2O molecules bound to the lanthanide ion(s) will be replaced by organic sensitizing molecules. Thus, the lanthanide ions will be bound to the sensitizing molecule as well as to the polyoxometalate, in a "ternary" system. We are taking two approaches: 1) to employ the crystal, **1**, as a solid, where the POM anchors the Eu(III) ions in three binding modes, for reaction with organic ligands and 2) to render a simple 1:1 Eu: POM soluble in organic solution and react that with sensitizing ligands. We report here the synthesis and crystal

structure of the cluster, **1**, and preliminary solid-state luminescence data of **1** and the 1:1 $[Eu(\alpha_2\text{-}P_2W_{17}O_{61}]^{7-}$ species, **2**,[21] after reaction with organic ligands and the synthesis, characterization of organic soluble $TBA_3H[EuPW_{11}O_{39}]$, **3**, $TBA_5H_2[Eu(\alpha_1\text{-}P_2W_{17}O_{61}]$, **4**, and $TBA_5H_2[Eu(\alpha_2\text{-}P_2W_{17}O_{61}]$, **5**, and preliminary luminescence data for their titration with the sensitizing ligands, phenanthroline and 2,2'-bipyridine.

5.2 Experimental Section

5.2.1 General

All reagents were commercially available and used without further purification. Elemental analyses were carried out by Inductive Coupled Plasma Atomic Emission Spectrometry (ICP-AES, SPECTROFLAME M120E) using a method described previously. [22] Steady-state emission and excitation spectra were acquired using a Fluorolog ISA JOBIN YVON SPEX Spectrofluorimeter. NMR data were collected as described previously. [22]

5.2.2 Preparation and Crystallization of $[Eu(H_2O)_3(\alpha_2\text{-}P_2W_{17}O_{61})(Eu_2(H_2O)_7]_4^{4-}$ (1).

The lacunary $K_{10}[\alpha\text{-}2P_2W_{17}O_{61}]$ (3.14 g, 0.639 mmol) was dissolved in 30 ml of 0.5 M sodium acetate buffer at pH = 5.5 at 70°C to form a clear solution. $EuCl_3$ (0.82 g, 2.24 mmol) was dissolved in a minimum amount of water and added dropwise to the stirring $K_{10}[\alpha\text{-}2P_2W_{17}O_{61}]$ solution. $AlCl_3$ (3.08 g, 12.77 mmol) was added to the reaction mixture, and the clear solution was allowed to slowly evaporate at room temperature, after one night, colorless small diamond - like crystals were formed. X-ray quality crystals were selected from the bulk crystals. Yield: 2.32 g, 65%. Anal. Calcd for $Al(H_3O)_2[Eu(H_2O)_3(\alpha_2\text{-}P_2W_{17}O_{61})(Eu_2(H_2O)_7]_4Cl{\cdot}20H_2O$; W, 59.82; Eu, 8.16; P, 1.19;

Al, 0.52. Found: W, 61.29; Eu, 8.22; P, 1.20; Al, 0.56. ^{31}P NMR Spectroscopy: H_2O/D_2O:δ, ppm: 8.4391 and 8.3475 and –12.2054.

5.2.3 Sample preparation for solid-state luminescence

1) Cluster, **1**, and 1:1 Eu^{3+}: α_2-$P_2W_{17}O_{61}^{10-}$, **2**, prepared by reacting 0.055 g (0.15 mmol) of $EuCl_3$ and 0.74 g (0.15 mmol) of α_2-$P_2W_{17}O_{61}^{10-}$ in water[21] and precipitating out with ether and methanol, were employed in these studies. Solid samples (0.15 mmol) were suspended in methanol for reaction with organic sensitizing ligands. To wash away any excess Eu^{3+} that may be occluded in the crystals, the solid samples of **1** and **2** were suspended in 1mL of methanol and vortexed; the supernatant was decanted; this procedure was repeated. 2) Solutions of organic sensitizing ligands (phenanthroline, bipyridine, phthalic acid, 0.01M) were made by dissolving the ligands in methanol. Dipicolinic acid was also used and that was a suspension in methanol. Samples of phthalic acid and dipicolinic acid were used as is and also were deprotonated by the addition of a stoichiometric amount of sodium methoxide. The sodium dipicolinate was also a suspension. 3) Suspensions of **1** and **2** were placed into small plastic tubes; the suspensions were centrifuged (5.5 x1000 rpm) for 1 minute, followed by decanting the supernatant. Organic ligands (0.02mL) were added to the solid, followed by 0.1mL of methanol; the suspension was vortexed for 15 seconds and centrifuged. The supernatant was decanted. Two drops of methanol was added to the remaining pellet, resulting in a slurry; the slurry was micropipetted on a microscope slide in a thin layer and allowed to dry. For the control reactions, $EuCl_3$ was suspended in methanol and mixed with a suspension of the organic ligand. The mixture was vortexed for 15 seconds, centrifuged; the supernatant was decanted and the slurry was spread on a microscope slide, as

described above. Excitation and emission spectra were recorded of the microscope slides containing dried suspensions of the Eu polyoxometalates, Eu POMs with organic ligands and control Eu(III) with organic ligands.

5.2.4 Preparation of organic soluble 1:1 Eu(III): POM

5.2.4.1 1:1 Eu(III): ($PW_{11}O_{39}$), $TBA_3H[EuPW_{11}O_{39}]$, 3.

Method A. $EuCl_3 \cdot 6H_2O$ (0.75 g, 2.047 mmol) was dissolved in 10 ml of distilled H_2O. To this solution, $K_7PW_{11}O_{39}$ (6.09 g, 2.047 mmol), dissolved in 25 ml of distilled H_2O at 40°C, was added dropwise. The resulting solution was stirred vigorously for 1 minute followed by the simultaneous addition of 4.62 g of saturated TBABr and 0.2 M HCl to control the pH at 3.6. The mixture was stirred for 1-2 minutes; the white precipitate was separated by filtration, and dried under air suction.

Method B. A solution of $K_7PW_{11}O_{39}$ (6.09 g, 2.047 mmol), dissolved in 25 ml of distilled H_2O at 40°C, was added dropwise to a solution of $EuCl_3 \cdot 6H_2O$ (0.75 g, 2.047 mmol, 10 ml H_2O). The resulting solution was stirred vigorously for a few minutes, followed by the addition of LiCl (0.87 g, 20.47 mmol) and 105 ml of EtOH. A white precipitate formed quickly and was collected by filtration, and dried under suction, ^{31}P NMR shows the formation of only 1:1 $[EuPW_{11}O_{39}]^{4-}$ complex. This white solid was dissolved in 15 ml of H_2O; 4.62 g of saturated TBABr and 0.2 M HCl were simulataneously added dropwise to control the pH at 3.6. The mixture was stirred for 1-2 minutes; the white precipitate was separated by filtration, and dried under air suction.

The protonation states were calculated as described above. Elemental anal. Calcd for $TBA_3H[Eu(H_2O)_4PW_{11}O_{39}]$: Eu, 4.18; W, 55.72; P, 0.85. Found: Eu, 4.36; W, 57.96; P, 0.89. The ^{31}P NMR spectra vary slightly with solution content:^{31}P NMR: δ, 5.6 ppm

(CD_3CN, H_2O), 9.6 ppm, (CD_3CN). This compound is identical to the species isolated from the reaction of Eu(III) and A- $PW_9O_{34}^{9-}$ in H_2O, in both 1:1 or 2:1 Eu: A- $PW_9O_{34}^{9-}$ stoichiometry, with the addition of TBA^+ or TEA^+. [25]

5.2.4.2 1:1 Eu^{3+}: α_1-$P_2W_{17}O_{61}^{10-}$, $TBA_5H_2[Eu(\alpha_1\text{-}P_2W_{17}O_{61}]$, 4.

$K_9Li[\alpha_1\text{-}P_2W_{17}O_{61}]$(3.04 g, 0.612 mmol) was dissolved in 40 ml distilled water at room temperature (~25°C), 806 µl of 0.76 M $EuCl_3$ (0.612 mmol) was added dropwise to the solution of $K_{10}[\alpha_1\text{-}P_2W_{17}O_{61}]$. The resulting solution was stirred for 30 min, then 1.5 g of TBABr in 5ml of distilled water was added dropwise, followed by adding extra 2 g of TBABr as solid into the above solution. The mixture was stirred for 3-4 minutes; the large amount of white precipitate formed by adding about 1.2 mL of Lithium acetate buffer (1M, pH 4.75). The precipitate was separated by filtration, washed with water and dried under air suction.

The protonation states was determined by titration with phenolphthalein[23]: 0.5 g of $TBA_5H_2[Eu(\alpha_1\text{-}P_2W_{17}O_{61}]$ was dissolved in 20 ml of CH_3CN. Argon was bubbled through the solution for at least 15 mins to remove any dissolved CO_2 after which time the solution was kept under a constant argon stream above the solution surface to prevent dissolution of atmospheric CO_2. Three drops of phenolphthalein indicator were added and the solution was titrated to a phenolphthalein endpoint with 0.05874 M of aqueous TBAOH. Elemental anal. Calcd for TBA_5H_2 $[Eu(H_2O)_4(\alpha_1\text{-}P_2W_{17}O_{61})]$: Eu, 2.39; W, 49.18; P, 0.97. Found: Eu, 2.51; W, 51.68; P, 1.02. Multinuclear NMR data: ^{31}P NMR: CD_3CN, δ, 5.14, -12.64 ppm are assigned to the TBA salt of $[Eu(\alpha_1\text{-}P_2W_{17}O_{61})]^{7-}$ in organic solvent, the chemical shifts are comparable with the δ 6.3, -12.5 ppm of the well-characterized $[Eu(\alpha_1\text{-}P_2W_{17}O_{61})]^{7-}$ in aqueous solution.[24] ^{183}W NMR reported for

TBA_5H_2 $[Lu(\alpha_1\text{-}P_2W_{17}O_{61})]^{7-}$ are consistent with the the 1:1 $[Lu(\alpha_1\text{-}P_2W_{17}O_{61})]^{7-}$ structure. [24]

5.2.4.3 1:1 Eu^{3+}: $\alpha_2\text{-}P_2W_{17}O_{61}^{10-}$, $TBA_5H_2[Eu(\alpha_2\text{-}P_2W_{17}O_{61}]$, 5.

$K_{10}[\alpha_2\text{-}P_2W_{17}O_{61}$ (3.00 g, 0.610 mmol) was dissolved in 40 ml of distilled H_2O at 70°C, $EuCl_3{\cdot}6H_2O$ (0.224 g, 0.610 mmol) was dissolved in minimum amount of distilled H_2O, and was added dropwise to the solution of $K_{10}[\alpha_2\text{-}P_2W_{17}O_{61}$. The resulting solution was stirred vigorously for 1 minute. Adjust the pH of the solution at 4.3 with 0.2 M HCl, then 1.5 g of saturated TBABr and 0.2 M HCl was added dropwise at the same time to keep the pH at 4.3. The mixture was stirred for 1-2 minutes; the white precipitate was separated by filtration while solution was hot, washed with water and dried under air suction.

5.2.5 Characterization of $TBA_3H[EuPW_{11}O_{39}]$, $TBA_5H_2[Eu(\alpha_2\text{-}P_2W_{17}O_{61}]$ and $TBA_5H_2[Eu(\alpha_1\text{-}P_2W_{17}O_{61}]$ by ^{31}P NMR

NMR spectra were obtained on a Jeol GX-400 spectrometer. ^{31}P NMR spectra at 161.8 MHz were acquired using the broad band decoupler coil of a 5 mm inverse detection probe. Typical acquisition parameters for ^{31}P spectra included: spectral width: 10, 000 Hz; acquisition time: 0.8 s; pulse delay: 1 s; pulse width: 50 μsec. From 200 to 2000 scans were acquired. For all spectra, the temperature was controlled at 20±0.5°C. ^{31}P NMR were referenced to 85% H_3PO_4. For ^{31}P chemical shifts, the convention used is that the more negative chemical shift denote up field resonance. All the samples were prepared in ACN-d3.

5.2.6 Determination of stock concentration of $TBA_3H[EuPW_{11}O_{39}]$, $TBA_5H_2[Eu(\alpha_2\text{-}P_2W_{17}O_{61}]$ and $TBA_5H_2[Eu(\alpha_1\text{-}P_2W_{17}O_{61}]$ in acetonitrile by ICP.

i) *Standard solution preparation.* The standard solution of P (0.2, 0.4, 0.6, 0.8, 1.2 ppm), Eu (1, 2, 4, 6 ppm), La (1, 2, 4, 6 ppm), W (20, 40, 60, 80, 120 ppm), Al (0.5, 1, 1.5, 2.5 ppm), Na (1, 3, 5, 7 ppm), and K (1, 3, 5, 7 ppm) was prepared by diluting 1000 ppm ICP standard solution (GFS Chemicals, Inc.) with distilled water. ii) *Sample preparation.* Crystals of complex $[Ln(\alpha\text{-}1\text{-}P_2W_{17}O_{61})_2]^{17-}$ ($Ln=La^{3+}$, Eu^{3+}) were collected by filtration, and were placed in uncovered, carefully labeled, small vials, then were put into a dessicator ($CaSO_4$ as drying agent), vacuum for 1.5 hour. The samples were left in the closed evacuated dessicator overnight. Afterwards, 0.0148 g of $[Eu(\alpha\text{-}1\text{-}P_2W_{17}O_{61})_2]^{17-}$ and 0.0106 g of $[La(\alpha\text{-}1\text{-}P_2W_{17}O_{61})_2]^{17-}$ was dissolved in a 25 ml volumetric flask with distilled water. 2 and 4 ml of solution from each flask was filled in to 25 ml of volumetric flask individually to make ICP samples. iii) *Method*: The sensitive wavelength for different element was selected (P: 213.618 nm; Eu: 381.970 nm; La: 379.478 nm, W: 239.709 nm; Na: 589.592 nm; K: 766.496 nm). A calibration curve for each element was constructed. The measurement of each sample was then performed.

5.2.7 Single Crystal X-ray Structure Determination.

Crystals of **1** was examined under a thin layer of mineral oil using a polarizing microscope. Selected crystals were mounted on a glass fiber and quickly placed in a stream cold nitrogen on a Bruker SMART CCD diffractometer equipped with a sealed tube Mo anode (K_∂ radiation, λ=0.71073 Å) and graphite monochromator or Nonius Kappa CCD diffractometer. The data were collected at around 100K. The SHELX package of software was used to solve and refine the structure. [26] The heaviest atoms were located by direct methods, and the remaining atoms were found in subsequent

Table 1. Crystal Data and Structure Refinement for the Complex **1**

	1
empirical formula	Al Cl Eu_{12} O_{376} P_8 W_{68}
Fw	5257.70
cryst syst	monoclinic
space group	P2(1)/n
temp, K	100 (2)
wavelength, Å	0.71073
a, Å	17.378(4)
b, Å	23.650(5)
c, Å	19.124(4)
α, deg	90
β, deg	101.41(3)
γ, deg	90
Vol, $Å^3$	7705(3)
Z	4
calcd density, g/cm^3	4.491
abs coeff, mm^{-1}	27.889
F (000)	9036
θ range, deg	2.10 to 20.82
limiting indices	$-17 \le h \le 17, -23 \le k \le 23, -19 \le l \le 19$
Reflns collected/unique	30967 / 8051 [R(int)=0.0675]
Refinement meth	full-matrix least- squares on F^2
data/ restraints/ parameters	8051 / 0 / 583
GOF on F^2	1.067
final R indices [$I>2\sigma(I)$]	R1= 0.0657, wR2=0.1727
R indices (all data)	R1=0.0737, wR2= 0.1818
largest diff.peak and hole ($eÅ^{-3}$)	4.652 and -8.644

Fourier difference syntheses. For the ammonium salt 1, the data did not support discrimination between oxygen and nitrogen atoms. All refinements were full-squares on F^2. Crystal data and structure refinement parameters for 1 are listed in Table 1s. Selected bond distances for 1 are given in Table 2. The final thermal parameters for oxygen atoms in the encapsulated phosphate are very small (<0.0001) and thus beyond the lower limit of the defined thermal parameter. As a result there is a remaining shift of 0.25 for Uij in the final structure.

5.2.8 Luminescence Spectroscopy

5.2.8.1 Solid State

The excitation spectra for each sample were measured by scanning over the range 250 to 500 nm while monitoring the emission at 614 nm. The Eu(III) emission spectra were measured by exciting at 280 nm and using a longpass filter (OG-570 nm, size 50.80 x 50.80, thickness 2.00 mm) to avoid interference from harmonic doubling.

5.2.8.2 Solution

Luminescence excitation spectra and emission spectra of titrating $TBA_3H[EuPW_{11}O_{39}]$, $TBA_5H_2[Eu(\alpha_2\text{-}P_2W_{17}O_{61}]$ and $TBA_5H_2[Eu(\alpha_1\text{-}P_2W_{17}O_{61}$ with organic ligands (1, 10-Phenanthroline and 2, 2'-Dipyridyl) were measured using Fluorespectrometer. The excitation (monitored at 614 nm) and emission (excited at 319 nm) spectra were collected at each data point. The relative luminescence intensity was plotted as a function of added ligand.

5.2.8.2.1 Titrating $TBA_3H[EuPW_{11}O_{39}]$ with 1, 10-Phenanthroline

605 μl of 0.009336 M $TBA_3H[EuPW_{11}O_{39}]$ stock solution (concentration was determined by ICP measurements of Eu, P, W) and 1395 μl of ACN was placed in a clean 0.5 ml of luminescence cuvatte. Using a volumetric pipette, a total of 22.38 mmol of 1, 10-Phenanthroline ACN solution was added in 20 μl (N0.1-20) and 40 μl (No.21-30) increments of 0.02797 M 1, 10-Phenanthroline stock solution.

5.2.8.2.2 Titrating $TBA_3H[EuPW_{11}O_{39}]$ with 2, 2'-Dipyridyl

310 μl of 0.009336 M $TBA_3H[EuPW_{11}O_{39}]$ stock solution and 2190 μl of ACN was placed in a clean 0.5 ml of luminescence cuvatte. Using a volumetric pipette, a total of 11.26 mmol of 2, 2'-Dipyridyl ACN solution was added in 15 μl (No.1-10), 20 μl (No.11-14) and 40 μl (No. 15-18) increments of 0.02888 M 2, 2'-Dipyridyl stock solution.

5.2.8.2.3 Titrating $TBA_5H_2[Eu(\alpha_2\text{-}P_2W_{17}O_{61}]$ with 1, 10-Phenanthroline

400 μl of 0.01382 M $TBA_5H_2[Eu(\alpha_2\text{-}P_2W_{17}O_{61}]$ stock solution and 2100 μl of ACN was placed in a clean 0.5 ml of luminescence cuvatte. Using a volumetric pipette, a total of 21.25 mmol of 1, 10-Phenanthroline ACN solution was added in 15 μl (No.1-10), 20 μl (No.11-15) and 40 μl (No. 16-17) increments of 0.05593 M 1, 10-Phenanthroline stock solution.

5.2.8.2.4 Titrating $TBA_5H_2[Eu(\alpha_1\text{-}P_2W_{17}O_{61}]$ with 1, 10-Phenanthroline

358 μl of 0.01589 M $TBA_5H_2[Eu(\alpha_1\text{-}P_2W_{17}O_{61}]$ stock solution and 2142 μl of ACN was placed in a clean 0.5 ml of luminescence cuvatte. Using a volumetric pipette, a total of 22.77 mmol of 1, 10-Phenanthroline ACN solution was added in 15 μl (No.1-8), 20 μl (No.9-14) and 40 μl (No. 15-18) increments of 0.05693 M 1, 10-Phenanthroline stock solution.

5.2.8.2.5 Titrating $TBA_5H_2[Eu(\alpha_1\text{-}P_2W_{17}O_{61}]$ with 2, 2'-Dipyridyl

360 μl of 0.01589 M $TBA_5H_2[Eu(\alpha_1\text{-}P_2W_{17}O_{61}]$ stock solution and 2140 μl of ACN was placed in a clean 0.5 ml of luminescence cuvatte. Using a volumetric pipette, a total of 22.88 mmol of 2, 2'-Dipyridyl ACN solution was added in 20 μl (No.1-2), 40 μl (No.3-11) and 80 μl (No. 12-18) increments of 0.02888 M 2, 2'-Dipyridyl stock solution.

5.2.8.2.6 Titrating $EuCl_3 \cdot 6H_2O$ with 1, 10-Phenanthroline

285 μl of 0.0197 M $EuCl_3 \cdot 6H_2O$ stock solution and 2215 μl of ACN was placed in a clean 0.5 ml of luminescence cuvatte. Using a volumetric pipette, a total of 22.37 mmol of 1, 10-Phenanthroline ACN solution was added in 20 μl (N0.1-12) and 40 μl (No.13-16) increments of 0.05593 M 1, 10-Phenanthroline stock solution.

5.3 Results and Discussions

5.3.1 Solid-State Chemistry

5.3.1.1 Description of Crystal Structure

The polyoxometalate unit in the crystal structure of **1** is the 1:1 $[Eu(H_2O)_3(\alpha_2\text{-}P_2W_{17}O_{61})]_2^{14-}$ where the Eu^{3+} (Eu2) ions are each substituted for a $[WO]^{4+}$ unit in the "cap" region of the tungsten-oxygen framework of the parent Wells-Dawson ion. In the solid-state, the Eu(III) ions are bound to four oxygen atoms of the POM and to three water molecules. To complete eight coordination, the Eu(III) ions are also bound to terminal W=O of the "belt" region of the adjacent $[Eu(H_2O)_3(\alpha_2\text{-}P_2W_{17}O_{61})]^{7-}$ unit, thus forming the dimeric unit. The bond lengths of the Eu2-$O_{bridging}$ and Eu2-O_{H2O} in the vacancy average 2.360 Å and 2.456 Å, respectively. These bond lengths as well as the Eu2-O_{H2O} bond length of 2.451 Å are similar to other $[Eu(H_2O)_3(\alpha_2\text{-}P_2W_{17}O_{61})]_2^{14-}$ species. [21,25]

The dimeric structure of **1** is similar to the crystal structure of the 1:1 $[Eu(H_2O)_3(\alpha_2\text{-}P_2W_{17}O_{61})]_2^{14-}$ prepared by reacting $(\alpha_2\text{-}P_2W_{17}O_{61})^{10-}$ with a slight excess of Eu(III) [Luo, 2002 #380] and also similar to the 1:1 $[Eu(H_2O)_3(\alpha_2\text{-}P_2W_{17}O_{61})]_2^{14-}$ prepared by reaction of A-α-$PW_9O_{34}^{9-}$ with Eu(III) and Al(III) under acidic conditions. [25] The structure of **1** is distinguished from those $[Eu(H_2O)_3(\alpha_2\text{-}P_2W_{17}O_{61})]_2^{14-}$ crystalline complexes due to the surface bound Eu(III) ions, Eu1 and Eu3, that are themselves, bound to at least six and four water molecules respectively.

Eu1 and Eu3 are bound to the terminal W=O oxygen atoms in the same "cap" region that is substituted with Eu2. The monomeric unit, showing the three nonequivalent Eu^{3+} ions is presented in Figure 1. The dimeric unit, including the surface bound Eu(III) ions and the Al(III) bound to a terminal W=O in a cap that is remote from the substitution site is shown in Figure 2 (A).

The two surface bound aquated Eu(III) ions (Eu1 and Eu3) further connect the $[Eu(H_2O)_3(\alpha_2\text{-}P_2W_{17}O_{61})]_2^{14-}$ units. This is shown in Figure 2, B and C, where, the dimeric unit is viewed along the a and c crystal axes, respectively. The aquated Eu1 of one dimer connects to Eu3 of another dimer via an oxo bridge to form a network of dimeric $[Eu(H_2O)_3(\alpha_2\text{-}P_2W_{17}O_{61})]_2^{14-}$ units. This network, viewed along the crystallographic a axis, is shown in Figure 3; some of the dimeric units are shown in boxes.

5.3.1.2 ^{31}P NMR

There is slight difference on the ^{31}P NMR spectroscopy compared with that of 1:1 $[Eu(H_2O)_3(\alpha_2\text{-}P_2W_{17}O_{61})]_2^{14-}$. [21] The downfield peak found at 8.23 ppm on the K^+ salt of the dimer is split into doublet at 8.4391 and 8.3475 ppm in this new compound, **1,**

indicating the slight difference of the environment of P atom which is close to Eu^{3+} binding site in the molecule.

Table 2. Selected Bond Lengths (Å) for Eu-O bonds in complex **1.**

Eu1		**Eu2**		**Eu3**	
Eu(1)-O(67)	2.35(6)	Eu(2)-O(23)	2.33(2)	Eu(3)-O(51)	2.36(2)
Eu(1)-O(28)	2.41(2)	Eu(2)-O(22)	2.36(2)	Eu(3)-O(75)	2.38(9)
Eu(1)-O(63)	2.47(5)	Eu(2)-O(48)	2.37(2)	Eu(3)-O(73)	2.43(8)
Eu(1)-O(68)	2.49(10)	Eu(2)- O(50)	2.39(2)	Eu(3)-O(64)#1	2.75(6)
Eu(1)-O(65)	2.49(4)	Eu(2)-O(71)	2.45(2)	Eu(3)-O(72)	2.77(15)
Eu(1)-O(62)	2.50(4)	Eu(2)-O(55)#2	2.45(2)	Eu(3)-O(74)	3.2(2)
Eu(1)-O(64)	2.52(6)	Eu(2)-O(70)	2.46(3)		
		Eu(2)-O(69)	2.46(3)		

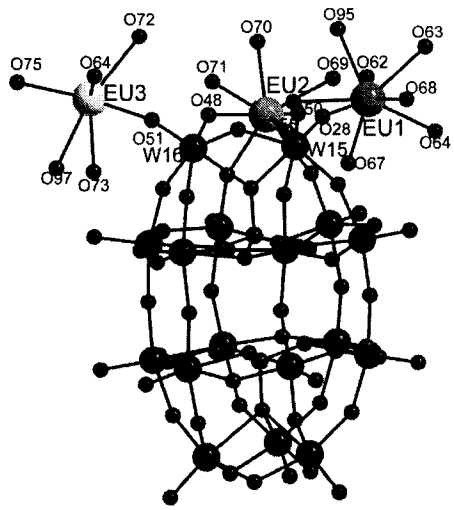

Figure 1. Representation of the monomeric unit of 1, $[Eu(H_2O)_3(\alpha_2\text{-}P_2W_{17}O_{61})(Eu_2(H_2O)_7]^-$, as 50% ellipsoids, showing the types of Eu(III) atoms in the structure. One Eu(III) is bound in the (α_2-$P_2W_{17}O_{61}$) defect. The other two Eu(III) are bound to terminal W=O atoms from the "cap" region. Legend: W: blue; O: red; Eu (cyan: Eu2 incorporated into defect, green: Eu1 that is 8-coordinate, yellow: Eu3 that is 6-coordinate); P: purple

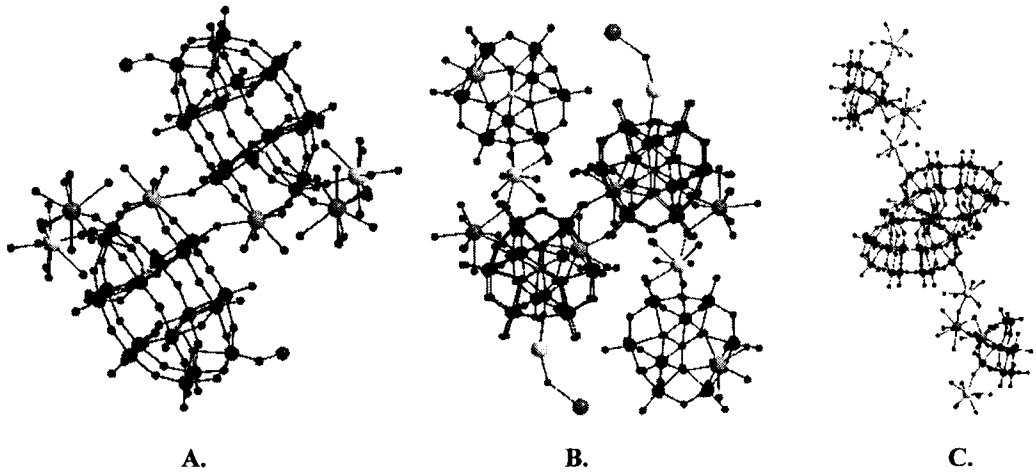

Figure 2. Representation of the polyoxometalate unit of 1, $[Eu(H_2O)_3(\alpha_2\text{-}P_2W_{17}O_{61})(Eu_2(H_2O)_7]_4^{4-}$, as 50% ellipsoids, showing the $[Eu\ (\alpha_2\text{-}P_2W_{17}O_{61})]_2^{14-}$ cluster and connectivity of the two surface bound Eu(III) ions. **A**. The dimeric unit including the surface bound Eu(III) ions. Eu2 is colored green and Eu3 is colored yellow. An Al(III) ion is bound to a terminal W=O in the remote cap. **B**. The dimer viewed along the a crystal axis showing the connectivity of the surface bound Eu2. C. the dimer viewed along the c axis showing the connectivity of the surface bound Eu3.

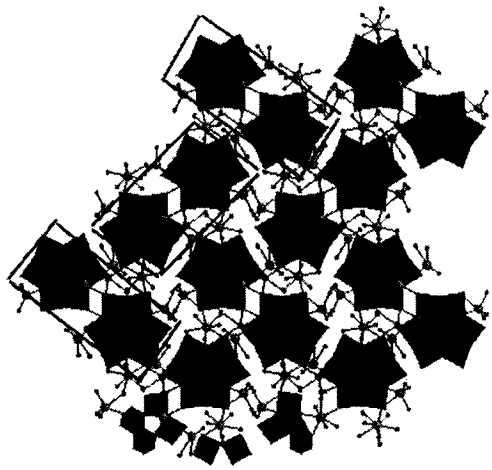

Figure 3. Representation of the polyoxometalate unit of 1, $[Eu(H_2O)_3(\alpha_2\text{-}P_2W_{17}O_{61})(Eu_2(H_2O)_7]_4^{4-}$, viewed along the crystallographic a axis, showing the extended structure. Boxes surround some of the dimeric units.

5.3.1.3 Solid-State Luminescence

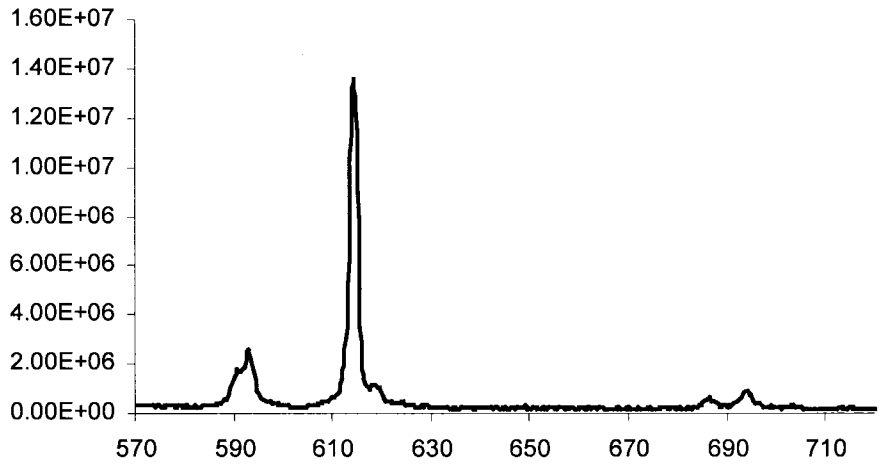

Figure 4. Emission spectrum of cluster **1** reacted with sodium dipicolinate in methanol. Excitation wavelength: 280 nm.

All of the organic ligands that were reacted with the cluster, **1** and the 1:1 $[Eu(H_2O)_3(\alpha_2\text{-}P_2W_{17}O_{61})]_2^{14-}$, **2**, behaved in a similar fashion, sensitizing the Eu(III) in **1** and **2**. Figure 4 shows a typical example of the solid-state emission spectrum of a suspension of the cluster, **1**, contacted with a suspension of sodium dipicolinate. Upon excitation at 280 nm, the emission spectra all showed a peak at 614 nm, assigned to the hypersensitive $^5D_0 \rightarrow {}^7F_2$ transition that results in the typical red emission of Eu(III). Also observed are broad peaks in the region of 590 nm; these are typically assigned to non-degenerate $^5D_0 \rightarrow {}^7F_0$ transitions, where each sharp band represents an unique Eu(III) environment. This band is broad and likely represents more than one Eu(III) chemical environment. Usually, high resolution spectra are required to identify the Eu(III) speciation in this region. The electric dipole allowed $^5D_0 \rightarrow {}^7F_4$ transition is found at 690 nm.

The excitation spectrum for this sample, Figure 5, clearly shows a strong, broad band at 280 nm, that is assigned to the organic sensitizing ligand and a sharp band at 394 nm; the latter band arises from the Eu POM framework and has been observed in solid state excitation spectra of $Eu(P_2W_{17}O_{61})_2^{17-}$. Eu(III) complexes of $PW_{11}O_{39}^{7-}$ also show this feature. Also, the typical oxygen to metal charge transfer bands usually found in polyoxometalate Eu(III) complexes in the 250-360 nm range are absent for $Eu(P_2W_{17}O_{61})_2^{17-}$ [27,28] and $Eu(PW_{11}O_{39})_2^{13-}$ [29]; each show only a feature at 394 nm with some broader features to higher energy. The observation of these bands at ca. 394 suggests that the Eu(III) polyoxometalate part is contributing to the luminescence along with the excitation into the organic sensitizing moiety.

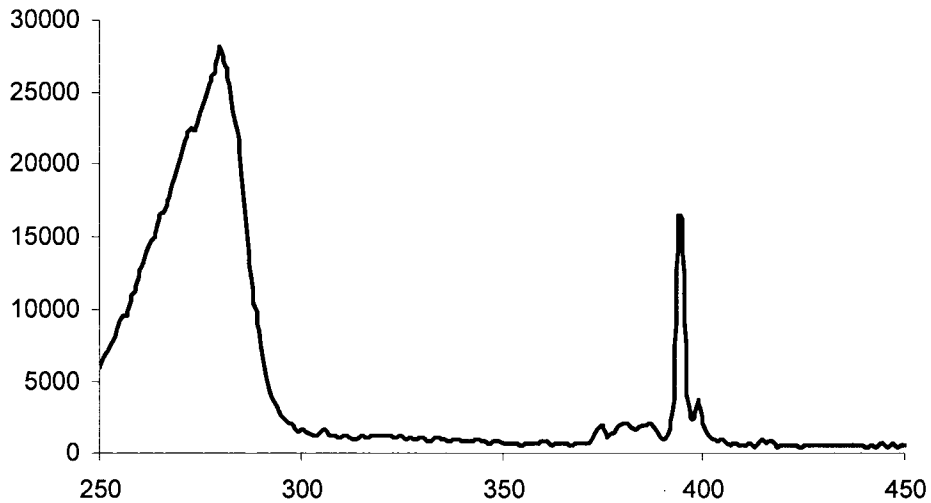

Figure 5. Excitation spectrum of cluster **1** reacted with sodium dipicolinate in methanol. Emission monitored at 614 nm; filter (OG-570 nm filter, size 50.80x 50.80, thickness 2.00 mm) was used to avoid interference from harmonic doubling.

Figure 6 shows a visualization of the slides on which the emission and excitation spectra were collected. In this Figure, the cluster, **1**, was reacted, as a suspension, with a palette of organic ligands. Excitation was achieved using a simple short wavelength

(254-344nm) UV lamp. There is no luminescence from the cluster alone (Figure 6A), as expected. All other samples display luminescence and the phthalic acid and dipicolinic acid, both deprotonated and untreated, appear to luminesce brightly. The phthalic acid and dipicolinic acid form stronger bonds to the Eu(III) center through the carboxylate moieties than the soft heterocyclic nitrogen atoms of the phenanthroline and bipyridine. The strong bonding likely contributes to the luminescence intensity. Efforts are underway to quantitate the luminescence of these complexes.

The controls, 1:1 $[Eu(H_2O)_3(\alpha_2\text{-}P_2W_{17}O_{61})]_2^{14-}$, **2**, and $EuCl_3$, that are both components of the cluster, show similar excitation and emission spectra, compared to **1**, when reacted with organic ligands. Both of the controls show similar luminescence when excited with short wavelength light

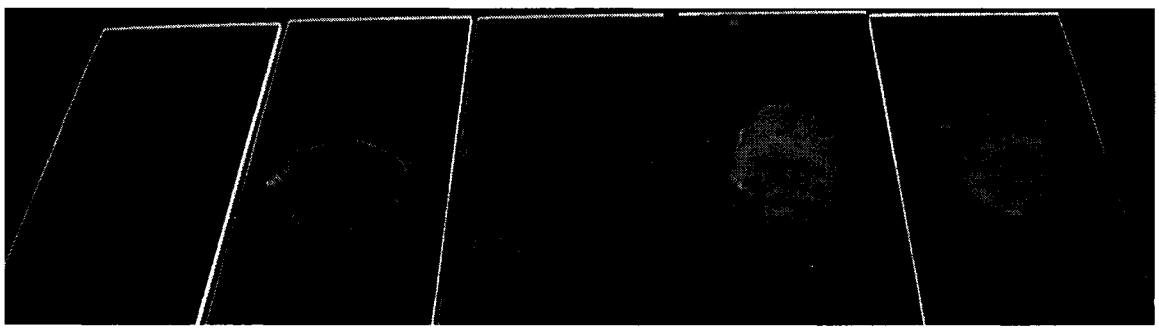

A. **B.** **C.** **D.** **E.**

Figure 6. Images of cluster **1** with different organic ligands under UV light (short wavelength, 254-344nm). A. cluster **1**without any organic ligand, B. phenanthroline, C. bipyridine, D. deprotonated pthalic acid, E. deprotonated dipicolinic acid.

5.3.1.4 Characterization of organic soluble 1:1 Eu(III): POM

5.3.1.4.1 TBA salt of $[EuPW_{11}O_{39}]^{4-}$, 3.

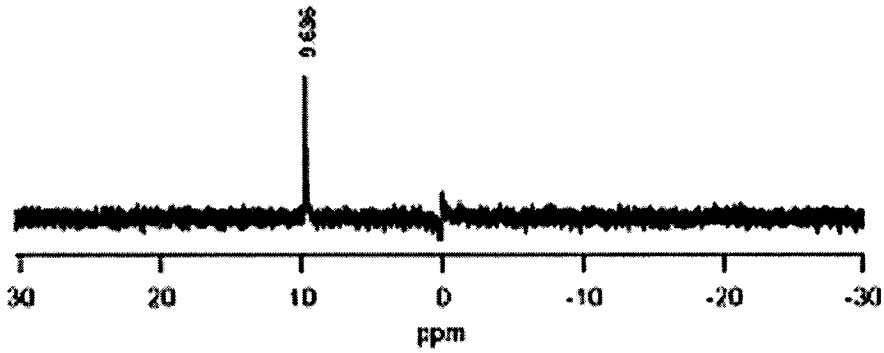

Figure 7. ^{31}P NMR spectra of TBA salt of $[EuPW_{11}O_{39}]^{4-}$ in acetonitrile

The ^{31}P NMR spectra of TBA salt of $[EuPW_{11}O_{39}]^{4-}$ in acetonitrile-d_3 (one drop of water was added to deproton) is shown in Figure 7, the clean peak at δ 9.2 ppm, compare with the species of $[EuPW_{11}O_{39}]^{4-}$ in aqueous solution at δ 5.6 ppm, is assigned to the species of TBA salt of $[EuPW_{11}O_{39}]^{4-}$ in organic solvent, which also indicate that the TBA salt of $[EuPW_{11}O_{39}]^{4-}$ synthesized at pH 3.6 is pure.

5.3.1.4.1.1 ^{31}P NMR titration to determine 1:1 $[EuPW_{11}O_{39}]^{4-}$ in organic solvent

In an attempt to observe the formation of 1:1 $[EuPW_{11}O_{39}]^{4-}$ in organic solvent, the titration of $TBA_4H_3PW_{11}O_{39}$ by $Eu(ClO_4)_3$ with different stoichiometric ratio of 4:1, 2:1, 1:1 and 1:2 respectively in acetonitrile was monitored by ^{31}P NMR. (Figure 8)

This is the first datebase to monitor the titration of $TBA_4H_3PW_{11}O_{39}$ with $Eu(ClO_4)_3$ in organic solvent by ^{31}P NMR. When $TBA_4H_3PW_{11}O_{39}$: $Eu(ClO_4)_3$ is 4:1, there are two species present in the solution, one is 1:2 $[Eu(PW_{11}O_{39})_2]^{11-}$, another one is ligand $[PW_{11}O_{39}]^{7-}$ due to the over amount of $[PW_{11}O_{39}]^{7-}$ in the solution, As $TBA_4H_3PW_{11}O_{39}$:

$Eu(ClO_4)_3$ goes to 2:1, three species are present including the previous two, a new peak at δ 5.6 ppm appears which represent 1:1 $[EuPW_{11}O_{39}]^{4-}$; As $TBA_4H_3PW_{11}O_{39}$: $Eu(ClO_4)_3$

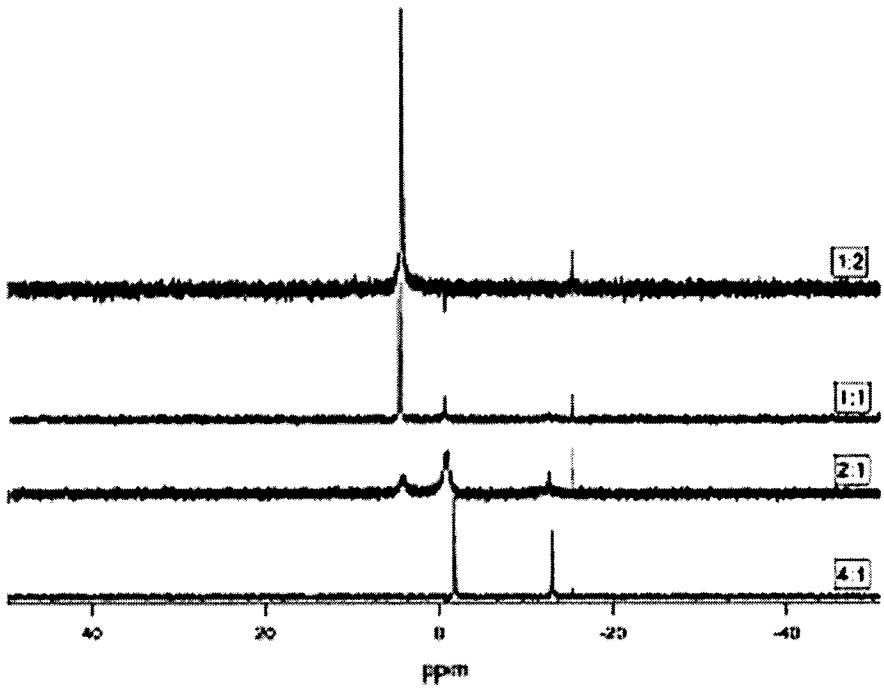

Figure 8. ^{31}P NMR spectra of titrating $TBA_4H_3PW_{11}O_{39}$ with $Eu(ClO_4)_3$ (mole ratio = $TBA_4H_3PW_{11}O_{39}$: $Eu(ClO_4)_3$)

goes up to 1:1, the peak at δ 5.6 ppm intense, both peaks at –1.1 ppm and –10.2 ppm turn weak. As $TBA_4H_3PW_{11}O_{39}$: $Eu(ClO_4)_3$ goes up to 2:1, the major species present in the solution is 1:1 $[EuPW_{11}O_{39}]^{4-}$, the minor species present is ligand $[PW_{11}O_{39}]^{7-}$. From this experiment, we can confirm the formation of 1:1 $[EuPW_{11}O_{39}]^{4-}$ in the organic solvent.

5.3.1.4.1.2 Proton titration to determine the proton numbers in the TBA salt of $[EuPW_{11}O_{39}]^{4-}$ ($TBA_xH_{4-x}EuPW_{11}O_{39}$)

To determine the proton numbers in the TBA salt of $[EuPW_{11}O_{39}]^{4-}$, the proton titration of $TBA_xH_{4-x}EuPW_{11}O_{39}$ by aqueous TBAOH solution was performed. The color

change at the end point was indicated by phenolphthalein. The calculation to get the proton numbers (4-x) is as follow:

In the experiment, 0.99 ml of 0.2937 M of aqueous TBAOH was used to titrate 1.0025 g of $TBA_xH_{7-x}[Eu(\alpha_2\text{-}P_2W_{17}O_{61}]$ acetonitrile solution.

$$TBA_xH_{4-x}EuPW_{11}O_{39} + (4\text{-}x)TBAOH \longrightarrow \text{End point}$$

$$1 \qquad\qquad 4\text{-}x$$

1.0025 g/(2829.28+4-x+242.48)g/mol = 0.2937 M * 0.99 ml /(1000*(4-x))

$x = 2.96 \approx 3$

There are 3 TBA^+ in the TBA salt of $[EuPW_{11}O_{39}]^{4-}$

Proton number = 4-x =1

Therefore, the chemical formula of the TBA salt of $[EuPW_{11}O_{39}]^{4-}$ is $TBA_3H[EuPW_{11}O_{39}]$.

5.3.1.4.2 TBA salt of $[Eu(\alpha_1\text{-}P_2W_{17}O_{61}]^{7-}$, 4, and $[Eu(\alpha_2\text{-}P_2W_{17}O_{61}]^{7-}$, 5.

The ^{31}P NMR spectra of TBA salt of $[Eu(\alpha_2\text{-}P_2W_{17}O_{61}]^{7-}$ and $[Eu(\alpha_1\text{-}P_2W_{17}O_{61}]^{7-}$

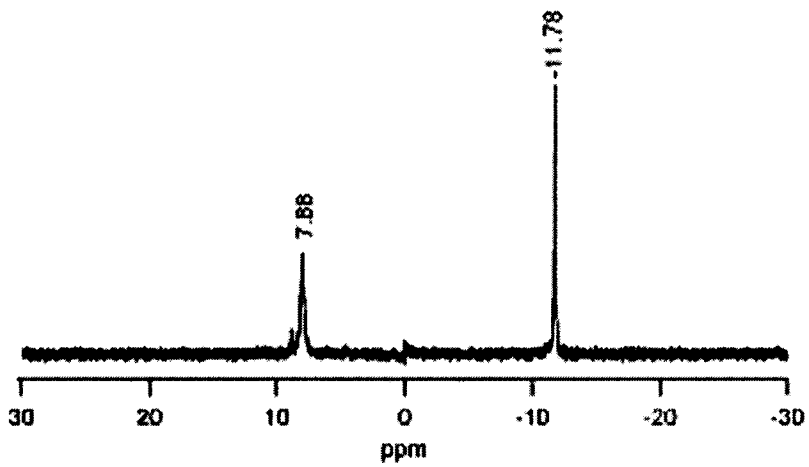

Figure 9. ^{31}P NMR spectra of TBA salt of $[Eu(\alpha_2\text{-}P_2W_{17}O_{61}]^{7-}$ in acetonitrile.

in acetonitrile-d_3 (one drop of water was added to deproton) are shown in Figure 9 and 10. Compare with δ 8.39, -12.33 ppm of $[Eu(\alpha_2\text{-}P_2W_{17}O_{61}]^{7-}$ in aqueous solution, the δ of TBA salt of $[Eu(\alpha_2\text{-}P_2W_{17}O_{61}]^{7-}$ in organic solvent shift to 7.88, -11.78 ppm respectively. As shown in Figure 10, the two peaks at δ 5.14, -12.64 ppm are assigned to the species of TBA salt of $[Eu(\alpha_1\text{-}P_2W_{17}O_{61}]^{7-}$ in organic solvent, a little chemical shift can be observed compared with the δ 6.3, -12.5 ppm of $[Eu(\alpha_1\text{-}P_2W_{17}O_{61}]^{7-}$ in aqueous solution. In both figures, the two clean peaks show the TBA salt of $[Eu(\alpha_2\text{-}P_2W_{17}O_{61}]^{7-}$ and $[Eu(\alpha_1\text{-}P_2W_{17}O_{61}]^{7-}$ we synthesized under different experimental conditions (pH, temperature) are very pure.

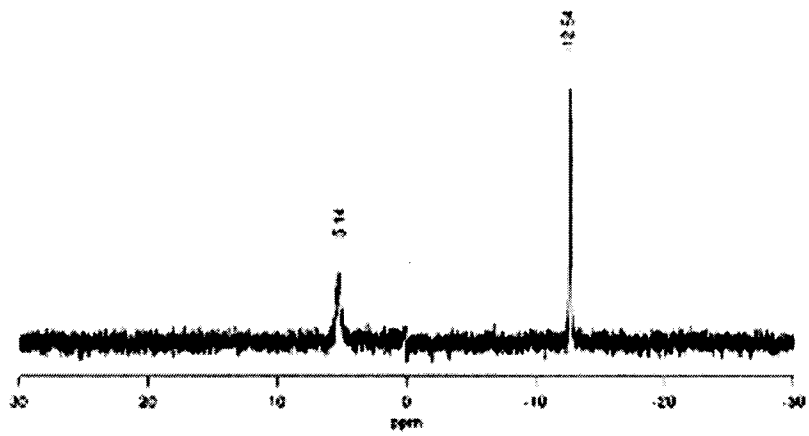

Figure 10. ^{31}P NMR spectra of TBA salt of $[Eu(\alpha_1\text{-}P_2W_{17}O_{61}]^{7-}$ in acetonitrile.

5.3.1.4.2.1 Proton titration to determine the proton numbers in the TBA salt of $[Eu(\alpha_1\text{-}P_2W_{17}O_{61}]^{7-}$ and $[Eu(\alpha_2\text{-}P_2W_{17}O_{61}]^{7-}$

To determine the proton numbers in the TBA salt of $[Eu(\alpha_1\text{-}P_2W_{17}O_{61}]^{7-}$ and $[Eu(\alpha_2\text{-}P_2W_{17}O_{61}]^{7-}$, the proton titration of $TBA_xH_{7-x}[Eu(\alpha_1\text{-}P_2W_{17}O_{61}]$ or $TBA_xH_{7-x}[Eu(\alpha_2\text{-}P_2W_{17}O_{61}$ by aqueous TBAOH solution was performed. The color change at the

end point was indicated by phenolphthalein. The calculation to get the proton numbers (7-x) is as follow:

In the experiment, 1.21 ml of 0.2837 M of aqueous TBAOH was used to titrate 1.0686 g of $TBA_xH_{7-x}[Eu(\alpha_2\text{-}P_2W_{17}O_{61}]$ acetonitrile solution.

$$TBA_xH_{7-x}[Eu(\alpha_2\text{-}P_2W_{17}O_{61}] + (7\text{-}x)TBAOH \longrightarrow \text{End point}$$

$$1 \qquad\qquad 7\text{-}x$$

$1.0686/(241.48x+5075.36)=1.21*0.2937/(1000*(7-x))$

$x=4.91\approx5$

There are 5 TBA^+ in the $TBA_xH_{7-x}[Eu(\alpha_2\text{-}P_2W_{17}O_{61}]$

Proton number = 7-x =2

Therefore, the chemical formula of TBA salt of $[Eu(\alpha_2\text{-}P_2W_{17}O_{61}]^{7-}$ is $TBA_5H_2[Eu(\alpha_2\text{-}P_2W_{17}O_{61}]$. The chemical formula of $TBA_5H_2[Eu(\alpha_1\text{-}P_2W_{17}O_{61}]$ is obtained in the same manner.

5.3.2 Solution Chemistry

To investigate the formation of soluble ternary organic: Eu(III) POM species and their luminescent properties, the 1:1 $TBA_5H_2[Eu(\alpha_1\text{-}P_2W_{17}O_{61})]$, 1:1 $TBA_5H_2[Eu(\alpha_2\text{-}P_2W_{17}O_{61})]$ and the 1:1 $TBA_3H[EuPW_{11}O_{39}]$ were reacted with organic ligands in acetonitrile. The 1:1 $TBA_5H_2[Eu(\alpha_1\text{-}P_2W_{17}O_{61})]$ species was chosen because it was clear, according to stability constant measurements, that the 1:1 formulation is maintained across the lanthanide series in aqueous solution and also in organic solution without contamination of the 1:2 species.[30,24] Preliminary titration data for the 1:1 $TBA_3H[EuPW_{11}O_{39}]$ in CH_3CN also suggest that the 1:1 species is maintained in organic solution.[31] Experiments wherein phenanthroline (phen) or bipyridine (bipy) are titrated into

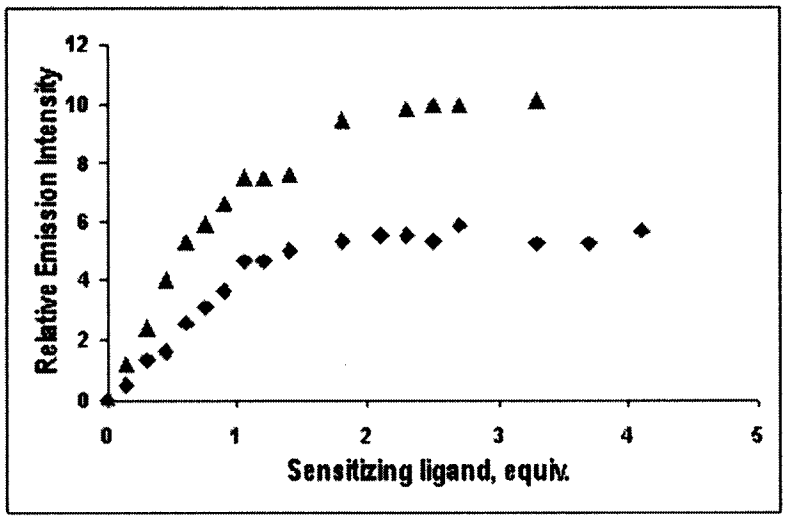

Figure 11. Relative emission intensity of $[Eu(\alpha_1\text{-}P_2W_{17}O_{61}]^{7-}$ upon addition of ▲ 2,2'-bipyridine ◆ Phenanthroline in CH_3CN, $[TBA_5H_2Eu(\alpha_1\text{-}P_2W_{17}O_{61})] = 7.02 \times 10^{-4}$ M, $\lambda_{exc} = 319$ nm.

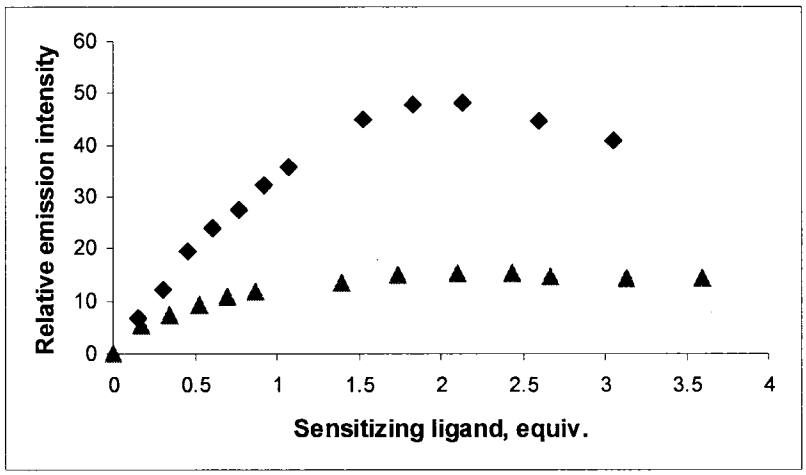

Figure 12. Relative emission intensity of $[Eu(PW_{11}O_{39}]^{4-}$ upon addition of ▲ 2,2'-bipyridine ◆ Phenanthroline in CH_3CN, $[TBA_3H(EuPW_{11}O_{39})]=7.47 \times 10^{-4}$ M, $\lambda_{exc} = 319$ nm.

the TBA salts of 1:1 Eu: $\alpha_1\text{-}P_2W_{17}O_{61}^{10-}$ in CH_3CN with λ_{exc}=350 nm, show an increase in emission ($\lambda_{emission}$= 614 nm) of the Eu(III) that levels off at 2 equivalents of organic ligand per equivalent of $[Eu(\alpha_1\text{-}P_2W_{17}O_{61})]$, consistent with 2:1 ligand: EuPOM formulation and energy transfer from the organic sensitizing ligand to the Eu(III) center (Figure 11). This is

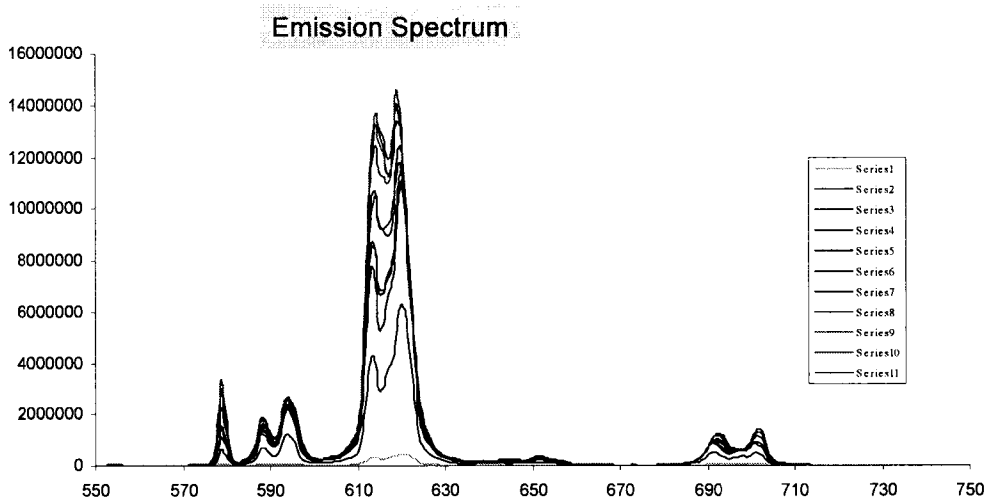

Figure 13. The emission spectra of $Eu(\alpha\text{-}PW_{11}O_{39})^{4-}$ with phenanthroline.

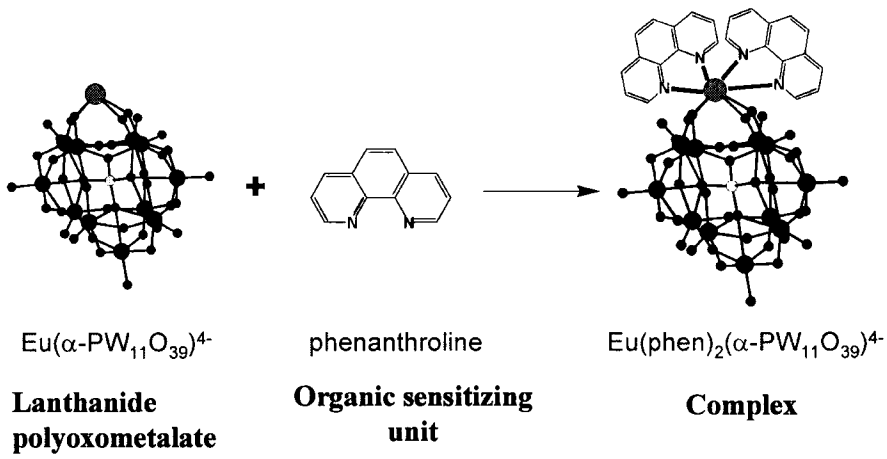

Scheme 2. The proposed reaction of $Eu(\alpha\text{-}PW_{11}O_{39})^{4-}$ with phenanthroline in organic solution

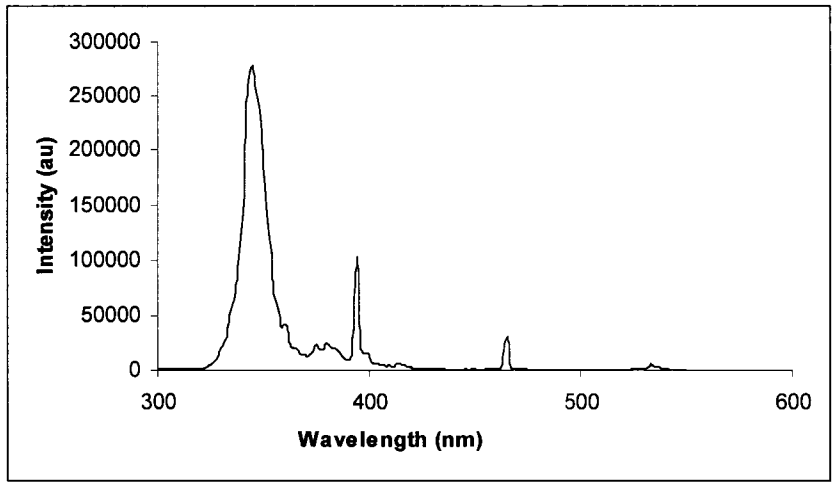

Figure 14. Excitation spectra of $[EuPW_{11}O_{39}]^{4-}$ with phenanthroline in CH_3CN. $[TBA_3H(EuPW_{11}O_{39})]=7.47 \times 10^{-4}$ M, λ_{em} =585 nm

expected because two bidentate organic ligands bind to the $[Eu(\alpha_1\text{-}P_2W_{17}O_{61})]$ unit to complete the eight coordination of Eu(III). Excitation spectra taken at each titration point confirm the energy transfer process from the organic moiety to the Eu(III). A typical example of Emission, Excitation spectra and a proposed reaction of $Eu(\alpha\text{-}PW_{11}O_{39})^{4-}$ with phenanthroline in organic solution are shown in Figure 13, Figure 14 and Scheme 2. Quantum yields are 0.12 for the bipy:Eu: $\alpha_1\text{-}P_2W_{17}O_{61}$ compared to < 0.01 for $Eu(\alpha_2\text{-}P_2W_{17}O_{61})_2^{17-}$ and other 1:2 Ln: POM complexes, measured against a rhodamine dye standard. [32, 33]

As seen in Figure 15, ^{31}P NMR shows slight shifts for both resonances from the parent 1:1 $[Eu(\alpha_1\text{-}P_2W_{17}O_{61})]$ complex upon addition of two equivalents of phenanthroline, suggesting that the Eu POM remains intact during the titration. The

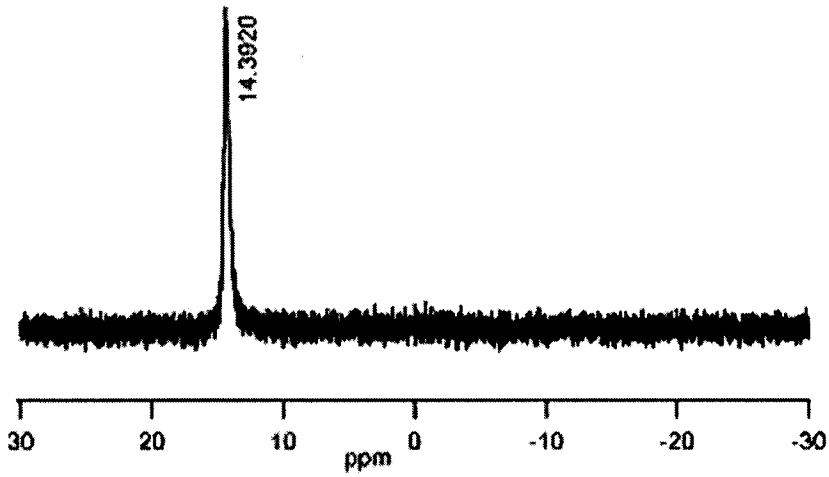

Figure 15. ^{31}P NMR of ternary complex of $[EuPW_{11}O_{39}]^{4-}$ with phenanthroline in CH_3CN.

control, $Eu(ClO_4)_3$ shows (see Figure 16) a peak at 4-5 equivalents of organic ligand added, consistent with all of the 8-9 coordination sites taken up by the bidentate ligand. Similar luminescence titrations have been performed for crown ether lanthanide complexes with sensitizing organic ligands to indicate ternary Ln (crown ether) (sensitizer ligand) complexes. [34]

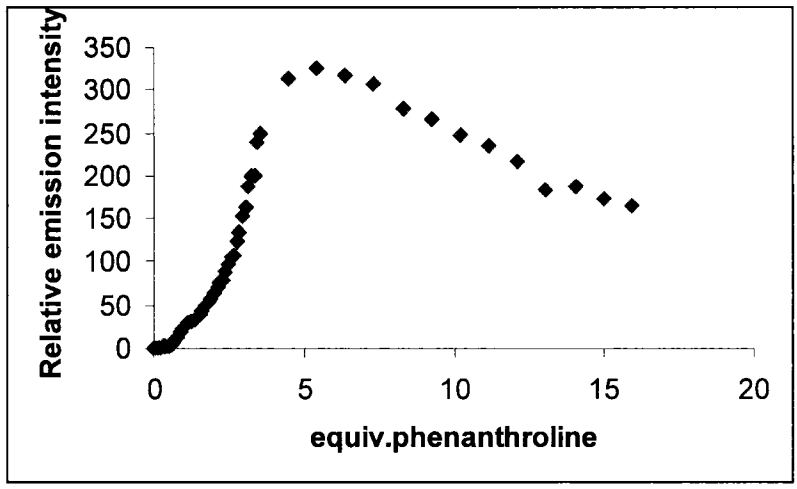

Figure 16. Relative emission intensity of $Eu(ClO_4)_3$ upon addition of phenanthroline in CH_3CN, $[Eu(ClO_4)_3]= 8.0 \times 10^{-4}$ M, $\lambda_{exc} = 319$ nm.

Similar behavior was observed in the luminescence titrations of $TBA_3H[EuPW_{11}O_{39}]$ with phen and bipy, shown in Figure 12. ^{31}P NMR spectra monitoring the titration of phenanthroline into $EuPW_{11}O_{39}^{4-}$ (D_2O added to prevent multiple peaks due to protonation) confirm that the EuPOM remains intact during and after reaction (EuPOM plus phen: ^{31}P, δ +14.50 ppm; free $EuPW_{11}O_{39}^{4-}$: ^{31}P, δ +5.5 ppm). The proton (^1H) NMR taken, in CD_3CN, as $TBA_3H[EuPW_{11}O_{39}]$ is added to phenanthroline, Figure 17, or the reverse addition, shows that the resonances of the phenanthroline shift upon complexation to the paramagnetic Eu(III). However, a dynamic process is also occurring that results in a broadening of the resonances representing the free and bound phenanthroline. Upon addition of the $EuPW_{11}O_{39}^{4-}$ to phenanthroline, the four phenanthroline resonances broaden and coalesce into two peaks at ca 8.2 ppm, an average of the four original resonances. As the EuPOM content increases, a broad peak around 5.9 ppm is observed along with small peaks in the range of 4.8 to 7.2 ppm; these are likely due to phen bound to EuPOM. The broad peak at ca 5.9 ppm is due to exchange of these phen ligands bound to the Eu POM with themselves and with the unbound phen. When the Eu POM: phen stoichiometry is 4:1 (Figure 9e) there are no broad peaks, only five relatively sharp peaks at 4.77, 5.04, 5.32, 6.04, and 7.28, ppm and three broader peaks at 6.50, 6.77, and 7.41, each integrating for about 1, suggesting that two phen ligands are bound to the Eu center. Exchange of bound bipy or phen with free ligand is expected and found, even under rigorous anhydrous conditions, due to the relatively low log K of phenanthroline bound to lanthanide(III) ions. [35]

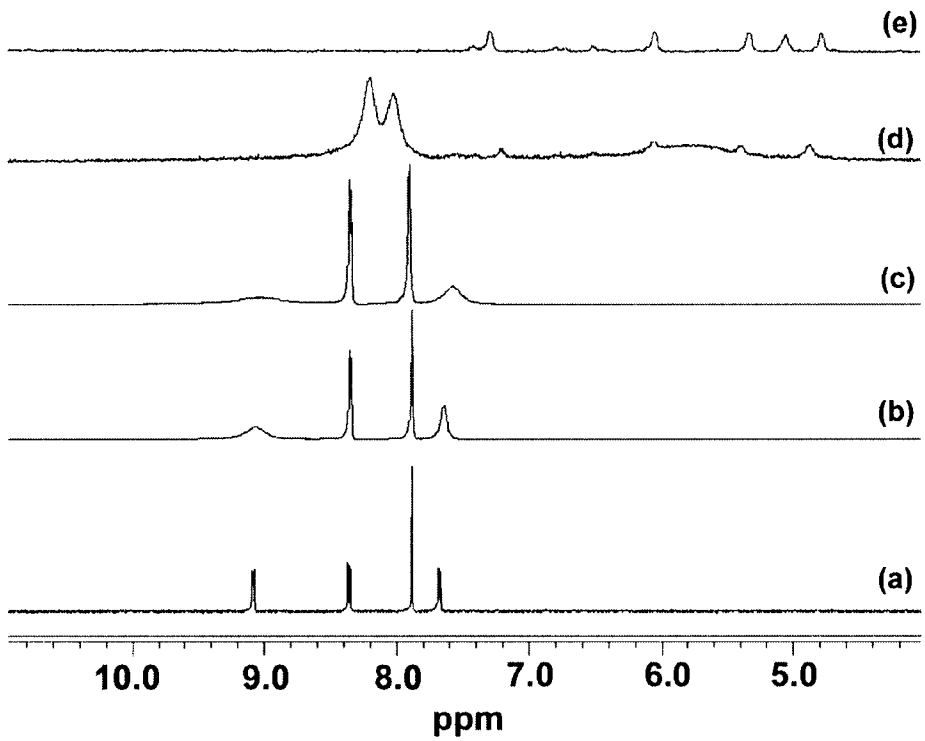

Figure 17. ^{31}P NMR spectra of titration of phenanthroline with $[EuPW_{11}O_{39}]^{4-}$ in acetonitrile, showing resonances assigned to phenanthroline. TBA resonances are found between 0 and 3.4 ppm and are not seen on these spectra. Phenanthroline: $[EuPW_{11}O_{39}]^{4-}$ a. phenanthroline only b. 20: 1 c. 1:1 d. 1:2 e. 1:4

5.4 Conclusion

We have prepared an unique cluster, $[Eu(H_2O)_3(\alpha_2\text{-}P_2W_{17}O_{61})(Eu_2(H_2O)_7]_4^{4-}$, **1**, in high yield and the preparation and crystallization is highly reproducible. The crystal structure shows three types of Eu(III) ions, Eu2 is bound in the defect of the cap region of the $\alpha_2\text{-}P_2W_{17}O_{61}$. The other two Eu(III) ions, Eu1 and Eu3 are each bound to two terminal oxygen atoms in that defect cap region. These two Eu(III) ions are bound through a bridging oxygen to other $[\mathbf{Eu}(\alpha_2\text{-}P_2W_{17}O_{61})]_2^{14-}$ clusters (Eu1 of one dimer is bound to Eu3 of another dimer) to form a network of $[\mathbf{Eu}(\alpha_2\text{-}P_2W_{17}O_{61})]_2^{14-}$ dimers connected by aquated Eu(III) ions.

Preliminary luminescence studies of a crystalline sample of 1, suspended in methanol and reacted with organic ligands, show that the organic ligands indeed are capable of sensitizing the luminescence of the Eu(III). For comparison in solution, the organic soluble $TBA_5H_2[Eu(\alpha_1\text{-}P_2W_{17}O_{61})]$, **3**, $TBA_5H_2[Eu(\alpha_2\text{-}P_2W_{17}O_{61})]$, **4**, and $TBA_3H[EuPW_{11}O_{39}]$, **5**, were prepared and characterized. As shown from luminescence titrations and ^{31}P and ^{1}H NMR spectroscopy, these species react with phenanthroline and bipyridine, in acetonitrile, to form the 2:1 organic ligand: $[Eu(\alpha_1\text{-}P_2W_{17}O_{61})]$ adduct.

5.5 References

(1) Sadakane, M.; Dickman, M. H.; Pope, M. T. *Angew. Chem. Int. Ed.* **2000**, *39*, 2914-2916.

(2) Mialane, P.; Lisnard, L.; Mallard, A.; Marrot, J.; Antic-Fidancev, E.; Aschehoug, P.; Vivien, D.; Secheresse, F. *Inorg. Chem.* **2003**, *42*, 2102-2108.

(3) Muller, A.; Peters, F.; Pope, M. T.; Gatteschi, D. *Chemical Reviews* **1998**, *98*, 239-271.

(4) Muller, A.; Krickemeyer, E.; Bogge, H.; Schmidtmann, M.; Peters, F. *Angew. Chem. Int. Ed.* **1998**, *37*, 3360-3365.

(5) Muller, A.; Sarkar, S.; Shah, S. Q. N.; Bogge, H.; Schmidtmann, M.; Sarker, S.; Kogerler, P.; Hauptfleish, B.; Trautwein, A. X.; Schunemann, V. *Angew. Chem. Int. Ed.* **1999**, *38*, 3238-3241.

(6) Wassermann, K.; Dickman, M. H.; Pope, M. T. *Angew. Chem. Int. Ed. Engl.* **1997**, *36*, 1445-1448.

(7) Belai, N.; Sadakane, M.; Pope, M. T. *J. Am. Chem. Soc.* **2001**, *123*, 2087-2088.

(8) For key references to lanthanide luminescence: a. Kido, J.; Okamoto, Y., *Chem. Rev.* **2002**, *102*, 2357-2368. b. Bruce, J. I.; Dickins, R. S.; Govenlock, L. J.; Gunnlaugsson, T.; Lopinski, S.; Lowe, M. P.; Parker, D.; Peacock, R. D.; Perry, J. J. B.; Aime, S.; Botta, M., *J. Am. Chem. Soc.* **2000**, *122*, 9674-9684. c. Dickins, R. S.; Aime, S.; Batsanov, A. S.; Beeby, A.; Botta, M.; Bruce, J. I.; Howard, J. A. K.; Love, C. S.; Parker, D.; Peacock, R. D.; Puschmann, H., *J. Amer. Chem. Soc.* **2002**, *124*, 12697-12705. d. Parker, D.; Dickins, R. S.; Puschmann, H.; Crossland, C.; Howard, J. A. K., "*Chem. Rev.* **2002**, *102*, 1977-2010.

(9) For key reviews on new functional materials, particularly electrochromic, electroluminescent, photochromic and photoluminescent materials, a. Katsoulis, D.E. *Chem. Rev.*, **1998,** *98*, 359-387. b.Yamase, T. *Chem. Rev.*, **1998**, *98*, 307-325. For recent applications of lanthanide polyoxometalates incorporated into materials: electrochromic device preparation, c. Liu, S.; Kurth, D. G.; Mohwald, H.; Volkmer, D., *Advanced Materials* **2002**, *14*, 225-228. photoluminescent films, d. Mo, Y.-G.; Dillon, R. O.; Snyder, P. G.; Tiwald, T. E., *Thin Solid Films* **1999**, *355-356*, 1-5. e. Xu, L.; Zhang, H.; Wang, E.; Kurth, D. G.; Li, Z., *J. Mater. Chem.* **2002**, *12*, 654-657. f. Xu, L.; Zhang, H.; Wang, E.; Wu, A.; Li, Z., *Materials Chemistry and Physics* **2002**, *77*, 484-488. g. Wang, Y.; Wang, X.; Hu, C.; Shi, C., *J. Mater. Chem.* **2002**, *12*, 703-707. h. Wang, J.; Liu, F.; Fu, L.; Zhang, H., *Materials Lett* **2002**, *56*, 300-304. i. Wang, Y.; Wang, X.; Hu, C., *Journal of Colloid and Interface Science* **2002**, *249*, 307-315. j. Wang, J.; Wang, H. S.; Fu, L. S.; Liu, F. Y.; Zhang, H. J., *Thin Solid Films* **2002**, *414*, 256-261.

(10) For key references to lanthanide Lewis Acid catalysis: a. Aspinall, H. C., *Chem. Rev.* **2002**, *102*, 1807-1850. b. Molander, G. A., *Chemtracts-Organic Chemistry* **1998**, *11*, 237-263. c. Molander, G., *Chem. Rev.* **1992**, *92*, 29-67. d. Shibasaki, M.; Yoshikawa, N.,*Chem. Rev.* **2002**, *102*, 2187-2209. e. Kobayashi, S.; Kawamura, M., *J. Am. Chem. Soc.* **1998**, *120*, 5840-5841. f. Kobayashi, S., *Pure and Appl. Chem.* **1998**, *70*, 1019-1026. g. Aspinall, H. C.; Dwyer, J. L. M.; Greeves, N.; McIver, E. G.; Woolley, J. C., *Organometallics* **1998**, *17*, 1884-1888. h. Xie, W.-H.; Yu, L.; Chen, D.; Li, J.; Ramirez, J.; Miranda, N. F.; Wang, P. G.*Lanthanide-Catalyzed organic synthesis in protic solvents*; Anastas, P. T.

and Williamson, T. C., Ed.; Oxford University Press: Oxford, UK, **1998**; pp 129-149.

(11) Jenkins, A. L.; Uy, O. M.; Murray, G. M. *Analytical Communications* **1997**, *34*, 221-224.

(12) Lester, E. D.; Bearman, G.; Ponce, A. *IEEE Engineering in Medicine and Biology Magazine* **2004**, *January/February, 2004*, 130-135.

(13) de Silva, A. P.; Fox, D. B.; Moody, T. S.; Weir, S. M. *Pure Appl. Chem.* **2001**, *73*, 503-511.

(14) Horrocks, W. D., Jr.; Sudnick, D. R. *J. Amer. Chem. Soc.* **1979**, *101*, 334-340.

(15) Horrocks, W. D., Jr. *Methods in Enzymology* **1993**, *226*, 495-538.

(16) *Luminescent Probes*; Bunzli, J.-C., G., Ed.; Elsevier: Amsterdam, 1989.

(17) Yamase, T.; Kobayashi, T.; Sugeta, M.; Naruke, H. *J. Phys. Chem. A* **1997**, *101*, 5046-5053.

(18) Yamase, T. *Chem. Rev.* **1998**, *98*, 307-325.

(19) Dexter, D. L. *J. Chem. Phys.* **1953**, *21*, 836-850.

(20) Klink, S. I.; Grave, L.; Reinhoudt, D. N.; van Veggel, F. C. J. M.; Werts, M. H. V.; Geurts, F. A. J.; Hofstraat, J. W. *J. Phys. Chem. A.* **2000**, *104*, 5457 - 5468.

(21) Luo, Q.; Howell, R. C.; Bartis, J.; Dankova, M.; Horrocks, W. D., Jr.; Rheingold, A. L.; Francesconi, L. C. *Inorg. Chem.* **2002**, *41*, 6112-6117.

(22) Zhang, C.; Howell, R. C.; Scotland, K. B.; Perez, F.; Luo, Q. L.; Todaro, L.; Francesconi, L. C. *Inorg. Chem.* **2004**, *in press*.

(23) Weiner, H.; Aiken, I., J.D.; Finke, R. G. *Inorg. Chem.* **1996**, *35*, 7905-7913.

(24) Bartis, J.; Dankova, M.; Lessmann, J. J.; Luo, Q.-H.; Horrocks, W. D., Jr.; Francesconi, L. C. *Inorganic Chemistry* **1999**, *38*, 1042-1053.

(25) Zhang, C.; Howell, R. C.; Scotland, K. B.; Perez, F. G.; Todaro, L.; Francesconi, L. C. *Inorg. Chem.* **2004**, *in press*.

(26) *SHELXTL, Brucker AXS, Inc., Bruker Advanced X-ray Solutions, 1999* **1999**.

(27) Blasse, G.; Dirksen, G. J.; Zonnevijlle, F. *J. Inorg. Nucl. Chem.* **1981**, *43*, 2847-2853.

(28) Lis, S.; But, S. *Journal of Alloys and Compounds* **2000**, *300-301*, 370-376.

(29) Yusov, A. B.; Fedoseev, A. M. *Radiokhimiya* **1992**, *34*, 61-70.

(30) Zhang, C.; Howell, R. C.; Luo, Q.; Fieselmann, H. L.; Todaro, L.; Francesconi, L. C. *manuscript in preparation* **2004**.

(31) Zhang, C.; Howell, R. C.; McGregor, D.; Bensaid, L.; Francesconi, L. C., unpublished work, **2004**.

(32) Hasegawa, Y.; Yamamuro, M.; Wada, Y.; Kanehisa, N.; Kai, Y.; Yanagida, S. *J. Phys. Chem. A.* **2003**, *107*.

(33) Huignard, A.; Gacoin, T.; Boilot, J.-P. *Chem. Mater.* **2000**, *12*, 1090-1094

(34) Magennis, S. W.; Craing, J.; Gardner, A.; Fucassi, F.; Cragg, P. J.; Robertson, N.; Parsons, S.; Pikramenou, Z. *Polyhedron* **2003**, *22*, 745-754.

(35) Riviere, C.; Nierlich, M.; Ephritikhine, M.; Madic, C. *Inorg. Chem.* **2001**, *40*, 4428-4435.

Chapter 6. Incorporating Ln POMs into layered Double Hydroxides (LDHs)

6.1 Introduction

Layered double hydroxides (LDHs) are the only known family of layered materials with permanent positive charge on the layers.[1] The general LDH formula is $[M^{2+}_{1-x}M^{3+}_{x}(OH)_2][A^{n-}]_{x/n}\cdot zH_2O$, where M^{2+} and M+ are divalent and trivalent metal cations such as Mg^{2+}, Zn^{2+} and Al^{3+} respectively, x is the ratio $M^{3+}/(M^{2+}+M^{3+})$ and A^{n-} is a simple organic or inorganic anion such as Cl^-, NO_3^-, CO_3^{2-}, SO_4^{2-} or $C_8H_4O_4^{2-}$. Such LDHs may be used as precursors of pillared layered structures which can be talor-made by modification of the host structure chemical composition or by chemical or structural modification of the guest species domains [2]. Currently, LDHs pillared by polyoxometalates anions have attracted considerable attentions as a potentially important class of catalytically active, microporous materials [24, 26-27]. Approaches to the preparation of pillared LDH-POM intercalated have been studied on Keggin ion α-$H_2W_{12}O_{40}^{6-}$ with a molecular diameter (~10Å) approximately two times as large as the LDH layer thickness (~4.8Å), Dawson ion α-$P_2W_{18}O_{62}^{6-}$ and Finke $Co_4(H_2O)_2(PW_9O_{34})_2^{10-}$ with molecular diameters much larger than 4.8Å. As illustrated in Scheme 1, each class of the POM can impart a different gallery pore structure upon pillaring reaction, resulting in new members of the class of LDH-POM derivatives. Owing to the diversity to approaches to the design of these

nanoscale materials, a wide range of structural, chemical, electronic, ionic, optical, and magnetic applications are possible.[26]

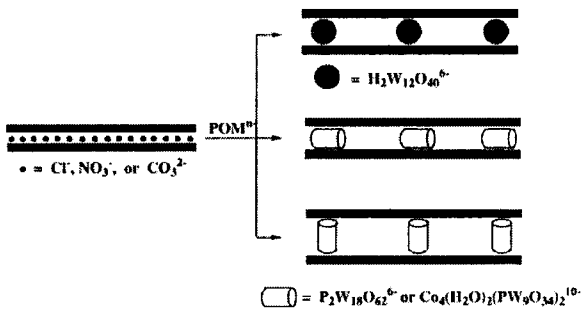

Scheme 1. Schematic representation of the formation of LDH derivatives pillared by Keggin, Dawson and Finke POM^{n-}. [24]

Lanthanide derivatives of the monovacant, lacunary Wells-Dawson and Keggin polyoxoanion ligands have attracted great interest because of their potential applications in catalysis, medicine and nuclear waste treatment. In particular, europium incorporated complexes have excited interest because of their structural and luminescence properties, connected with their potential use in lasers and luminescent materials.

There is only one reference describing incorporation of a lanthanide POM, $[Ln(W_5O_{18})_2]^{9-}$ (Ln=Eu,Tb) into (acidic) Zn/Al LDH, XRD and emission spectroscopy data suggest that the molecule decomposes and the Eu $W_5O_{18}^{3-}$ unit binds to the oxygen atoms of the brucite-like layer.[43]

In our group, we are incorporating well characterized Dawson-like $[Eu(\alpha_1\text{-}P_2W_{17}O_{61}]^{7-}$ (**1**) and Keggin-like $[Eu(H_2O)_2(PW_{11}O_{39})]^{4-}$ (**2**) into both acidic and basic LDHs with the aims of creating composite materials as novel photoluminescent materials and catalysts.

In this paper, we exchanged polyoxometalate **1** and **2** into "expanded" Mg_3Al-LDH-adipate material at 50°C and refluxing temperatures following the method of Yun and Pinnavaia [24]. Since **1** and **2** are hydrolytically unstable at weakly acidic to basic pH, in addition to proceed the pillaring reaction into the basic Mg/Al LDH layers, we also try using the acidic Zn/Al LDH to minimize the co-formation of impurity phase that deposits on the surface of the LDH crystallites. The synthetic route was illustrated in Scheme **2**.

The structural, textural and luminescence properties of the pillared products were examed based on PXRD, FTIR, N_2 adsorption/desorption studies, Raman, Fluorescence, and solid state NMR spectroscopies.

$$\text{LDH-}CO_3^{2-} \xrightarrow[2.\ H_2O,\ 25\ ^\circ C]{1.\ \Delta\ (500^\circ C)} \text{LDH-}OH^- \xrightarrow{\text{adipic acid}}$$

$$\text{LDH-[adipate]} \xrightarrow[100\ ^\circ C]{POM^{n-}} \text{LDH-[}POM^{n-}\text{]}$$

Scheme 2. Synthetic routes to prepare LDH-POM^{n-}

6.2 Experimental Section

6.2.1 Materials preparation

6.2.1.1 LDH carbonate

The Mg_3Al LDH carbonate and Zn_3Al LDH carbonate were prepared by a modification of the literature methods. [25-27] A 2 l, three-neck, round-bottom flask was equipped with a pH probe, a thermometer, and two 30-ml syringes. The flask was

charged with 500 ml of fresh DDI water, and the pH was prejusted to 10.0 by the addition of 2 M NaOH. A 250 ml of 1.0 M mixed-metal nitrate solution of Mg^{2+}, and Al^{3+} (Mg^{2+}/Al^{3+}=3.0) was added dropwise via two 30-ml of syringes needles to the vigorously stirred flask at a constant temperature of 40C. The reaction pH was kept at 10.0 first by the coaddition of a mixed base solution of 1 M Na_2CO_3 and 2 M NaOH (CO_3^{2-}/Al^{3+} = 1.5) and then by the addition of 2 M NaOH solution. The resultant white suspension was allowed to stir for 2 h at 40°C, and then for an additional 48h at 70°C. The final product was centrifuged, and washed two times with fresh DDI water, and then dried overnight in an oven at 75°C.

6.2.1.2 LDH hydroxide

1.2 g of the LDH carbonate was calcined in a quartz tube furnace for 5 h at 500°C under a nitrogen flow to form the solid oxide. 0.6 g of the resulting mixed oxide solid solution was slurried in 100 ml of fresh degassed DDI water under flowing nitrogen for 5 days to form the LDH hydroxide.

6.2.1.3 LDH adipate

The temperature of the above slurry was increased to 50°C, and a 200% excess of adipic acid (0.56g) dissolved in 65 ml of slightly warmed fresh DDI water was added all at once, followed by 1 h of stirring at 50°C.

6.2.1.4 Anion exchange of polyoxoanions for adipate

After stirring, the above suspension was allowed to settle and then decanted, leaving a slurry of the LDH-adipate precursor. The temperature was then increased to 100°C, a 100 ml of degassed boiling water was added to the fresh LDH-adipate slurry. Hot POM solution (for **1**, 1.2 g in 23 mL of DDI water, for **2**, 1.8 g in 35 mL of DDI water) was placed in a pressure equalized addition funnel above the flask, and added

dropwise at ambient pH to the vigorously stirred slurry. After the addition was complete, stirred for an additional 8 min at reflux temperature under N_2, and then the product was quickly cooled in an icebath for 2-3 h, centrifuged, and washed twice with water. The final product was air dried at room temperature, ground and stored in vials.

6.2.2 Preparation of $[Eu(\alpha\text{-}2\text{-}P_2W_{17}O_{61}]_2^{14-}$, 1, $[EuPW_{11}O_{34}(H_2O)_2]^{4-}$, 2

6.2.2.1 $[Eu(\alpha\text{-}2\text{-}P_2W_{17}O_{61}]_2^{14-}$, 1

Solid $Na_9[A\text{-}PW_9O_{34}]\cdot xH_2O$ (2.19 g, 0.9 mmol) was added slowly to a solution of $EuCl_3\cdot 6H_2O$ (0.33 g, 0.9 mmol) in 7.5 ml of H_2O. The resulting suspension was heated to about 80°C, within a few seconds, a clear solution formed. Solid $AlCl_3$ (1.74 g, 7.2 mmol) was added to the hot solution, the resulting clear solution was heated for an additional 10 min. Traces of a precipitate were removed by filtration. The solution was stored in a vial at room temperature. After a month, plate-like crystals were grown, and x-ray quality crystals were chosen. (yield: 1.19 g, 47% based on $EuCl_3\cdot 6H_2O$).

To get high yield of complex **1** to incorporate into the LDH material, a direct method of synthesizing complex **1** was used [3]. The lacunary $K_{10}[\partial\text{-}2P_2W_{17}O_{61}]$ (5 g, 1.017mmol) was dissolved in 50 ml of 0.5 M sodium acetate buffer at pH = 5.5 at 70°C to form a clear solution. $EuCl_3$ (1.2 g, 3.08 mmol) was dissolved in a minimum amount of water and added dropwise to the stirring $K_{10}[\partial\text{-}2P_2W_{17}O_{61}]$ solution. KCl (5 g,) was added to the reaction mixture, and the clear solution was cooled in the refrigerator. After 2 h, a white precipitate formed, which contained a small impurity of the 1:2 sandwich complex, according to ^{31}P NMR spectroscopy. The precipitate was dissolved in 50 ml of sodium acetate buffer at pH 5.5 at 70°C, and 1.5 mL of 1.0 M $EuCl_3$ was added, followed by the addition of 3 g of KCl. The clear solution was cooled to 0°C. A white precipitate formed

after a few hours and was collected and was collected and recrystallized twice from hot water at 70°C.

6.2.2.2 $[EuPW_{11}O_{34}(H_2O)_2]^{4-}$, 2

To a solution of $EuCl_3 \cdot 6H_2O$ (0.66 g, 1.8 mmol) in 15 ml of H_2O was added slowly with vigorous stirring $Na_9[A\text{-}PW_9O_{34}] \cdot 18H_2O$ (2.19 g, 0.9 mmol). The solution was stirred for 20 min. The resulting suspension was heated to about 80°C. $AlCl_3$ (1.74 g, 7.2 mmol) was added. Within a few seconds, the resulting solution turned clear. Stirring continued for 20 min. Traces of a precipitate were removed by filtration. The solution was stored in a beaker open to air. After a week, different shapes of crystals were grown, collect the plate-like crystals by removing the square-shape crystals, which was confirmed to be $AlCl_3$. Yield: 0.6g (21%). X-ray quality crystals were grown in this fashion. IR (KBr disk) in metal-oxygen stretching region: $\Im$=1092 (m), 1055(m), 1025(m), 951(s), 935(s), 820(vs), 790 cm^{-1} (s).

To get high yield of complex **2** to incorporate into the LDH material, a method directly from $K_7(PW_{11}O_{39})$ was used. To a solution of $EuCl_3 \cdot 6H_2O$ (1.32 g, 3.6 mmol) in 25 mL of 0.2 M sodium acetate buffer at pH = 4 at 50°C was added slowly with vigorous stirring $K_7(PW_{11}O_{39})$ (2.12 g, 0.72 mmol). After the solution has been stirred at this temperature (50°C) for 20 min, KCl (0.5 g) was added, the reaction mixture was allowed to cool to room temperature and filtered. Addition of a threefold excess of ethanol to the cooled filtrate yielded a precipitate, which was collected by filtration. The precipitate was dissolved in 50 mL of sodium acetate buffer at pH 4 at 50°C, the clear solution was cooled in the refrigerator, after two days, the colorless crystals was formed. (yield: 1.7 g, 76.7% based on $[PW_{11}O_{39}]^{7-}$).

6.2.3 Physical Measurements

The FTIR spectra of the samples pressed in KBr pellets were obtained at a resolution of 8 cm^{-1} between 4000 and 400 cm^{-1} on a Perkin-Elmer 1625 series FTIR spectrometer, using 64 sample scans and 64 background scans. UV-Vis spectra were measured with a Cray 3 spectrophotometer. Steady-state emission and excitation spectra were acquired using a SPEX Fluorolog-τ2 Spectrofluorimeter. Powder X-ray diffraction (PXRD) patterns were recorded with a Rigaku diffractometer, using $CuK_{\partial 1}$ (0.154 nm) x-rays: typically run at a voltage 40 kV and current of 30 mA. Raman spectra were excited with laser radiation of wavelength 488 nm from a Coherent Innova 200 argon-ion laser. The excitation power was maintained at 100 mW and the Raman scattering was collected and dispersed by a Spex 1877, 0.6-meter spectrometer. A cooled (140 K) Spex Spectrum-1 CCD camera was coupled to the spectrometer and used as the detector.

6.3 Results and Discussion

6.3.1 Crystal Structures

In the solid state the $[Eu(H_2O)_3(\alpha_2\text{-}P_2W_{17}O_{61})]^{7-}$ (**1**) (Figure 1) is a dimer where the Eu is bound to the four oxygen atoms in the cap vacancy of the Dawson-like polyanion and to three water molecules and to a terminal tungsten oxygen of another $(\alpha_2\text{-}P_2W_{17}O_{61})^{10-}$ unit. The luminescence spectroscopy and ^{183}W NMR show good evidence that $[Eu(H_2O)_3(\alpha_2\text{-}P_2W_{17}O_{61})]_2^{14-}$ in aqueous solution dissociate into a monomeric species wherein the Eu is bound to four water molecule and one $[\alpha_2\text{-}P_2W_{17}O_{61}]^{10-}$ moiety [7]. The size of this monomeric form is 10Å and 20Å for the minor and major dimensions, respectively. In the solid state, $[Eu(H_2O)_2(PW_{11}O_{39})]^{4-}$ (**2**) (Figure 2) is a

polymer where the Eu is bound to the four oxygen atoms in the cap vacancy of the Keggin-like polyanion and to two water molecules and to a terminal tungsten oxygen of another $PW_{11}O_{39}^{7-}$ unit. Both ^{31}P NMR and ^{183}W NMR show good evidence that $[Eu(H_2O)_2(PW_{11}O_{39})]_2^{8-}$ in aqueous solution dissociate into a monomeric species [8]. The size of this monomeric form is 10Å.

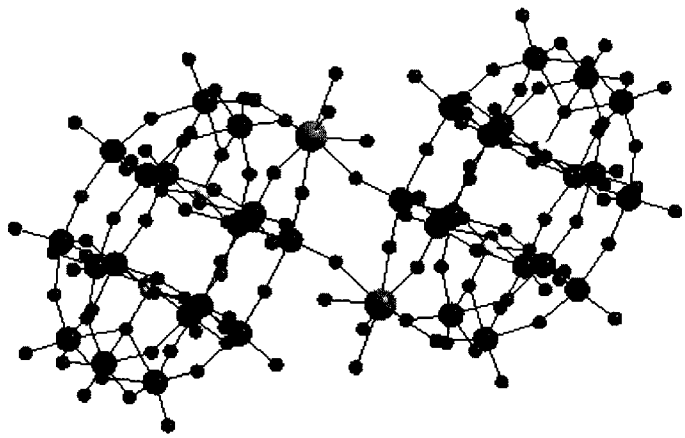

Figure 1. Dimeric form of $[Eu(H_2O)_3(\alpha\text{-}2\text{-}P_2W_{17}O_{61})]^{7-}$ (**1**)

6.3.2 Incorporation into Mg_3Al-LDH

To facilitate the incorporation of bulky polyoxoanions **1** and **2** into the LDH layers, adipic acid was used in the synthesis to expand the interlayer distances from about 8.0Å to 12.9Å, which is anticipated to be sufficiently large to allow the **1** or **2** to be incorporated into the "expanded" layers. The IR of the composite Mg_3Al-[**1**], Mg_3Al-[**2**] and Zn_3Al-[**1**], Zn_3Al-[**2**] materials, in both cases, showed bands for the POMs, suggesting retention in the LDH substituted materials. The FTIR are shown in **Figure 3** (e, g) and **Figure 4** (c, d). In order to evaluate each step of the synthetic route (**scheme 2**) that proceeds through LDH-CO_3, mixed oxide, LDH-OH, and LDH-adipate precursors, FTIR was also taken on each precursor material. The FTIR spectra indicated that

complete exchange of adipate anions in the precursor material by POM anions was achieved except for the Zn/Al analogues. (**Figure 3 and 4**).

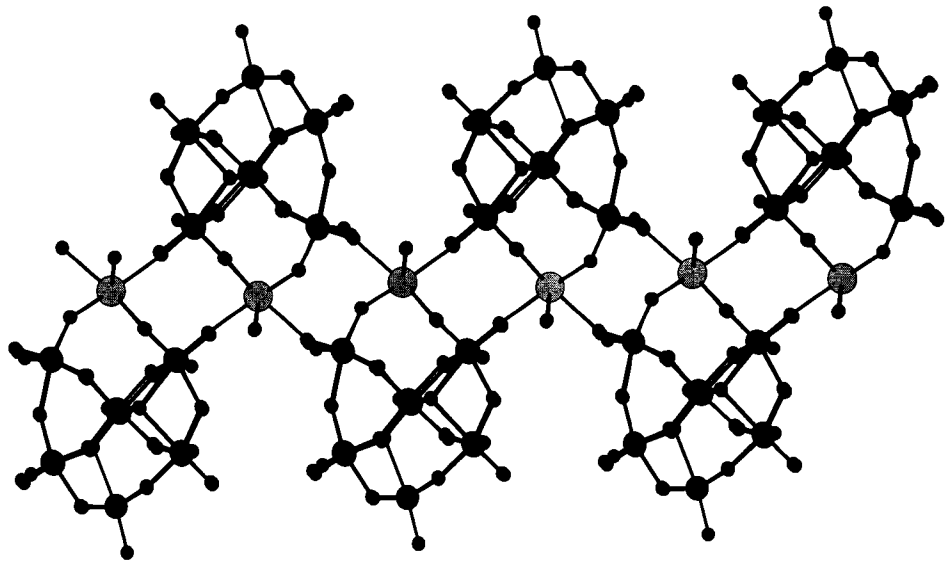

Figure 2. Polymeric form of $[Eu(H_2O)_2(PW_{11}O_{39})]^{4-}$ (**2**)

The XRD data for Mg_3Al-LDH-[**1**] showed multiple phases in the XRD, including some amorphous phase and the phases characterized by a broad reflection at low angles (2θ = 7-11°). Peaks observed at 15.694Å, 8.258Å and 4.1Å were indexed to the d_{003}, d_{006}, and d_{009} reflections corresponding to an interlayer spacing of ca. 12.9Å. This may represent the situation where the Cs axis of **1** is oriented parallel to the brucite – like layers as shown in Figure 5. Transition metal substituted Wells-Dawson $(M(H_2O)\partial_2\text{-}P_2W_{17}O_{61})^{8-}$ ($M=Co^{II}$, Cu^{II}, and Zn^{II}) molecules, incorporated into Zn_2Al-LDH showed similar layer spacing [10]. The interlayer $[EuPW_{11}O_{39}]^{4-}$ ion most likely has the C_2 axis of the oxygen framework orthogonal to the LDH layers to optimize H bonding to the gallery hydroxyl groups, as proposed in Figure 5.

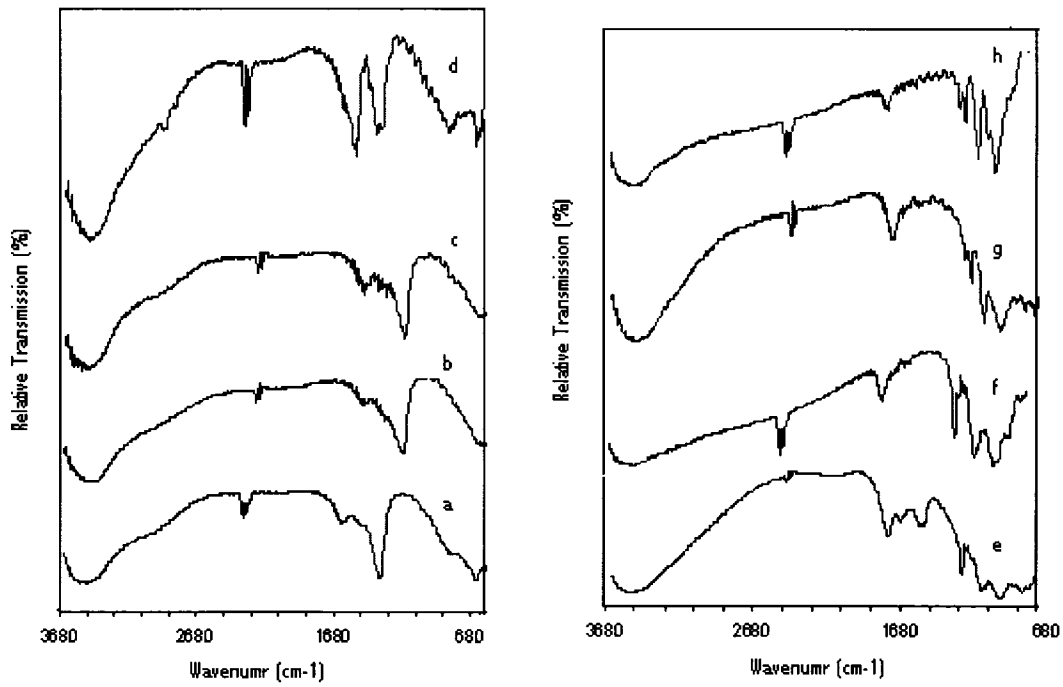

Figure 3. FTIR spectra of (a) Mg_3Al LDH-CO_3, (b) Mg_3Al LDH-CO_3 calsinate, (c) Mg_3Al LDH-OH, (d) Mg_3Al LDH-adipate, (e) Mg_3Al LDH-[**2**], (f) pure solid **2**, (g) Mg_3Al LDH-[**4**], (h) pure solid **4**

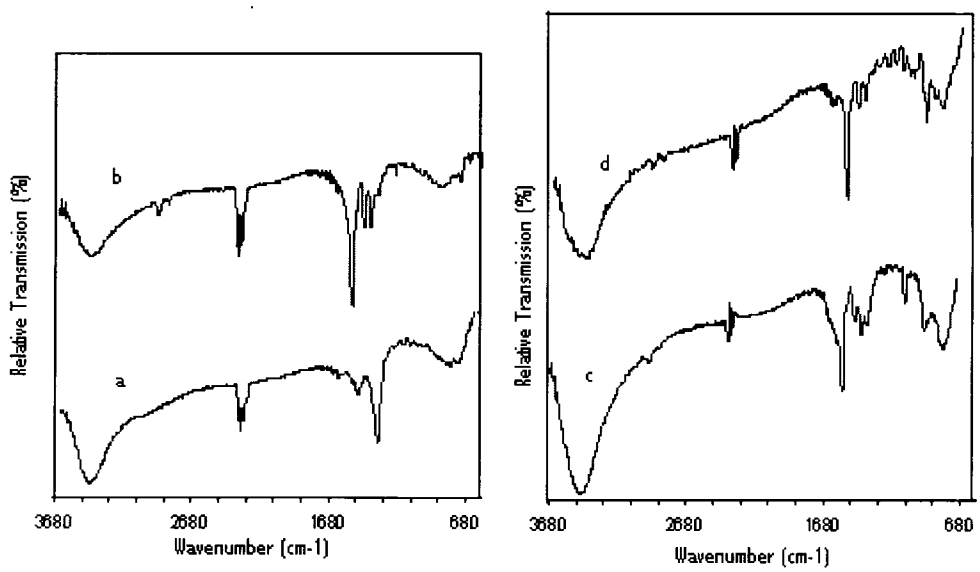

Figure 4. FTIR spectra of (a) Zn_3Al LDH-CO_3, (b) Zn_3Al LDH-adipate, (c) Zn_3Al LDH-[**4**], (d) Zn_3Al LDH-[**2**]

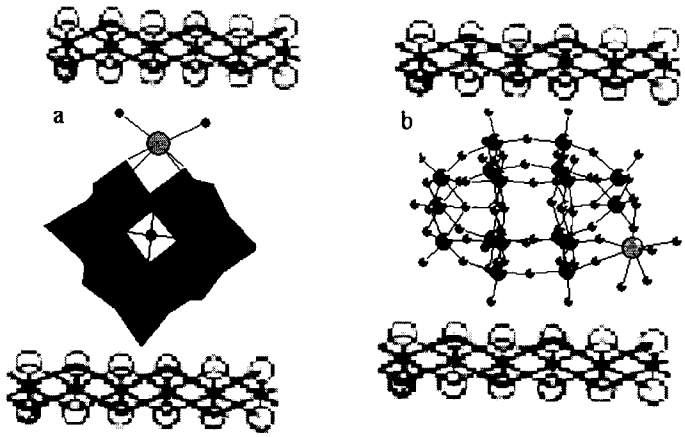

Figure 5. proposed POM^{n-} gallery orientations for the LDH intercalates. (a) **2**, (b) **1**

6.3.3 Luminescence of the pillered LDH materials

The luminescence behavior of the Mg_3Al-LDH-[**2**], Mg_3Al-LDH-[**1**] and Zn_3LDH-[**2**] has been investigated at 25°C by direct excitation at 395 nm. Representative emission spectra of the pure solid **2**, the composite Mg_3Al-LDH-[**2**], Zn_3Al-LDH-[**2**] and pure solid **1**, the composite Mg_3Al-LDH-[**1**] are shown in **Figure 6** and **7**. It is to be noted that the emission spectra for both samples are quite similar, indicating the weak interactions between the intercalated polyoxoanion and the LDH layer hydroxyls and the maintenance of the integrity of the structure of **2** and the integrated character of the composite. Eu^{3+} ions have five emission lines corresponding to the $^5D_0 \rightarrow {}^7F_J$ transitions, where J=0-4. The $^5D_0 \rightarrow {}^7F_2$ emission around 618 nm is the most predominant transition, and is the characteristic "europium red" luminescence. [34] The most important probe transitions for Eu^{3+} complexes are $^5D_0 \rightarrow {}^7F_{0,1,2}$, whose intensities are governed by selection rules which depend on the local symmetry of the crystal field around the ion.[35-39] It can be concluded that there is only one type of Eu^{3+} binding site in our pillared

materials from the splitting numbers of the $^5D_0 \rightarrow {}^7F_0$ (1line), $^5D_0 \rightarrow {}^7F_1$ (no more that 3 lines), and $^5D_0 \rightarrow {}^7F_2$ (no more than 5 lines). It is interesting to note that the luminescence intensity of **2** was enhanced after the intercalation of **2** into Mg_3Al-LDH and Zn_3Al-LDH layers (**Figure 6**). The emission spectra of **1** and Mg_3Al-LDH-[**1**] show similar patterns as in **Figure 6**, but the luminescence intensity of **4** was greatly reduced after the intercalation of **1** into Mg_3Al-LDH layers (**Figure 7**), probably due to the smaller amount of **1** into the layers.

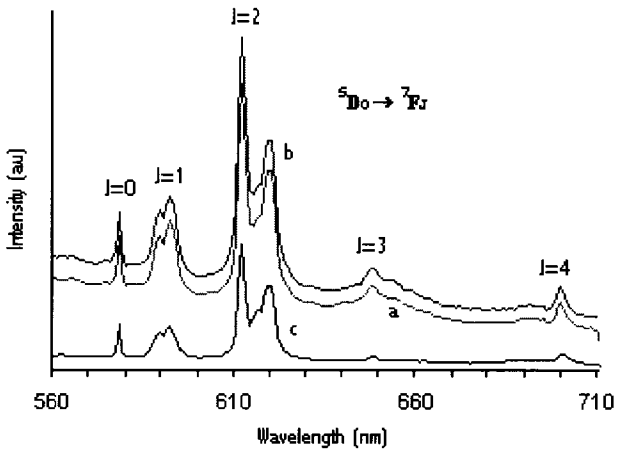

Figure 6. Emission spectra of (a) Zn_3Al-[**2**], (b) Mg_3Al-[**2**], (c) pure solid **2**

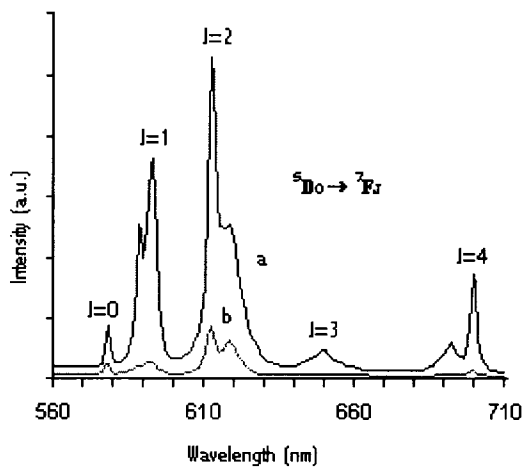

Figure 7. Emission spectra of (a) pure solid **1**, (b) Mg_3Al-[**1**],

6.3.4 Raman absorptions of the pillared LDH materials

Raman spectra of solid state of **2,** Mg_3Al-LDH-[**2**], Zn_3Al-LDH-[**2**] and **1**, Mg_3Al-LDH-[**1**], Zn_3Al-LDH-[**1**] are shown in **Figure 8** and **9**. Similar Raman patterns for the samples in **Figure 8** are found, which indicate that polyoxoanion **1** remains intact in the LDH layers. Raman spectra in **Figure 8** have characteristic vibration peaks at ca.

232, 967 and 981 cm^{-1}, assigned to symmetric stretching γ_s (W-Ot) (where Ot represent terminal oxygen), asymmetric stretching γ_{as} (W-Ot); and symmetric stretching γ_s (P-O-W). [40,41] respectively. The relative weak bands at ca. 374 and 1015cm^{-1} are assigned to bending δ (W-O-W) and γ_{as} (W-O-P), respectively. It is interesting to note that certain Raman bands for the pillared vis-à-vis the respective bands for solid state **1** show red shift, e. g., the 230, and 232 cm^{-1}, for γ_s (W-Ot) and the 976 and 981 cm^{-1} for γ_s (P-O-W), respectively, indicating the weak host-guest interaction between the LDH layer hydroxyls and the oxygen framework. However, slightly different Raman patterns for pure solid **2** and the composite Mg_3Al-LDH-[**2**], Zn_3Al-LDH-[**2**] are found (**Figure 9**), which can be explained that the interaction between the host LDH layer and the guest POM anion is probably stronger than that in the intercalated Mg_3Al-LDH-[**1**].

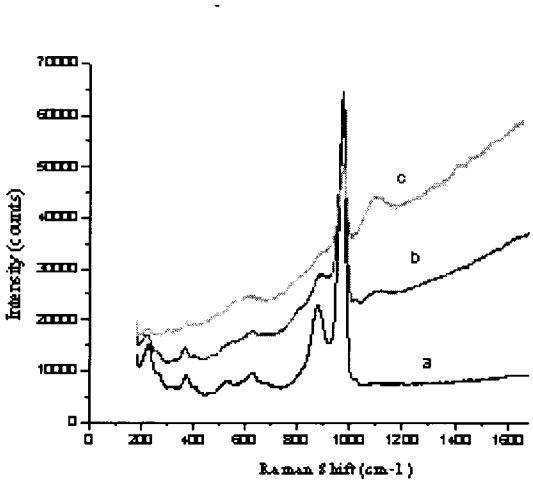

Figure 8. Raman spectra of (a) pure solid **1**, (b) Mg_3Al-[**1**], (c) Zn_3Al-[**1**]

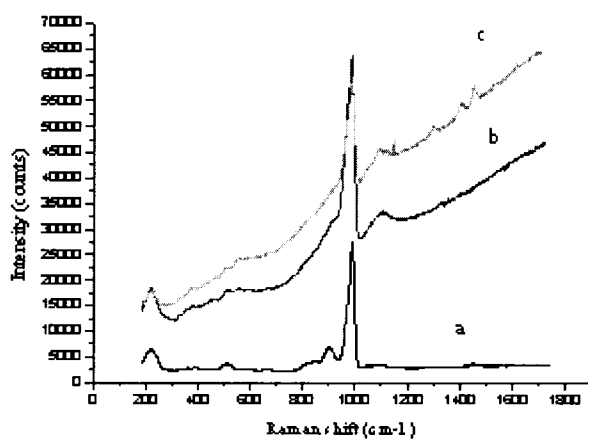

Figure 9. Raman spectra of (a) pure solid **2**, (b) Mg_3Al-[**2**], (c) Zn_3Al-[**2**]

6.2 Conclusion

Dawson-like $[Eu(\alpha_1\text{-}P_2W_{17}O_{61}]^{7-}$ (**1**) and Keggin-like $[Eu(H_2O)_2(PW_{11}O_{39})]^{4-}$ (**2**) were incorporated into the layered double hydroxide (LDH-Mg/Al, LDH-Zn/Al). Structure and luminescence properties of these pillared products have been examined based on PXRD, FTIR, Fluorescence and Raman spectroscopies studies. PXRD data show some multiple phases, probably due to the different orientations of the POMs in the LDH layers. For Mg_3Al LDH-[**1**], a d_{003} value at 15.694Å was obtained, indicating that the $[Eu(H_2O)_3(\alpha_2\text{-}P_2W_{17}O_{61}]]^{7-}$ ions have been successfully intercalated between the LDH layers. The FTIR of the composite Mg_3Al-[**2**], Mg_3Al-[**1**] and Zn_3Al-[**2**], Zn_3Al-[**1**] materials, showed bands for the POMs, suggesting retention in the LDH substituted materials. Similar emission and Raman pattern of the pillared products, indicated the weak host-guest interaction between the LDH layer hydroxyls and the oxygen framework of the POM anions. It is interesting to note that the luminescence intensity of **2** was enhanced after the intercalation of **2** into Mg_3Al-LDH and Zn_3Al-LDH layers, while the luminescence intensity of **1** was greatly reduced after the intercalation of **1** into LDH layers probably due to the smaller amount of **1** into the layers.

6.4 References

[1] S. K. Yun and T. Pinnavaia, *Inorg. Chem.* 1996, 35, 6853-6860.

[2] C. Barriga, W. Jones; P. Malet; V. Rives, and M. A. Ulibarri. *Inorg. Chem.* 1998, 37, 1812-1820.

[3] Kwon, T.; Pinnavaia, T. *J. Chem. Mater.* 1989, 1, 381.

[4] Drezdzon, M. A. *Inorg. Chem.* 1989, 27, 4628.

[5] Evans, J.; Pillinger, M.; Zhang, J. *J. Chem. Soc., Dalton Trans.* 1996, 2963.

[6] Alvin P. Ginsberg, *Inorganic syntheses* V27, 1992.

[7] Q-H Luo, R.C. Howell, J. Bartis, M. Dankova, W. D. Horrocks, Jr. A. L. Rheingold, and L. C. Francesconi, *Inorg. Chem.* 2002, accepted.

[8] C. Zhang; R. C. Howell; K. B. Scotland; F. G. Perez and L. C. Francesconi. manuscript, 2002.

[9] M. R. Weir; R. Kydd, *Microporous and Mesoporous Materials*, 20 (1998) 339-347.

[10] Guo, J.; Li, Y.; Jiao, Q.; Jiang, D.; Min, E., *Chemical research in Chinese Universities* 1998; 14, 176-178.

[11] F. Embert; A. Mehdi; C. Reye; R. J. P. Corriu. *Chem. Mater.* 2001, 13, 4542-4529.

REFERENCES

Chapter 1

(1) Jeffrey T. Rhuce, Craig L. Hill, Deborah A. Juad. *Chem. Rev.*,**1998**, 98, 327-357

(2) Pierre Gouzerh, Anna Proust, *Chem. Rev.*, **1998**, 98, 77-111

(3) Hill, C. L., *Chem Review*. 1998, 98, 3

(4) Gouzerh, P.; Proust, A., *Chem. Rev.* 1998, 98, 77.

(5) Contant, R.; Teza, A. *Inorg. Chem.* **1985**, 24, 4610.

(6) Jeannin, Y. *J. Cluster. Sci.* **1992**, 3, 55

(7) Creaser, I.; Heckel, M. C.; Neitz, R. J.; Pope, M. T. *Inorg. Chem.* **1993**, 32, 1573.

(8) Antonio, M. R.; Soderholm, L. *J. Cluster Sci.* **1996**, 7, 585.

(9) Dickman, M. H.; Gama, G. J.; Kim, K. C.; Pope, M. T. *J. Cluster Sci.* **1996**, 7, 567.

(10) Harrup, M. K.; Hill, C. L. *Inorg. Chem.* **1994**, 33, 5448.

(11) Kim, K.; Pope, M. T. *Inorg. Chem.*, **1999**,

(12) Kim, G.S.; Judd, D.A.; Hill, C. L.; Schinazi, R. F.; J. Med. Chem. **1994**, 37, 816

(13) Bartis J.; Dankova M.; Lessmann J.; Luo Q-H.; Horrocks, Jr.; W. Dew.; Francesconi L. C., *Inorganic. Chem.*, **1999**, 38, 1042-1053

(22) Zhang, X.; Chen, Q.; Duncan,D. C.; Lachiotte, R. J.; Hill, C. L. *Inorg. Chem.* 1997, 36, 4381.

(23) Finke, R. G.; droege, M.; Hutchinso, J. R.; gansow, O. *J. Am. Chem. Soc.* 1981, 103, 1587-1589.

(24) Massart, R.; Contant, R.; Fruchart, J.-M.; Ciabrini, J. –P.; Fournier, M. *Inorg. Chem.* 1977, 16, 2916-2921.

(25) (a) Weakley, T. J. R.; Finke, R. G. *Inorg. Chem.* 1990, 29, 1235-1241. (b) Weakley, T. J. R.; Evans, H. T., Jr.; Showell, J. S.; Tourne, C. M. *J. Chem. Soc., Chem. Commun.* 1973, 139-140. (c) Evans, H. T.; Tourne, G. F.; Tourne, C. M.; Weakly, T. J. R.; *J. Chem. Soc., Dalton Trans.* 1986, 2699. (d) Finke, R. G.; Droege, M. W.; Domaile, P. J. *Inorg. Chem.* 1987, 26, 3886.

(26) (a) Coronado, E.; Gomez-Garcia, C. J. *Comments Inorg. Chem.* 1995, 17, 255. (b) Gomez-Garcia, C.; Coronado, E.; Gomez-Romero, P.; Casan-Pastor, N. Inorg. Chem. 1993, 32, 3378.

(27) (a) Zhang, X.; Jameson, G. B.; O'Connor, C. J.; Pope, M. T. *Polyhedron* 1996, 15, 917.

(28) (a) Knoth, W. H.; Domaille, P. J.; Harlow, R. L. *Inorg. Chem.* 1986, 25, 1577. (b) Knoth, W. H.; Domaille, P. J.; Farlee, R. D. *Organometallics* 1985, 4, 62.

(29) Weakley, T. J. R. *J. Chem. Soc. Chem. Commun.* 1984, 1406.

(22) Luo, Q. H.; Howell, R. C.; Bartis, J.; Dankova, M.; Horroks, W. D. Jr.; Rheingold, L.; Francesconi, L. C., *Inorg.Chem.* Accepted.

(23) S. K. Yun and T. Pinnavaia, *Inorg. Chem.* 1996, 35, 6853-6860.

(24) Luo, Q.; Howell, R. C.; Bartis, J.; Dankova, M.; Horrocks, W. D., Jr.; Rheingold, A. L.; Francesconi, L. C. *Inorg. Chem.* 2002, *41*, 6112-6117.

(25) a. Kozik, M.; Hammer, C. F.; Baker, L. C. W.,*J. Am. Chem. Soc.* **1986,** *108*, 2748-2749. b.Kozik, M.; Baker, L. C. W.,*J. Am. Chem. Soc.* **1990,** *112*, 7604-7611. c. Keita, B.; Levy, B.; Nadjo, L.; Contant, R.,*New. J. Chem.* **2002,** *26*, 1314-1319. d. Lopez, X.; Bo, C.; Poblet, J. M.,*J. Am. Chem. Soc.* **2002,** *124*, 12574-12582.

(26) Contant, R.; Abbessi, M.; Canny, J.; Belhouari, A.; Keita, B.; Nadjo, L., *Inorg. Chem.* **1997,** *36*, 4961-4967. b. Contant, R.; Richet, M.; Lu, Y. W.; Keita, B.; Nadjo, L.,*Eur. J. Inorg. Chem.* **2002,** c. Keita, B.; Girard, F.; Nadjo, L.; Contant, R.; Canny, J.; Richet, M.,*J. Electroanal. chem.* **1999,** *478*, 76-82.

(27) a. Bartis, J.; Dankova, M.; Lessmann, J. J.; Luo, Q.-H.; Horrocks, W. D., Jr.; Francesconi, L. C., *Inorg. Chem* **1999,** *38*, 1042-1053. b. Luo, Q.; Howell, R.C.; Bartis, J.; Dankova, M.; Williams, C.; Horrocks, W.DeW., Jr.; Young, V.C., Jr,; Rheingold, A.L.; Francesconi, L.C.; Antonio, M.R.*Inorg. Chem.* **2001**, *40*, 1894.

(28) For key references to lanthanide luminescence: a.Bunzli, J.-C. G. "Luminescent Probes" in Lanthanide Probes in Chemistry, Biology and Earth Sciences; Bunzli, J.-C.G.; Choppin, G. Eds.; 1989; Elsevier, Amsterdam. b. Kido, J.; Okamoto, Y. *Chem. Rev.* **2002**, *102*, 2357-2368. c. Bruce, J. I.; Dickins, R. S.; Govenlock, L. J.; Gunnlaugsson, T.; Lopinski, S.; Lowe, M. P.; Parker, D.; Peacock, R. D.; Perry, J. J. B.; Aime, S.; Botta, M., *J. Am. Chem. Soc.* **2000**, *122*, 9674-9684. d. Dickins, R. S.; Aime, S.; Batsanov, A. S.; Beeby, A.; Botta, M.; Bruce, J. I.; Howard, J. A. K.; Love, C. S.; Parker, D.; Peacock, R. D.; Puschmann, H.*J. Amer. Chem. Soc.* **2002**, *124*, 12697-12705. e. Parker, D.; Dickins, R. S.; Puschmann, H.; Crossland, C.; Howard, J. A. K. *Chem. Rev.* **2002**, *102*, 1977-2010..

(29) For key reviews on new functional materials, particularly electrochromic, electroluminescent, photochromic and photoluminescent materials, a. Katsoulis, D.E. *Chem. Rev.*, **1998**, *98*, 359-387. b.Yamase, T. *Chem. Rev.*, **1998**, *98*, 307-325. *For recent applications of lanthanide polyoxometalates incorporated into materials: electrochromic device preparation*, c. Liu, S.; Kurth, D. G.; Mohwald, H.; Volkmer,

D.*Advanced Materials* **2002**, *14*, 225-228. *photoluminescent films*, d. Mo, Y.-G.; Dillon, R. O.; Snyder, P. G.; Tiwald, T. E. *Thin Solid Films* **1999**, *355-356*, 1-5. e. Xu, L.; Zhang, H.; Wang, E.; Kurth, D. G.; Li, Z. *J. Mater. Chem.* **2002**, *12*, 654-657. f. Xu, L.; Zhang, H.; Wang, E.; Wu, A.; Li, Z. *Materials Chemistry and Physics* **2002**, *77*, 484-488. g. Wang, Y.; Wang, X.; Hu, C.; Shi, C. *J. Mater. Chem.* **2002**, *12*, 703-707. h. Wang, J.; Liu, F.; Fu, L.; Zhang, H. *Materials Lett.* **2002**, *56*, 300-304. i. Wang, Y.; Wang, X.; Hu, C. *Journal of Colloid and Interface Science* **2002**, *249*, 307-315. j. Wang, J.; Wang, H. S.; Fu, L. S.; Liu, F. Y.; Zhang, H. J. *Thin Solid Films* **2002**, *414*, 256-261.

(30) For key references to lanthanide Lewis Acid catalysis: a. Aspinall, H. C. *Chem. Rev.* **2002**, *102*, 1807-1850. b. Molander, G. A. *Chemtracts-Organic Chemistry* **1998**, *11*, 237-263. c. Molander, G. *Chem. Rev.* **1992**, *92*, 29-68. d. Shibasaki, M.; Yoshikawa, N. *Chem. Rev.* **2002**, *102*, 2187-2209. e. Kobayashi, S.; Kawamura, M. *J. Am. Chem. Soc.* **1998**, *120*, 5840-5841. f. Kobayashi, S. *Pure and Appl. Chem.* 1998, *70*, 1019-1026. g. Aspinall, H. C.; Dwyer, J. L. M.; Greeves, N.; McIver, E. G.; Woolley, J. C. *Organometallics* **1998**, *17*, 1884-1888. h. Xie, W.-H.; Yu, L.; Chen, D.; Li, J.; Ramirez, J.; Miranda, N. F.; Wang, P. G . in *Environmentally Benign Chemistry: Green Chemistry*; Anastas, P. T. and Williamson, T. C., Ed.; Oxford University Press: Oxford, UK, **1998**; Vol. , pp 129-149.

(39) Sadakane, M.; Dickman, M. H.; Pope, M. T. *Angew. Chem. Int. Ed.* **2000**, *39*, 2914-2916.

(40) Mialane, P.; Lisnard, L.; Mallard, A.; Marrot, J.; Antic-Fidancev, E.; Aschehoug, P.; Vivien, D.; Secheresse, F. *Inorg. Chem.* **2003**, *42*, 2102-2108.

(41) Luo, Q-H., Doctoral Dissertation, Chemistry Department of the City University of New york, **2002**.

(42) a. Jeffrey T. Rhuce, Craig L. Hill, Deborah A. Juad. *Chem. Rev.*,**1998**,98,327-357, b. Pierre Gouzerh, Anna Proust, *Chem. Rev.,* **1998**, 98, 77-111, c. Kim, G.S.; Judd, D.A.; Hill, C. L.; Schinazi, R. F.; J. Med. Chem. **1994**, 37, 816

(43) Zhang, C.; Howell, R. C.; Francesconi, L. C., *J. cluster. Sci.*, **2004**, in press.

(44) Zhang, C.; Howell, R.C.; Perez, F.; Scotland, K.; Todaro L. J., Francesconi, L.C., ***Inorg. Chem.***, **2004**, 43, 7691-7701.

(45) Zhang C.; Fang X.; Luo, Q-H; Howell R. C.; Hill, C. L.; Francesconi L. C., ***Inorg. Chem.***, submitted, **2004**.

(46) Zhang, C.; Howell, R. C.; Luo, Q-H; Fieselmann, H. L.; Todaro, L. J.; Francesconi, L. C., ***J. Am. Chem. Soc.***, accepted, **2004**.

Chapter 2

(1) For key references to lanthanide luminescence: a.Bunzli, J.-C. G. "Luminescent Probes" in Lanthanide Probes in Chemistry, Biology and Earth Sciences; Bunzli, J.-C.G.; Choppin, G. Eds.; 1989; Elsevier, Amsterdam. b. Kido, J.; Okamoto, Y. *Chem. Rev.* **2002**, *102*, 2357-2368. c. Bruce, J. I.; Dickins, R. S.; Govenlock, L. J.; Gunnlaugsson, T.; Lopinski, S.; Lowe, M. P.; Parker, D.; Peacock, R. D.; Perry, J. J. B.; Aime, S.; Botta, M., *J. Am. Chem. Soc.* **2000**, *122*, 9674-9684. d. Dickins, R. S.; Aime, S.; Batsanov, A. S.; Beeby, A.; Botta, M.; Bruce, J. I.; Howard, J. A. K.; Love, C. S.; Parker, D.; Peacock, R. D.; Puschmann, H.*J. Amer. Chem. Soc.* **2002**, *124*, 12697-12705. e. Parker, D.; Dickins, R. S.; Puschmann, H.; Crossland, C.; Howard, J. A. K. *Chem. Rev.* **2002**, *102*, 1977-2010..

(2) For key reviews on new functional materials, particularly electrochromic, electroluminescent, photochromic and photoluminescent materials, a. Katsoulis, D.E. *Chem. Rev.*, **1998**, *98*, 359-387. b.Yamase, T. *Chem. Rev.*, **1998**, *98*, 307-325. *For recent applications of lanthanide polyoxometalates incorporated into materials*: *electrochromic device preparation*, c. Liu, S.; Kurth, D. G.; Mohwald, H.; Volkmer, D.*Advanced Materials* **2002**, *14*, 225-228. *photoluminescent films*, d. Mo, Y.-G.; Dillon, R. O.; Snyder, P. G.; Tiwald, T. E. *Thin Solid Films* **1999**, *355-356*, 1-5. e. Xu, L.; Zhang, H.; Wang, E.; Kurth, D. G.; Li, Z. *J. Mater. Chem.* **2002**, *12*, 654-657. f. Xu, L.; Zhang, H.; Wang, E.; Wu, A.; Li, Z. *Materials Chemistry and Physics* **2002**, *77*, 484-488. g. Wang, Y.; Wang, X.; Hu, C.; Shi, C. *J. Mater. Chem.* **2002**, *12*, 703-707. h. Wang, J.; Liu, F.; Fu, L.; Zhang, H. *Materials Lett.* **2002**, *56*, 300-304. i. Wang, Y.; Wang, X.; Hu, C. *Journal of Colloid and Interface Science* **2002**, *249*, 307-315. j. Wang, J.; Wang, H. S.; Fu, L. S.; Liu, F. Y.; Zhang, H. J. *Thin Solid Films* **2002**, *414*, 256-261.

(3) For key references to lanthanide Lewis Acid catalysis: a. Aspinall, H. C. *Chem. Rev.* **2002**, *102*, 1807-1850. b. Molander, G. A. *Chemtracts-Organic Chemistry* **1998**, *11*, 237-263. c. Molander, G. *Chem. Rev.* **1992**, *92*, 29-68. d. Shibasaki, M.; Yoshikawa, N. *Chem. Rev.* **2002**, *102*, 2187-2209. e. Kobayashi, S.; Kawamura, M. *J. Am. Chem. Soc.* **1998**, *120*, 5840-5841. f. Kobayashi, S. *Pure and Appl. Chem.* 1998, *70*, 1019-1026. g. Aspinall, H. C.; Dwyer, J. L. M.; Greeves, N.; McIver, E. G.; Woolley, J. C. *Organometallics* **1998**, *17*, 1884-1888. h. Xie, W.-H.; Yu, L.; Chen, D.; Li, J.; Ramirez, J.; Miranda, N. F.; Wang, P. G . in *Environmentally*

Benign Chemistry: Green Chemistry; Anastas, P. T. and Williamson, T. C., Ed.; Oxford University Press: Oxford, UK, **1998**; Vol. , pp 129-149.

(4) Sadakane, M.; Dickman, M. H.; Pope, M. T. *Angew. Chem. Int. Ed.* **2000**, *39*, 2914-2916.

(5) Mialane, P.; Lisnard, L.; Mallard, A.; Marrot, J.; Antic-Fidancev, E.; Aschehoug, P.; Vivien, D.; Secheresse, F. *Inorg. Chem.* **2003**, *42*, 2102-2108.

(6) Muller, A.; Peters, F.; Pope, M. T.; Gatteschi, D. *Chemical Reviews* **1998**, *98*, 239-271.

(7) Muller, A.; Krickemeyer, E.; Bogge, H.; Schmidtmann, M.; Peters, F. *Angew. Chem. Int. Ed.* **1998**, *37*, 3360-3365.

(8) Muller, A.; Sarkar, S.; Shah, S. Q. N.; Bogge, H.; Schmidtmann, M.; Sarker, S.; Kogerler, P.; Hauptfleish, B.; Trautwein, A. X.; Schunemann, V. *Angew. Chem. Int. Ed.* **1999**, *38*, 3238-3241.

(9) Wassermann, K.; Dickman, M. H.; Pope, M. T. *Angew. Chem. Int. Ed. Engl.* **1997**, *36*, 1445-1448.

(10) Belai, N.; Sadakane, M.; Pope, M. T. *J. Am. Chem. Soc.* **2001**, *123*, 2087-2088.

(11) Bartis, J.; Dankova, M.; Blumenstein, M.; Francesconi, L. C. *Journal of Alloys and Compunds* **1997**, *249*, 56-68.

(12) Bartis, J.; Sukal, S.; Dankova, M.; Kraft, E.; Kronzon, R.; Blumenstein, M.; Francesconi, L. C. *J. Chem. Soc., Dalton Trans* **1997**, 1937-1944.

(13) Bartis, J.; Dankova, M.; Lessmann, J. J.; Luo, Q.-H.; Horrocks, W. D., Jr.; Francesconi, L. C. *Inorganic Chemistry* **1999**, *38*, 1042-1053.

(14) Luo, Q.; Howell, R. C.; Dankova, M.; Bartis, J.; Williams, C. W.; Horrocks, W. D., Jr.; Young, J., V.G.; Rheingold, A. L.; Francesconi, L. C.; Antonio, M. R. *Inorg. Chem.* **2001**, *40*, 1894-1901.

(15) Luo, Q.; Howell, R. C.; Bartis, J.; Dankova, M.; Horrocks, W. D., Jr.; Rheingold, A. L.; Francesconi, L. C. *Inorg. Chem.* **2002**, *41*, 6112-6117.

(16) Sadakane, M.; Dickman, M. H.; Pope, M. T. *Inorg. Chem.* **2001**, *40*, 2715-2719.

(17) Sadakane, M.; Ostuni, A.; Pope, M. T. *J. Chem. Soc. Dalton Trans.* **2002**, 63-67.

(18) Howell, R. C.; Perez, F. G.; Jain, S.; Horrocks, W. D., Jr.; Rheingold, A. L.; Francesconi, L. C. *Angew. Chem. Int. Ed.* **2001**, *40*, 4301-4304.

(19) Domaille, P. J. *Inorg. Synth.* **1990**, *27*, 100-101.

(20) SHELXTL, Brucker AXS, Inc., Bruker Advanced X-ray Solutions, **1999**

(21) Contant, R. *Inorg. Synth.* **1990**, *27*, 71.

(22) Contant, R.; Herve, G. *Reviews in Inorganic Chemistry* **2002**, *22*, 63-111.

(23) Hill, C. L.; Weeks, M. S.; Schinazi, R. F. *J. Med. Chem.* **1990**, *33*, 2767-2772.

(24) Ho, R. K. C.; Klemperer, W. G. *J. Amer. Chem. Soc.* **1978**, *100*, 6772-6774.

(25) When A-α- $PW_9O_{34}^{9-}$ was directly dissolved in NaAc (0.5 M, pH 6.5, 30% D_2O), the peak at 1.99 ppm along with other small peaks was observed.

(26) Thorp, H. H. *Inorg. Chem.* **1992**, *31*, 1585-1588.

(27) Brown, I. D.; Altermatt, D. *Acta Cryst.* **1985**, *B41*, 244-247.

(28) Spek, A. L. *Acta Cryst.* **1990**, *A 46*, C34.

(29) Peacock, R. D.; Weakley, T. J. R. *J. Chem. Soc.* **1971**, *A*, 1836-39.

(30) Fedotov, M. A.; Pertsikov, B. Z.; Danovich, D. K. *Polyhedron* **1990**, *9*, 1249-1256.

(31) We have also observed Eu(III)and Eu(III)-OH-Eu(III) dimeric units serving as countercations. These moieties bind to terminal W=O bonds of polyoxometalates. (Zhang, C.; Howell, R.C.; Francesconi, L.C., manuscript in preparation).

(32) Kirby, J. F.; Baker, L., C.W. *Inorganic Chemistry* **1998**, *37*, 5537-5545.

(33) Laronze, N.; Marrot, J.; Herve, G. *Inorg. Chem.* **2003**, *42*, 5857-5862.

(34) Grigoriev, V. A.; Hill, C. L.; Weinstock, I. A. *J. Am. Chem. Soc.* **2000**, *122*, 3544-3545.

(35) Grigoriev, V. A.; Cheng, D.; Hill, C. L.; Weinstock, I. A. *J. Am. Chem. Soc.* **2001**, *123*, 5292-5307.

(36) Cheng, Z.; Howell, R. C.; Luo, Q.; Fieselmann, H. L.; Todaro, L.; Francesconi, L. C., manuscript in preparation.

(37) Fang, X.; Anderson, T. M.; Neiwert, W. A.; Hill, C. L. *Inorg. Chem.* **2003**, *42*, 8600-8602.

(38) Knoth, W. H.; Domaille, P. J.; Harlow, R. L. *Inorg. Chem.* **1986**, *25*, 1577-1584.

Chapter 3

(1) a. Katsoulis, D. E.,*Chem. Rev.* **1998,** *98*, 359-387. b. Mizuno, N.; Misono, M.,*Chem. Rev.* **1998,** *98*, 199-217.

(2) Weinstock, I. A.; Barbuzzi, E. M. G.; Wemple, M. W.; Cowan, J. J.; Reiner, R. S.; Sonnen, D. M.; Heintz, R. A.; Bond, J. S.; Hill, C. L.,*Nature* **2001,** *414*, 191-195.

(3) a. Sadakane, M.; Dickman, M. H.; Pope, M. T.,*Angew. Chem. Int. Ed.* **2000,** *39*, 2914-2916. b. Mialane, P.; Lisnard, L.; Mallard, A.; Marrot, J.; Antic-Fidancev, E.;

Aschehoug, P.; Vivien, D.; Secheresse, F.,*Inorg. Chem.* **2003,** *42*, 2102-2108. c. Wassermann, K.; Dickman, M. H.; Pope, M. T.,*Angew. Chem. Int. Ed. Engl.* **1997,** *36*, 1445-1448.

(4) Belai, N.; Sadakane, M.; Pope, M. T.,*J. Am. Chem. Soc.* **2001,** *123*, 2087-2088.

(5) a. Kozik, M.; Hammer, C. F.; Baker, L. C. W.,*J. Am. Chem. Soc.* **1986,** *108*, 2748-2749. b.Kozik, M.; Baker, L. C. W.,*J. Am. Chem. Soc.* **1990,** *112*, 7604-7611. c. Keita, B.; Levy, B.; Nadjo, L.; Contant, R.,*New. J. Chem.* **2002,** *26*, 1314-1319. d. Lopez, X.; Bo, C.; Poblet, J. M.,*J. Am. Chem. Soc.* **2002,** *124*, 12574-12582.

(6) Contant, R.; Abbessi, M.; Canny, J.; Belhouari, A.; Keita, B.; Nadjo, L.,*Inorg. Chem.* **1997,** *36*, 4961-4967. b. Contant, R.; Richet, M.; Lu, Y. W.; Keita, B.; Nadjo, L.,*Eur. J. Inorg. Chem.* **2002,** c. Keita, B.; Girard, F.; Nadjo, L.; Contant, R.; Canny, J.; Richet, M.,*J. Electroanal. chem.* **1999,** *478*, 76-82.

(7) a. Bartis, J.; Dankova, M.; Lessmann, J. J.; Luo, Q.-H.; Horrocks, W. D., Jr.; Francesconi, L. C., *Inorg. Chem* **1999,** *38*, 1042-1053. b. Luo, Q.; Howell, R.C.; Bartis, J.; Dankova, M.; Williams, C.; Horrocks, W.DeW., Jr.; Young, V.C., Jr,; Rheingold, A.L.; Francesconi, L.C.; Antonio, M.R.*Inorg. Chem.* **2001**, *40*, 1894.

(8) Contant, R., *Inorg. Synth*, 1990, 27, 71

(9) Luo, Q-H., Doctoral Dissertation, Chemistry Department of the City University of New york, **2002**.

(10) Sluis & Spek, *Acta Cryst.* **1990**, *A46*, 194

(11) Ortega, F.; Pope, M. T.; Evans, J., H.G. *Inorg. Chem.* **1997**, *36*, 2166-2169., Sazani, G.; Dickman, M. H.; Pope, M. T. *Inorg. Chem.* **2000**, *39*, 939-943; Wasserman, K.; Lunck, H. J.; Palm, R.; Fuchs, J.; Steinfeldt, N.; Stoesser, R.; Pope, M. T. *Inorg.*

Chem. **1996**, *35*, 3273-9; Xin, F.; Pope, M. F. *Inorg. Chem.* **1996**, *35*, 5693-5695; Zhang, X. Y.; O'Connor, C. J.; Jameson, G. B.; Pope, M. T. *Inorg. Chem.* **1996**, *35*, 30-34).

(12) Ciabrini, J.-P.; Contant, R.,*J. Chem. Research (M).* **1993,** 2720-2744.

(13) Bion, L.; Mercier, F.; Decambox, P.; Moisy, P.,*Radiochim. Act*a **1999**; 161-166.

(14) Luo, Q.-H.; Zhang, C.; Howell, R.C.; Francesconi, L.C., manuscript in preparation.

(15) Van Pelt, C. E.; Crooks, W. J., III; Choppin, G. R.,*Inorg. Chim. Acta.* **2003,** 1-8.

(16) q= 0.34, 0.5M KCl; Horrocks, W. D., Jr.,*Methods in Enzymology* **1993,** *226*, 495-538.

Chapter 4

(1) a. Sadakane, M.; Dickman, M. H.; Pope, M. T. *Angew. Chem. Int. Ed.* 2000, *39*, 2914-2916. b. Mialane, P.; Lisnard, L.; Mallard, A.; Marrot, J.; Antic-Fidancev, E.; Aschehoug, P.; Vivien, D.; Secheresse, F. *Inorg. Chem.* 2003, *42*, 2102-2108.

(2) a. Muller, A.; Krickemeyer, E.; Bogge, H.; Schmidtmann, M.; Peters, F. *Angew. Chem. Int. Ed.* 1998, *37*, 3360-3365. b. Muller, A.; Sarkar, S.; Shah, S. Q. N.; Bogge, H.; Schmidtmann, M.; Sarker, S.; Kogerler, P.; Hauptfleish, B.; Trautwein, A. X.; Schunemann, V. *Angew. Chem. Int. Ed.* 1999, *38*, 3238-3241. c. Wassermann, K.; Dickman, M. H.; Pope, M. T. *Angew. Chem. Int. Ed. Engl.* 1997, *36*, 1445-1448.

(3) Belai, N.; Sadakane, M.; Pope, M. T. *J. Am. Chem. Soc.* 2001, *123*, 2087-2088.

(4) For key references to lanthanide luminescence: a.Bunzli, J.-C. G. "Luminescent Probes" in Lanthanide Probes in Chemistry, Biology and Earth Sciences; Bunzli,

J.-C.G.; Choppin, G. Eds.; 1989; Elsevier, Amsterdam. b. Kido, J.; Okamoto, Y. *Chem. Rev.* **2002**, *102*, 2357-2368. c. Bruce, J. I.; Dickins, R. S.; Govenlock, L. J.; Gunnlaugsson, T.; Lopinski, S.; Lowe, M. P.; Parker, D.; Peacock, R. D.; Perry, J. J. B.; Aime, S.; Botta, M., *J. Am. Chem. Soc.* **2000**, *122*, 9674-9684. d. Dickins, R. S.; Aime, S.; Batsanov, A. S.; Beeby, A.; Botta, M.; Bruce, J. I.; Howard, J. A. K.; Love, C. S.; Parker, D.; Peacock, R. D.; Puschmann, H.*J. Amer. Chem. Soc.* **2002**, *124*, 12697-12705. e. Parker, D.; Dickins, R. S.; Puschmann, H.; Crossland, C.; Howard, J. A. K. *Chem. Rev.* **2002**, *102*, 1977-2010..

(5) For key references to lanthanide Lewis Acid catalysis: a. Aspinall, H. C. *Chem. Rev.* **2002**, *102*, 1807-1850. b. Molander, G. A. *Chemtracts-Organic Chemistry* **1998**, *11*, 237-263. c. Molander, G. *Chem. Rev.* **1992**, *92*, 29-68. d. Shibasaki, M.; Yoshikawa, N. *Chem. Rev.* **2002**, *102*, 2187-2209. e. Kobayashi, S.; Kawamura, M. *J. Am. Chem. Soc.* **1998**, *120*, 5840-5841. f. Kobayashi, S. *Pure and Appl. Chem.* 1998, *70*, 1019-1026. g. Aspinall, H. C.; Dwyer, J. L. M.; Greeves, N.; McIver, E. G.; Woolley, J. C. *Organometallics* **1998**, *17*, 1884-1888. h. Xie, W.-H.; Yu, L.; Chen, D.; Li, J.; Ramirez, J.; Miranda, N. F.; Wang, P. G . in *Environmentally Benign Chemistry: Green Chemistry*; Anastas, P. T. and Williamson, T. C., Ed.; Oxford University Press: Oxford, UK, **1998**; Vol. , pp 129-149.

(6) a. Bartis, J.; Dankova, M.; Blumenstein, M.; Francesconi, L. C. *Journal of Alloys and Compunds* 1997, *249*, 56-68. b. Bartis, J.; Sukal, s.; Dankova, M.; Kraft, E.; Kronzon, R.; Blumenstein, M.; Francesconi, L. C. *J. Chem. Soc., Dalton Trans* 1997, 1937-1944. c. Bartis, J.; Dankova, M.; Lessmann, J. J.; Luo, Q.-H.;

Horrocks, W. D., Jr.; Francesconi, L. C. *Inorganic Chemistry* 1999, *38*, 1042-1053. e. Luo, Q.; Howell, R. C.; Dankova, M.; Bartis, J.; Williams, C. W.; Horrocks, W. D., Jr.; Young, J., V.G.; Rheingold, A. L.; Francesconi, L. C.; Antonio, M. R. *Inorg. Chem.* 2001, *40*, 1894-1901. f. Luo, Q.; Howell, R. C.; Bartis, J.; Dankova, M.; Horrocks, W. D., Jr.; Rheingold, A. L.; Francesconi, L. C. *Inorg. Chem.* 2002, *41*, 6112-6117.

(7) Sadakane, M.; Ostuni, A.; Pope, M. T. *J. Chem. Soc. Dalton Trans.* 2002, 63-67.

(8) Luo, Q.; Howell, R. C.; Dankova, M.; Bartis, J.; Williams, C. W.; Horrocks, W. D., Jr.; Young, J., V.G.; Rheingold, A. L.; Francesconi, L. C.; Antonio, M. R. *Inorg. Chem.* 2001, *40*, 1894-1901.

(9) Bartis, J.; Dankova, M.; Lessmann, J. J.; Luo, Q.-H.; Horrocks, W. D., Jr.; Francesconi, L. C. *Inorganic Chemistry* 1999, *38*, 1042-1053.

(10) Vogel, A. I. *A text-book of quantitative inorganic analysis_including elementary instrumental analysis*; 3rd edition ed.; Longmans, 1961.

(11) Zhang, C.; Howell, R. C.; Scotland, K. B.; Perez, F. G.; Todaro, L.; Francesconi, L. C. *Inorg. Chem.* 2004, *43*, 7691-7701.

(12) Kirby, J. F.; Baker, L., C.W. *Inorganic Chemistry* 1998, *37*, 5537-5545.

(13) Laronze, N.; Marrot, J.; Herve, G. *Inorg. Chem.* 2003, *42*, 5857-5862.

(14) Grigoriev, V. A.; Hill, C. L.; Weinstock, I. A. *J. Am. Chem. Soc.* 2000, *122*, 3544-3545.

(15) Grigoriev, V. A.; Cheng, D.; Hill, C. L.; Weinstock, I. A. *J. Am. Chem. Soc.* 2001, *123*, 5292-5307.

(16) Cheng, Z.; Howell, R. C.; Luo, Q.; Fieselmann, H. L.; Todaro, L.; Francesconi, L. C. 2004.

(17) Barrett, D. M. Y.; Kawha, I. A.; Mague, J. T.; McPherson, G. L. *J. Org. Chem.* 1995, *60*, 5946-5953

(19) Peacock, R. D.; Weakley, T. J. R. *J. Chem. Soc.* 1971, *A*, 1836-1839.

(20) Ciabrini, J.-P.; Contant, R. *J. Chem. Research (M).* 1993, 2720-2744.

(21) a. Bion, L.; Moisy, P.; Madic, C. *Radiochimica Acta* 1995, *69*, 251-257. b. Bion, L.; Moisy, P.; Vaufrey, F.; Meot-Reymond, S.; Simoni, E.; Madic, C. *Radiochim. Acta* 1997, *78*.

(22) Van Pelt, C. E.; Crooks, W. J., III; Choppin, G. R. *Inorg. Chim. Acta.* 2003, *346*, 215-222.

Chapter 5

(1) Sadakane, M.; Dickman, M. H.; Pope, M. T. *Angew. Chem. Int. Ed.* **2000**, *39*, 2914-2916.

(2) Mialane, P.; Lisnard, L.; Mallard, A.; Marrot, J.; Antic-Fidancev, E.; Aschehoug, P.; Vivien, D.; Secheresse, F. *Inorg. Chem.* **2003**, *42*, 2102-2108.

(3) Muller, A.; Peters, F.; Pope, M. T.; Gatteschi, D. *Chemical Reviews* **1998**, *98*, 239-271.

(4) Muller, A.; Krickemeyer, E.; Bogge, H.; Schmidtmann, M.; Peters, F. *Angew. Chem. Int. Ed.* **1998**, *37*, 3360-3365.

(5) Muller, A.; Sarkar, S.; Shah, S. Q. N.; Bogge, H.; Schmidtmann, M.; Sarker, S.; Kogerler, P.; Hauptfleish, B.; Trautwein, A. X.; Schunemann, V. *Angew. Chem. Int. Ed.* **1999**, *38*, 3238-3241.

(6) Wassermann, K.; Dickman, M. H.; Pope, M. T. *Angew. Chem. Int. Ed. Engl.* **1997**, *36*, 1445-1448.

(7) Belai, N.; Sadakane, M.; Pope, M. T. *J. Am. Chem. Soc.* **2001**, *123*, 2087-2088.

(8) For key references to lanthanide luminescence: a. Kido, J.; Okamoto, Y., *Chem. Rev.* **2002**, *102*, 2357-2368. b. Bruce, J. I.; Dickins, R. S.; Govenlock, L. J.; Gunnlaugsson, T.; Lopinski, S.; Lowe, M. P.; Parker, D.; Peacock, R. D.; Perry, J. J. B.; Aime, S.; Botta, M., *J. Am. Chem. Soc.* **2000**, *122*, 9674-9684. c. Dickins, R. S.; Aime, S.; Batsanov, A. S.; Beeby, A.; Botta, M.; Bruce, J. I.; Howard, J. A. K.; Love, C. S.; Parker, D.; Peacock, R. D.; Puschmann, H., *J. Amer. Chem. Soc.* **2002**, *124*, 12697-12705. d. Parker, D.; Dickins, R. S.; Puschmann, H.; Crossland, C.; Howard, J. A. K., "*Chem. Rev.* **2002**, *102*, 1977-2010.

(9) For key reviews on new functional materials, particularly electrochromic, electroluminescent, photochromic and photoluminescent materials, a. Katsoulis, D.E. *Chem. Rev.*, **1998,** *98*, 359-387. b.Yamase, T. *Chem. Rev.*, **1998**, *98*, 307-325. For recent applications of lanthanide polyoxometalates incorporated into materials: electrochromic device preparation, c. Liu, S.; Kurth, D. G.; Mohwald, H.; Volkmer, D., *Advanced Materials* **2002**, *14*, 225-228. photoluminescent films, d. Mo, Y.-G.; Dillon, R. O.; Snyder, P. G.; Tiwald, T. E., *Thin Solid Films* **1999**, *355-356*, 1-5. e. Xu, L.; Zhang, H.; Wang, E.; Kurth, D. G.; Li, Z., *J. Mater. Chem.* **2002**, *12*, 654-657. f. Xu, L.; Zhang, H.; Wang, E.; Wu, A.; Li, Z.,

Materials Chemistry and Physics **2002**, *77*, 484-488. g. Wang, Y.; Wang, X.; Hu, C.; Shi, C., *J. Mater. Chem.* **2002**, *12*, 703-707. h. Wang, J.; Liu, F.; Fu, L.; Zhang, H., *Materials Lett* **2002**, *56*, 300-304. i. Wang, Y.; Wang, X.; Hu, C., *Journal of Colloid and Interface Science* **2002**, *249*, 307-315. j. Wang, J.; Wang, H. S.; Fu, L. S.; Liu, F. Y.; Zhang, H. J., *Thin Solid Films* **2002**, *414*, 256-261.

(10) For key references to lanthanide Lewis Acid catalysis: a. Aspinall, H. C., *Chem. Rev.* **2002**, *102*, 1807-1850. b. Molander, G. A., *Chemtracts-Organic Chemistry* **1998**, *11*, 237-263. c. Molander, G., *Chem. Rev.* **1992**, *92*, 29-67. d. Shibasaki, M.; Yoshikawa, N.,*Chem. Rev.* **2002**, *102*, 2187-2209. e. Kobayashi, S.; Kawamura, M., *J. Am. Chem. Soc.* **1998**, *120*, 5840-5841. f. Kobayashi, S., *Pure and Appl. Chem.* **1998**, *70*, 1019-1026. g. Aspinall, H. C.; Dwyer, J. L. M.; Greeves, N.; McIver, E. G.; Woolley, J. C., *Organometallics* **1998**, *17*, 1884-1888. h. Xie, W.-H.; Yu, L.; Chen, D.; Li, J.; Ramirez, J.; Miranda, N. F.; Wang, P. G.*Lanthanide-Catalyzed organic synthesis in protic solvents*; Anastas, P. T. and Williamson, T. C., Ed.; Oxford University Press: Oxford, UK, **1998**; pp 129-149.

(11) Jenkins, A. L.; Uy, O. M.; Murray, G. M. *Analytical Communications* **1997**, *34*, 221-224.

(12) Lester, E. D.; Bearman, G.; Ponce, A. *IEEE Engineering in Medicine and Biology Magazine* **2004**, *January/February, 2004*, 130-135.

(13) de Silva, A. P.; Fox, D. B.; Moody, T. S.; Weir, S. M. *Pure Appl. Chem.* **2001**, *73*, 503-511.

(14) Horrocks, W. D., Jr.; Sudnick, D. R. *J. Amer. Chem. Soc.* **1979**, *101*, 334-340.

(15) Horrocks, W. D., Jr. *Methods in Enzymology* **1993**, *226*, 495-538.

(16) *Luminescent Probes*; Bunzli, J.-C., G., Ed.; Elsevier: Amsterdam, 1989.

(17) Yamase, T.; Kobayashi, T.; Sugeta, M.; Naruke, H. *J. Phys. Chem. A* **1997**, *101*, 5046-5053.

(18) Yamase, T. *Chem. Rev.* **1998**, *98*, 307-325.

(19) Dexter, D. L. *J. Chem. Phys.* **1953**, *21*, 836-850.

(20) Klink, S. I.; Grave, L.; Reinhoudt, D. N.; van Veggel, F. C. J. M.; Werts, M. H. V.; Geurts, F. A. J.; Hofstraat, J. W. *J. Phys. Chem. A.* **2000**, *104*, 5457 - 5468.

(21) Luo, Q.; Howell, R. C.; Bartis, J.; Dankova, M.; Horrocks, W. D., Jr.; Rheingold, A. L.; Francesconi, L. C. *Inorg. Chem.* **2002**, *41*, 6112-6117.

(22) Zhang, C.; Howell, R. C.; Scotland, K. B.; Perez, F.; Luo, Q. L.; Todaro, L.; Francesconi, L. C. *Inorg. Chem.* **2004**, *in press*.

(23) Weiner, H.; Aiken, I., J.D.; Finke, R. G. *Inorg. Chem.* **1996**, *35*, 7905-7913.

(24) Bartis, J.; Dankova, M.; Lessmann, J. J.; Luo, Q.-H.; Horrocks, W. D., Jr.; Francesconi, L. C. *Inorganic Chemistry* **1999**, *38*, 1042-1053.

(25) Zhang, C.; Howell, R. C.; Scotland, K. B.; Perez, F. G.; Todaro, L.; Francesconi, L. C. *Inorg. Chem.* **2004**, *in press*.

(26) *SHELXTL, Brucker AXS, Inc., Bruker Advanced X-ray Solutions, 1999* **1999**.

(27) Blasse, G.; Dirksen, G. J.; Zonnevijlle, F. *J. Inorg. Nucl. Chem.* **1981**, *43*, 2847-2853.

(28) Lis, S.; But, S. *Journal of Alloys and Compounds* **2000**, *300-301*, 370-376.

(29) Yusov, A. B.; Fedoseev, A. M. *Radiokhimiya* **1992**, *34*, 61-70.

(30) Zhang, C.; Howell, R. C.; Luo, Q.; Fieselmann, H. L.; Todaro, L.; Francesconi, L. C. *manuscript in preparation* **2004**.

(31) Zhang, C.; Howell, R. C.; McGregor, D.; Bensaid, L.; Francesconi, L. C., unpublished work, **2004**.

(32) Hasegawa, Y.; Yamamuro, M.; Wada, Y.; Kanehisa, N.; Kai, Y.; Yanagida, S. *J. Phys. Chem. A.* **2003**, *107*.

(33) Huignard, A.; Gacoin, T.; Boilot, J.-P. *Chem. Mater.* **2000**, *12*, 1090-1094

(34) Magennis, S. W.; Craing, J.; Gardner, A.; Fucassi, F.; Cragg, P. J.; Robertson, N.; Parsons, S.; Pikramenou, Z. *Polyhedron* **2003**, *22*, 745-754.

(35) Riviere, C.; Nierlich, M.; Ephritikhine, M.; Madic, C. *Inorg. Chem.* **2001**, *40*, 4428-4435.

Chapter 6

(1) S. K. Yun and T. Pinnavaia, *Inorg. Chem.* 1996, 35, 6853-6860.

(2) C. Barriga, W. Jones; P. Malet; V. Rives, and M. A. Ulibarri. *Inorg. Chem.* 1998, 37, 1812-1820.

(3) Kwon, T.; Pinnavaia, T. *J. Chem. Mater.* 1989, 1, 381.

(4) Drezdzon, M. A. *Inorg. Chem.* 1989, 27, 4628.

(5) Evans, J.; Pillinger, M.; Zhang, J. *J. Chem. Soc., Dalton Trans.* 1996, 2963.

(6) Alvin P. Ginsberg, *Inorganic syntheses* V27, 1992.

(7) Q-H Luo, R.C. Howell, J. Bartis, M. Dankova, W. D. Horrocks, Jr. A. L. Rheingold, and L. C. Francesconi, *Inorg. Chem.* 2002, accepted.

(8) C. Zhang; R. C. Howell; K. B. Scotland; F. G. Perez and L. C. Francesconi. manuscript, 2002.

(9) M. R. Weir; R. Kydd, *Microporous and Mesoporous Materials*, 20 (1998) 339-347.

(10) Guo, J.; Li, Y.; Jiao, Q.; Jiang, D.; Min, E., *Chemical research in Chinese Universities* 1998; 14, 176-178.

(11) F. Embert; A. Mehdi; C. Reye; R. J. P. Corriu. *Chem. Mater.* 2001, 13, 4542-4529.